

**METHODS FOR ASYNCHRONOUS AND NON-INVASIVE EEG-BASED
BRAIN-COMPUTER INTERFACES. TOWARDS INTELLIGENT
BRAIN-ACTUATED WHEELCHAIRS**

**MÈTODES PER INTERFÍCIES CEREBRALS ASÍNCRONES NO
INVASIVES ORIENTADES AL CONTROL DE CADIRES DE RODES
INTEL·LIGENTS**

A Thesis Submitted For the Degree of Doctor of Philosophy

BY

FERRAN GALÁN MOLES

BIOMETRICS AND STATISTICS PROGRAM 2001-2003

DEPARTMENT OF STATISTICS

UNIVERSITY OF BARCELONA

Supervisors:

Dr. Joan Guàrdia i Olmos

Dr. Francesc Oliva i Cuyàs

Dr. José del R. Millán Ruiz

Barcelona, UB
2008

...PER A LA MARIA...
A MIS PADRES

Preface

This thesis has been developed in two stages. The first stage corresponds to my stay as research fellow at the Dept. of Methodology for Behavioural Sciences of the University of Barcelona. During this period jointly with my supervisors we started from scratch working in brain-computer interfaces research, mainly working on databases and data recorded during open-loop protocols. The main innovation from this period was the introduction of mental tasks transitions detection and canonical variates analysis in BCI field. The second stage corresponds to my stay at IDIAP Research Institute as research assistant where I worked for MAIA¹ EU project which aimed at developing asynchronous and non-invasive brain-computer interfaces to control robots and wheelchairs. During this period all my work was focused on developing and adapting experimental protocols, methods and algorithms to enhance the robustness and performance of the brain-computer interface system integrated in the brain-actuated wheelchair. The compilation of publications included in this thesis describe some of the work carried out for this purpose.

¹MAIA—*Mental Augmentation through Determination of Intended Action*, <http://www.maia-project.org>

Acknowledgements

As introduced in the preface this thesis has been developed in two stages. During the first stage of the process I joined the Department of Methodology for Behavioural Sciences and the Department of Statistics of the University of Barcelona, and I was external student at the Biomedical Engineering Research Center of the Technical University of the Catalonia. During the second stage I joined IDIAP Research Institute at Martigny, Switzerland.

In the course of this adventure, I have been fortunate to interact with many people who have influenced me greatly. One of the pleasures of writing this manuscript is the opportunity to thank them. It also allows me to thank people that played a key role giving me chances and motivating me to start a research career, and of course my people, people that is always there even if they are in front of a *desaparecido*...

Primerament, m'agradaria mostrar el meu agraïment a en Joan i en Francesc per haver-me dirigit la tesi, per haver confiat en mi i el meu treball en tot moment, per donar-me total llibertat i recolzament, tant personal com acadèmic, a l'hora d'embrancar-nos en un àmbit de recerca que en aquell moment a qualsevol li sonava a ciència ficció. Gràcies a tots dos per tot el que heu fet per mi i per el que continueu fent, sempre me'n recordaré dels nostres eventuals esmorzars, dinars i/o aperitius quan jo feia estades llampec a Barcelona escapant-me de Suïssa.

Gràcies Jose. Gràcies per haver acceptat la meva sol·licitud per fer una estada de curta durada a l'IDIAP. Gràcies per haver-me ofert la possibilitat de quedar-m'hi, gràcies per obrir-me les portes i guiar-me en l'art de barallar-se amb problemes desafiants en un entorn tant estimulant com és l'IDIAP, i gràcies per haver accedit a dirigir la tesi. Treballar sota la teva supervisió per MAIA, assolir els objectius i superar moments difícils ha estat la millor manera d'aprendre aquest ofici. Finalment, gràcies també per presentar-me al Sr. Brandy, el del teu poble.

Thanks to my KUL colleagues: Johan, Dirk, Gerolf and Marnix. Has been a pleasure to work with you. This thesis would not be possible without your contribution on the robotic side.

Voldria agrair al Departament de Metodologia de les Ciències del Comportament de la Universitat de Barcelona, a la M^a Lluïsa, aleshores la seva directora, al Toni, aleshores el seu secretari, i a la resta de companys haver-me posat a l'abast tots els recursos que he necessitat. Durant la meua estada sempre em vaig considerar un becari afortunat, realment

vaig ser un privilegiat.

Gràcies a la Maribel, la Maite i en Xavi, les meves primeres companyes i company de despatx al Departament de Metodologia, per acollir-me i fer-me sentir com a casa des de el primer dia. Gràcies al Natx i la Meri pels dinars divertits a la fàcul, sempre recordaré a la Meri amb el seu *tupper* i l'abric vermell, i al Natx con sus pelos *Polopelo*. Gràcies als que van portar la vidilla al departament i van ser els meus companys en el nou despatx de becaris, la Jor, el David i l'Ana, gràcies per ser capaços de conviure amb la meva psicopatia.

I also would like to thank many IDIAPers for their friendship and support at different moments. Some already left, I started snowboarding thanks to Mike and Anna. Gerwin was my buddy in the art of learning how to land appropriately. Christos was always at the next office to talk, to have dinner, to go hiking...and Guillaume was the climb master. Some still at IDIAP, Sarah showed me bits of Valais. Deepu and Sriram introduced me to the marvellous Indian food. Tristan showed me how to enjoy Café des Alps and introduced me to Marcel, the dominican-swiss. Vincent, the web-rock master, during spring and summer was every Wednesday ready to enjoy the rock's touch. I really enjoyed multicultural dinners, drinks, ski days, the carpet and the chocolates with Phil, Yoko and Hari. I improved my English thanks to Bastian, my *Alias* supplier. I improved my French thanks to Michel, my French teacher. Well, he was not only a French teacher, he always organized activities to help us to integrate ourselves in the Swiss way of life. I always will remember the *brisoleés*, the snow hike-fondue-sledging evenings, and dinners at his place. Petr was always ready and available to take me hiking, climbing and to the slopes. Bertrand enhanced my quality of life at Martigny, his sister's snowboard has been the channel to discover the snow culture up there. The BCI guys, Pierre, Ricardo, Nicolas, Eileen and Ganga, crazy people from who I have learned a lot. Pierre was my baby foot master, my roommate and party mate at many travels (I always will remember the Tarantino hotel at Leuven) and one of my EEG recordings mates. He is also the lab master. As I told you, you are another hard worker psychopath. Without your work this thesis could not be possible. Ricardo, ha sido un placer trabajar contigo. Gracias por estar siempre disponible para revisar mis papers y para mantener discusiones productivas. He aprendido mucho observando como trabajas y siempre ha sido reconfortante tenerte al lado. Nicolas was my snowboarding master, his advices took me to another level. I really admire you because you are dealing with some of the hardest problems nowadays a researcher in pattern recognition and neuroscience can face. Eileen was my other EEG recordings mate. I always will remember your cookies, brownies and supporting staff for the experimental sessions, and those *Big Tasty* lunches wearing the cap. But overall, I always will remember the first time you drove the wheelchair along the slalom. You gave me the best moment of my life as a scientist. Mr. Gangadhar Garipelli, Ganga. I do not have enough words or space to tell all what I should to tell. Ganga was, he is and he will be *The Crazy Indian*. He has been my buddy at Martigny. I enjoyed his company, his enthusiasm, his advices and our discussions. He always was there helping me to pass difficult moments and encouraging me. There are people that his mere presence makes better the live of the others. He is one of them. I tu Guillermo,

Torrente. He estat afortunat al haver-te conegut. Gràcies per venir al meu despatx quan vaig arribar a l'IDIAP. Hem fet i desfet moltes coses junts (aikido, mur, roca, snowboarding, sopars, *LOST*, festes, i més coses...). Ets una persona especial. M'encanta passar estones i parlar amb tu, és difícil trobar algú que parli el mateix idioma o s'hagi empassat la mateixa pastilla. Finally, thank all the IDIAPers to be there at the right moment.

Vull aprofitar aquesta ocasió per mostrar també el meu sentit d'agraïment a la Montse, la persona que em va donar la primera oportunitat d'introduir-me en la recerca quan jo era simplement un estudiant de primer curs de Psicologia. Després van ser el José Antonio, el Josep Maria, el Reynaldo i el Carles. Posteriorment, la Montse em va ajudar novament en decidir-me a realitzar el doctorat quan jo m'estava plantejant tornar a Barcelona. Gràcies a tots per haver-me deixat col·laborar amb vosaltres i ser una esponja. Els estudis de llicenciatura sense vosaltres haguessin estat avorrits i incomplets. Finalment, gràcies al Pep per haver-me ensenyat com segmentar manualment les diferents fases del son i a lidar amb CPAPs. En el període en el que vam treballar junts és on va néixer la motivació de desenvolupar algorismes de classificació de fenòmens EEG.

El torn de la meva gent. Vull agrair-vos a tots vosaltres que sempre estigueu amb mi encara que jo estigui lluny. Amb tots vosaltres he compartit moments inoblidables.

Gràcies al Toni, el meu amic de la infància i veï. Als meus amics de llicenciatura amb els seus respectius, respectives, fills i filles: Oscar, Eva, Aroa, Clara, Albert, Conchi, Ivan (Joan), Sonia, Juan Carlos, Laura, Santi, Vanessa, Eugenio, Cristian i Ariela. Als *Algarrobos* i família extensa, especial menció pel Pascual, la Yolanda i el Marc. A la Pili i al Roger. Al Reynaldo, definitivament eres de otra galaxia, gracias por escucharme, orientarme, dar tu opinión, pensar en mí y cuidarme. A mi familia dominicana, a Joel, Aricel, Luís, Eva María y Felipe.

Gracias a mi familia. Cada uno de vosotros ha contribuido de una manera u otra en mi forma de caminar por la vida.

Gracias a mis padres. Gracias a los dos por quererme como me queréis, por entenderme como me entendéis, por educarme como me habéis educado, por creer ciegamente en mí, y por haber puesto todos los medios para que estas líneas sean una realidad. Sois los mejores padres del mundo y esta tesis está dedicada a vosotros.

Finalment, gràcies a la millor persona que he conegut. Maria, aquesta tesi no hagués estat possible sense tu i no hi ha ni suficients paraules ni suficient espai per expressar els meus sentiments. Em limitaré a dir que aquesta tesi, malgrat tot, ha estat realitzada per a tu. És teva.

This research was supported in part by the Agència de Gestió d'Ajuts Universitaris i de Recerca, Departament d'Universitats Recerca i Societat de la Informació, Generalitat de Catalunya, under Grants 2002FI00437 and 2005BE00110, by the Swiss National Science Foundation through the National Centre of Research on "Interactive Multimodal Information Management (IM2)" and by the European IST Programme FET Project FP6-003758. This manuscript only reflects the author's views and founding agencies are not liable for any use that may be made of the information contained herein.

Contents

1	Introduction	1
1.1	Measuring Brain Activity	2
1.2	EEG Features Utilized in BCI Research	4
1.2.1	EEG Oscillatory Rhythms	4
1.2.2	Event Related Potentials (ERP)	6
1.3	Non-Invasive EEG-based BCIs	7
1.4	The IDIAP BCI	8
1.4.1	Spontaneous Asynchronous Operation	9
1.4.2	The Machine Learning Way to BCI	9
1.4.3	Blending of Intelligences	10
1.4.4	Recognition of High-Level Cognitive States	10
1.5	MAIA Project	11
1.6	Aim of the Thesis	12
2	Summary of Contents	15
2.1	Using MTTD to Improve Spontaneous Mental Activity Classification	15
2.1.1	Introduction	15
2.1.2	Methods	15
2.1.3	Results and Conclusions	19
2.2	Detecting Intentional Mental Transitions in an Asynchronous BCI	20
2.2.1	Introduction	20
2.2.2	Methods	21
2.2.3	Results and Conclusions	28
2.3	Feature Extraction for Multi-class BCI using CVA	34
2.3.1	Introduction	34
2.3.2	Methods	34
2.3.3	Results and Conclusions	37
2.4	Visuo-Spatial Attention Frame Recognition for BCI's	40
2.4.1	Introduction	40
2.4.2	Methods	41

2.4.3	Results and Conclusions	42
2.5	A Brain-Actuated Wheelchair	44
2.5.1	Introduction	44
2.5.2	Methods	45
2.5.3	Results and Conclusions	50
3	Conclusions	55
A	Non-Invasive Brain-Machine Interaction	59
B	Using Mental Tasks Transitions Detection to Improve Spontaneous Mental Activity Classification	73
C	Detecting Intentional Mental Transitions in an Asynchronous BCI	83
D	Feature Extraction for Multi-class BCI using Canonical Variates Analysis	101
E	Visuo-Spatial Attention Frame Recognition for Brain-Computer Interfaces	109
F	A Brain-Actuated Wheelchair: Asynchronous and Non-Invasive Brain-Computer Interfaces for Continuous Control of Robots	115
G	Adaptive Shared Control of a Brain-Actuated Simulated Wheelchair	145
H	Context-based Filtering for Assisted Brain-Actuated Wheelchair Driving	153
I	Demonstrations	167
J	Resum	169
J.1	Interfícies Cerebrals a l'IDIAP Research Institute	169
J.1.1	Protocol Asíncron i Espontani	171
J.1.2	La Via de l'Aprenentatge Estadístic en Interfícies Cerebrals	171
J.1.3	Combinació d'Intel·ligències	172
J.1.4	Reconeixement d'Estats Cognitius	172
J.2	Projecte MAIA	173
J.3	Objectius de la Tesi	173
J.4	Resultats i Conclusions	176
	Bibliography	179

Abbreviations

BCI = Brain-computer interface

CNV = Contingent Negative Variation

CVA = Canonical Variates Analysis

CVT = Canonical Variates Transformation

DBDA = Distance Based Discriminant Analysis

DP = Discriminant Power

ECoG = Electrocorticogram

EEG = Electroencephalogram

EMG = Electromyogram

EOG = Electrooculogram

ERD = Event-Related Desynchronization

ERS = Event-Related Synchronization

ERP = Event-Related Potentials

fMRI = Functional Magnetic Resonance Imaging

MAIA = Mental Augmentation through Determination of Intended Action

MEG = Magnetoencephalogram

MTTD = Mental Tasks Transition Detection

NIRS = Near-Infrared Radiation Spectroscopy

PET = Positron Emission Tomography

PSD = Power Spectral Density

SCP = Slow Cortical Potentials

SSVEP = Steady State Visual Evoked Potentials

TTD = Thought Translation Device

VEP = Visual Evoked Potentials

Chapter 1

Introduction

The idea of controlling machines not by manual operation, but by mere thinking (i.e., the brain activity of human subjects) has fascinated humankind since ever, and researchers working at the crossroads of computer science, neurosciences, and biomedical engineering have started to develop the first prototypes of brain-computer interfaces (BCI) over the last decade or so (Millán et al., 2008).

This chapter introduces readers not familiar with brain-computer interfaces an insight into this research field, and put the contributions of this thesis in context. To this end, after defining what is a brain-computer interface (BCI) system and describing its architecture, section 1.1 presents the most utilized methods for measuring brain activity, section 1.2 introduces the main electroencephalogram (EEG) features utilized in BCI research, section 1.3 briefly describes different EEG-based BCI systems, section 1.4 describes the IDIAP BCI and its principles, section 1.5 introduces MAIA project, and finally section 1.6 describes the aim of the thesis and put its contributions in MAIA project context.

A BCI is a close loop system that monitors the user's brain activity and translates their intentions into actions without using activity of any muscle or peripheral nerve (Wolpaw et al., 2002). The central tenet of a BCI is the capability to distinguish different patterns of brain activity, each being associated to a particular intention or mental task. Thus, a BCI system can be described as an assistive technology that bridges the users with the environment.

The brain activity recorded with an acquisition system is processed and transformed by a signal processing module to select relevant features that are fed to a pattern recognition module. This module, usually a statistical classifier, identifies the kind of brain activity generated by the user and associates it to commands that permit to control a device. Finally, feedback plays a key role in the user's learning providing information about the performance of the BCI executing the intended task. Fig. 1.1 shows the BCI general architecture.

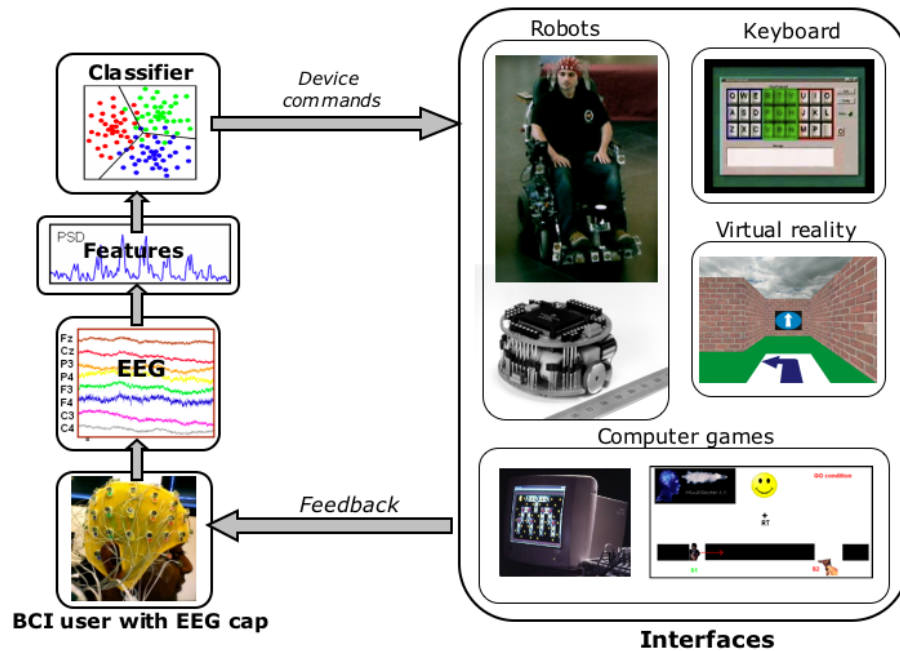


Figure 1.1: Schematic representation of a BCI architecture.

1.1 Measuring Brain Activity

BCI systems acquire brain activity in order to infer users intent utilizing several techniques that can be classified according to their invasiveness and the nature of the recording, namely based on electrical or metabolic activity. Different techniques are now briefly introduced starting with two invasive techniques, namely implanted microelectrodes and electrocorticogram (ECoG), followed by non-invasive techniques based on metabolic activity, functional magnetic resonance imaging (fMRI), positron emission tomography (PET) and near-infrared spectroscopy (NIRS), and finishing with two non-invasive techniques based on magnetic and electrical activity, magnetoencephalogram (MEG) and electroencephalogram (EEG).

- Implanted microelectrodes** allow to record the electrophysiological activity (action potentials) from single neurons or local field potentials (LFP) that reflect the combined activity of nearby neurons and synapses. Although this technique offers the highest temporal and spatial resolution providing, most BCI work has been limited in animals (Carmena et al., 2003; Serruya et al., 2002; Taylor et al., 2002) given the risk of insertion of multiple electrode arrays within brain tissue and unresolved issues related to acute and chronic tissue damage and long term recording stability (Grill and Mortimer, 2000; Polikov et al., 2005; Szarowski et al., 2003; Vetter et al., 2004). The number of studies with humans is reduced (Kennedy et al., 2000;

Hochberg et al., 2006).

- **ECoG** records electrical fields produced by the brain placing electrode arrays on the cortical surface without penetrating into the brain. Despite the acceptable temporal and spatial resolution and the impressive results reported (Leuthardt et al., 2004), its application to BCI research has been very limited and restricted to patients implanted with ECoG electrode arrays for a few days prior to epilepsy surgery.
- **fMRI** works by detecting the changes in blood oxygenation and flow that occur in response to neural activity. Haemoglobin is diamagnetic when oxygenated but paramagnetic when deoxygenated. This difference in magnetic properties leads to small differences in the MR signal of blood depending on the degree of oxygenation. Since blood oxygenation varies according to the levels of neural activity these differences can be used to detect brain activity. Although fMRI provides a good spatial resolution its use on BCI research has been also limited (Weiskopf et al., 2004) mainly because two reasons, the lack of enough temporal resolution given that the hemodynamic response rises to a peak with a delay of 4-5 seconds, and the expensiveness of the equipment.
- **PET** is a nuclear medical imaging technique that produces a three-dimensional image or map of brain functional processes. A short-lived radioactive tracer isotope, which decays by emitting a positron, is incorporated into a metabolically active molecule, typically fluorodeoxyglucose, and is injected into blood circulation. Therefore it is possible to measure metabolic activity of a brain area by detecting positron emission. As in the case of fMRI, PET provides a good spatial resolution but its use on BCI research has been also limited because the same reasons. In addition, this technique also presents a small risk for the subject since radioactive compounds are injected in the blood circulation.
- **NIRS** uses transmittance measurements of near-infrared (NIR) radiation (from about 1000 nm to 2500 nm) to monitor the degree of oxygenation of different metabolites. Oxygenated and deoxygenated hemoglobin have different optical properties. As for fMRI, since blood oxygenation is correlated with neuronal activity, differences in optical response can be used to measure brain activity. Different than PET and fMRI, NIRS does not need radioisotopes or other contrast agents. This propriety has motivated its use in BCI research (Chen et al., 1999; Coyle et al., 2004a; Coyle et al., 2004b) but its spatial and temporal resolutions are low.
- **MEG** is an imaging technique used to measure the magnetic fields produced by electrical activity in the brain, typically from current flows in the long apical dendrites of the cortical pyramidal cells. This technique has a very high temporal resolution (in the range of milliseconds) but the use of MEG in BCI research (Georgopoulos

et al., 2005) has been limited mainly because the expensiveness and the size of the required equipments.

- **EEG** is the neurophysiologic measurement of the electrical activity of the brain recorded from electrodes placed on the scalp. The voltage fluctuations (20-100 μV) registered by EEG are the summations of the continually ongoing electrical activity of large populations of cortical neurons. It reflects the extracellular currents resulting from postsynaptic membrane depolarization and hyperpolarization of cortical pyramidal neurons. Its main limitation is its poor spatial resolution since EEG is most sensitive to a particular set of post-synaptic potentials, those which are generated in superficial layers of the cortex, on the crests of gyri directly abutting the skull and radial to the skull. Dendrites which are deeper in the cortex, inside sulci, are in midline or deep structures (such as the cingulate gyrus or hippocampus) or produce currents which are tangential to the skull have far less contribution to the EEG signal. In addition, the meninges, cerebrospinal fluid and skull contaminates the EEG signal, obscuring its intracranial source. Despite these limitations, EEG temporal resolution is very high (in the range of milliseconds) and is easily recorded comparatively to other risky, expensive and non-portable equipments, key issues to widen real time BCI applications (Bayliss, 2003; Blankertz et al., 2006a; Millán et al., 2004; Galán et al., 2008a) and to bring BCI technology to a large population.

1.2 EEG Features Utilized in BCI Research

As introduced in the previous section, EEG brings interesting properties to BCI research, namely high temporal resolution, non-invasiveness, economy and portability. This section describes a variety of EEG features that have been exploited by different BCI systems. These features are mainly extracted from the changes on the ongoing EEG produced by internally or externally events. These changes can be classified in two groups, namely phase unlocked or phase locked. The former case it is mainly observed in frequency domain and reflects the modulation of different EEG oscillatory rhythms. The second case has been mainly defined in temporal domain and reflects the brain electrical activity triggered by the event (event related potentials).

1.2.1 EEG Oscillatory Rhythms

EEG is mainly described by a variety of oscillatory rhythms that have different functional correlates. These rhythms have been divided into several groups according to their frequency range. (see Fig. 1.2)

- **Delta** is the lowest frequency range, below 4Hz. Occurs in very deep sleep, in infancy, and serious organic brain diseases.

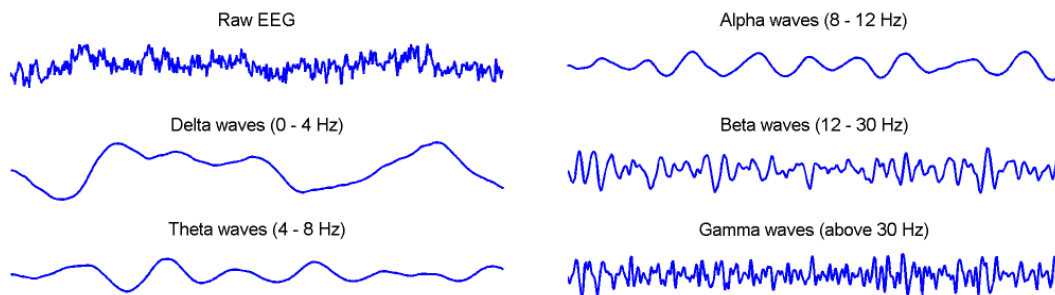


Figure 1.2: EEG oscillatory rhythms. The top left plot shows one second of raw EEG signal and the five other plots illustrate five frequency ranges.

- **Theta** is the frequency range from 4 to 8 Hz and it is associated to creativity, intuition, daydreaming, and fantasizing and is a repository for memories, emotions, sensations. Theta rhythm is strong during internal focus, meditation, prayer, and spiritual awareness. It reflects the state between wakefulness and sleep. It is abnormal in awake adults but is perfectly normal in children up to 13 years old. It is also normal during sleep. Theta is believed to reflect activity from the limbic system and hippocampal regions. Theta is observed in anxiety, behavioral activation and behavioral inhibition.
- **Alpha** is the frequency range from 8 to 12 Hz. It is associated to alertness and sleep, but not actively processing information. They are strongest over the occipital (back of the head) cortex and also over frontal cortex. During deep sleep it disappear.
- **mu** is the frequency range from 8 to 12 Hz as Alpha but with specific topography and different functional correlates. It is not always present in adult people, and it has a short duration. It is highly related with the motor cortex functions and it is salient in precentral - prerolandic circumvolution and postcentral gyrus.
- **Beta** is the frequency range from 12 to 30 Hz. It is generally regarded as a normal rhythm and is the dominant rhythm during extra activation of the central nervous system. It is associated with arousal, problem solving, attention and concentration, and information processing.
- **Gamma** is the frequency range from approximately 30 to 100 Hz. Gamma rhythms are thought to represent binding of different populations of neurons together into a network for the purpose of carrying out a certain cognitive or motor function. Gamma rhythms may be involved in higher mental activity, including perception, problem solving, fear, and consciousness.

Phase unlocked changes consist on Event-Related Desynchronization (ERD) or Event-Related Synchronization (ERS) effects (Pfurtscheller and Lopes da Silva, 1999), decreases

or increases of power in given frequency bands that reflect decreases or increases of synchrony of the underlying neuronal populations. The reported results showing the feasibility of voluntary modulating different EEG rhythms by executing motor imagery and cognitive tasks (Babiloni et al., 2000; Curran et al., 2004; Penny et al., 1998; Pfurtscheller and Neuper, 2001) have shown its potential use as mental commands for BCI applications.

1.2.2 Event Related Potentials (ERP)

As introduced before, event related potentials are phase locked changes that refers to brain electrical activity triggered by an event. There are two main types of them, namely exogenous (also known as evoked potentials) and endogenous. While exogenous ERP represent the processing of the physical stimulus and the propagation of activity in the sensory pathways, they have been mainly used for diagnostic purposes (Goff et al., 1978; Barber, 1988), endogenous are caused by "higher" cognitive processes that might involve memory, expectation, attention, or changes in the mental state, among others (Hillyard and Woods, 1979; Callaway et al., 1978; Karrer et al., 1984; Picton and Hillyard, 1988). The use of ERP in BCI technology is based on their detection in order to keep track of the event that elicited them, which is associated to a command. The most utilized ERP so far have been visual evoked potentials (VEP), P300, and slow cortical potentials (SCP).

Visual Evoked Potentials (VEP)

VEP are exogenous evoked potentials caused by sensory stimulation of a subject's visual field. Commonly used visual stimuli are flashing lights, or checkerboards on a video screen that flicker between black on white to white on black (invert contrast). When the repetition rate of the visual stimulus is faster than 6 Hz, the new stimulus is presented before the last response of the visual system vanishes, then a periodic response called steady state VEP (SSVEP) is generated. SSVEP is composed of a series of components whose frequencies are exact integer multiples of the stimulus frequency. Since exogenous ERP present modality-specific scalp topography, VEP are localized in occipital locations.

P300

P300 (Sutton et al., 1965) are endogenous ERP which temporal shape is a positive deflection approximately 300 ms after the event presentation. The P300 appears following unexpected sensory stimuli or stimuli that provide useful information to the subjects according to the task in execution. The P300 only peaks in the vicinity of 300 ms for very simple decisions. More generally, its latency appears to reflect the amount of time necessary to come to a decision about the stimulus. The harder the decision, the longer it takes for the P300 to appear.

Slow Cortical Potentials

Slow cortical potentials (SCP) are endogenous potentials in the latency range from 0.5 up to 10 seconds. They are typically seen as a slow negativation associated with cortical activation, either preceding voluntary movements, in that case called *Bereitschaftspotentials* (PB) or readiness potentials (Kornhuber and Deeck, 1964), or preceding an expected imperative external event, in that case called *Contingent Negative Variation* (CNV) (Walter et al., 1964). Contrarily, positive shifts indicate cortical relaxation (Birbaumer et al., 1999). Early studies described the feasibility of learning SCP control (Elbert et al., 1980) showing its potential use as mental commands.

1.3 Non-Invasive EEG-based BCIs

The first designed BCI prototype was non-invasive EEG-based. The original idea comes from the 70's when Vidal (Vidal, 1973; Vidal 1977) developed a VEP-based BCI whose tenet was the recognition of VEP over the visual cortex to recognize the direction of the user's visual fixation point and translate it into a command. The main drawback of this kind of systems is that strictly speaking they are not BCI's because the users need of peripheral nerves or muscular control to shift the gaze (Sutter, 1992; Middendorf et al., 2000; Gao et al., 2003). In recent years, the number of EEG-based BCI systems has grown and they utilize different EEG features than VEP that do not need the use of peripheral nerves. These new systems enable navigation in virtual environments (Bayliss, 2003), controlling prosthetic devices (Pfurtscheller et al., 2000), driving mobile devices such as robots (Millán et al., 2004) or wheelchairs (Galán et al., 2008a), and writing using virtual keyboards (Birbaumer et al., 1999; Millán, 2003; Oberbaimer et al., 2003; Wolpaw et al., 2003).

As introduced in section 1.2, the EEG features utilized as control commands are mainly extracted from the changes on the ongoing EEG produced by external or internal events. Present-day non-invasive EEG-based BCIs can be classified into 2 groups according to the kind of events utilized. The first group, utilizing external events, work under a synchronous or system-paced control paradigm where the device-user interaction is time-locked to a external cue (the event) periodically provided by the system. The BCI systems included in this group are P300, SCP based. The second group, utilizing internal events, enables working under an asynchronous or self-paced control paradigm where the device-user interaction is self-initiated by the user becoming spontaneous and natural. The BCI systems included in this group are based on modulation of oscillatory rhythms.

P300-based BCI developed by Donchin and cols. (Farwell and Donchin, 1988; Donchin et al., 2000) have the advantage that they require no prior training because P300 is a stereotyped response to a desired choice. Nevertheless, the amplitude of P300 diminishes over time so that the performances of the BCI could decrease. While the user faces a (6×6) , its rows or columns flash alternatively every 125 ms in random order. The user then selects

a symbol by counting how many times the row or column containing the desired selection flashes. Thus, the user should pay attention to flash events of the desired symbol. In users with visual impairments, auditory or tactile modalities can be used (Glover et al., 1986).

SCP-based BCI is referred as "Thought Translation Device" (TTD) (Birbaumer et al., 1999). Its main disadvantage is the long training period required to learn how to increase or decrease the SCP. During the first 2 seconds before the presentation of a first external cue, the system measures the user baseline state, then an active period of another 2 seconds where the user tries to increase or decrease the SCP (to produce positive or negative shifts) by selecting one of the two targets follows. The end of the active period acts as the expected imperative external event.

The first oscillatory rhythms-based BCIs (Wolpaw et al., 2003, Pfurtscheller and Neuper, 2001, Kostov and Polak, 2000, Penny and Roberts, 2000) were developed implementing synchronous modes of interaction. In such BCIs, the user induces ERD/ERS effects by motor imagery or different cognitive tasks, such as arithmetic operations, when a external cue is provided by the system. However, the modulation of oscillatory rhythms can be self-paced by the user following his/her intent at any time without needing any external cue. This fact has lead to the appearance of a second generation of oscillatory rhythms-based BCIs implementing asynchronous modes of interaction (Birch et al., 2002; Blankertz et al., 2006a; Millán et al., 2002; Millán et al., 2004; Scherer et al., 2004).

1.4 The IDIAP BCI

This section introduces the contents of the publication included in Appendix A (Millán et al., 2008) that reviews IDIAP BCI research.

The IDIAP BCI relies on four principles. The first one is an asynchronous protocol where subjects decide voluntarily when to switch between mental tasks and perform those mental tasks at their own pace. The second principle is mutual learning, where the user and the BCI are coupled together and adapt to each other. In other words, IDIAP BCI uses machine learning approaches to discover the individual EEG patterns characterizing the mental tasks executed by the user while users learn to modulate their brainwaves so as to improve the recognition of the EEG patterns. The third principle is the combination of the user's intelligence with the design of intelligent devices that facilitate interaction and reduce the user's cognitive workload. This is particularly useful for mental control of mobile devices such as robots and wheelchairs. Finally, the fourth principle is the recognition of high-level cognitive states related to the user's awareness of erroneous responses. Thus, user's commands are executed only if no error is detected, what enables the BCI to interact with the user in a much more meaningful way. In the next subsections the four principles are described.

1.4.1 Spontaneous Asynchronous Operation

As described before, EEG-based BCIs can be classified as synchronous or asynchronous. The necessity of external stimulation in case of synchronous systems restrict their applicability to a limited range of tasks. A more natural and suitable alternative for interaction is to analyze components associated with spontaneous "intentional" mental activity. This is particularly the case when controlling robotics devices. Synchronous BCIs are limited by a low channel capacity, below 0.5 bits/s (Wolpaw et al., 2002). The main reason is that the external cues are repeated every 4-10 s and the response of the BCI is the overall decision over this period (Birbaumer et al., 1999; Pfurtscheller et al., 2001; Wolpaw et al., 2004). Such synchronous protocols facilitate EEG analysis since the starting time of mental states are precisely known and differences with respect to background EEG activity can be amplified. Unfortunately, they are slow and BCI systems that use them normally recognize only 2 mental states. On the contrary, IDIAP BCI utilizes more flexible asynchronous protocols where the subject makes self-paced decisions on when to stop doing a mental task and start immediately the next one (Birch et al., 2002; Millán et al., 2004). In such asynchronous protocols the subject can voluntarily change the mental task being executed at any moment without waiting for external cues. The time of response of an asynchronous BCI can be below 1 second. For instance, in IDIAP approach the system responds every 1/2 second. The rapid responses of IDIAP asynchronous BCI, together with its performance, give a theoretical channel capacity between 1 and 1.5 bits/s.

1.4.2 The Machine Learning Way to BCI

Except for P300-based BCIs, a critical issue for the development of a EEG-based BCI is training—i.e., how users learn to operate the BCI. Some groups have demonstrated that some subjects can learn to control their brain activity through appropriate, but lengthy, training in order to generate fixed EEG patterns that the BCI transforms into external actions (Birbaumer et al., 1999; Wolpaw et al., 2004). In this case the subject is trained over several months to modify the amplitude of their EEG signals. IDIAP BCI follows a mutual learning process to facilitate and accelerate the user's training period. Indeed, IDIAP approach allows subjects to achieve good performances in just a few hours of training in the presence of feedback (Millán et al., 2004; Galán et al., 2008a). Most EEG-based BCI systems deal with the recognition of just 2 mental tasks (Babiloni et al., 2000; Pfurtscheller et al., 2001; Blankertz et al., 2006a; Birch et al., 2002). IDIAP approach achieves error rates below 30% for 3 mental tasks. This is mainly because the use of machine learning techniques at two levels, namely feature extraction and training the classifier embedded into the BCI. The approach aims at discovering subject-specific spatio-frequency patterns embedded in the continuous EEG signal—i.e., EEG rhythms over local cortical areas that differentiate the mental tasks. At the first level, those features that are more relevant for discriminating among the mental tasks are selected. The selected features are those that satisfy two cri-

teria: maximization of the separability of the mental tasks and stability over time. Indeed, EEG signals are non-stationary and, so, change over time. Feature extraction is based on canonical variates analysis (Galán et al., 2007a). IDIAP BCI uses a statistical Gaussian classifier (see Millán et al. (2004) for more details). The output of this statistical classifier is an estimation of the posterior class probability distribution for a sample; i.e., the probability that a given single trial belongs to each mental task (or class). See Appendix E for more details.

1.4.3 Blending of Intelligences

BCI systems are being used to operate a number of brain-actuated applications that augment people's communication capabilities, provide new forms of entertainment, and also enable the operation of physical devices. Until recently, EEG-based BCIs have been considered too slow for controlling rapid and complex sequences of movements. But IDIAP BCI has shown that asynchronous analysis of EEG signals is sufficient for humans to continuously control a mobile robot along non-trivial trajectories requiring fast and frequent switches between mental tasks (Millán et al., 2004). Two human subjects learned to mentally drive the robot between rooms in a house-like environment visiting 3 or 4 rooms in the desired order. A key element of this brain-actuated robot is shared control between two intelligent agents, the human user and the robot, so that the user only gives high-level mental commands that the robot performs autonomously. In particular, the user's mental states are associated with high-level commands and that the robot executes these commands autonomously using the readings of its on-board sensors. Another critical feature is that a subject can issue high-level commands at any moment. This is possible because the operation of the BCI is asynchronous and, unlike synchronous approaches, does not require waiting for external cues. The robot relies on a behavior-based controller to implement the high-level commands to guarantee obstacle avoidance and smooth turns. In this kind of controller, on-board sensors are read constantly and determine the next action to take. As explained in next section, we have recently extended this work to the mental control of both a simulated and a real wheelchair.

1.4.4 Recognition of High-Level Cognitive States

EEG-based brain-computer interfaces provide disabled people with new tools for control and communication. However, as any other interaction modality based on physiological signals and body channels (e.g., muscular activity, speech and gestures), BCIs are prone to errors in the recognition of subject's intent, and those errors can be frequent. Indeed, even well-trained subjects rarely reach 100% of success. In contrast to other interaction modalities, a unique feature of the "brain channel" is that it conveys both information from which it is possible to derive mental control commands to operate a brain-actuated device as well as information about cognitive states that are crucial for a purposeful interaction, all this on



Figure 1.3: Subject driving the brain-actuated wheelchair through EEG.

the millisecond range. One of these states is the awareness of erroneous responses, which a number of groups have recently started to explore as a way to improve the performance of BCIs (Schalk et al., 2000; Blankertz et al., 2003). Ferrez and Millán's work (Ferrez and Millán, 2005; Ferrez and Millán, 2007a; Ferrez and Millán, 2007b) have reported the presence of a new kind of error related potentials (ErrP) elicited by the erroneous responses of the BCI during the recognition of the user's intent. It has recently shown the feasibility of simultaneously classifying mental commands for BCI control and detecting ErrP to filter out erroneous commands in a real-time system, all this at the single-trial level (Ferrez, 2007).

1.5 MAIA Project

The goal of the EU project called MAIA (Mental Augmentation through determination of Intended Action) was to develop non-invasive brain-computer interfaces that recognize the subject's voluntary imagination of motor actions and transmits this intention to a device that performs the necessary low-level steps to achieve complex tasks. This project was founded under the Information Society Technologies (IST) programme of the Sixth Framework Programme (FP6), it started in September 2004 and ended in December 2007. The partners were the IDIAP Research Institute (coordinator, Switzerland), the Katholieke Universiteit Leuven (Belgium), The University Hospital of Geneva (Switzerland), the Fondazione Santa Lucia in Rome (Italy) and the Helsinki University of Technology (Finland). The main innovative principles were the use of estimates of intracranial activity from scalp EEG for the recognition of the subject's motor intent, the adaptive shared autonomy between the human and the robot, the use of vibrotactile feedback to speed up training of the

subject, the integration of high-level cognitive states such as errors to increase the reliability of the interface and the online adaptation of the interface to the subject to constantly track the changes of brain activity. The main achievement of the MAIA project were the two demonstrations in 2006 and 2007 of the first brain-actuated wheelchair (shown in Fig. 1.3) controlled by a subject sitting on it in the laboratories of the Katholieke Universiteit Leuven (see supplementary .WMV files included in Appendix I). In this case, we incorporated shared control principles into the BCI (Philips et al., 2007; Vanacker et al., 2007). In shared control, the intelligent controller relieves the human from low level tasks without sacrificing the cognitive superiority and adaptability of human beings that are capable of acting in unforeseen situations.

1.6 Aim of the Thesis

This thesis is aimed at developing methods for asynchronous and non-invasive EEG-based brain computer interfaces to enhance the robustness of brain-actuated devices. Within MAIA project framework, these methods have been developed to enhance the robustness of the brain-actuated wheelchair.

The MAIA brain-actuated wheelchair is integrated by two entities, the intelligent wheelchair and the BCI system. Environmental information from the wheelchair's sensors feeds a contextual filter that builds a probability distribution $P_{Env}(C)$ over the possible user's mental steering commands, $C = \{Left, Right, Forward\}$. The BCI system estimates the probabilities $P_{EEG}(C)$ of the different mental commands from the EEG data. Both streams of information are combined to produce a filtered estimate of the user's intent $P(C) = P_{EEG}(C) \cdot P_{Env}(C)$. The shared control system also uses the environmental information from the wheelchair's sensors to map these high-level commands into appropriate motor commands, translational and rotational velocities, in order to generate a smoother driving behavior. This is done by an intelligent controller that activates an appropriate assisting behavior when the user needs help. Thus, the system constantly adapt the level of assistance to a specific situation. It will help significantly when the subject's performance (BCI accuracy) is low whereas it will decrease its role when the BCI accuracy is higher. Fig. 1.4 depicts a schematic representation of the shared control architecture of the brain-actuated wheelchair. See Appendices G and H (Philips et al., 2007; Vanacker et al., 2007) for a detailed description.

Three are the main contributions of this thesis. First, the use of mental tasks transitions detection (MTTD) as inferred a priori information to guide postprocessing algorithms which goal is to denoise the decision making of the brain-computer interface system. Second, the use of a new feature extractor method for multi-class brain-computer interfaces with canonical solution that provides a reduced number of canonical discriminant spatial patterns and rank the channels sorted by power discriminability between classes. Third, the introduction of frames approach recognizing intermittent induced electroencephalo-

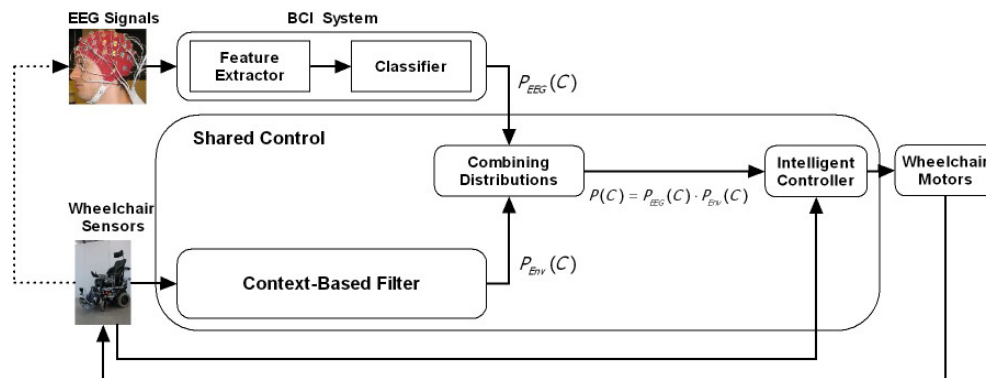


Figure 1.4: Architecture of the brain-actuated wheelchair.

graphic spatial patterns of amplitude modulation to guide a novel decision making process. While the first two consist in adding or substituting modules on the current architecture of the brain-actuated wheelchair in agreement with current asynchronous BCI approaches (Blankertz et al., 2006a; Birch et al., 2002; Millán et al., 2004), the third one implies a radical departure from current approaches and would imply to change the BCI decision making process. Fig. 1.5 depicts where the aforementioned contributions are integrated on the architecture of the brain-actuated wheelchair.

The IDIAP BCI research and the three contributions of this thesis have been described in the following publications:

1. J.del R. Millán, P. W. Ferrez, F. Galán, E. Lew, and R. Chavarriaga. Non-Invasive Brain-Machine Interaction. *International Journal of Pattern Recognition and Artificial Intelligence*, 2008. To appear.
2. F. Galán, F. Oliva, and J. Guàrdia. Using Mental Tasks Transitions Detection to Improve Spontaneous Mental Activity Classification. *Medical and Biological Engineering and Computing*, 45: 603-609, 2007b.
3. F. Galán, F. Oliva, J. Guàrdia, P.W. Ferrez, and J. del R. Millán. Detecting Intentional Mental Transitions in an Asynchronous Brain-Computer Interface. *Medical and Biological Engineering and Computing*, 2008b. Submitted.
4. F. Galán, P. W. Ferrez, F. Oliva, K. Guàrdia, and J. del R. Millán. Feature Extraction for Multi-class BCI using Canonical Variates Analysis. In *Proceedings of the 2007 IEEE International Symposium on Intelligent Signal Processing, WISP 2007*, Alcalá de Henares, Spain, 2007a.
5. F. Galán, J. Palix, R. Chavarriaga, P.W. Ferrez, C.A. Hauert, and J. del. R. Millán. Visuo-spatial Attention Frame Recognition for Brain-computer Interfaces. In: Wang,

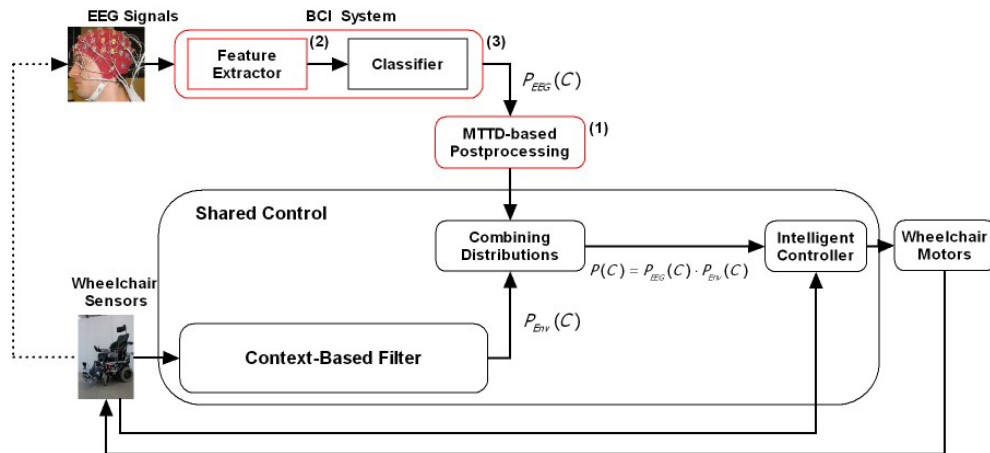


Figure 1.5: Architecture of the modified brain-actuated wheelchair after including the three contributions of this thesis (highlighted by red squares). (1) MTTD-based postprocessing module would represent a new module between the BCI system and combining distributions. (2) The proposed feature extractor method it is placed in the feature extractor module. (3) The frames approach would imply change the complete BCI system decision making process.

R., Gu, F., and Shen, F. (Eds.) *Advances in Cognitive Neurodynamics ICCN 2007. Proceedings of the International Conference on Cognitive Neurodynamics. ICCN 2007 Proceedings*. Springer, Shanghai, China, 2007c. To appear.

6. F. Galán, M. Nuttin, E. Lew, P. W. Ferrez, G. Vanacker, J. Phillips, H. Van Brussel, and J. del R. Millán. A Brain-Actuated Wheelchair: Asynchronous and Non-Invasive Brain-Computer Interfaces for Continuous Control of Robots, *Clin. Neurophysiol.*, 2008a. To appear.

Publication 1 reviews IDIAP BCI research. Publications 2 and 3 include two versions of the MTTD algorithm, publication 4 describes the use of CVA for Multi-class BCI feature extraction, publication 5 proposes the neural frames approach, and finally publication 6 describes the current version of the simulated brain-actuated wheelchair. This version and the real wheelchair incorporated the feature extractor described in publication 4.

The outline of this thesis is the following. Chapter 2 summarizes the contents of the references 2-6. The published and preprint accepted versions are collected in appendices A, B, C, D, E and F. Appendices G and H include the published versions of Phillips and Vanacker's works (Phillips et al, 2007; Vanacker et al., 2007) in order to provide a more complete description of the shared control introduced in MAIA brain-actuated wheelchair. Appendix I includes three .WMV files with demonstrations of the simulated and real brain-actuated wheelchairs, and finally appendix J includes a Catalan version of the summary.

Chapter 2

Summary of Contents

This chapter introduces the contents of the five publications collected in appendices B, C, D, E and F that describe the three contributions of this thesis.

2.1 Using Mental Tasks Transitions Detection to Improve Spontaneous Mental Activity Classification

2.1.1 Introduction

This section describes the algorithm that won the BCI Competition III -Data Set V: Multiclass Problem, Continuous EEG- (Blankertz, et al., 2006b). The algorithm is based on canonical variates transformation (CVT) and distance based discriminant analysis (DBDA) combined with a mental tasks transitions detector (MTTD) to classify spontaneous mental activity in order to operate a brain-computer interface working under an asynchronous protocol. The algorithm achieved an averaged classification accuracy over three subjects of 68.65% (79.60%, 70.31% and 56.02% respectively) in a 3-class problem.

2.1.2 Methods

Data Acquisition, Task and Preprocessing

Data were acquired by IDIAP Research Institute as described by Millán (2004) and Blankertz et al. (2006b). Data were recorded from three healthy subjects meanwhile they were executing three different mental tasks: imagination of self-paced left hand movements, imagination of self-paced right hand movements, and generation of words beginning with the same random letter. Each subject participated in four sessions acquired in the same day. The duration of each session was 4 min, with a intersession break of 5-10 min. In each session, each subject performed a given task for 15 s, switching randomly to another task at the operator request. Thus, the EEG data were not split into trials since the subjects were always performing one of the mental tasks. Subjects did not received any feedback.

EEG potentials were recorded at 32 electrodes placed at standard positions of the International 10-20 system. The sampling rate was 512 Hz.

Data were provided in two ways: the raw EEG potentials and precomputed features (data used by the algorithm introduced here). The precomputed features were obtained spatially filtering by means of a surface Laplacian computed globally by spherical spline of order 2. Then, every 65 ms (16 times per second) was estimated the power spectral density (PSD) in the band 8-30 Hz over the last second of data with a resolution of 2 Hz for eight channels (C3, Cz, C4, CP1, CP2, P3, Pz, and P4). Thus, an EEG sample is a 96-dimensional vector (eight channels times 12 frequency components).

The algorithm should provide an output every 0.5 s using the last second of data. That is, the goal for the competition was to estimate the class labels for every input vector of the fourth session of each subject. Since input vectors were computed 16 times per second, the labels needed to be estimated providing the average of eight consecutive samples (to get a response every 0.5 s).

The performance measure was the classification accuracy averaged over the three subjects.

Algorithm Description

Preprocessing and Feature Extraction First of all, data is transformed by means of normalizing each PSD sample estimation. Each spectral component h of channel i from sample recorded at time t $PSD_{h_t}(i)$ is normalized by dividing it by the energy of the channel

$$\widetilde{PSD}_{h_t}(i) = \frac{PSD_{h_t}(i)}{\sum_{h=1}^{12} PSD_{h_t}(i)} \quad (2.1)$$

Therefore, the transformed sample at time t $\widetilde{\mathbf{PSD}}_t$ is a 96-dimensional concatenated vector (8 channels times 12 normalized frequency components) as the original data \mathbf{PSD}_t . After normalization, the feature extraction process is guided by CMT. This transformation permits the projection of a p -dimensional data set, constituted by n_l samples from $l = 1, \dots, c$ different classes, in a $(c-1)$ -dimensional feature space defined by the canonical discriminant functions that maximize the separation between the class centroids and minimize the intra-class variance (see Krzanowski (1988) for a detailed description). This is achieved by finding the eigenvectors \mathbf{A} of $\mathbf{W}^{-1}\mathbf{B}$ with eigenvalues larger than zero, where

$$\mathbf{B} = \sum_{l=1}^c n_l (\mathbf{m}_l - \mathbf{m})(\mathbf{m}_l - \mathbf{m})' \quad (2.2)$$

and

$$\mathbf{W} = \sum_{l=1}^c \sum_{j=1}^{n_l} (\widetilde{\mathbf{PSD}}_{l_j} - \mathbf{m}_l)(\widetilde{\mathbf{PSD}}_{l_j} - \mathbf{m}_l)' \quad (2.3)$$

are dispersion matrices between and within classes respectively, and

$$\mathbf{m}_l = \frac{1}{n_l} \sum_{j=1}^{n_l} \widetilde{\mathbf{PSD}}_{lj} \quad (2.4)$$

and

$$\mathbf{m} = \frac{1}{n} \sum_{l=1}^c n_l \mathbf{m}_l \quad (2.5)$$

are the class and total centroids respectively. Note that $n = \sum_{l=1}^c n_l$. The new feature space \mathbf{Y} is defined by the projection of $\widetilde{\mathbf{PSD}}$ samples induced by \mathbf{A} :

$$\mathbf{Y} = \widetilde{\mathbf{PSD}} \mathbf{A} \quad (2.6)$$

Discriminant Analysis After normalization and CVT, the algorithm discriminates between mental tasks using DBDA (Cuadras et al., 1997) with Euclidean distance. With this approach the Mahalanobis distance is implicitly used, as well as allowing a reduced spatial representation. The special interest applying DBDA is the possibility of using any distance function between individuals. Among them we have tested absolute value, chord and Hellinger distances achieving similar overall performances, although further studies should be explored. To obtain a reduced spatial representation DB canonical variate analysis could be used (in fact CVT is the particular case when the distance between individuals is the Mahalanobis distance).

Given c subpopulations or classes C_1, \dots, C_c and a defined distance function d_l for class C_l , the proximity measurement for pattern $\widetilde{\mathbf{PSD}}_t$ with vector $\mathbf{y}_t = \widetilde{\mathbf{PSD}}_t \mathbf{A}$, is defined as

$$\phi_l(\mathbf{y}_t) = V_l(\mathbf{y}_{C_l} | \mathbf{y}_t) - V_l(\mathbf{y}_{C_l}) \quad (2.7)$$

where

$$V_l(\mathbf{y}_{C_l}) = \frac{1}{2} E_{C_l C_l} [d_l^2(\mathbf{y}_{C_l}, \mathbf{y}_{C_l})] \quad (2.8)$$

and

$$V_l(\mathbf{y}_{C_l} | \mathbf{y}_t) = E_{C_l} [d_l^2(\mathbf{y}_t, \mathbf{y}_{C_l})] \quad (2.9)$$

are the geometric variability and the relative geometric variability to pattern \mathbf{y}_t . Note that \mathbf{y}_{C_l} refers to those patterns belonging to class C_l . Thus, the DBDA assigns $\widetilde{\mathbf{PSD}}_t$ to C_l , if

$$\phi_l(\mathbf{y}_t) = \min_{s=1, \dots, c} [\phi_s(\mathbf{y}_t)] \quad (2.10)$$

In practice, suitable estimates of geometric variability and relative geometric variability to pattern \mathbf{y}_t are

$$\hat{V}_l(\mathbf{y}) = \frac{1}{2n_l^2} \sum_{j,j'=1}^{n_l} d^2(\mathbf{y}_{lj}, \mathbf{y}_{lj'}) \quad (2.11)$$

$$\hat{V}_l(\mathbf{y}|\mathbf{y}_t) = \frac{1}{n_l} \sum_{j=1}^{n_l} d^2(\mathbf{y}_t, \mathbf{y}_{lj}), \quad (2.12)$$

where \mathbf{y}_{lj} is the sample j of class l . Therefore, the estimate of the proximity function is

$$\hat{\phi}_l(\mathbf{y}_t) = \frac{1}{n_l} \sum_{j=1}^{n_l} d^2(\mathbf{y}_t, \mathbf{y}_{lj}) - \frac{1}{2n_l^2} \sum_{j,j'=1}^{n_l} d^2(\mathbf{y}_{lj}, \mathbf{y}_{lj'}). \quad (2.13)$$

Following the competition requirements, we have taken into account eight consecutive samples. Thus, the final decision obtained every 62.5 milliseconds is based on the last 0.5 seconds. The projected sample incoming from a testing set is assigned to class C_l in time t if

$$\bar{\phi}_l(\mathbf{y}_t) = \min_{s=1, \dots, c} [\bar{\phi}_s(\mathbf{y}_t)] \quad (2.14)$$

where

$$\bar{\phi}_l(\mathbf{y}_t) = \frac{1}{N_{av}} \sum_{i=1}^{N_{av}} \hat{\phi}_l(\mathbf{y}_{t-i+1}) \quad (2.15)$$

is an average proximity over $N_{av} = 8$ consecutive samples.

Mental Tasks Transitions Detector (MTTD) With the aim to improve classification accuracy, we have designed a parallel discriminant process guided by a MTTD. For each new incoming sample, after normalization and canonical variates projection, the algorithm works as follows:

1. Compute an index to detect transitions. It is easy to detect a mental task transition at time t with the index

$$I(\widetilde{\mathbf{PSD}}_t) = |\Psi(\widetilde{\mathbf{PSD}}_{t-1}, \widetilde{\mathbf{PSD}}_t) - \Psi(\widetilde{\mathbf{PSD}}_{t-2}, \widetilde{\mathbf{PSD}}_{t-1})| \quad (2.16)$$

if $\min[I(\widetilde{\mathbf{PSD}}_{t-1}), I(\widetilde{\mathbf{PSD}}_t)] > \theta$, where θ is a fixed threshold and $\Psi(\cdot)$ is a dissimilarity function. In this work we use the Euclidean distance. It is worth noting that the detection of a mental task transition needs only four $\widetilde{\mathbf{PSD}}$ patterns, and does not introduce any delay given that detects a sudden change at time t .

2. Classify the sample with DBDA.

Table 2.1: Classification accuracy over the three subjects according to different test conditions

Subject	MTTD	Test Condition				Competition Test
		1 → 2	1 → 3	2 → 3	1 + 2 → 3	1 + 2 + 3 → 4
1	No	67.4%	69.73%	72.87%	74.86%	75.14%
	Yes	72.84%	72.09%	75.64%	76.46%	79.60%
2	No	51.94%	59.99%	58.64%	62.41%	62.18%
	Yes	59.58%	68.03%	64.86%	68.72%	70.31%
3	No	52.31%	42.97%	38.69%	42.73%	50.83%
	Yes	61.68%	46.45%	39.10%	43.49%	56.02%
Average	No	57.33%	57.56%	56.73%	60.00%	62.72%
	Yes	64.70%	62.19%	59.87%	62.89%	68.65%

For each subject and average, the first row refers to the performance of the algorithm without including MTTD, and the second one to the complete algorithm.

3. If $\min[I(\widetilde{\mathbf{PSD}}_{t-1}), I(\widetilde{\mathbf{PSD}}_t)] > \theta$, compute class proportions $p(C_i)$ assigned by DBDA in the gap limited by two last transitions or by first sample and first transition. Otherwise, do nothing.
4. If $\max_h[p(C_h)] > \xi$, where ξ is a fixed threshold, until next transition remove from training data those samples labeled as C_h and reclassify the new sample once again with DBDA into resting classes. Otherwise, do nothing (maintain classification from step 2).

Note that mental tasks transitions detection yields to use transitions to discard the class that can be assumed as predominant (with a proportion bigger than ξ) in the gap limited by the two last transitions, improving chance classification in next incoming samples from 0.33 to 0.50.

2.1.3 Results and Conclusions

The algorithm was first tested with *sessions 2 and 3*. In order to do this, when the algorithm was tested with the second session, it had been trained with the first session; and when it was tested with the third session, it had been trained with the first two sessions, both individually and jointly. The transition detector threshold was fixed at $\theta = 0.2$, and the probability threshold, at $\xi = 0.55$.

Table 2.1 shows the algorithm performance over the three subjects, according to the test conditions mentioned above. For each subject, the first row refers to the performance of the algorithm without including MTTD while the second one refers to the complete

algorithm. These results showed two aspects worth highlighting that were considered in the competition testing with *session 4*. On the one hand, the inclusion of MTTD systematically improved the performance of the classification. On the other hand, when the algorithm was tested with the third session, the results indicated it was advisable to train it with the two first sessions jointly. This action produced the best performance over the two first subjects. Similar results to the best performance were obtained over the third subject, which was achieved when only the first session was used to train the algorithm. Thus, all patterns from the first three sessions jointly were taken as a training set for the competition, and the thresholds were fixed at $\theta = 0.2$ and $\xi = 0.55$. Likewise, Table 2.1 shows the competition results too: the algorithm without MTTD inclusion provides a mean classification accuracy of 62.72% (75.14%, 62.18% and 50.83% for each subject), whereas the complete algorithm improves this mean classification accuracy up to 68.65% (79.60%, 70.31% and 56.02%).

Despite the promising results showed by this algorithm, some drawbacks as the sampling rate MTTD dependency as well as the simplicity of the heuristic rule implemented on it call for future extensions of this approach to avoid undesired effects of artifacts detection. The showed results also call for further studies assessing the algorithm performance on BCI's working in different conditions where the subjects receive online feedback. Next section introduces a modified version of the algorithm that addresses these issues.

2.2 Detecting Intentional Mental Transitions in an Asynchronous BCI

2.2.1 Introduction

As showed in section 2.1 (see also Appendix B; Galan et al., 2007b) the inclusion of MTTD has been proven as a useful tool in guiding the transduction process of a BCI working under an asynchronous protocol. MTTD allows for the extraction of the signal's contextual information in order to infer the user's intentionality at a given moment and thus correcting possible classification errors. Despite the good results shown, the algorithm previously proposed is sampling rate depending, introduces a simple heuristic rule and does not show good behavior in contexts where the user gets online feedback. The algorithm proposed in this section, like its antecessor, is based on canonical variates transformation (CVT) and on distance-based discriminant analysis (DBDA), but it has a new transitions detector based on Kalman filtering that solves the sampling rate dependency. In addition, it includes a classifier supervisor based on heuristics rules that exploit transition detection as well as inconsistencies between subject's mental intention and the associated EEG. These heuristic rules lead to significant improvements of the BCI in terms of both classification accuracy and channel capacity, adapting itself to the user's needs. The algorithm has been also tested with data recorded during experimental sessions where two subjects were receiving continuous visual feedback from virtual and real brain-actuated robots.

2.2.2 Methods

Data Acquisition, Task and Preprocessing

For the offline assessment of the algorithm two data sets have been used. The first one, the BCI Competition III -Data Set V: Multiclass Problem, Continuous EEG- (Blankertz, et al., 2006b), where subjects did not receive any feedback indicating their performance. The second one comes from feedback experiments. In both data sets, EEG signals were recorded with a portable Biosemi acquisition system from 32 (first data set) or 64 (second data set) electrodes. The sampling frequency was 512 Hz. The signal was spatially filtered using a surface Laplacian (first data set) or common average reference (CAR) (second data set) previous to the estimation every 62.5 ms. (16 times per second) of the PSD in the band 8-30-Hz, with a resolution of 2Hz over the last 1-second windows. In the first data set the PSD was estimated on the electrodes C3, Cz, C4, CP1, CP2, P3, Pz, P4; thus obtaining a 96-dimensional vector (8 electrodes \times 12 frequency components) as a pattern. In the second data set the PSD was estimated on F3, F4, FC1, FC2, C3, C1, C2, C4, CP1 and CP2 obtaining a 120-dimensional vector (10 electrodes \times 12 frequency components). The computation of the EEG patterns, the vector **PSD**, is described in Millán (2004) and Blankertz et al. (2006b).

Data come from 5 healthy voluntary subjects. Subjects 1, 2 and 3 from the first data set carried out three mental tasks, two motor imagination tasks (right-left hand movement imagination) and one cognitive task (search of words with the same initial letter) for 15 seconds switching randomly between them at the operator's request. EEG signals were recorded during 4 non-feedback sessions. Subjects 4 and 5 executed the same mental tasks also during 4 sessions while receiving continuous visual feedback from the movement of a virtual robot in the case of subject 4, or from a real mobile robot in the case of subject 5. The robots were controlled by the association between the subject's mental states and high-level commands (right-left hand imagination with right-left turns, and word search with forward movements). In addition, the brain-actuated robots relied on a behavior-based controller that guarantee obstacle avoidance and smoothed turns (Millán et al., 2004). These two subjects were at the very beginning of their training with the robots.

For every subject, the first three sessions were used as training and validation sets while the fourth session was the test set.

Algorithm Description

The algorithm incorporates three components: an *inconsistencies detector* between the user's intent and the measured EEG patterns that assigns a provisional label to each incoming pattern, a *transitions detector* based on Kalman filtering that detects patterns not similar to their predecessors, and a *classifier supervisor* based on three heuristic rules that determine which of these patterns identified as transitions by the transitions detector are intentional transitions between different mental tasks. Fig. 2.1 depicts a schematic representation

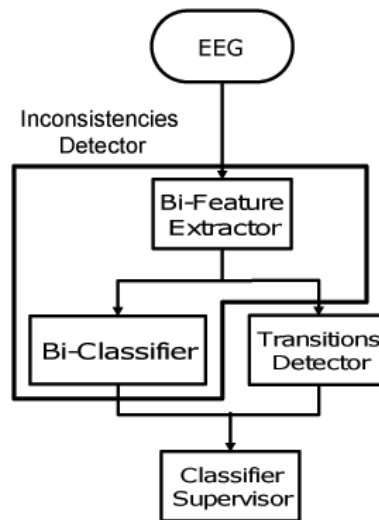


Figure 2.1: Schematic representation of the whole algorithm. Note that the inconsistencies detector (based on a bi-feature extractor and a bi-classifier) and the transitions detector work in parallel. The output of the two previous components is used by the classifier supervisor.

of the overall algorithm. The inconsistencies detector, based on a bi-feature extractor and a bi-classifier, works in parallel with the transition detector. Thus, each incoming pattern is first checked for inconsistency and transition. Next, based on three heuristic rules and only using the labels of the three last patterns identified as transitions, the classifier supervisor eventually changes the label of the pattern provided by the inconsistencies detector. Next, each component is described.

Inconsistencies Detector One of the main difficulties of classifying spontaneous brain activity is its variability over time. Physiological reasons, like endogenous brain processes and fatigue, cause slow changes of EEG over time. An approach to deal with this type of non-stationary behavior is to build adaptive classifiers that track this variability (Millán, 2004). In addition, rapid shifts in the user’s motivational and attentional states¹ may lead to a mismatch between the user’s intent and the user’s EEG patterns. The aim of the inconsistencies detector is to identify those patterns that likely are inconsistent with the user’s intent.

In order to identify inconsistent patterns two canonical spaces by means of a canonical variates transformation (CVT) are built, as in section 2.1.2 (see Appendix D; Galán et al., 2007a). The first one is based on the original labelling that corresponds to the user’s

¹For instance, erroneous responses of the BCI, especially if they are frequent as it is the case at the beginning of the user’s training, may disconcert and frustrate the user.

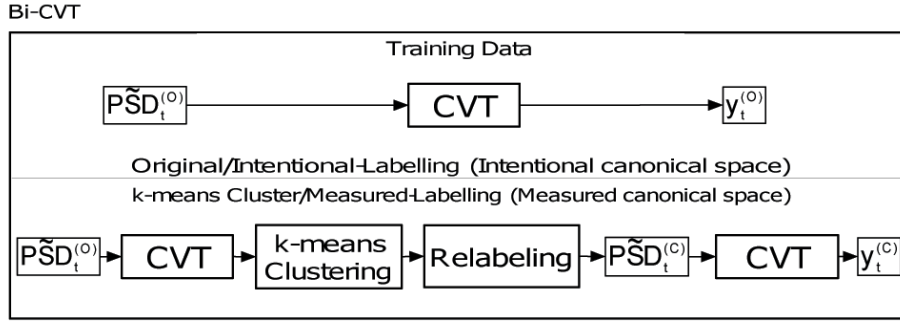


Figure 2.2: Bi-feature extractor based on CVT (Bi-CVT). From the training data we build two canonical spaces, the intentional canonical space using the original labelling (top), and the measured canonical space using the k-means cluster labelling (bottom). Patterns whose projections onto the canonical spaces do not match are potentially inconsistent and the Bi-DBDA labels them as *unknown*.

intent (*intentional* labelling)—i.e., it is obtained by a direct CVT on the training set. In the second case, after building the canonical space as in the first case, k-means cluster analysis (using Euclidean distance) generating as many clusters as mental tasks (3, in this case) is carry out. Then, the patterns in the training set are relabelled with the labels obtained from the clustering process (*measured* labelling) and a new canonical space is built. This Bi-CVT process yields two different canonical spaces, the intentional and the measured canonical spaces (see Fig. 2.2). Afterwards, the patterns of the test set are projected onto both canonical spaces and the resulting projections are sent to each DBDA classifier. The outputs of these two classifiers are combined to obtain a final decision, called Bi-DBDA, which labels a pattern as *unknown* if the outputs of the two previous DBDA classifiers are inconsistent—i.e, they are different.

The different steps of the inconsistencies detector are the following²:

1. *Normalization*: Each spectral component h of channel i from the pattern recorded at time t , $PSD_{h_t}(i)$, is normalized by the energy of the channel

$$\widetilde{PSD}_{h_t}(i) = \frac{PSD_{h_t}(i)}{\sum_{h=1}^n PSD_{h_t}(i)} \quad (2.17)$$

2. *Bi-CVT*: Eigenvectors $\mathbf{A}^{(O)}$ and $\mathbf{A}^{(C)}$ of $\mathbf{W}^{-1(O)}\mathbf{B}^{(O)}$ and $\mathbf{W}^{-1(C)}\mathbf{B}^{(C)}$ with eigenvalues greater than zero are found, where $\mathbf{B}^{(\cdot)}$ and $\mathbf{W}^{(\cdot)}$ are the between- and within-

²Note that the first step is the normalization of the frequency components of each electrode as described in section 2.1.2

classes dispersion matrices, obtained from the matrices $\widetilde{\mathbf{PSD}}^{(O)}$ and $\widetilde{\mathbf{PSD}}^{(C)}$ of patterns with the original labels (*intentional* labelling) or with the cluster-analysis labels (*measured* labelling), respectively. Then, projections

$$\mathbf{y}_t^{(O)} = \widetilde{\mathbf{PSD}}_t^{(O)} \mathbf{A}^{(O)} \quad (2.18)$$

$$\mathbf{y}_t^{(C)} = \widetilde{\mathbf{PSD}}_t^{(C)} \mathbf{A}^{(C)} \quad (2.19)$$

are computed

3. *Bi-DBDA*: The label ν_t of the incoming pattern at time t with projections $\mathbf{y}_t^{(O)}$ and $\mathbf{y}_t^{(C)}$ is

$$\nu_t = \begin{cases} g & \text{if } (\bar{\phi}_g(\mathbf{y}_t^{(O)}) = \min_k [\bar{\phi}_k(\mathbf{y}_t^{(O)})]) \cap (\bar{\phi}_g(\mathbf{y}_t^{(C)}) = \min_k [\bar{\phi}_k(\mathbf{y}_t^{(C)})]) \\ unknown & \text{otherwise} \end{cases} \quad (2.20)$$

where k is the number of classes and $\bar{\phi}_g(\mathbf{y}^{(\cdot)})$ is the average of DBDA proximity estimates, $\hat{\phi}_g(\mathbf{y}^{(\cdot)})$ (see section 2.1.2 and Appendices B and C; Galán et al., 2007b; Galán et al., 2008b), in the corresponding canonical space over $N_{av} = 4$ consecutive patterns

$$\bar{\phi}_g(\mathbf{y}_t^{(\cdot)}) = \frac{1}{N_{av}} \sum_{i=1}^{N_{av}} \hat{\phi}_g(\mathbf{y}_{t-i+1}^{(\cdot)}) \quad (2.21)$$

Thus, the final decision is obtained every 0.250 s. In this way, the new pattern is assigned to class C_g only if the two DBDA classifiers agree. See Fig. 2.3 for an example.

Transitions Detector Based on Kalman Filtering Kalman filtering is a principled approach to detect abrupt changes in temporal series (Baseville et al., 1993). Here it is used to build a more robust transitions detector independent of the sampling rate. While the inconsistencies detector filters patterns given the relative positions of its projections on both training canonical spaces, the transitions detector checks for patterns whose distances to their predecessors on the measured canonical space are larger than expected. Thus, the transitions detector filters those patterns that are likely intentional transitions between different mental tasks. Using the projected patterns ($\mathbf{y}_t^{(C)}$) in the canonical space obtained with labels computed by k-means cluster analysis (*measured* labelling), the following linear state dynamical system is built:

$$\begin{aligned} \mathbf{x}_t &= \mathbf{A}\mathbf{x}_{t-1} + \mathbf{w}_{t-1} \\ \mathbf{y}_{t-1}^{(C)} &= \mathbf{H}\mathbf{x}_{t-1} + \mathbf{v}_{t-1} \end{aligned} \quad (2.22)$$

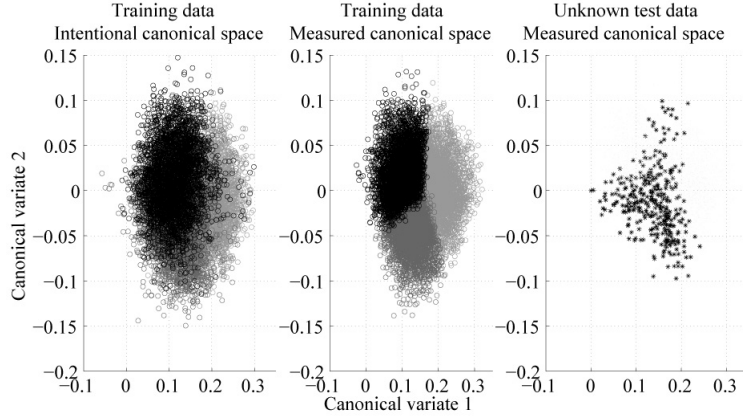


Figure 2.3: Bi-DBDA example, subject 1. *Left:* Training data projection with original labels on the intentional canonical space (black: imagination of left hand movement; dark grey: imagination of left hand movement, light grey: word search). *Middle:* Training data projection with cluster labels on the measured canonical space. *Right:* Test data labelled by Bi-DBDA as unknown projected on the measured canonical space. These inconsistent patterns are those projected onto the mismatch areas of the two canonical spaces.

where \mathbf{x}_t , \mathbf{A} and \mathbf{H} are the state vector, the state matrix and the measurement matrix, respectively. The state noise \mathbf{w}_{t-1} and the measurement noise \mathbf{v}_{t-1} are assumed to be uncorrelated zero-mean Gaussian white-noise processes with covariance matrices \mathbf{Q} and \mathbf{R} . The Kalman filter finds the optimal state estimate $\hat{\mathbf{x}}_t$ (minimizing the variance error estimator, defined as $E[\|\mathbf{x}_t - \hat{\mathbf{x}}_t\|^2]$) given a set of past observations $\{\mathbf{y}_1^{(C)}, \dots, \mathbf{y}_t^{(C)}\}$ in a prediction-correction approach:

1. **Prediction equations.** In this step, the prediction of the state of the system at time t $\hat{\mathbf{x}}_{t|t-1}$ and his variance $\mathbf{P}_{t|t-1}$ are computed from the estimates and $\mathbf{P}_{t-1|t-1}$ at time $t-1$ and the noise covariance \mathbf{Q} :

$$\hat{\mathbf{x}}_{t|t-1} = \mathbf{A}\hat{\mathbf{x}}_{t-1|t-1} \quad (2.23)$$

$$\mathbf{P}_{t|t-1} = \mathbf{A}\mathbf{P}_{t-1|t-1}\mathbf{A}^T + \mathbf{Q} \quad (2.24)$$

Initial matrices \mathbf{A} , \mathbf{H} , \mathbf{Q} and \mathbf{R} are estimated with EM algorithm (Digalakis et al., 1993) using the third session. As initial values estimates, $\hat{\mathbf{x}}_{t-1|t-1} = \mathbf{y}_{t-1}^{(C)}$ and $\mathbf{P}_{t-1|t-1} = \mathbf{R}$ are fixed.

2. **Correction equations.** The obtained estimates in the prediction step are corrected by the innovation process

$$\epsilon_t = \mathbf{y}_t^{(C)} - \mathbf{H}\hat{\mathbf{x}}_{t|t-1} \quad (2.25)$$

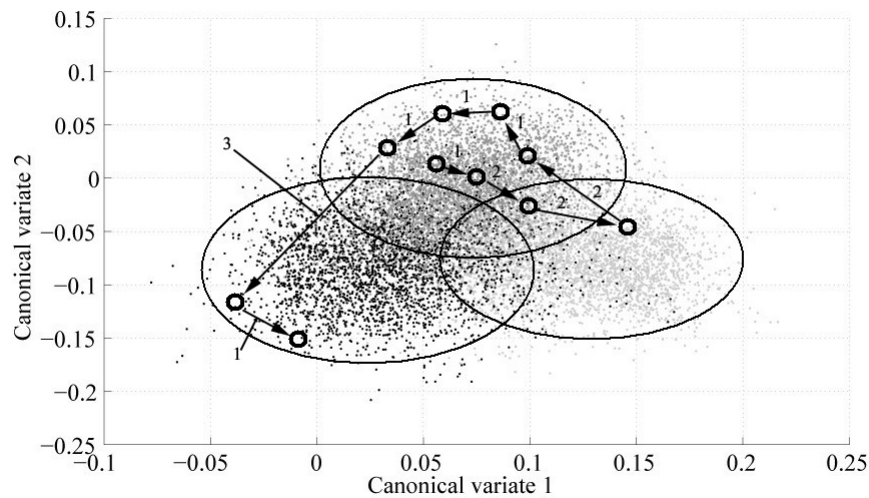


Figure 2.4: Examples of projected test patterns identified as transitions on the training measured canonical space (black: imagination of left hand movement; dark grey: imagination of right hand movement; light grey: word search). Dots show the projected training patterns. Big circles represent the location of the three mental tasks in the canonical space. Small circles indicate transitions; i.e., patterns exhibiting leaps in the measured canonical space with respect to their predecessors. In this example the user executes first imagination of right hand movement and then imagination of left hand movement. This example illustrates the three kinds of transitions: **1**, within-class; **2**, unintentional between-class; **3**, intentional between-class transition.

defined as the difference between the new measured value $\mathbf{y}_t^{(C)}$ and the hypothetical measured value given the estimate $\hat{\mathbf{x}}_{t|t-1}$ at time t . Then, the corrected estimates are

$$\hat{\mathbf{x}}_{t|t} = \hat{\mathbf{x}}_{t|t-1} + \mathbf{K}_t[\mathbf{y}_t^{(C)} - \mathbf{H}\hat{\mathbf{x}}_{t|t-1}] \quad (2.26)$$

$$\mathbf{P}_{t|t} = [\mathbf{I} - \mathbf{K}_t\mathbf{H}]\mathbf{P}_{t|t-1} \quad (2.27)$$

where the Kalman gain matrix is

$$\mathbf{K}_t = \mathbf{P}_{t|t-1}\mathbf{H}^T\mathbf{S}_t^{-1} \quad (2.28)$$

and the innovation covariance matrix is

$$\mathbf{S}_t = \mathbf{H}\mathbf{P}_{t|t-1}\mathbf{H}^T + \mathbf{R} \quad (2.29)$$

If the system works properly, the normalized innovation process $\tilde{\epsilon}_t = \mathbf{S}_t^{-1/2}\epsilon_t$ is a zero-mean Gaussian white-noise process with identity covariance matrix $E[\tilde{\epsilon}_t] = 0$, $E[\tilde{\epsilon}_t\tilde{\epsilon}_t^T] = \mathbf{I}$. Thus, any transition or variation in the model is reflected by a change in the aforementioned statistics.

In order to detect transitions, the sequence of innovation process sample covariance matrices is used (Hajiyev and Caliskan, 1999)

$$\mathbf{U}_t = \frac{1}{N_{av} - 1} \sum_{i=t-N_{av}+1}^t [\tilde{\epsilon}_i - \bar{\tilde{\epsilon}}_t][\tilde{\epsilon}_i - \bar{\tilde{\epsilon}}_t]^T \quad (2.30)$$

where

$$\bar{\tilde{\epsilon}}_t = \frac{1}{N_{av}} \sum_{i=t-N_{av}+1}^t \tilde{\epsilon}_i \quad (2.31)$$

and $N_{av} = 2$ consecutive patterns. Given a threshold θ , we consider that there is a transition if the following inequality is satisfied

$$I(\mathbf{U}_t) > \theta > I(\mathbf{U}_{t-1}) \quad (2.32)$$

where

$$I(\mathbf{U}_t) = \Psi[d(\mathbf{U}_t), d(\mathbf{U}_{t-1})] \quad (2.33)$$

is the Euclidean distance $\Psi[\cdot]$ between the diagonal vectors $d(\mathbf{U}_t)$ and $d(\mathbf{U}_{t-1})$ (variance vectors) of two consecutive sample covariance matrices. In this way, using (2.32) only abrupt changes in time are kept. Consecutive changes are not considered to be intentional—rather they may indicate periods where the subject cannot sustain attention.

Classifier Supervisor As previously described, incoming patterns identified as transitions exhibit leaps in the training measured canonical space with respect to their predecessors. Thus these transitions patterns are probably located in different canonical subspaces from their predecessors and Bi-DBDA will have labelled such a transition pattern either as the majority of its predecessors (*within-class transition*) or differently (*intentional* or *unintentional between-class transition*) (see Fig. 2.4). This last scenario reflects a mismatch between the user’s intent and the user’s EEG patterns. The goal of the classifier supervisor is to infer the different kinds of transitions and correct the labelling produced by Bi-DBDA.

To do so we have designed three heuristic rules (HR1, HR2, and HR3). HR1 is the simplest and most conservative rule as it rejects a large number of patterns (labels them as *unknown*) rule from which HR2 and HR3 are derived (see Fig. 2.5 and 2.6 for a detailed description). The three HR label a new pattern, always every 0.250 s, using information from the last three transitions. The three HR seek to infer the intentional label of the patterns identified as transitions and then reclassify the subsequent patterns, until the next transition, with the same label. In this way the classifier supervisor only changes the labels when a intentional transition between different mental tasks is inferred.

2.2.3 Results and Conclusions

The advantages of a inconsistencies detector and a classifier supervisor in an asynchronous BCI have been assessed offline by using the first three sessions of each subject as training and validation³ data and the fourth as test data. Performance has been measured in terms of classification accuracy and channel capacity. Given that the different components of the algorithm may reject responses (*unknown* responses), the estimator proposed by Millán et al. (2004) has been used as a measure of the channel capacity. Table 2.2 shows the results for subjects 1, 2 and 3, whose data were used in BCI Competition III. Table 2.3 shows the results obtained on the subjects who received online feedback.

Regarding the first data set, all the components of the new algorithm give the best performance for subject 1 and the worst for subject 3, paralleling the results obtained by the different algorithms that participated in the BCI Competition III. $DBDA^{(O)}$ classifier (DBDA trained with the intentional canonical space) and $DBDA^{(C)}$ classifier (DBDA trained with measured canonical space) exhibit a very similar performance over the three subjects in terms of both channel capacity and classification accuracy. Note that although the classification accuracy of these simple classifiers are slightly worse than the original classifier BCI-III, the channel capacity is similar (or even better) due to the fact that the new algorithm yields faster responses. But the real advantage of the new algorithm appears when the two new components process sequentially the outputs of the two DBDA classifiers. Indeed, the detection of inconsistent patterns (7.82%, 12.18% and 30.75% un-

³k-fold cross-validation was done to select the values of the different hyper parameters of the algorithm—e.g., thresholds of the MTTD.

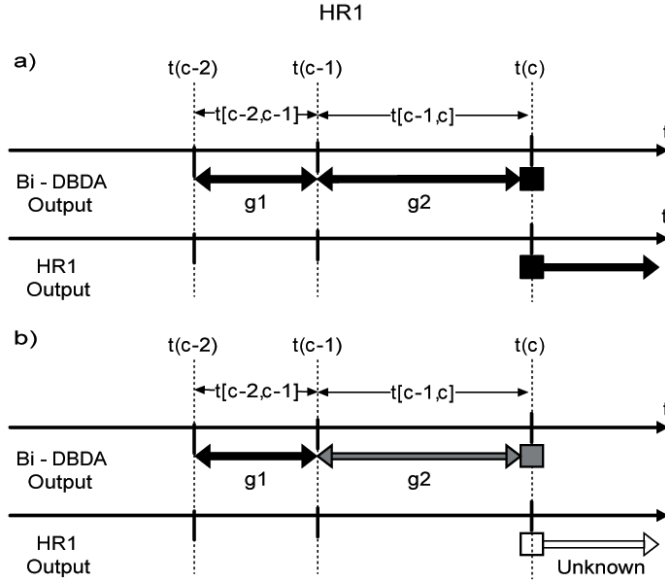


Figure 2.5: HR1 changes the label of all *unknown* patterns after a transition if the C_{g1} and C_{g2} classes with maximum labelling proportion assigned by Bi-DBDA, $\max_{k+1}[p(\nu_{t[c-1,c]} = g1))]$ and $\max_{k+1}[p(\nu_{t[c-2,c-1]} = g2))]$, in the two gaps $t[c-2, c-1]$, $t[c-1, c]$ limited by the last three transitions are the same and equal to the label of the last transition $t(c)$ (**HR1.a**). Otherwise, HR1 labels as *unknown* the last transition $t(c)$ and all following patterns (**HR1.b**). Note that the number of classes $k+1$ corresponds to the k mental tasks plus the *unknown* class. Although this labelling rule may delay the detection of an intentional transition, it allows for the filtering of a great number of unintentional transitions. This rule yields a large number of unknown patterns, which limits its suitability to situations where it is useful to be conservative (e.g., at the very early stages of training where there is a higher degree of mismatch between the user's intent and the EEG patterns). Empty squares referred to unknown labels.

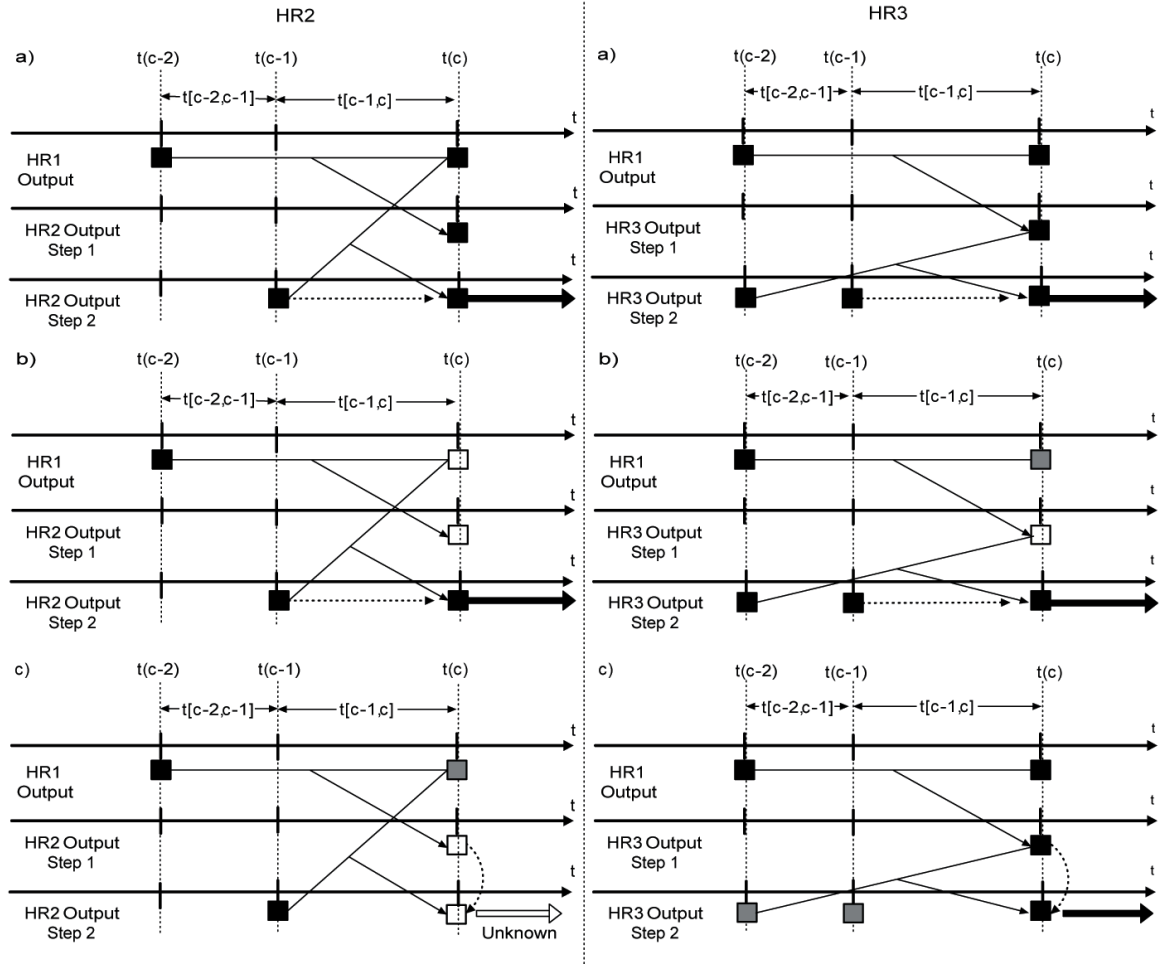


Figure 2.6: Rules HR2 and HR3 incorporate two different ways to extend the filtering of unintentional transitions generated by HR1, allowing a more extensive supervision with different degrees of caution. Both of them share the first step where the new transition $t(c)$ keeps the label it received from HR1 if it is the same as the label HR1 assigned to transition $t(c-2)$, otherwise $t(c)$ is classified as *unknown*. HR2 and HR3 differ in the second step. HR2 re-labels the new transition $t(c)$ as the previous one $t(c-1)$ if HR1 labelled $t(c)$ either as HR2 labelled $t(c-1)$ (**HR2.a**) or as *unknown* (**HR2.b**), otherwise the output of the first step of HR2 is kept (**HR2.c**). HR3 re-labels the new transition $t(c)$ as the previous one $t(c-1)$ if HR3 in the first step labelled $t(c)$ either as HR3 labelled $t(c-2)$ in the second step (**HR3.a**) or as *unknown* (**HR3.b**), otherwise the output of the first step of HR3 is kept (**HR3.a**). The difference between both rules is the amount of *unknown* labels generated: HR3 rejects a shorter number of patterns. Empty squares referred to unknown labels.

known responses for subjects 1, 2 and 3, respectively) leads to a significant increase of the Bi-DBDA channel capacity since the percentage of patterns incorrectly classified is greatly reduced. In particular, the effects of the inconsistencies detection in subject 3 stands out: the percentages of correctly and incorrectly classified patterns are inverted.

These results are further improved with the use of the different heuristic rules (HR) of the classifier supervisor. HR1 allows to increase the channel capacity for the three subjects, even though it rejects an extremely high percentage of patterns. HR2 rejects much less patterns and improves significantly the channel capacity. Finally, HR3 achieves a still further significant increase of the channel capacity (due to a remarkable increase in classification accuracy) for the first two subjects, but it shows a dramatic decline in performance in terms of channel capacity for subject 3.

Concerning the second data set where subjects received continuous feedback, the same trend is observed; i.e., the first two DBDA classifiers already achieved similar classification accuracy than the original classifier (and, hence, better channel capacity due to their faster responses), and the channel capacity is further improved through the sequential processing of the outputs of those classifiers by the inconsistencies detector (Bi-DBDA) and classifier supervisor. However, the effects of the different HR on the subjects' performance is not the same as before. For subject 4 is also appreciable a significant improvement after the application of HR1 on the output of the Bi-DBDA and even a higher one with HR2. HR3 also increases the channel capacity with respect to Bi-DBDA, but in a lesser extent than HR1 and HR2. Significantly, all three heuristic rules invert the percentages of correctly and incorrectly classified patterns. For subject 5, only HR1 and HR2 increase the channel capacity with respect to Bi-DBDA, with HR1 outperforming HR2. The disadvantage of HR3 for these two subjects is that it rejects a very short number of patterns and, given that these two subjects are at the very beginning of their training, the BCI makes risky decisions, thus generating a high percentage of misclassifications. Under this condition, more conservative heuristic rules are better suited.

In conclusion, the incorporation of the inconsistencies detector and the classifier supervisor outperforms the original classifier, winner of the BCI Competition III, on all five subjects for both working conditions of a BCI—namely with or without online feedback. Of the three heuristic rules, HR3 only seems suitable when the user's performance is already satisfactory (i.e., subjects 1 and 2). Otherwise, it is recommendable to use HR1 or, preferably, HR2. This is the case of subject 3, who has still a poor performance, and of subjects 4 and 5, who are at the beginning of their training or do not yet master the complexity of the online feedback coming from moving robots. Although HR1 and HR2 present a lower performance in terms of classification accuracy than HR3, they succeed notably in limiting the number of incorrect responses, an important aspect in order to avoid processes of discouragement, confusion and frustration that can easily interfere with attentional processes, and thus achieving acceptable levels of channel capacity.

Summarizing, in this section has been shown that the inclusion of a inconsistencies detector and a classifier supervisor based on intentional mental transitions detection leads to

Table 2.2: Classifiers performance on the BCI Competition III data set.

Subject1				
Classifier	Channel Capacity	Accuracy	Error	Rejection
<i>DBDA</i> ^(O)	1.69 b/s	70.80 %	29.20 %	-
<i>DBDA</i> ^(C)	1.68 b/s	70.72 %	29.28 %	-
Bi-DBDA	1.96 b/s	67.47 %	24.71 %	7.82 %
HR1	2.90 b/s	54.02 %	5.61 %	40.37 %
HR2	3.91 b/s	72.37 %	4.60 %	23.03 %
HR3	4.34 b/s	90.77 %	8.14 %	1.09 %
BCI-III	1.30 b/s	79.60 %	20.40 %	-

Subject2				
Classifier	Channel Capacity	Accuracy	Error	Rejection
<i>DBDA</i> ^(O)	.85 b/s	59.92 %	40.08 %	-
<i>DBDA</i> ^(C)	.82 b/s	59.44 %	40.56 %	-
Bi-DBDA	1.17 b/s	54.51 %	33.31 %	12.18 %
HR1	1.89 b/s	38.24 %	11.84 %	49.92 %
HR2	2.68 b/s	58.31 %	11.31 %	30.38 %
HR3	2.75 b/s	80.12 %	19.04 %	.84 %
BCI-III	.82 b/s	70.31 %	29.69 %	-

Subject3				
Classifier	Channel Capacity	Accuracy	Error	Rejection
<i>DBDA</i> ^(O)	.30 b/s	48.74 %	51.16 %	-
<i>DBDA</i> ^(C)	.30 b/s	48.77 %	51.13 %	-
Bi-DBDA	.98 b/s	37.00 %	32.25 %	30.75 %
HR1	1.46 b/s	28.78 %	14.52 %	56.70 %
HR2	1.71 b/s	41.81 %	18.49 %	39.70 %
HR3	.49 b/s	52.52 %	46.46 %	1.02 %
BCI-III	.31 b/s	56.02 %	43.98 %	-

DBDA^(O): DBDA trained with training data, original labelling.

DBDA^(C): DBDA trained with training data, cluster labelling.

BCI-III: Winner classifier of the BCI Competition III, which yields a decision every 0.5 s. Note that the new algorithm yields a response every 0.250 s, hence achieving a higher channel capacity than the original algorithm for similar classification accuracies.

Table 2.3: Classifiers performance of subjects receiving online feedback.

Subject4				
Classifier	Channel Capacity	Accuracy	Error	Rejection
$DBDA^{(O)}$.11 b/s	42.73 %	57.27 %	-
$DBDA^{(C)}$.10 b/s	42.30 %	57.70 %	-
Bi-DBDA	.22 b/s	40.00 %	52.89 %	7.11 %
HR1	1.10 b/s	17.95 %	13.75 %	68.30 %
HR2	1.48 b/s	26.57 %	10.41 %	63.02 %
HR3	.55 b/s	54.40 %	45.29 %	.31 %
BCI-III*	.06 b/s	43.75 %	56.25 %	-

Subject5				
Classifier	Channel Capacity	Accuracy	Error	Rejection
$DBDA^{(O)}$.04 b/s	39.04 %	60.96 %	-
$DBDA^{(C)}$.04 b/s	39.06 %	60.94 %	-
Bi-DBDA	.12 b/s	36.47 %	56.46 %	7.07 %
HR1	.92 b/s	14.25 %	19.11 %	66.64 %
HR2	.85 b/s	18.14 %	27.02 %	54.84 %
HR3	.07 b/s	40.51 %	59.26 %	.23 %
BCI-III*	.02 b/s	39.75 %	60.25 %	-

$DBDA^{(O)}$: DBDA trained with training data, original labelling.

$DBDA^{(C)}$: DBDA trained with training data, cluster labelling.

BCI-III: Winner classifier of the BCI Competition III, which yields a decision every 0.5 s. Note that the new algorithm yields a response every 0.250 s, hence achieving a higher channel capacity than the original algorithm for similar classification accuracies.

an effective inference of the user's intended mental task. This approach yields a significant increase of the channel capacity mainly because it allows to decrease the error rates. Experimental results show the benefits of our algorithm in both working conditions of a BCI, namely with or without online feedback. The main limitation of this approach is the use of ad-hoc heuristic rules. The next step is to formalize these heuristic rules in a Bayesian framework and build probabilistic models for the inference of the user intent as in (Verma and Rao, 2006).

2.3 Feature Extraction for Multi-class BCI using Canonical Variates Analysis

2.3.1 Introduction

IDIAP BCI is focused on asynchronous and non-invasive EEG-based BCI to control robots and wheelchairs (Millán et al., 2004; Galán et al., 2008a). It means that the users drive such devices by learning to voluntarily control specific EEG features. To facilitate this learning process it is necessary to select those subject-specific features that allow to generate the maximum number of discriminant patterns. This process becomes crucial to facilitate the generation of those patterns that permit an easier execution of those commands needed to drive the different devices. To this end, Common Spatial Patterns (CSP) (Ramoser et al., 2000) and his extension Common Spatio Spectral Patterns (CSSP) (Lemm et al., 2005) have been proven very useful. However, *there is no canonical way to choose the relevant CSP patterns for multi-class CSP and only approximative solutions can be obtained* (Dornhege et al., 2004). This section describes a feature extraction method with canonical solution for multi-class BCI. The proposed method provides a reduced number of canonical discriminant spatial patterns (CDSP) and ranks the channels sorted by power discriminability (DP) between classes. It relies in Canonical Variates Analysis (CVA) which has been utilized previously in Galán et al. (2007a).

2.3.2 Methods

Canonical Variates Analysis

Utilizing IDIAP BCI system the users employ the voluntary modulation of different oscillatory rhythms by executing of different mental tasks (motor and cognitive) to drive robots and wheelchairs in virtual and real environments. In these applications the users utilize more than two commands. To facilitate this voluntary modulation it is necessary to find those subject-specific spatial patterns that maximize the separability between the patterns generated by executing the different mental tasks. In this way, from band-pass filtered EEG signals, the CSP algorithm extracts canonical discriminant spatial patterns which directions

maximizes the differences in variance between two classes. *Since the variance of a band-pass filtered signal is a measure for the energy in the corresponding frequency band, the patterns reflect the spatial distributions of event-related (de)synchronization (ERS/ERD) effects* (Dornhege, 2003). However, *there is no canonical way to choose the relevant CSP patterns for multi-class CSP and only approximative solutions can be obtained* (Dornhege, 2004). This limitation can be avoided in two ways, namely working in frequency domain or working with the squared band-pass filtered EEG signal. In the former case, the energy in the corresponding frequency band is measured by its spectral power. In this domain the spatial distributions of ERS/ERD effects are identified by changes on the spectral power. In the later case, their distributions are identified by changes on the mean, given that the variance of a band-pass filtered EEG signal becomes the mean when the signal is squared (Galán et al., 2007a). Thus, using CVA it is easy to extract CDSP which directions maximize the differences in mean, either spectral power in the first case or energy of the original band-pass filtered EEG signal in the second case, between a given number of classes.

Given the $n_i \times c$ matrix, either with the estimated spectral power of a frequency band or the squared band-pass filtered EEG signal, $\mathbf{S}_i = (\mathbf{s}_{i1}, \dots, \mathbf{s}_{in_i})'$ of class $i = 1, \dots, k$, where n_i is the number of samples and c is the number of channels, and $\mathbf{S} = (\mathbf{S}'_1, \dots, \mathbf{S}'_k)'$, the $k - 1$ CDSP of \mathbf{S} are the eigenvectors \mathbf{A} of $\mathbf{W}^{-1}\mathbf{B}$ which eigenvalues $\lambda_u, (u = 1, \dots, k - 1)$ are larger than 0. Note that the direction of eigenvectors \mathbf{A} maximize the quotient between the between-classes dispersion matrix

$$\mathbf{B} = \sum_{i=1}^k n_i (\mathbf{m}_i - \mathbf{m})(\mathbf{m}_i - \mathbf{m})' \quad (2.34)$$

and the pooled within-classes dispersion matrix

$$\mathbf{W} = \sum_{i=1}^k \sum_{j=1}^{n_i} (\mathbf{s}_{ij} - \mathbf{m}_i)(\mathbf{s}_{ij} - \mathbf{m}_i)' \quad (2.35)$$

where

$$\mathbf{m}_i = \frac{1}{n_i} \sum_{j=1}^{n_i} \mathbf{s}_{ij} \quad (2.36)$$

and

$$\mathbf{m} = \frac{1}{n} \sum_{i=1}^k n_i \mathbf{m}_i \quad (2.37)$$

are the class and total centroids respectively. Thus, the new features are obtained by the projection

$$\mathbf{Y} = \mathbf{S}\mathbf{A} \quad (2.38)$$

Once the CDSP are computed, it is useful to know how the original features (electrodes) are contributing in the separability between the classes. It also permits to interpret the space generated by the CDSP, specially when the number of classes is high. In this way, it is possible to rank the channels given their contribution on the new space. It is possible to define a new *Discriminant Power* (DP) (Gonzalez Andino et al., 2006) measure for each channel from the *structure matrix*, pooled correlation matrix between original channels in \mathbf{S} and the new features in \mathbf{Y} . Given the $c \times k - 1$ structure matrix \mathbf{T} , where $\mathbf{T} = \sum_{i=1}^k \mathbf{T}_i$, $e = 1, \dots, c$, and the normalized eigenvalues $\gamma_u = \lambda_u / \sum_{u=1}^{k-1} \lambda_u$, the proposed DP can be computed as follows

$$DP_e = \left(\sum_{u=1}^{k-1} \gamma_u t_{eu}^2 / \sum_{e=1}^c \sum_{u=1}^{k-1} \gamma_u t_{eu}^2 \right) \times 100 \quad (2.39)$$

Data Acquisition, Task and Preprocessing

Data were recorded from 4 subjects with a portable Biosemi acquisition system using 64 channels sampled at 512Hz and high-pass filtered at 1Hz. The subjects were sitting in a chair looking at a fixation cross placed at the center of a monitor. The subjects were instructed to execute three different mental tasks (left hand imagination movement, rest, and words association) in a self-paced way. The mental task to be executed was previously specified by the operator in order to counterbalance the order, the subjects specify when they started to execute the mental task. Each subject participated in 20 sessions integrated by 6 trials each, 2 trials of each class. The duration of each trial was 7 seconds but only the last 6 seconds were utilized in the analysis to avoid preparation periods. Subjects 1 and 2 had previous experience with the selected mental tasks, while it was the first time for subjects 3 and 4.

To work in frequency domain the signal was spatially filtered using common average reference (CAR) previous to the estimation every 62.5 ms. (16 times per second) of the power spectral density (PSD) in the band 10-14Hz with 2Hz resolution over the last 1-second windows. PSD was estimated by Welch method with 5 overlapped (25%) Hanning windows of 500 ms. length. To work in temporal domain the signal was also spatially filtered by CAR, band-pass filtered in the frequency range 8-16Hz (to get a band-pass filtered signal in the same frequency ranges analyzed in the frequency domain, taking in account the FIR filter transition band) and finally squared. Single trials were obtained by averaging samples within last 1-second window. In both cases only 45 electrodes were utilized, namely: F1, F3, F5, FC1, FC3, FC5, C1, C3, C5, CP1, CP3, CP5, P1, P3, P5, P7, PO3, PO7, O1, Fz, FCz, Cz, CPz, Pz, POz, Oz, F2, F4, F6, FC2, FC4, FC6, C2, C4, C6, CP2, CP4, CP6, P2, P4, P6, P8, PO4, PO8, O2.

Table 2.4: LDA Classification accuracy over the four subjects according to the different test sessions using CVA in frequency and temporal domains

Subject	Domain	Test Session					Average
		1	2	3	4	5	
1	F ^a	66.25%	76.04%	71.04%	70.41%	62.92%	69.33%
	T ^b	60.34%	87.05%	74.13%	73.54%	72.42%	73.50%
2	F	72.71%	59.79%	73.54%	69.37%	64.38%	67.95%
	T	62.36%	56.70%	69.81%	61.76%	71.14%	64.35%
3	F	43.54%	49.38%	55.00%	60.21%	50.63%	51.75%
	T	60.32%	60.04%	61.41%	50.28%	55.83%	57.57%
4	F	35.83%	61.45%	48.33%	33.54%	34.16%	42.66%
	T	31.24%	62.17%	35.71%	46.57%	35.95%	42.33%
Average	F						57.89%
	T						59.43%

^afrequency domain, ^btemporal domain

Analysis

To assess the canonical discriminant spatial patterns (CDSP) stability over time, data were split in two sets, the training set integrated by the trials from the first 15 sessions, and the test set integrated by the trials from the last 5 sessions. In frequency domain a trial was defined by each PSD estimation whereas in temporal domain each trial was defined as the averaged squared band-pass signal over the last second. After obtain the CDSP from the training set of each domain, training and test trials where projected in the new space using eq. 2.38. Then, one Linear Discriminant Analysis (LDA) classifier was built per subject and per domain whose parameters were estimated on the corresponding training sets. Finally, these LDA classifiers were used to assess the generalization performances of each subject. Given that the main problem in BCI research is to deal with EEG instability over time, the use of k-fold cross validation was avoided. This non-parametric classification error estimator uses as training and test sets data from all sessions, what never occurs in on-line applications and yields optimistic error estimations.

2.3.3 Results and Conclusions

Table 2.4 reports the LDA classification accuracy over the 5 test sessions using CVA in frequency and temporal domain. In average, the classification accuracies for both domains are equivalent (57.89% in frequency domain vs. 59.43% in temporal domain, random level is 33.3% for a 3-class problem). In the temporal domain, higher classification accuracies were obtained for two subjects, namely subjects 1 and 3 (73.50% and 57.57% vs. 69.33%

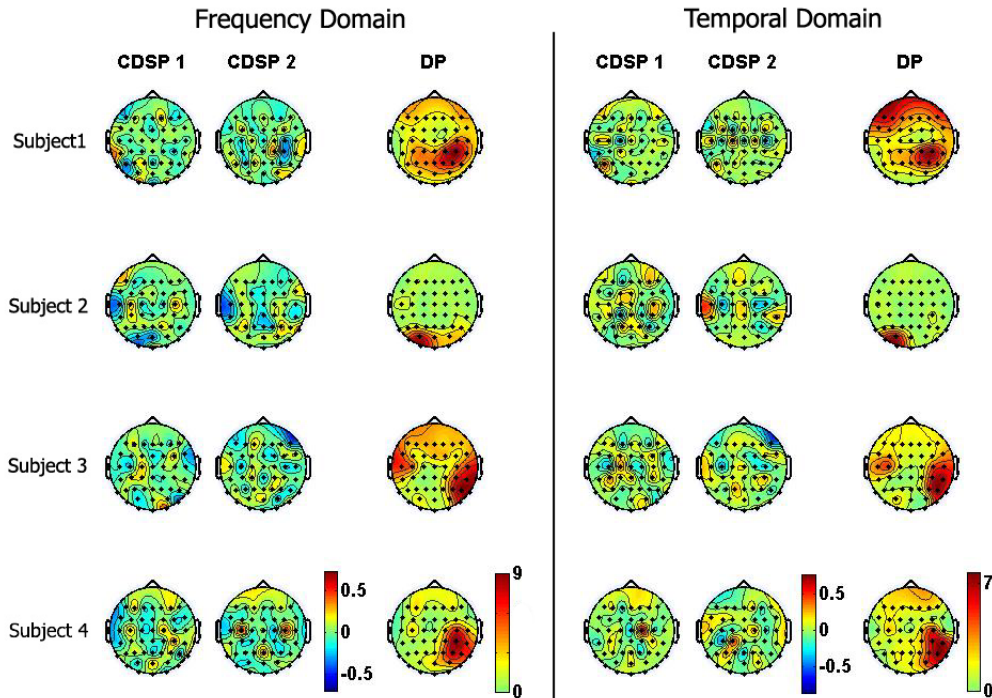


Figure 2.7: CDSP and DP for each subject in frequency and temporal domains computed from training set. Note that DP scale is in %.

and 51.75%). In the frequency domain, higher classification accuracies were obtained only for one subject, namely subject 2 (67.95% vs. 64.35%). The performance is equivalent on subject 4 (42.66% vs. 42.33%). Fig. 2.7 depicts the two CDSP and the DP obtained for each subject in frequency and temporal domains computed on the training set. The CDSP interpretation as a whole is facilitated by DP maps. DP maps show the electrodes contribution, in percentage, on the space defined by the CDSP. As expected according to the results obtained in terms of classification accuracy, DP maps obtained from both domains show a similar distribution of electrodes contribution in all subjects.

Fig. 2.8 and 2.9 depict the DP for each subject in the frequency and temporal domains, respectively, computed joining all test sessions (first column) and also from every single test session (next five columns). These figures show the origin of the intersession variability and allow also to understand the results in terms of classification accuracy (see Table 2.4). In both domains, the classification accuracy is related to the level of similarity between DP maps obtained from the training set (see DP maps in Fig. 2.7) and DP maps obtained from test sessions (see Fig. 2.8, frequency domain, and Fig. 2.9, temporal domain), either joining

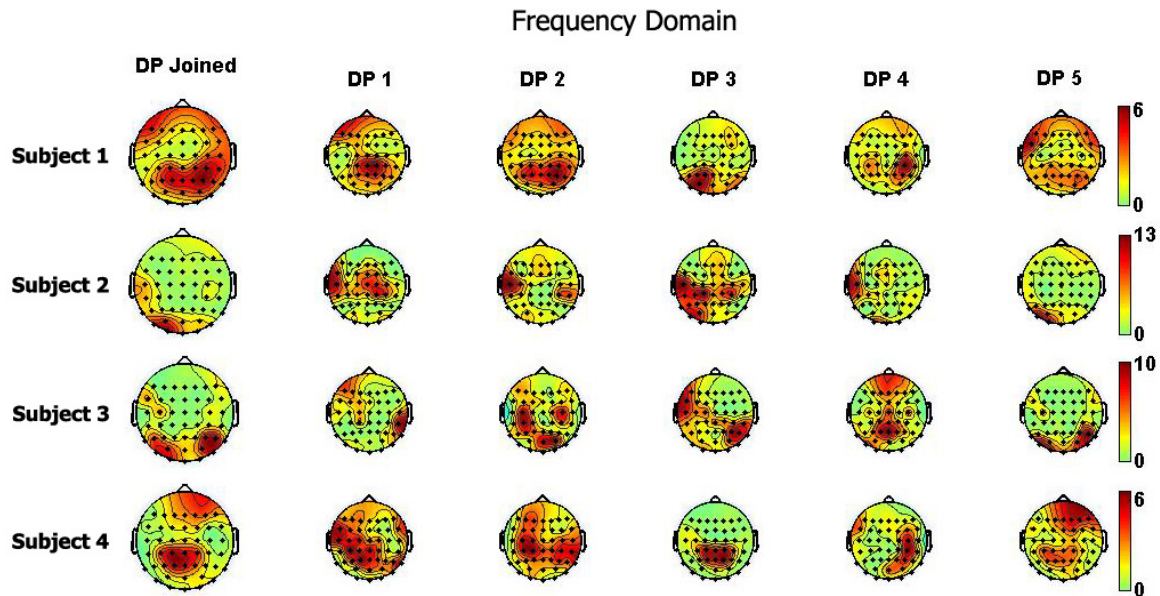


Figure 2.8: DP for each subject in frequency domain computed joining all test sessions and from every single test session. Note that DP scale is in %.

all test sessions or for each single test session. Higher classification accuracies correspond to higher similarity between the maps, what means that the canonical spaces defined by the CDSP estimated on the training sets are more stable over time. It is also worth noting that the similarity between DP maps obtained from both domains (DP joined in Fig. 2.8 and 2.9, first column) decreases on those subjects with lower classification accuracies.

The objective of this paper was to propose a new feature extraction method with a canonical solution for multi-class BCI. The estimated CDSP yield the space of maximum separability between ERS/ERD effects involved in the execution of different mental tasks. The proposed DP measure rank the electrodes sorted by their contribution in the new space. The average LDA classification accuracies obtained working on frequency and temporal domains are equivalent. Performances are not very high for a 3-class problem because, for comparative purposes, it has been classified every single trial obtained from the last second window. The equivalent results, in terms of classification accuracies, are also reflected in the similarity between the DP maps obtained from the training sets of both domains. On the other hand, the level of similarity between DP maps obtained from the testing sets of both domains decreases for those subjects with lower classification accuracies (subjects 3 and 4). A possible explanation that needs to be explored is that energy (temporal domain) and

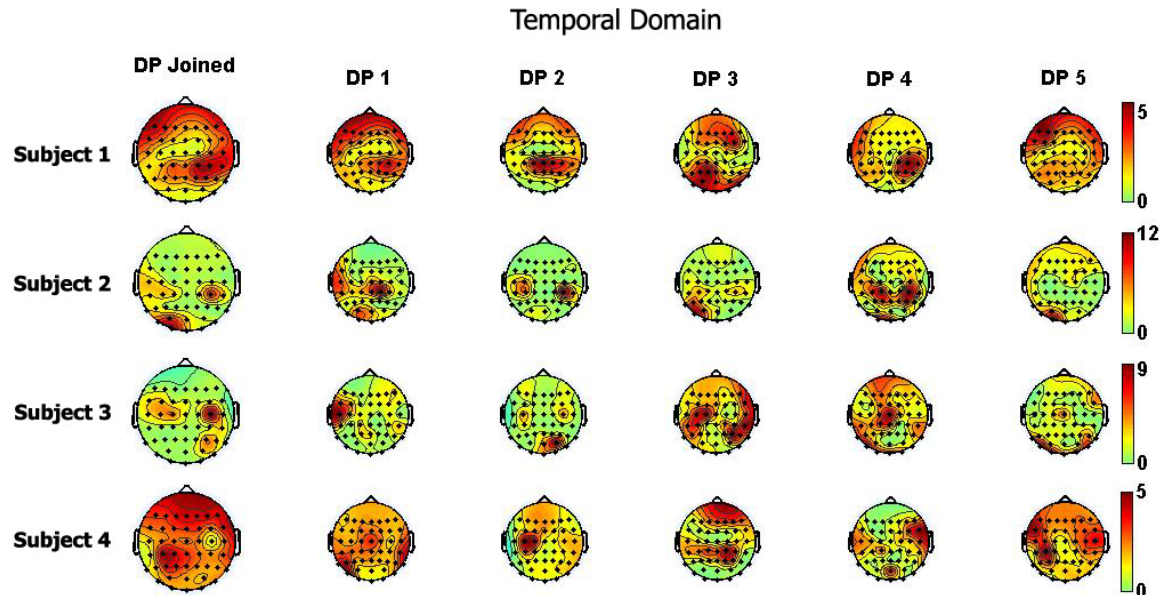


Figure 2.9: DP for each subject in temporal domain computed joining all test sessions and from every single test session. Note that DP scale is in %.

PSD estimation (frequency domain) do not reflect the same phenomena when the signal is less stationary, what occurs when the subject have difficulties to generate stable EEG patterns during the execution of the mental tasks. Future work will focus on testing different extensions of CVA, assessing the sources of performance variability between both domains on different subjects, and exploring the relation between energy and spectral estimation.

2.4 Visuo-Spatial Attention Frame Recognition for Brain-Computer Interfaces

2.4.1 Introduction

As introduced before, asynchronous EEG-based BCI allow users to control devices spontaneously and at their own pace. To this end, people learn how to voluntary modulate different oscillatory EEG rhythms by the execution of different mental tasks. A limitation of using mental tasks as control commands (e.g., imagining movements or doing arithmetic operations) is that subjects need to keep performing those mental tasks during the

whole interaction, what can be exhausting, especially for novel users. An alternative is to exploit conscious behaviors that do not require sustained attention. Recent studies have demonstrated the possibility to modulate EEG alpha band by orienting visuo-spatial attention (Thut et al., 2006). In an ideal case, BCI users could make the wheelchair *turn left* just by orienting their attention (without any eye movement) to some location in the left visual field, what is more natural than, for instance, imagining a left hand movement. Moreover, once the wheelchair just turn left, users will simply stop attending to any particular spot of their visual field and the wheelchair, endowed with an intelligent controller (Millán et al., 2004), will move forward.

In this section it is assessed the feasibility of recognizing user's voluntary modulation of EEG rhythms associated to visuo-spatial attention in an experimental setup close to the ecological conditions of asynchronous EEG-based BCIs. To this end, two approaches are compared, a *traditional BCI approach* and a *frames approach*. These frames, as described by Freeman (Freeman, 2005), correspond to active intermittent induced spatial patterns of amplitude modulation of beta-gama oscillations in response to conditioned stimuli. Based on those findings, the following questions are addressed: (i) Does this discontinuous mode of function (i.e., frames) also appear in response to voluntary modulation of EEG rhythms? (ii) In this case, is it possible to classify these frames with respect to the attended location? (iii) Which frequency ranges yields better classification accuracy? (iv) Can this approach improve BCI performance? We hypothesize that *traditional approaches* (assuming sustained modulation of EEG rhythms over time) would face methodological problems: they will label (for training purposes) and classify samples extracted from periods of time where the underlying brain phenomena is either not present or is not salient enough. Then, a *frames approach* (which only classifies those samples where the induced episodic frames are detected) would be more appropriate. This section addresses these questions and presents some hints for future work.

2.4.2 Methods

Data were recorded from 2 subjects with a portable Biosemi acquisition system using 64 channels sampled at 512Hz and high-pass filtered at 1Hz. The sampling rate was fixed at 512Hz to ensure a good estimation of the highest frequency component under analysis. The subjects were sitting in a chair looking at a fixation cross placed at the center of a monitor. The subjects were instructed to covertly attend to one of two possible target locations (lower-left and lower-right monitor's corners). The target location was specified by the operator in a pseudo-random balanced order. The subjects specified when they started to shift their attention. Each subject participated in 10 sessions composed by 4 trials each, 2 trials for each target. The duration of each trial was 7 seconds but only the first 600ms were utilized in this study.

The signal was spatially filtered using common average reference (CAR) previous to estimate the continuous Morlet wavelet coefficients on 18 frequency components (7, 8, 9,

10, 11, 12, 28, 32, 36, 40, 44, 48, 56, 64, 72, 80, 88, and 96 Hz) and 16 electrodes (F5, FC5, C5, CP5, P5, AFz, Fz, FCz, Cz, PCz, Pz, F6, FC6, C6, CP6, P6). The selection of electrodes was based on preliminary analysis of continuous Morlet wavelet coefficients scalp topography. Thus, each trial is composed by 512×0.6 samples and 18×16 features. The analysis carried on aims to compare the recognition rates over the different frequency components using two different approaches, namely the *traditional BCI approach* and the *frames approach*. The process was structured in two steps:

1. One canonical space was built per each frequency component (18 canonical spaces) (Galán et al, 2007a) using 16-dimensional vectors (estimated wavelet coefficients at 16 electrodes). Since it is a 2-class problem, canonical spaces are defined by 1 canonical function.
2. Two classifiers were built following two different approaches:
 - (a) *Traditional BCI approach*: an LDA was built using all the training projected samples on the canonical space and classifying all the test projected samples.
 - (b) *Frames approach*: only a subset of the projected samples (i.e. frames) were used for training and classification. A sample was considered as a frame if its projection on the training canonical space was located on the opposite tails of each class distribution. Eight percentiles were utilized as thresholds: P_{40} , P_{35} , P_{30} , P_{25} , P_{20} , P_{15} , P_{10} and P_5 . Thus, a sample was identified as a frame either its projection was below a given percentile (i.e: P_5) of class 1 or above the opposite percentile (i.e: P_{95}) of class 2. From now, the reference to one percentile also includes its opposite.

Both approaches were assessed using k -fold cross validation, $k = 20$. Each fold was integrated per one trial of each condition respecting the timing when they were recorded.

2.4.3 Results and Conclusions

The average LDA classification accuracy is higher utilizing the frames approach. For both subjects, the maximum classification accuracy is reached utilizing P_5 . Only the results obtained on this percentile are reported on detail. The maximum average classification accuracy classifying all the samples (i.e. traditional approach) is 58.41% at 10Hz and 63.08% at 12Hz for subject 1 and 2 respectively (see Fig. 2.10 *left*), both in the alpha range. Utilizing frames approach, the maximum average classification accuracies are 80.64% at 72Hz, and 87.31% at 32Hz for subject 1 and 2 respectively (see Fig. 2.10 *center*), both in the gamma range. It represents an absolute increase of 22.23% and 27.13% for subject 1 and 2 respectively. Notice that these classification accuracies are computed only on those samples identified as frames. The average percentage of samples identified as frames out of the total of samples of a trial is 5.85% for subject 1 and 5.92% for subject 2 (see Fig. 2.10

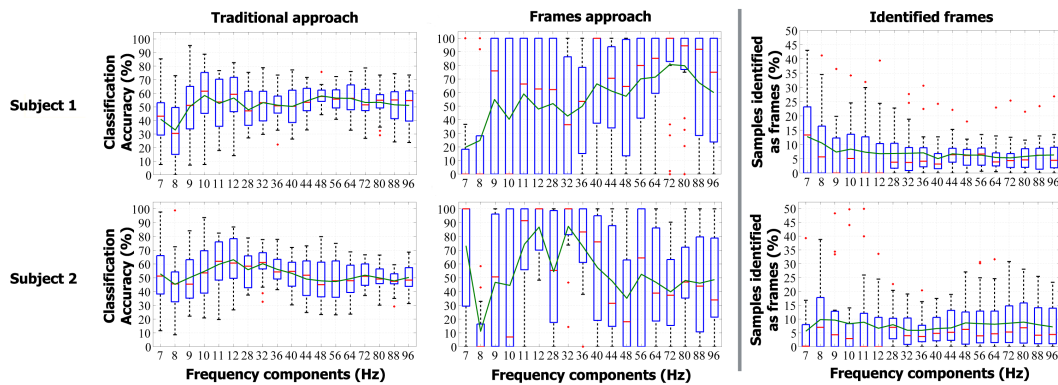


Figure 2.10: Classification results using 20-fold crossvalidation over the 18 frequency components. Solid line represents the mean. LDA classification accuracy distributions utilizing traditional approach (*left*) and frames approach (*center*). *Right*, percentage of the total trial samples identified as frames.

right) at 72Hz and 32Hz respectively. In case of subject 1, only in 1 fold out of 20 it was not possible to identify any frame. In case of subject 2, it was not possible in 4 out of 20 folds. To understand the implication of these results in a real BCI application, each trial has been labelled according to the class maximum recognized by the classifier, using all the samples in case of traditional approach, and using only frames in case of frames approach. In the first case, the trial classification accuracies are 60.00% and 57.50% for subjects 1 and 2 respectively, what implies that channels capacities are .05 bits/second and .03 b/s (using estimator proposed in Millán et al., (2004)). Using frames approach, the trial classification accuracies are 60.00% and 47.50%, but with only 12.50% of error recognition in both cases, what implies that channels capacities are .55 b/s and .46 b/s. Using frames approach the BCI theoretical channel capacity is boosted by 10.

This preliminary study on visuo-spatial attention frame recognition for BCI provides relevant hints for further research. First, it is possible to voluntarily modulate EEG rhythms by orienting visuo-spatial attention in order to use asynchronous noninvasive EEG-based BCI's. Second, the intensity of this modulation is not sustained over time. This fact can be related to the active intermittent induced spatial patterns of amplitude modulation (frames) in response to conditioned stimuli described by Freeman (Freeman, 2005). In this case these patterns are voluntarily driven by the subject. Third, it is possible to classify the frames generated by orienting the attention to different visual locations with high classification accuracies (above 80%). Fourth, these classification accuracies are maximum in gamma band ($> 30\text{Hz}$), corresponding to endogenous shifts of attention effects (Palix et al., 2006). Fifth, classification accuracies utilizing a traditional approach, i.e. assuming modulations sustained over time, are around the chance level. It suggests that this approach

is not optimal to recognize induced EEG phenomena, what is confirmed comparing the BCI theoretical channel capacity achieved using both approaches. Using frames approach the BCI theoretical channel capacity is drastically increased.

2.5 A Brain-Actuated Wheelchair: Asynchronous and Non-Invasive Brain-Computer Interfaces for Continuous Control of Robots

2.5.1 Introduction

One of the main challenges of a non-invasive BCI based on spontaneous brain activity is the non-stationary nature of the EEG signals. Shenoy and co-workers (Shenoy et al., 2006) describe two sources of non-stationary behavior, namely differences between samples extracted from calibration measurements (training data set) and samples extracted during the online operation of the BCI system (test data set), and changes in the user's brain processes during the online operation (e.g., due to fatigue, change of task involvement, etc). Such kind of phenomena have motivated that BCI research groups develop adaptive algorithms to deal with these shifts in the distributions of samples (Shenoy et al., 2006; Buttfeld et al., 2006; Millán et al., 2007). Unfortunately, current adaptive solutions have two main limitations. Firstly, they are based on supervised approaches requiring the correct output for every sample and so the user cannot operate the BCI autonomously. Secondly, adaptation in the wrong moment (e.g., when the user is not executing properly the mental tasks because of fatigue, distraction, etc) will incorrectly change the feedback (the device's behavior) and will disrupt user's learning process. Given this scenario, two questions arise. Is it possible to find (rather) stable subject-specific EEG features to reduce the differences between samples extracted from calibration and online operation sessions? How shared control techniques can minimize the impact of changes in the user's brain processes during the online operation?

This section describes an asynchronous brain-actuated wheelchair that can be operated autonomously (without the help of any expert operator) and report results obtained by two subjects while driving a simulated version of the wheelchair. The brain-actuated wheelchair exhibits two key components, namely the selection of stable user-specific EEG features that maximize the separability between the different mental tasks, and the implementation of a shared control system (Philips et al., 2007; Vanacker et al., 2007) between the BCI and the intelligent wheelchair. The experiments carried out aimed to assess the robustness of the system. In experiment 1 two subjects were asked to mentally drive both a real and a simulated wheelchair from a starting point to a goal along a pre-specified path. Here only are reported the experiments with the simulated wheelchair for which we have extensive data in a complex environment that allows a sound analysis. Each subject participated in 5

experimental sessions integrated by 10 trials each. The experimental sessions were carried out with different elapsed times between them (since one hour to two months) to assess the system robustness over time. The pre-specified path was divided in 7 stretches to assess the system robustness in different contexts. To further assess the performance of the brain-actuated wheelchair, subject 1 participated in a second experiment consisting of 10 trials where he was asked to drive the simulated wheelchair following 10 different complex and random paths.

2.5.2 Methods

EEG Data Acquisition and Preprocessing

EEG Data were recorded from 2 healthy subjects with a portable Biosemi acquisition system using 64 channels sampled at 512Hz and high-pass filtered at 1Hz. Then, the signal was spatially filtered using a common average reference (CAR) before estimating the power spectral density (PSD) in the band 8-48 Hz with 2 Hz resolution over the last 1 second. The PSD was estimated every 62.5 ms (i.e., 16 times per second) using the Welch method with 5 overlapped (25%) Hanning windows of 500 ms. Thus, an EEG sample is a 1344-dimensional vector (64 channels times 21 frequency components).

System Description

The system is integrated by two entities, the intelligent wheelchair and the BCI system. Environmental information from the wheelchair's sensors feeds a contextual filter that builds a probability distribution $P_{Env}(C)$ over the possible user's mental steering commands, $C = \{Left, Right, Forward\}$. The BCI system estimates the probabilities $P_{EEG}(C)$ of the different mental commands from the EEG data. Both streams of information are combined to produce a filtered estimate of the user's intent $P(C) = P_{EEG}(C) \cdot P_{Env}(C)$. The shared control system also uses the environmental information from the wheelchair's sensors to map these high-level commands into appropriate motor commands, translational and rotational velocities, in order to generate a smoother driving behavior. This is done by an intelligent controller that activates an appropriate assisting behavior when the user needs help. Thus, the system constantly adapts the level of assistance to a specific situation. It will help significantly when the subject's performance (BCI accuracy) is low whereas it will decrease its role when the BCI accuracy is higher. In these experiments the assisting behavior utilized was obstacle avoidance, which calculates a proper translational and rotational velocities pair to steer the wheelchair away from obstacles. Fig. 1.4 depicts a schematic representation of the shared control architecture of the brain-actuated wheelchair. See (Philips et al., 2007; Vanacker et al., 2007) for a detailed description. The BCI has two components, namely a feature extractor and a Gaussian classifier. The former selects the most relevant features of the EEG signals based on CVA (Galán et al., 2007a).

Based on these features, the Gaussian classifier estimates the probability distributions of the three mental commands (Millán et al., 2004).

Out of the system components, here it is only described the statistical Gaussian classifier. A complete description of the shared control architecture is included in Appendices G and H (Philips et al., 2007; Vanacker et al., 2007), and the feature extractor has already described in section 2.3 (see Appendix D; Galán et al., 2007a).

The classifier utilized is a statistical Gaussian classifier, (Millán et al., 2004) for more details. The output of this statistical classifier is an estimation of the posterior class probability distribution for a sample; i.e., the probability that a given single trial belongs to each mental task (or class). Each class is represented by a number of Gaussian prototypes, typically less than four. That is, it is assumed that the class-conditional probability function of class k is a superposition of N_k Gaussian prototypes. It is also assumed that all classes have equal prior probability. All classes have the same number of prototypes N_p , and for each class each prototype has equal weight $1/N_k$. Then, dropping constant terms, the activity of the i^{th} prototype of class k for a given sample \mathbf{x} is the value of the Gaussian with center μ_k^i and covariance matrix Σ_k^i . From this we calculate the posterior probability y_k of the class k , which is the sum of the activities of all the prototypes of class k divided by the sum of the activities of all the prototypes of all the classes. The classifier output for input vector \mathbf{x} is then the class with the highest probability. In order to smooth this output, we average the class-conditioned probabilities of the last 8 consecutive input vectors \mathbf{x} . Thus, the classifier responds every 0.5 s. Usually each prototype of each class would have an individual covariance matrix Σ_k^i , but to reduce the number of parameters the model has a single diagonal covariance matrix common to all the prototypes of the same class. During offline training of the classifier, the prototype centers are initialized by any clustering algorithm or generative approach. This initial estimate is then improved by stochastic gradient descent to minimize the mean square error $E = \frac{1}{2} \sum_k (y_k - t_k)^2$, where \mathbf{t} is the target vector in the form 1-of-C; that is, if the second of three classes was the desired output, the target vector is (0,1,0). The covariance matrices are computed individually and are then averaged over the prototypes of each class to give Σ_k .

Calibration Sessions and Feature Extraction

To extract stable discriminant EEG features and build the statistical Gaussian classifier, both subjects participated in 20 calibration sessions recorded in the same day than the test driving session 1. The calibration sessions were recorded during the morning and the test driving session 1 during the afternoon. As in the driving sessions, the subjects were sitting in a chair looking at a fixation point placed at the center of a monitor. The display was also the same, the simulated wheelchair in a first person view (see Fig. 2.11 *Left*). The subjects were instructed to execute the three mental tasks (left hand imagination movement, rest, and words association) in a self-paced way. The mental task to be executed was selected by the operator in order to counterbalance the order, while the subjects decided when they

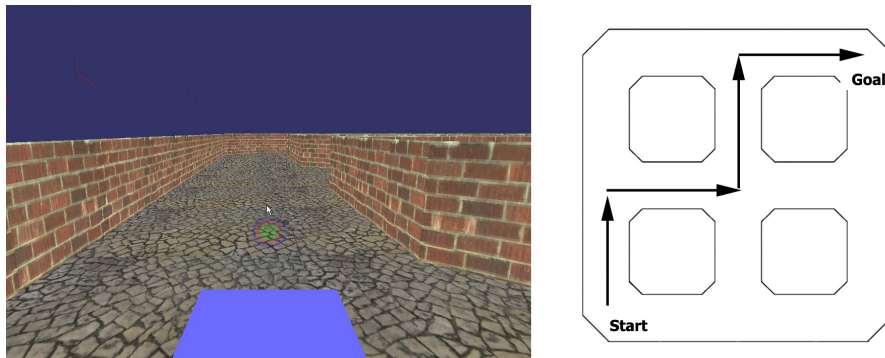


Figure 2.11: *Left:* monitor display in a first person view from the Start. The white cursor at the center is the fixation point. The rectangle at the bottom is the simulated wheelchair. *Right:* top view of the simulated world and the pre-specified path.

started to execute the mental task. Each calibration session was integrated by 6 trials each, 2 trials of each class. The duration of each trial was 7 seconds but only the last 6 seconds were utilized in the analysis to avoid preparation periods. In these sessions the subjects did not receive any feedback, so the monitor display was static.

The data from the 20 calibration sessions were grouped in 4 blocks (B1, B2, B3 and B4) of 5 consecutive sessions. Taking into account the recordings timing, different configurations of training and testing sets (train-test) were set: B1–B2, B1–B3, B1–B4, B2–B3, B2–B4, B3–B4, (B1+B2)–B3, (B1+B2)–B4, (B1+B2+B3)–B4. Feature selection was done in a sequential way, where first were picked stable frequency components and then the best electrodes. To assess the stability of the frequency components 20 CVA were applied, one per frequency component, on the training set of each configuration. For each canonical space the electrodes were ranked according to their contribution to this space (see Section 2.3). Then, up to 15 linear discriminant classifiers were built, each using those electrodes that contributed more than $c\%$, with $c \in \{1.0, 2.0, \dots, 15.0\}$. The stability of the classifier accuracy over the different configurations was used to select the frequency components. Afterwards, for each selected frequency, it was taken the configuration of electrodes (out of the 15 possible ones), that yielded the highest classification accuracy on the configuration (B1+B2+B3)–B4. Finally, the different combinations of selected frequencies (with their associated electrodes) was tested on the configuration (B1+B2+B3)–B4, choosing the best one. At the end of this sequential process the selected frequencies were 12 Hz for subject 1 and $\{10, 12, 14\}$ Hz for subject 2. Then it was built the statistical Gaussian classifier for each subject using their individual selected features from all the data of the calibration sessions. Fig. 2.12 depicts the electrodes contribution for each selected frequency component for each subject.

An issue to be ruled out in any BCI system is the use of eye movements or muscular

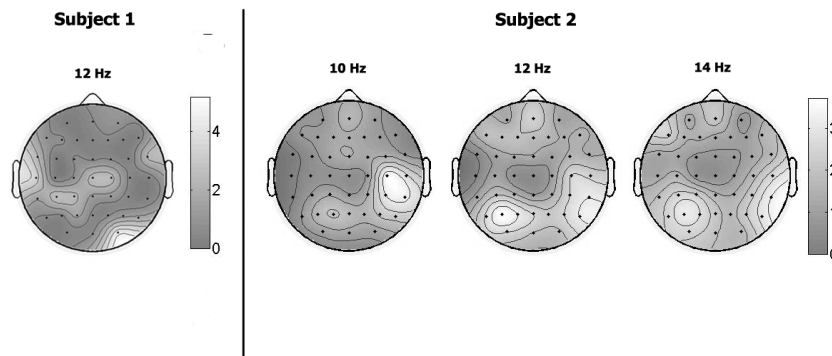


Figure 2.12: Electrode discriminant power DP_e (see Section 2.3) for the selected frequencies for each subject. For subject 1 the main contributions come from left temporal, central and right occipital areas. For subject 2, at 10 Hz the main contributions come from right central-parietal areas, and at 12 and 14 Hz from bilateral parietal areas.

activity components embedded in the EEG as control signals. In the experiments described in this paper this issue was not assessed but it was in posterior experiments with the real wheelchair where the same statistical Gaussian classifiers were utilized. In the later ones the eye movement and muscular activity were monitored by means of bipolar electromyogram (EMG) using 2 surface electrodes placed on the forearm muscle Extensor Digitorum, and by bipolar electrooculogram (EOG) using surface electrodes placed below and laterally to the left eye respectively. These experiments showed that the eye movements and muscular activity components embedded in the EEG were equally distributed among the classes.

Experimental Tasks

Task 1 Both subjects were sitting in a chair looking at a fixation point placed at the center of a monitor. The monitor displayed a simulated wheelchair in a first person view placed in a simulated world. The subjects were asked to mentally drive the simulated wheelchair from a starting point to a goal following a pre-specified path by executing three different mental tasks (*left* hand imagination movement to turn *Left*, rest to go *Forward*, and words association to go *Right*). Fig. 2.11 depicts the monitor display and the pre-specified path. Every subject participated in 5 experimental sessions, each consisting of 10 trials. The time elapsed between two consecutive experimental sessions was variable to assess the system robustness over time: 1 day between sessions 1 and 2, 2 months between sessions 2 and 3, 1 hour between sessions 3 and 4, and finally 1 day between sessions 4 and 5.

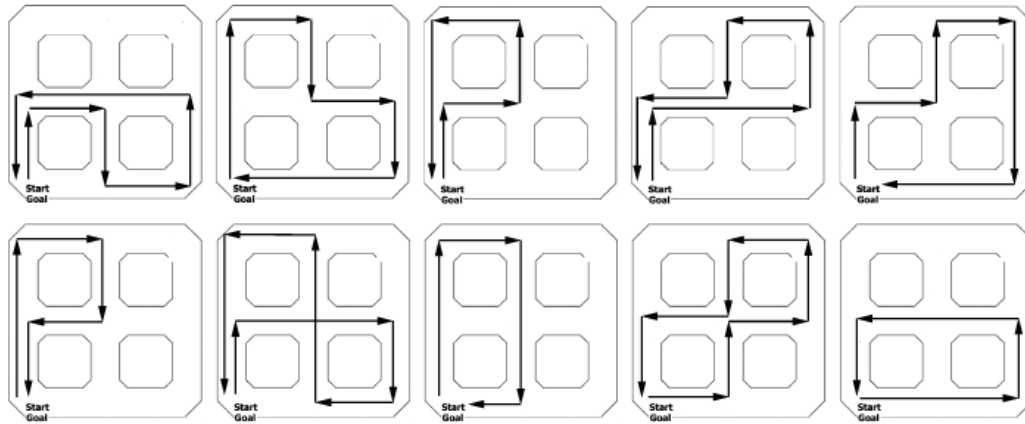


Figure 2.13: Top view of the random paths in Task 2. Trial 1 placed in upper row, first column. Trial 10 placed in second row, last column.

Task 2 To further assess the performance of the brain-actuated wheelchair, Subject 1 participated in a second experiment four months later. He performed 10 trials in the same simulated environment where he was asked to drive the simulated wheelchair following 10 different complex and random paths never tried before. Fig. 2.13 depicts the 10 complex and random paths. Subject 2 did not participated in this task because she was not available.

Analysis

The system's robustness was assessed in task 1 on three criteria, namely the percentage of goals reached, the BCI classification accuracy, and the shared control (the actual mental commands sent to the wheelchair after combining the probability distributions from the BCI and contextual filter) accuracy. The three criteria were analyzed over time (5 sessions) and context. For the contextual analysis, the path was split in 7 stretches. Thus, the system's performance was measured over the final goal (complete path) and subgoals (path stretches). Additionally, to assess the subjects brain-actuated control executing this task, a random BCI (random statistical Gaussian classifier) was utilized. Its percentage of goals reached was used as a reference.

The analysis of the accuracies of the BCI and shared control has a main limitation since it requires to know the subject's intent. It is true, however, that in the experiments subjects had to inform the operator whenever they switched mental task so that the latter could label the data. Unfortunately, this approach is far from optimal. Indeed, providing this information interferes with, and so hampers, the driving task. As a consequence, the subject may deliver wrong or delayed mental commands leading to poor trajectories that the subject needs to correct by rapidly switching between mental commands—and the subject

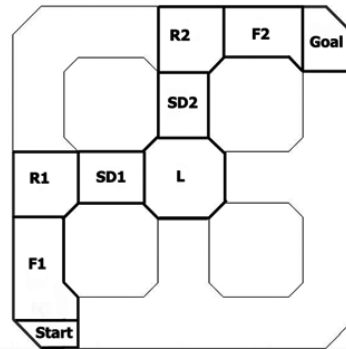


Figure 2.14: Top view of the world and the path stretches. Stretches F1 and F2 were labelled as *Forward*, R1 and R2 labelled as *Right*, L labelled as *Left*, and SD1 and SD2 labelled as strategy dependent. The subjects can go through SD1 by means of two strategies, either executing *Forward* or executing *Right* followed by *Left*. Through SD2, subjects can execute either *Forward* or *Left* followed by *Right*.

does not have time to inform the operator of all those switches and their exact timing. It follows that using the subject's stated intent for labelling data yields a pessimistic estimate of the accuracies of the BCI and the shared control. For this reason the accuracies were estimated in different way. Each path stretch was labelled with the command that makes the wheelchair reach the next subgoal, and the subject stated his intent. Only those samples where the subject's stated intent coincided with the path labelling were utilized to compute the accuracies. Fig. 2.14 shows the 7 labelled stretches.

To avoid the limitations described before, in task 2 the subject drove the wheelchair without informing the operator about the mental command he was executing. In this way, the subject could drive the simulated wheelchair in real conditions that allow a better assessment of the brain-actuated wheelchair. In this case only the behavioral performance (percentage of goals reached) was assessed.

2.5.3 Results and Conclusions

Fig. 2.15 depicts the percentage of final goals reached over the 5 sessions of task 1. Subject 1 reached more final goals in all the sessions. For both subjects, session 1 and session 3 are the sessions with less reached final goals (40% and 10% in session 1, 50% and 40% in session 3). Note that between session 2 and session 3 passed 2 months, so sessions 1 and 3 can be considered as sessions where the subjects re-learn how to interact with the system and its dynamics. If these sessions were not considered, the average percentage of reached final goals are 86.7% and 66.7% for subjects 1 and 2, respectively. Regarding the maximum performances, subject 1 reached the final goal 100% of the trials in session 4, and subject 2

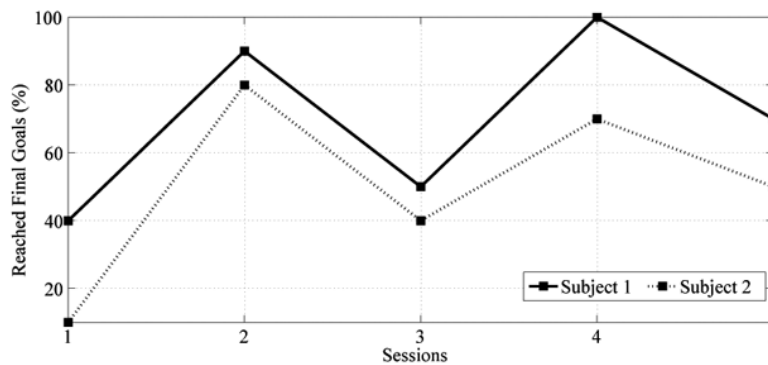


Figure 2.15: Percentage of reached final goals over sessions. The time elapsed between sessions was: 1 day between sessions 1 and 2, 2 months between sessions 2 and 3, 1 hour between sessions 3 and 4, and 1 day between sessions 4 and 5.

reached the final goal 80% of the trials in session 2. It is worth noting that even in the first session where the subjects had lower performance (40% and 10% of reached goals), it was significant compared to the percentage of goals reached by the random BCI (1%).

Table 2.5 displays the percentage of reached local goals, the average BCI classification accuracy and the shared control accuracy on each session over the 7 path stretches (local goals) for the two subjects, and the percentage of reached goals for the artificial random subject (random statistical Gaussian classifier). This table makes it clear the reasons why subjects couldn't reach the final goal—they failed sometimes to turn *Left* at the stretch L and/or to turn *Right* at the stretches R1 and R2. Interestingly, in these three stretches shared control performed generally worse than the BCI, what could indicate that subjects tried to deliver mental commands that the shared control system considers impossible to execute. On the contrary, shared control significantly improved the performance of BCI at stretches F1, SD1, SD2 and F2, where the wheelchair was supposed to go straight. The average difference over these stretches is 35% for subject 1 (24% BCI vs. 59% shared control) and 20% for subject 2 (34% BCI vs. 55% shared control). These 'poor' accuracies of the BCI and shared control indicate that to drive the wheelchair straight subjects cannot simply deliver the mental command *Forward*, but needed to steer *Left* and *Right*. Furthermore, shared control helped to generate smoother trajectories.

Subject 1 failed to reach the final goal in session 1 because he could not turn *Left* at stretch L in 30% of the cases and, afterwards, he failed to turn *Right* in 40% of the cases that he successfully arrived to stretch R2. In this session, subject 1 always performed correctly the optimal action for all other stretches he went through. As mentioned before, at these 'hard' stretches, L and R2, shared control degraded the BCI performance (50% vs. 62% in L and 47% vs. 53% in R2). Regarding session 3, subject 1 failed to reach the final goal because he could not turn *Left* at stretch L 50% of the cases. This was due to a low

Table 2.5: Percentage of local goals reached, average BCI classification accuracy and average shared control accuracy over the 7 path stretches

Subject	Criterion	Session	Path Stretch						
			F1	R1	SD1	L	SD2	R2	F2
1	Local Goals Reached (%)	1	100	100	100	70	100	57	100
		2	100	100	100	90	100	100	100
		3	100	100	100	50	100	100	100
		4	100	100	100	100	100	100	100
		5	100	90	100	89	100	88	100
	BCI / Shared Control Accuracy (%)	1	18/45	73/62	20/40	62/50	18/33	53/47	23/67
		2	22/52	73/70	26/53	57/55	20/58	68/67	19/58
		3	34/62	70/59	22/46	42/37	15/78	69/63	29/85
		4	28/55	70/63	22/66	54/51	16/57	69/64	25/68
		5	33/62	56/51	29/62	53/52	29/63	56/47	30/75
2	Local Goals Reached (%)	1	100	10	100	100	100	100	100
		2	100	100	100	90	100	89	100
		3	100	100	100	40	100	100	100
		4	100	80	100	88	100	100	100
		5	100	100	100	50	100	100	100
	BCI / Shared Control Accuracy (%)	1	40/61	29/29	17/42	89/89	25/83	61/68	36/50
		2	33/41	71/68	40/62	57/59	26/48	66/65	35/61
		3	40/55	77/75	40/57	38/37	26/56	73/67	48/70
		4	38/46	62/63	46/62	49/53	38/48	77/77	35/61
		5	31/42	65/63	27/43	48/39	27/43	77/74	24/54
Random	Local Goals Reached (%)	-	100	16	100	6	100	100	100

BCI accuracy (42%) and a lower shared control accuracy (37%). Finally, in sessions 2, 4 and 5 subject 1 reached the final goal 70% (or more) of the trials and each local goal over 88%.

Subject 2 failed to reach the final goal in session 1 because he could not turn *Right* at stretch R1 90% of the cases. This was due to a very low BCI and shared control accuracy (29%). In sessions 3 and 5, the poor final performance was due to failures in turning *Left* at stretch L—accuracies of 50% and 40%, respectively. As for subject 1, also in these two sessions shared control degraded the BCI performance although less severely (38% vs. 37% in session 3, 48% vs. 39% in session 5). Finally, in sessions 2 and 4 subject 2 reached the final goal 70% (or more) of the trials and each local goal over 80%.

The random BCI only reached the final goal 1% of the trials because only was able to turn *Right* at stretch R1 and to turn *Left* at stretch L in 16% and 6% of the trials respectively, percentages significant lower than achieved by subjects 1 and 2.

In task 2, subject 1 reached the final goal 80% of the trials. He failed in the last 2 trials, where he was not able to turn *Right* at the starting point. Making this first *Right* turn requires a very high BCI performance because the subject has to rotate the wheelchair by 90 degrees almost in place (i.e., without entering the corridor it is facing). Indeed, the execution of even a short number of wrong commands in this context makes the shared control system to move the wheelchair *Forward*. Once the wheelchair is in the corridor, the shared control system makes it very hard to turn back (180 degrees) rapidly and the trial is considered a failure. To illustrate the behavior of the brain-actuated wheelchair in this task, we have included in Appendix I a supplementary MOV file which contains the trajectories generated on trials 7 (successful) and 10 (unsuccessful).

In this section has been presented an asynchronous and non-invasive EEG-based BCI prototype for brain-actuated wheelchair driving. The system can be autonomously operated by the user without the need for adaptive algorithms externally tuned by a human operator to minimize the impact of the EEG non-stationary behavior. The brain-actuated wheelchair has two key components. First, the selection of stable user-specific EEG features that maximize the separability between the patterns generated by executing different mental tasks. Second, the inclusion of a shared control system between the BCI system and the intelligent simulated wheelchair. The reported experiments with two subjects have shown that both were able to reach 90% (subject 1) and 80% (subject 2) of the goals one day after the calibration of the BCI system, and 100% (subject 1) and 70% (subject 2) two months later. It is worth noting that both subjects reached less goals in the first session, one hour after the calibration of the BCI system, and in the third, first session after two months of the calibration of the BCI system, sessions where the subjects learn or re-learn how to interact with the system and its dynamics. However, even in these sessions, the subjects have shown significant brain-actuated control of the simulated wheelchair comparing their performance with a random BCI reached 1% of the goals.

In agreement with the results obtained in (Vanacker et al, 2007), the analysis over different path stretches has shown that the shared control system boosts the BCI performance

when it is low, while it may even degrade it when the BCI performance is higher because the user driving strategy it is not compatible with the context-based filter. As a consequence, the subject has to learn when these situations occur in order to develop successful driving strategies compatible with rules of the shared control system. On the other hand, a low BCI accuracy does *not* necessarily imply that the BCI is not working correctly. This accuracy is *estimated* according to the user's stated intent and/or the optimal command for each stretch, while for a proper control of the wheelchair subjects need to make steering corrections and so switch rapidly between mental commands. For this reason we believe that the assessment of an intelligent brain-actuated device cannot simply be based on the BCI performance. As illustrated by the results achieved in task 2, the current approach makes it possible for subject 1 to drive along complex paths once he was "free" to concentrate on the task.

Chapter 3

Conclusions

This thesis proposes methods for asynchronous and non-invasive brain computer interfaces to improve the robustness of a brain-actuated wheelchair. First, the use of mental tasks transitions detection as inferred a priori information to guide post-processing algorithms aiming at improving the decision making of the brain-computer interface system. Second, the use of a new feature extractor method for multi-class brain-computer interfaces with canonical solution that provides a reduced number of canonical discriminant spatial patterns and rank the channels sorted by power discriminability between classes. Third, the introduction of frames approach recognizing intermittent induced electroencephalographic spatial patterns of amplitude modulation to guide a novel decision making process.

The first MTTD-based post-processing algorithm proposed (see Appendix B; Galán et al. (2007b)) won the international BCI Competition III -Data Set V: Multiclass Problem, Continuous EEG- (Blankertz et al., 2006b) achieving an average classification accuracy over three subjects of 68.65% (79.60%, 70.31% and 56.02% respectively) in a 3-class problem. The inclusion of MTTD represents an absolute increase of 6% in average classification accuracy with respect to the algorithm version that does not include it. Despite these good off-line results, the algorithm have some drawbacks as the sampling rate dependency as well as the simplicity of the heuristic rule implemented. These limitations could explain the algorithm failure in some conditions where the subjects receive online feedback. In order to overcome them, a second algorithm has been proposed. The second algorithm (see Appendix C; Galán et al. (2008b)) has a new transitions detector based on Kalman filtering and includes a classifier supervisor based on heuristics rules that exploit transition detection as well as inconsistencies between subject's mental intention and the associated EEG. These heuristic rules lead to significant improvements of the BCI in terms of both classification accuracy and channel capacity, adapting itself to the user's needs. This approach yields a significant increase of the channel capacity mainly because it allows to decrease the error rates and because yields a response every 250 milliseconds (the first one yields a response every 500 milliseconds). The experimental results have shown the benefits of this algorithm in both working conditions, namely with or without online feedback. The main limitation is the use of ad-hoc heuristic rules. The next step is to formalize those

heuristic rules in a Bayesian framework and build probabilistic models for the inference of the user intent as in (Verma and Rao, 2005). It will permit to implement the MTTD-based post-processing algorithm in the brain-actuated wheelchair in order to combine the output posterior distributions with the ones coming from the context-based filter (see Fig. 1.4).

The proposed feature extractor method with canonical solution for multi-class BCI (see Appendix D; Galán et al. (2007a)) yields the space of maximum separability between ERD/ERS (Pfurtscheller and Lopes da Silva, 1999) associated to the execution of different mental tasks. In addition, the proposed DP measure ranks the electrodes sorted by their contribution in the mentioned space. It has been also shown that equivalent solutions are obtained working in different domains, namely frequency and temporal domains. In addition, experimental results show that the equivalent results, in terms of classification accuracies, are also reflected in the similarity between the DP maps obtained from the training and test sets of both domains. On the other hand, the level of similarity between DP maps obtained from the testing sets of both domains decreases for those subjects with lower classification accuracies. A possible explanation that needs to be explored is that energy (temporal domain) and PSD estimation (frequency domain) do not reflect the same phenomena when the signal is less stationary, what occurs when the subject has difficulties to generate stable EEG patterns during the execution of the mental tasks. The feature extractor has been successfully implemented in both MTTD-based post-processing algorithms and in the brain-actuated wheelchair. It also plays an essential role in the neural frame detection process. Future work will focus on developing algorithms to assess the DP stability of the original features over time in order to identify those features involved in ERD/ERS with a stable role.

The introduction of neural frames (Freeman, 2005) detection in asynchronous EEG-based BCIs (see Appendix E; Galán et al. (2007c)) implies a radical departure from current approaches. It transforms the scenario from a traditional EEG pattern recognition problem to a EEG event detection problem using pattern recognition tools. This approach has been preliminary assessed on visuo-spatial attention frame recognition. The results obtained have shown, first, the feasibility of voluntarily modulating EEG rhythms by orienting visuo-spatial attention in order to use asynchronous noninvasive EEG-based BCI's. Second, the intensity of this modulation is not sustained over time. This fact can be related to the active intermittent induced spatial patterns of amplitude modulation (frames). In this case these patterns are voluntary driven by the subject. Third, it is possible to classify the frames generated by orienting the attention to different visual locations with high classification accuracies (above 80%). Fourth, these classification accuracies are maximum in gamma band ($> 30\text{Hz}$), corresponding to endogenous shifts of attention effects (Palix et al., 2006). Fifth, classification accuracies utilizing a traditional approach, i.e. assuming modulations sustained over time, are around the chance level. It suggests that this approach is not optimal to recognize induced EEG phenomena, what is confirmed comparing the BCI theoretical channel capacity achieved using both approaches. Using frames approach the BCI theoretical channel capacity is boosted by 10. Future work will be oriented to extend the

presented study to more subjects and to develop algorithms for trial recognition based on the accumulation of evidence over time. These algorithms will yield responses on variable timing once a confident level of evidence is reached.

The three contributions of this thesis and the brain-actuated wheelchair represent research lines in progress with different degree of development. Up to date, only the feature extractor has been implemented in the BCI system integrated on the brain-actuated wheelchair.

The current version of the brain-actuated wheelchair has been described in Section 2.5 (see Appendix F; Galán et al. (2008a)). The system can be autonomously operated by the user without the need for adaptive algorithms externally tuned by a human operator to minimize the impact of the EEG non-stationary behavior. The brain-actuated wheelchair has two key components. First, the selection of stable user-specific EEG features that maximize the separability between the patterns generated by executing different mental tasks. Second, the inclusion of a shared control system between the BCI system and the intelligent simulated wheelchair. The reported experiments with two subjects have shown that both were able to reach 90% (subject 1) and 80% (subject 2) of the goals one day after the calibration of the BCI system, and 100% (subject 1) and 70% (subject 2) two months later. It is worth noting that both subjects reached less goals in the first session, one hour after the calibration of the BCI system, and in the third, first session after two months of the calibration of the BCI system, sessions where the subjects learn or re-learn how to interact with the system and its dynamics. However, even in these sessions, the subjects have shown significant brain-actuated control of the simulated wheelchair comparing their performance with a random BCI that only reached 1% of the goals.

In agreement with the results obtained in Vanacker et al. (2007) (see Appendix H), the analysis over different path stretches has shown that the shared control system boosts the BCI performance when it is low, while it may even degrade it when the BCI performance is higher because the user driving strategy it is not compatible with the context-based filter. As a consequence, the subject has to learn when these situations occur in order to develop successful driving strategies compatible with rules of the shared control system. On the other hand, a low BCI accuracy does *not* necessarily imply that the BCI is not working correctly. This accuracy is *estimated* according to the user's stated intent and/or the optimal command for each stretch, while for a proper control of the wheelchair subjects need to make steering corrections and so switch rapidly between mental commands. For this reason we believe that the assessment of an intelligent brain-actuated device cannot simply be based on the BCI performance. As illustrated by the results achieved in task 2, the current approach makes it possible for subject 1 to drive along complex paths once he was "free" to concentrate on the task.

In the last years asynchronous EEG-based BCI research has shown the feasibility to mentally control different kind of devices. The next step is to develop intelligent devices and to optimize the interaction between the user and these devices. The challenge is to promote intelligent brain interactions.

Appendix A

Non-Invasive Brain-Machine Interaction

J. del R. Millán, P. W. Ferrez, F. Galán, E. Lew, and R. Chavarriaga. Non-Invasive Brain-Machine Interaction. *International Journal of Pattern Recognition and Artificial Intelligence*, 2008. To appear.

Resum

Aquest article revisa breument la recerca que es porta a terme en el camp de les interfícies cerebrals, amb especial atenció a les interfícies no invasives basades en l'EEG, i descriu tres aplicacions desenvolupades a l'IDIAP Research Institute: un teclat virtual, un videojoc i una cadira de rodes. Finalment, es discuteixen algunes de les actuals línies de recerca del grup orientades a millorar el rendiment i la robustesa de les interfícies cerebrals desenvolupades per al control en temps real de dispositius robòtics.

La idea de controlar diferents tipus de dispositius amb el pensament (mitjançant l'activitat cerebral) ha fascinat a la humanitat des de sempre. Investigadors treballant en àrees multidisciplinars entre l'estadística, la ciència computacional, la neurociència i l'enginyeria biomèdica han començat a desenvolupar les primeres proves de concepte d'interfícies cerebrals que permeten navegar en entorns virtuals, controlar pròtesis, conduir dispositius mòbils com robots o cadires de rodes, i escriure utilitzant teclats virtuals.

Una interfície cerebral és un sistema de cicle tancat que monitoritza l'activitat cerebral de l'usuari i transforma la seva intencionalitat en accions sense necessitat d'utilitzar l'activitat muscular o el sistema nerviós perifèric. L'aspecte central d'aquest tipus d'interfície és la capacitat de reconèixer patrons d'activitat cerebral, patrons cadascun dels quals està associat a una intenció o tasca cognitiva. D'aquesta manera, una interfície cerebral és un desenvolupament tecnològic assistencial que estableix una nova modalitat interactiva entre l'usuari i l'entorn.

Com funciona una interfície cerebral? L'activitat cerebral, enregistrada amb un sistema d'adquisició, és posteriorment processada i transformada per un mòdul de processament de senyals on es seleccionen les característiques rellevants que permeten a un mòdul de reconeixement de patrons, normalment un classificador estadístic, identificar el tipus d'activitat

generada per l'usuari i associar-la a comandes que permetin controlar un dispositiu. Finalment, el feedback juga un paper essencial en el procés d'aprenentatge de l'usuari facilitant informació sobre la manera en que el sistema ha executat la comanda desitjada.

Les interfícies cerebrals desenvolupades a l'IDIAP Research Institute (IDIAP BCI) segueixen quatre principis. El primer, un protocol asíncron amb el qual els usuaris decideixen voluntàriament quan executar una tasca cognitiva, seguint el seu propi ritme, sense la necessitat d'un senyal extern que marqui la pauta d'execució. El segon, aprenentatge mutu entre la interfície i l'usuari. IDIAP BCI utilitza tècniques d'aprenentatge estadístic per descobrir els patrons EEG característics de cada usuari associats a l'execució de les diferents tasques cognitives que permeten la modulació voluntària dels diferents ritmes EEG. El tercer principi és la combinació de la intel·ligència de l'usuari i la intel·ligència artificial implementada en els diferents dispositius amb l'objectiu de facilitar la interacció i reduir la càrrega cognitiva de l'usuari. Aquest principi és particularment útil per al control de dispositius mòbils com robots i cadires de rodes. Finalment, el quart principi consisteix en el reconeixement d'estats cognitius de l'usuari associats a la percepció d'errors. D'aquesta manera, el sistema únicament executa aquelles comandes no percebudes per l'usuari com comandes erròniament reconegudes per la interfície.

NON-INVASIVE BRAIN-MACHINE INTERACTION

JOSÉ del R. MILLÁN*[†], PIERRE W. FERREZ*[†], FERRAN GALÁN*[‡], EILEEN LEW*[†],

RICARDO CHAVARRIAGA*

**IDIAP Research Institute, Centre du Parc, Av. des Prés-Beudin 20,
1920-Martigny, Switzerland*

[†]Ecole Polytechnique Fédérale de Lausanne (EPFL), Lausanne, Switzerland

*[‡]University of Barcelona, Barcelona, Spain
jose.millan@idiap.ch*

The promise of Brain-Computer Interfaces (BCI) technology is to augment human capabilities by enabling interaction with computers through a conscious and spontaneous modulation of the brainwaves after a short training period. Indeed, by analyzing brain electrical activity online, several groups have designed brain-actuated devices that provide alternative channels for communication, entertainment and control. Thus, a person can write messages using a virtual keyboard on a computer screen and also browse the internet. Alternatively, subjects can operate simple computer games, or brain games, and interact with educational software. Work with humans has shown that it is possible for them to move a cursor and even to drive a wheelchair. This paper briefly reviews the field of BCI, with a focus on non-invasive systems based on electroencephalogram (EEG) signals. It also describes three brain-actuated devices we have developed: a virtual keyboard, a brain game, and a wheelchair. Finally, it shortly discusses current research directions we are pursuing in order to improve the performance and robustness of our BCI system, especially for real-time control of brain-actuated robots.

Keywords: Brain-computer interfaces; electroencephalogram; asynchronous protocols; brain-actuated devices; statistical classifiers; feature selection.

1. Introduction

The idea of controlling machines not by manual operation, but by mere “thinking” (i.e., the brain activity of human subjects) has fascinated humankind since ever, and researchers working at the crossroads of computer science, neurosciences, and biomedical engineering have started to develop the first prototypes of *brain-computer interfaces (BCI)* over the last decade or so^{1, 2, 3, 4, 5, 6}. A BCI monitors the user’s brain activity and translates their intentions into actions—such as moving a wheelchair^{7, 8} or

selecting a letter from a virtual keyboard^{9, 10}—*without* using activity of any muscle or peripheral nerve. The central tenet of a BCI is the capability to distinguish different patterns of brain activity, each being associated to a particular intention or mental task.

Such a kind of BCI is a natural way to augment human capabilities by providing a new interaction link with the outside world and is particularly relevant as an aid for paralyzed humans, although it also opens up new possibilities in natural and direct interaction for able-bodied people. Figure 1 shows the general architecture of a BCI. Brain electrical activity is recorded with a portable device. These raw signals are first processed and transformed in order to extract some relevant features that are then passed on to some mathematical models (e.g., statistical classifiers or neural networks). This model computes, after some training process, the appropriate mental commands to control the device. Finally, visual feedback, and maybe other kinds such as tactile stimulation, informs the subject about the performance of the brain-actuated device so that they can learn appropriate mental control strategies and make rapid changes to achieve the task.

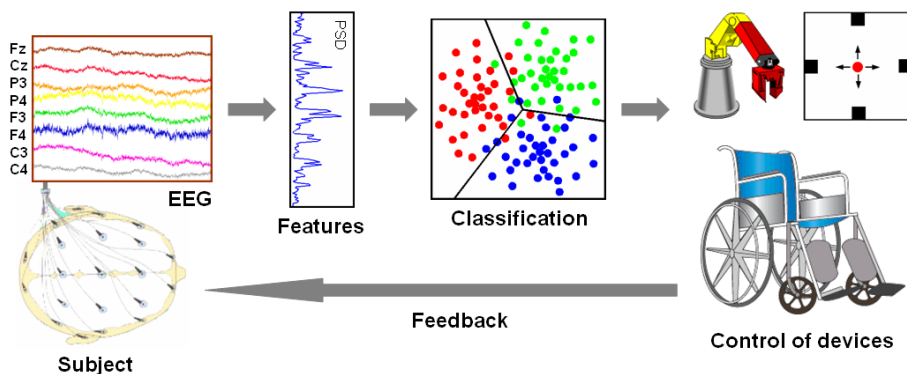


Fig. 1. General architecture of a brain-computer interface (BCI) for controlling devices such as a cursor, a robotic arm, or a motorized wheelchair. In this case the BCI measures electroencephalogram (EEG) signals recorded non-invasively from electrodes placed on the subject's scalp.

A BCI may monitor brain activity via a variety of methods, which can be coarsely classified as invasive and non-invasive. In invasive BCI systems the activity of single neurons (their spiking rate) is recorded from microelectrodes implanted in the brain. Less invasive approaches are based on the analysis of electrocorticogram (ECoG) signals from electrodes implanted under the skull. For humans, however, it is preferable to use non-invasive approaches to avoid the risks generated by permanent surgically implanted devices in the brain, and the associated ethical concerns. Most non-invasive BCI systems use electroencephalogram (EEG) signals; i.e., the electrical brain activity recorded from electrodes placed on the scalp. The main source of the EEG is the synchronous activity of thousands of cortical neurons. Measuring the EEG is a simple noninvasive way to

monitor electrical brain activity, but it does not provide detailed information on the activity of single neurons (or small brain areas). Moreover, it is characterized by small signal amplitudes (a few μ Volts) and noisy measurements (especially if recording outside shield rooms).

Besides electrical activity, neural activity also produces other types of signals, such as magnetic and metabolic, that could be used in a BCI. Magnetic fields can be recorded with magnetoencephalography (MEG), while brain metabolic activity—reflected in changes in blood flow—can be observed with positron emission tomography (PET), functional magnetic resonance imaging (fMRI), and optical imaging. Unfortunately, such alternative techniques require sophisticated devices that can be operated only in special facilities. Moreover, techniques for measuring blood flow have long latencies and thus are less appropriate for interaction.

From this short review it follows that, because of its low cost, portability and lack of risk, EEG is the ideal modality if we want to bring BCI technology to a large population. In the next sections we review the main components of our BCI system, which is based on the online analysis of spontaneous EEG signals and recognizes 3 mental tasks. Our approach relies on four principles. The first one is an asynchronous protocol where subjects decide voluntarily when to switch between mental tasks and perform those mental tasks at their own pace. The second principle is mutual learning, where the user and the BCI are coupled together and adapt to each other. In other words, we use machine learning approaches to discover the individual EEG patterns characterizing the mental tasks executed by the user while users learn to modulate their brainwaves so as to improve the recognition of the EEG patterns. The third principle is the combination of the user's intelligence with the design of intelligent devices that facilitate interaction and reduce the user's cognitive workload. This is particularly useful for mental control of robots. Finally, the fourth principle is the recognition of high-level cognitive states related to the user's awareness of erroneous responses, error potentials (ErrP). Thus, user's commands are executed only if no error is detected, what enables the BCI to interact with the user in a much more meaningful way. We also describe the three brain-actuated applications we have developed. Finally, we discuss current research directions we are pursuing in order to improve the performance and robustness of our BCI system, especially for real-time control of brain-actuated robots.

2. Spontaneous EEG and Asynchronous Operation

Non-invasive EEG-based BCIs can be classified as “evoked” or “spontaneous”. An evoked BCI exploits a strong characteristic of the EEG, the so-called evoked potential, which reflects the immediate automatic responses of the brain to some external stimuli. Evoked potentials are, in principle, easy to pick up with scalp electrodes. The necessity of external stimulation does, however, restrict the applicability of evoked potentials to a limited range of tasks. In our view, a more natural and suitable alternative for interaction is to analyze components associated with spontaneous “intentional” mental activity. This is particularly the case when controlling robotics devices. Spontaneous BCIs are based on

the analysis of EEG phenomena associated with various aspects of brain function related to mental tasks carried out by the subject at his/her own will. Such a kind of BCI can exploit two kinds of spontaneous, or endogenous, brain signals, namely slow potential shifts¹¹ or variations of rhythmic activity^{7, 9, 12, 13, 14, 15}. We will focus on the latter that are the most common.

EEG-based BCIs are limited by a low channel capacity*. Most of the current systems have a channel capacity below 0.5 bits/s³. One of the main reasons for such a low bandwidth is that they are based on synchronous protocols where EEG is time-locked to externally paced cues repeated every 4-10 s and the response of the BCI is the overall decision over this period^{11, 13, 14}. Such synchronous protocols facilitate EEG analysis since the starting time of mental states are precisely known and differences with respect to background EEG activity can be amplified. Unfortunately, they are slow and BCI systems that use them normally recognize only 2 mental states.

On the contrary, we utilize more flexible asynchronous protocols where the subject makes self-paced decisions on when to stop doing a mental task and start immediately the next one^{7, 9, 16}. In such asynchronous protocols the subject can voluntarily change the mental task being executed at any moment without waiting for external cues. The time of response of an asynchronous BCI can be below 1 second. For instance, in our approach the system responds every 1/2 second. The rapid responses of our asynchronous BCI, together with its performance (see Section 3), give a theoretical channel capacity between 1 and 1.5 bits/s.

3. The Machine Learning Way to BCI

A critical issue for the development of a BCI is training—i.e., how users learn to operate the BCI. Some groups have demonstrated that some subjects can learn to control their brain activity through appropriate, but lengthy, training in order to generate fixed EEG patterns that the BCI transforms into external actions^{11, 14}. In this case the subject is trained over several months to modify the amplitude of their EEG signals. We follow a mutual learning process to facilitate and accelerate the user's training period. Indeed, our approach allows subjects to achieve good performances in just a few hours of training in the presence of feedback⁹.

Most BCI systems deal with the recognition of just 2 mental tasks^{12, 13, 15, 16}. Our approach achieves error rates below 5% for 3 mental tasks, but correct recognition is 70%. In the remaining cases (around 20-25%), the classifier doesn't respond, since it considers the EEG samples as uncertain. The incorporation of rejection criteria (see below) to avoid making risky decisions is an important concern in BCI. From a practical point of view, a low classification error is a critical performance criterion for a BCI; otherwise users can become frustrated and stop utilizing it.

We use machine learning techniques at two levels, namely feature selection and training the classifier embedded into the BCI. In the next subsections we review both levels.

* Channel capacity is the maximum possible information transfer rate, or bit rate, through a channel.

3.1. Feature Selection

To facilitate and accelerate the mutual learning process where the user and the BCI are coupled together and adapt each other, it is necessary to select subject-specific spatio-frequency patterns embedded in the continuous EEG signal—i.e., EEG rhythms over local cortical areas that differentiate the mental tasks. The selected features are those that satisfy two criteria: maximization of the separability of the mental tasks and stability over time⁸. The feature selection process we use is based on canonical variates analysis (CVA)¹⁷, also known as multiple discriminant analysis¹⁸, which provides a canonical solution for multi-class problems. In our case, CVA extract canonical discriminant spatial patterns (CDSP) whose directions maximize the differences in mean spectral power between a given number of classes.

Let's $S_k = (s_{k1}, \dots, s_{kn_k})$ be the $n_k \times c$ matrix with the estimated spectral power of a frequency band for class $k = 1, \dots, l$ where n_k is the number of samples and c is the number of channels. Now, given $S = (S_1', \dots, S_l')$, the $l-1$ CDSP of S are the eigenvectors A of $W^{-1}B$ whose eigenvalues $\lambda_u, (u = 1, \dots, l-1)$ are larger than 0. Note that the direction of the eigenvectors A maximizes the quotient between the between-classes dispersion matrix B and the pooled within-classes dispersion matrix W . Thus, the CDSP are obtained by projecting $X = SA$. Once the CDSP are computed, we select the electrodes with higher contribution on the CDSP. This contribution is measured with a *Discrimination* index computed from the structure matrix—the pooled correlation matrix between the original channels in S and the CDSP X . Given the $c \times (l-1)$ structure matrix T , where $T = \sum_{k=1}^l T_k$ $e = 1, \dots, c$, and the normalized eigenvalues $\gamma_u = \lambda_u / \sum_{u=1}^{l-1} \lambda_u$, the proposed discrimination index is computed as

$$D_e = \left(\sum_{u=1}^{l-1} \gamma_u t_{eu}^2 / \sum_{e=1}^c \sum_{u=1}^{l-1} \gamma_u t_{eu}^2 \right) \times 100. \quad (1)$$

See Ref. 19 for more details.

3.2. Classifier

We use a statistical Gaussian classifier (see Ref. 7 for more details). The output of this statistical classifier is an estimation of the posterior class probability distribution for a sample; i.e., the probability that a given single trial belongs to each mental task (or class). Each class is represented by a number of Gaussian prototypes, typically less than four. That is, we assume that the class-conditional probability function of class C_k is a superposition of N_k Gaussian prototypes. We also assume that all classes have equal prior probability. All classes have the same number of prototypes N_p , and for each class each prototype has equal weight $1/N_k$. Then, dropping constant terms, the activity a_k^i of the i^{th} prototype of class C_k for a given sample x is the value of the Gaussian with centre μ_k^i

and covariance matrix Σ_k^i . From this we calculate the posterior probability y_k of the class C_k . The posterior probability y_k of the class C_k is now the sum of the activities of all the prototypes of class k divided by the sum of the activities of all the prototypes of all the classes. The classifier output for input vector x is now the class with the highest probability, provided that the probability is above a given threshold, otherwise the result is “unknown”. Usually each prototype of each class would have an individual covariance matrix Σ_k^i , but to reduce the number of parameters the model has a single diagonal covariance matrix common to all the prototypes of the same class. During offline training of the classifier, the prototype centers are initialized by any clustering algorithm or generative approach. This initial estimate is then improved by stochastic gradient descent to minimize the mean square error $E = \frac{1}{2} \sum_k (y_k - t_k)^2$, where t is the target vector in the form 1-of-C; that is, if the second of three classes was the desired output, the target vector is (0,1,0). The covariance matrices are computed individually and are then averaged over the prototypes of each class to give Σ_k .

4. Blending of Intelligences

To be fully operative, a BCI system has to facilitate an effective human–device interaction and reduce the user’s cognitive workload. It means the system has to be comfortable and, in the case of control of external devices such as robots and prostheses, to provide safe modes of operation. A way to promote this kind of interactions is to design smart devices, which recognize the user’s intent and execute it automatically so relieving the user from low-level detailed control, and then combine the intelligences of both, the user and the device. Section 7 introduces the brain-actuated devices developed in our lab and describes how we have developed this concept for mental control of robots and wheelchairs. Despite these initial attempts to facilitate brain interaction, the operation of brain-actuated devices requires a high degree of concentration and attentional levels.

5. Recognition of High-Level Cognitive States

EEG-based brain-computer interfaces provide disabled people with new tools for control and communication. However, as any other interaction modality based on physiological signals and body channels (e.g., muscular activity, speech and gestures), BCIs are prone to errors in the recognition of subject’s intent, and those errors can be frequent. Indeed, even well-trained subjects rarely reach 100% of success. In contrast to other interaction modalities, a unique feature of the “brain channel” is that it conveys both information from which we can derive mental control commands to operate a brain-actuated device as well as information about cognitive states that are crucial for a purposeful interaction, all this on the millisecond range. One of these states is the awareness of erroneous responses, which a number of groups have recently started to explore as a way to improve the performance of BCIs^{20, 21}. We have reported the presence of a new kind of error-related potentials (ErrP) elicited by the erroneous responses of the BCI during the recognition of the user’s intent^{22, 23, 24}. We have recently shown the feasibility of

simultaneously classifying mental commands for BCI control and detecting ErrP to filter out erroneous commands in a real-time system, all this at the single-trial level²⁵.

6. Hardware and Signal Acquisition

We acquire EEG potentials with a portable BioSemi system using a cap with either 32 or 64 integrated electrodes arranged in the modified 10/20 International System. The EEG recordings are monopolar and taken at 512Hz.

EEG signals are characterized by a poor signal-to-noise ratio and spatial resolution. Their quality is greatly improved by means of spatial filtering techniques. We use the common average reference (CAR) procedure, where at each time step the average potential over all the channels is subtracted from each channel. This re-referencing procedure removes the background activity, leaving activity from local sources beneath the electrodes. Alternatively, raw EEG potentials can be transformed by means of a Surface Laplacian (SL) derivation. The SL estimate yields new potentials that represent better the cortical activity originated in radial sources immediately below the electrodes. The superiority of SL- and/or CAR-transformed signals over raw potentials for the operation of a BCI has been demonstrated in different studies^{12, 26}.

7. Brain-Actuated Devices

BCI systems are being used to operate a number of brain-actuated applications that augment people's communication capabilities, provide new forms of entertainment, and also enable the operation of physical devices. In this section we briefly describe some of the brain-actuated devices we have developed over the years. All these systems have been largely demonstrated publicly.

Our asynchronous BCI can be used to select letters from a virtual keyboard on a computer screen and to write a message^{9, 10}. Initially, the whole keyboard (26 English letters plus the space to separate words, for a total of 27 symbols organized in a matrix of 3 rows by 9 columns) is divided in three blocks, each associated to one of the mental tasks. The association between blocks and mental tasks is indicated by the same colors as during the training phase. Each block contains an equal number of symbols, namely 9 at this first level (3 rows by 3 columns). Then, once the statistical classifier recognizes the block on which the subject is concentrating, this block is split in 3 smaller blocks, each having 3 symbols this time (1 row). As one of this second-level blocks is selected, it is again split in 3 parts. At this third and final level, each block contains 1 single symbol. Finally, to select the desired symbol, the user concentrates in its associated mental task as indicated by the color of the symbol. This symbol goes to the message and the whole process starts over again. Thus, the process of writing a single letter requires three decision steps. It goes without saying that the incorporation of statistical language models, or other techniques for word prediction such as T9 in cellular phones, will facilitate and speed up writing (cf. principle "blending of intelligences").

The second brain-actuated device is a simple computer game¹⁰, or “brain game”, but other educational software could have been selected instead. It is the classical Pacman. For the control of Pacman, two mental tasks are enough to make it turn left or right. Pacman changes direction of movement whenever one of the mental tasks is recognized twice in a row. In the absence of further mental commands, Pacman moves forward until it reaches a wall, where it stops and waits for instructions.

Finally, it is also possible to control mentally robots and prostheses. Until recently, EEG-based BCIs have been considered too slow for controlling rapid and complex sequences of movements. But we have shown for the first time^{7, 9} that asynchronous analysis of EEG signals is sufficient for humans to continuously control a mobile robot—emulating a motorized wheelchair—along non-trivial trajectories requiring fast and frequent switches between mental tasks (see Fig. 2). Two human subjects learned to mentally drive the robot between rooms in a house-like environment visiting 3 or 4 rooms in the desired order. Furthermore, mental control was only marginally worse than manual control on the same task. A key element of this brain-actuated robot is cooperative control between two intelligent agents—the human user and the robot—so that the user only gives high-level mental commands that the robot performs autonomously. In particular, the user’s mental states are associated with high-level commands (e.g., “turn right at the next occasion”) and that the robot executes these commands autonomously using the readings of its on-board sensors. Another critical feature is that a subject can issue high-level commands at any moment. This is possible because the operation of the BCI is asynchronous and, unlike synchronous approaches, does not require waiting for external cues. The robot relies on a behaviour-based controller to implement the high-level commands to guarantee obstacle avoidance and smooth turns. In this kind of controller, on-board sensors are read constantly and determine the next action to take. In particular, if from the robot’s sensor point of view a mental command is deemed to be unsafe, it will not be executed.

More recently, we have extended this work to the mental control of both a simulated and a real wheelchair (see Fig. 3). This has been done in the framework of the European project MAIA (<http://www.maia-project.org>) in cooperation with the KU Leuven. In this case, we have incorporated shared control principles into the BCI^{27, 28}. In shared control, the intelligent controller relieves the human from low level tasks without sacrificing the cognitive superiority and adaptability of human beings that are capable of acting in unforeseen situations. In other words, in shared control there are two intelligent agents—the human user and the robot—so that the user only conveys intents that the robot performs autonomously. Although our first brain-actuated robot had already some form of cooperative control, shared control is a more principled and flexible framework.

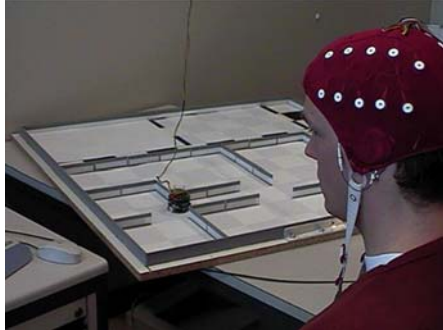


Fig. 2. One of the users while driving mentally the robot through the different rooms of the environment, making it turn right, turn left, or move forward. The robot has 3 lights on top to provide feedback to the user and 8 infrared sensors around its diameter to detect obstacles.



Fig. 3. Subject driving the wheelchair in a natural environment from non-invasive EEG. Note the laser scanner in front of the wheelchair, in between the subject's legs.

8. Current Directions of Research

For brain-actuated robots, contrarily to augmented communication through BCI, fast decision-making is critical. In this sense, real-time control of brain-actuated devices, especially robots and neuroprostheses, is the most challenging application for BCI. While brain-actuated robots have been demonstrated in the laboratory, this technology is not yet ready to be taken out and used in real-world situations. A critical issue is how to improve the robustness of BCIs with the goal of making it a more practical and reliable technology. A first avenue of research is online adaptation of the interface to the user to keep the BCI constantly tuned to its owner^{29, 30}. The point here is that, as subjects gain experience, they develop new capabilities and change their brain activity patterns. In addition, brain signals change naturally over time. In particular, this is the case from a session (with which data the classifier is trained) to the next (where the classifier is

applied). Thus, online learning can be used to adapt the classifier throughout its use and keep it tuned to drifts in the signals it is receiving in each session. Preliminary work shows the feasibility and benefits of this approach. As already mentioned, detection of error-related potentials (ErrP) prevents the execution of wrong mental commands (Sect. 5). But this is not the only way to take benefit from ErrP. Indeed, ErrP—which are generated in response to errors made by the BCI rather than by the user—can provide with performance feedback that, in combination with online adaptation, allows improving the BCI while it is being used in a fully unsupervised way³¹.

Another aspect we are currently investigating is the potential benefit of using neurocognitive knowledge to increase the recognition rate of ErrP and, more generally, the performance of the BCI. Recent findings³² have uncovered that ErrP are most probably generated in a deep fronto-central brain area called anterior cingulate cortex (ACC). We have verified this hypothesis for our ErrP using a well-known inverse method called sLORETA³³. Furthermore, in a preliminary study based on another inverse model called Cortical Current Density³⁴ we have found that the most relevant voxels (tiny cortical patches) for ErrP classification are in agreement with those neurophysiological findings and, more importantly, their use improves ErrP recognition compared to scalp EEG features²⁵. We will continue exploring the use of inverse methods for both ErrP recognition as well as for classification of mental commands.

Finally, the work on ErrP suggests that it could be possible to recognize in real time high-level cognitive and emotional states from EEG (as opposed, and in addition, to mental commands) such as alarm, fatigue, frustration, or attention that are crucial for an effective and purposeful interaction. Indeed, the rapid recognition of these states will lead to truly adaptive interfaces that customize dynamically in response to changes of the cognitive and affective states of the user.

Acknowledgements

This work is supported by the Swiss National Science Foundation through the National Centre of Competence in Research on “Interactive Multimodal Information Management (IM2)” and also by the European IST Programme FET Project FP6-003758. This paper only reflects the authors’ views and funding agencies are not liable for any use that may be made of the information contained herein.

References

1. Nicoletis, M.A.L.: Actions from Thoughts. *Nature* 409, 403–407 (2001)
2. Millán, J.d.R.: Brain-Computer Interfaces. In: Arbib, M.A. (ed.) *Handbook of Brain Theory and Neural Networks*, pp. 178–181. MIT Press, Cambridge, Massachusetts (2002)
3. Wolpaw, J.R., Birbaumer, N., McFarland, D.J., Pfurtscheller, G., Vaughan, T.M.: Brain-Computer Interfaces for Communication and Control. *Clin. Neurophysiol.* 113, 767–791 (2002)
4. Wickelgren, I.: Tapping the Mind. *Science* 299, 496–499 (2003)

5. Dornhege, G., Millán, J.d.R., Hinterberger, T., McFarland, D., Müller, K.-R. (eds.): *Towards Brain-Computer Interfacing*. MIT Press, Cambridge, Massachusetts (2007)
6. Millán, J.d.R., Ferrez, P.W., Galán, F., Lew, E., Chavarriaga, R.: Non-Invasive Brain-Actuated Interaction. In: Mele, F., Ramella, G., Santillo, S., Ventriglia, F. (eds.) *Advances in Brain, Vision, and Artificial Intelligence*, pp. 438–447. LCNS 4729, Springer, Berlin (2007).
7. Millán, J.d.R., Renkens, F., Mouriño, J., Gerstner, W.: Non-Invasive Brain-Actuated Control of a Mobile Robot by Human EEG. *IEEE Trans. Biomed. Eng.* 51, 1026–1033 (2004)
8. Galán, F., Nuttin, M., Lew, E., Ferrez, P.W., Vanacker, G., Philips, J., Van Brussel, H., Millán, J.d.R.: An Asynchronous and Non-Invasive Brain-Actuated Wheelchair. In: *13th International Symposium on Robotics Research*. Hiroshima, Japan (2007)
9. Millán, J.d.R., Renkens, F., Mouriño, J., Gerstner, W.: Brain-Actuated Interaction. *Artif. Intell.* 159, 241–259 (2004)
10. Millán, J.d.R.: Adaptive Brain Interfaces. *Comm. ACM* 46, 74–80 (2003)
11. Birbaumer, N., Ghanayim, N., Hinterberger, T., Iversen, I., Kotchoubey, B., Kübler, A., Perelmouter, J., Taub, E., Flor, H.: A Spelling Device for the Paralyzed. *Nature* 398, 297–298 (1999)
12. Babiloni, F., Cincotti, F., Lazzarini, L., Millán, J.d.R., Mouriño, J., Varsta, M., Heikkinen, J., Bianchi, L., Marciari, M.G.: Linear Classification of Low-Resolution EEG Patterns Produced by Imagined Hand Movements. *IEEE Trans. Rehab. Eng.* 8, 186–188 (2000)
13. Pfurtscheller, G., Neuper, C.: Motor Imagery and Direct Brain-Computer Communication. *Proc. IEEE* 89, 1123–1134 (2001)
14. Wolpaw, J.R., McFarland, D.J.: Control of a Two-Dimensional Movement Signal by a Noninvasive Brain-Computer Interface in Humans. *PNAS* 101, 17849–17854 (2004)
15. Blankertz, B., Dornhege, G., Krauledat, M., Müller, K.R., Kunzmann, V., Losch, F., Curio, G.: The Berlin Brain-Computer Interface: EEG-based Communication without Subject Training. *IEEE Trans. Neural Sys. Rehab. Eng.* 14, 147–152 (2006)
16. Birch, G.E., Bozorgzadeh, Z., Mason, S.G.: Initial On-Line Evaluation of the LF-ASD Brain-Computer Interface with Able-Bodied and Spinal-Cord Subjects using Imagined Voluntary Motor Potentials. *IEEE Trans. Neural Sys. Rehab. Eng.* 10, 219–224 (2002)
17. Krzanowski, W.J.: *Principles of Multivariate Analysis*. Oxford University Press, Oxford (1998)
18. Duda, R.O., Hart, P.E., Stork, D.G.: *Pattern Classification*. JohnWiley & Sons, 2nd ed. (2001)
19. Galán, F., Ferrez, P.W., Oliva, F., Guàrdia, J., Millán, J.d.R.: Feature Extraction for Multi-class BCI using Canonical Variates Analysis. In: *IEEE International Symposium on Intelligent Signal Processing*. Alcalá de Henares, Spain (2007)
20. Schalk, G., Wolpaw, J.R., McFarland, D.J., Pfurtscheller, G.: EEG-based Communication: Presence of an Error Potential. *Clin. Neurophysiol.* 111, 2138–2144 (2000)
21. Blankertz, B., Dornhege, G., Schäfer, C., Krepki, R., Kohlmorgen, J., Müller, K.R., Kunzmann, V., Losch, F., Curio, G.: Boosting Bit Rates and Error Detection for the Classification of Fast-Paced Motor Commands based on Single-Trial EEG Analysis. *IEEE Trans. Neural Sys. Rehab. Eng.* 11, 127–131 (2003)

22. Ferrez, P.W., Millán, J.d.R.: You Are Wrong!—Automatic Detection of Interaction Errors from Brain Waves. In: Proc. 19th International Joint Conference on Artificial Intelligence, Edinburgh, UK (2005)
23. Ferrez, P.W., Millán, J.d.R.: Error-Related EEG Potentials in Brain-Computer Interfaces. In: Dornhege, G., Millán, J.d.R., Hinterberger, T., McFarland, D., Müller, K.-R. (eds.) *Towards Brain-Computer Interfacing*. MIT Press, Cambridge, Massachusetts (2007)
24. Ferrez, P.W., Millán, J.d.R.: Error-Related EEG Potentials Generated during Simulated Brain-Computer Interaction. *IEEE Trans. Biomed. Eng.* To appear (2007)
25. Ferrez, P.W.: Error-Related EEG Potentials in Brain-Computer Interfaces. Ph.D. Thesis, Ecole Polytechnique Fédéral de Lausanne, Switzerland (2007)
26. Mouriño, J.: EEG-based Analysis for the Design of Adaptive Brain Interfaces. Ph.D. Thesis, Centre de Recerca en Enginyeria Biomèdica, Universitat Politècnica de Catalunya, Barcelona, Spain (2003)
27. Philips, J., Millán, J.d.R., Vanacker, G, Lew, E., Galán, F., Ferrez, P.W., Van Brussel, H., Nuttin, M.: Adaptive Shared Control of a Brain-Actuated Simulated Wheelchair. In: 10th International Conference on Rehabilitation Robotics, Noordwijk, The Netherlands (2007)
28. Vanacker, G, Millán, J.d.R., Lew, E., Ferrez, P.W., Galán, F., Philips, J., Van Brussel, H., Nuttin, M.: Context-based Filtering for Assisted Brain-Actuated Wheelchair Driving. *Computational Intelligence and Neuroscience* (2007)
29. Buttfeld, A., Ferrez, P.W., Millán, J.d.R.: Towards a Robust BCI: Error Recognition and Online Learning. *IEEE Trans. Neural Sys. Rehab. Eng.* 14, 164–168 (2006)
30. Millán, J.d.R., Buttfeld, A., Vidaurre, C., Krauledat, M., Schögl, A., Shenoy, P., Blankertz, B., Rao, R.P.N., Cabeza, R., Pfurtscheller, G., Müller, K.-R.: Adaptation in Brain-Computer Interfaces. In: Dornhege, G., Millán, J.d.R., Hinterberger, T., McFarland, D., Müller, K.-R. (eds.) *Towards Brain-Computer Interfacing*. MIT Press, Cambridge, Massachusetts (2007)
31. Chavarriaga, R., Ferrez, P.W., and Millán, J.d.R.: To Err is Human: Learning from Error Potentials in Brain-Computer Interfaces. In: 1st International Conference on Cognitive Neurodynamics, Shanghai, China (2007)
32. Holroyd, C.B., Coles, M.G.H.: The Neural Basis of Human Error Processing: Reinforcement Learning, Dopamine and the Error-related Negativity. *Psychological Rev.* 109, 679–709 (2002)
33. Pascual-Marqui, R.D.: Standardized Low Resolution Brain Electromagnetic Tomography (sLORETA): Technical Details. *Meth. Find. Exp. Clin. Pharmacol.* 24D, 5–12 (2002)
34. Babiloni, F., Babiloni, C., Locche, L., Cincotti, F., Rossini, P.M., Carducci, F.: High-Resolution Electroencephalogram: Source Estimates of Laplacian-Transformed Somatosensory-Evoked Potentials using Realistic Subject Head Model Constructed from Magnetic Resonance Imaging. *Med. Biol. Eng. Comput.* 38: 512–519 (2000)

Appendix B

Using Mental Tasks Transitions Detection to Improve Spontaneous Mental Activity Classification

F. Galán, F. Oliva, and J. Guàrdia. Using Mental Tasks Transitions Detection to Improve Spontaneous Mental Activity Classification. *Medical and Biological Engineering and Computing*, 45: 603-609, 2007b.

Resum

El present article proposa un algorisme basat en una transformació inicial en variables canòniques i anàlisi discriminant basat en distàncies, ambdós combinats amb un detector de transicions entre tasques cognitives, per a la classificació d'activitat cognitiva espontània amb l'objectiu d'operar una interfície cerebral asíncrona. L'algorisme va ser el guanyador de la BCI Competition III -Data Set V: Multiclass Problem, Continuous EEG- assolint una classificació correcta mitjana sobre tres subjectes de 68.65% (79.60%, 70.31% i 56.02% respectivament) en un problema de tres classes.

El BCI Competition III -Data Set V: Multiclass Problem, Continuous EEG- va ser enregistrat en tres subjectes sans mentre executaven tres tasques cognitives: imaginació de moviments de la ma esquerra, imaginació de moviments de la ma dreta i cerca de paraules que comencen per la mateixa lletra. Cada subjecte va participar en quatre sessions enregistrades en un mateix dia. En cada sessió, cada subjecte va executar una tasca durant 15 segons, canviant aleatòriament de tasca seguint les indicacions de l'operador. D'aquesta manera, atès que els subjectes van executar les diferents tasques cognitives de manera continuada, l'EEG no va ser segmentat en diferents assajos.

Els resultats obtinguts mostren que la inclusió d'un detector de transicions entre tasques cognitives incrementa sistemàticament la classificació correcta de les mateixes. Mentre que la versió de l'algorisme que no inclou la detecció de transicions proporciona una classificació correcta mitjana de 62.72% (75.14%, 62.18% i 50.83% per cada subjecte), l'algorisme

complet millora aquest rendiment fins a un 68.65% (79.60%, 70.31% i 56.02% respectivament).

Malgrat els resultats prometedors d'aquest algorisme, algunes limitacions, com la seva dependència respecte la freqüència de mostreig així com la simplicitat de la regla heurística implementada, fan necessari el desenvolupament de noves extensions per minimitzar l'impacte d'efectes no desitjables com artefactes.

Using mental tasks transitions detection to improve spontaneous mental activity classification

Ferran Galán · Francesc Oliva · Joan Guàrdia

Received: 3 January 2007 / Accepted: 8 May 2007 / Published online: 31 May 2007
© International Federation for Medical and Biological Engineering 2007

Abstract This paper presents an algorithm based on canonical variates transformation (CVT) and distance based discriminant analysis (DBDA) combined with a mental tasks transitions detector (MTTD) to classify spontaneous mental activities in order to operate a brain-computer interface working under an asynchronous protocol. The algorithm won the BCI Competition III -Data Set V: Multiclass Problem, Continuous EEG- achieving an averaged classification accuracy over three subjects of 68.65% (79.60, 70.31 and 56.02%, respectively) in a three-class problem.

Keywords Electroencephalogram · Brain-computer interface · Asynchronous protocol · Canonical variates transformation · Distance based discriminant analysis · Mental tasks transitions detection

1 Introduction

Brain-computer interface (BCI) research is in constant growing [9]. However, from a noninvasive approach, using electroencephalogram (EEG) signals, BCI's are still too slow to control complex sequences of movements. Some studies show the benefits to carry on mental practice and to develop concentration skills in order to improve the BCI performance [6], but the main reason for this slow control is the use of synchronous protocols where the user has to execute mental tasks when an external cue repeated in time indicates it is possible [3]. In order to overcome this disadvantage, some BCI groups are focusing their researches in developing noninvasive EEG-based BCI's that permit an asynchronous control of devices [1, 8], providing the user with the possibility to operate when he or she decides to, in a more flexible environment.

In this context, this paper presents an algorithm based on canonical variates transformation (CVT) [5] and distance based discriminant analysis (DBDA) [4] combined with a mental tasks transitions detector (MTTD) to classify spontaneous mental activities in order to operate a BCI working under an asynchronous protocol. The algorithm won the BCI Competition III -Data Set V: Multiclass Problem, Continuous EEG- [2].

This work was supported in part by Agència de Gestió d'Ajuts Universitaris i de Recerca, Departament d'Universitats Recerca i Societat de la Informació, Generalitat de Catalunya, under Grants 2002FI00437, 2001SGR00139 and 2001SGR00067, and by Ministerio de Educación y Ciencia, under Grant MTM2004-00440.

F. Galán (✉)
Departament de Metodologia de les Ciències
del Comportament, Facultat de Psicologia,
Universitat de Barcelona, Barcelona, Spain
e-mail: fgalan@ub.edu; Ferran.Galan@idiap.ch

Present Address:
F. Galán
IDIAP Research Institute, Martigny,
Switzerland

F. Oliva
Departament d'Estadística, Facultat de Biologia,
Universitat de Barcelona, Barcelona, Spain

J. Guàrdia
Departament de Metodologia de les
Ciències del Comportament, Facultat de Psicologia,
Universitat de Barcelona, Barcelona, Spain

2 Method

2.1 Data acquisition, task and preprocessing

Data were acquired by IDIAP Research Institute, Martigny, Switzerland, as described in [2, 7]. Data were recorded from three healthy subjects meanwhile they were executing three different mental tasks: imagination of self-paced left hand movements, imagination of self-paced right hand movements, and generation of words beginning with the same random letter. Each subject participated in four sessions acquired in the same day. The duration of each session was 4 min, with a inter-session break of 5–10 min. In each session, each subject performed a given task for 15 s, switching randomly to another task at the operator request. Thus, the EEG data were not split into trials since the subjects were always performing one of the mental tasks. Subjects did not received any feedback.

EEG potentials were recorded at 32 electrodes placed at standard positions of the International 10–20 system. The sampling rate was 512 Hz.

Data were provided in two ways: the raw EEG potentials and precomputed features (data used by the algorithm presented here). The precomputed features were obtained spatially filtering by means of a surface Laplacian computed globally by spherical spline of order 2. Then, every 65 ms (16 times per second) was estimated the power spectral density (PSD) in the band 8–30 Hz over the last second of data with a resolution of 2 Hz for eight channels (C3, Cz, C4, CP1, CP2, P3, Pz, and P4). Thus, an EEG sample is a 96-dimensional vector (8 channels times 12 frequency components).

The algorithm should provide an output every 0.5 s using the last second of data. That is, the goal for the competition was to estimate the class labels for every input vector of the fourth session of each subject. Since input vectors were computed 16 times per second, the labels needed to be estimated providing the average of eight consecutive samples (to get a response every 0.5 s).

The performance measure was the classification accuracy averaged over the three subjects.

2.2 Algorithm description

2.2.1 Preprocessing and feature extraction

First of all, data is transformed by means of normalizing each PSD sample estimation. Each spectral component h of channel i from sample recorded at time t $PSD_{h_t}(i)$ is normalized by dividing it by the energy of the channel

$$\widetilde{PSD}_{h_t}(i) = \frac{PSD_{h_t}(i)}{\sum_{h=1}^{12} PSD_{h_t}(i)} \quad (1)$$

Therefore, the transformed sample at time t $\widetilde{\mathbf{PSD}}_t$ is a 96-dimensional concatenated vector (8 channels times 12 normalized frequency components) as the original data \mathbf{PSD}_t . After normalization, the feature extraction process is guided by CVT. This transformation permits the projection of a p -dimensional dataset, constituted by n_l samples from $l = 1, \dots, c$ different classes, in a $(c-1)$ -dimensional feature space defined by the canonical discriminant functions that maximize the separation between the class centroids and minimize the intra-class variance [5]. This is achieved by finding the eigenvectors \mathbf{A} of $\mathbf{W}^{-1}\mathbf{B}$ with eigenvalues larger than zero, where

$$\mathbf{B} = \sum_{l=1}^c n_l (\mathbf{m}_l - \mathbf{m})(\mathbf{m}_l - \mathbf{m})' \quad (2)$$

and

$$\mathbf{W} = \sum_{l=1}^c \sum_{j=1}^{n_l} (\widetilde{\mathbf{PSD}}_{lj} - \mathbf{m}_l)(\widetilde{\mathbf{PSD}}_{lj} - \mathbf{m}_l)' \quad (3)$$

are dispersion matrices between and within classes, respectively, and

$$\mathbf{m}_l = \frac{1}{n_l} \sum_{j=1}^{n_l} \widetilde{\mathbf{PSD}}_{lj} \quad (4)$$

and

$$\mathbf{m} = \frac{1}{n} \sum_{l=1}^c n_l \mathbf{m}_l \quad (5)$$

are the class and total centroids respectively. Note that $n = \sum_{l=1}^c n_l$. The new feature space \mathbf{Y} is defined by the projection of $\widetilde{\mathbf{PSD}}$ samples induced by \mathbf{A} :

$$\mathbf{Y} = \widetilde{\mathbf{PSD}}\mathbf{A} \quad (6)$$

2.2.2 Discriminant analysis

After normalization and CVT, the algorithm discriminates between mental tasks using DBDA (see [4] for details). In this work we use the Euclidean distance but any other distance could be explored.

Given c subpopulations or classes C_1, \dots, C_c and a defined distance function d_l for class C_l , the proximity measurement for pattern \mathbf{PSD}_t with vector $\mathbf{y}_t = \widetilde{\mathbf{PSD}}_t\mathbf{A}$, is defined as

$$\phi_l(\mathbf{y}_t) = V_l(\mathbf{y}_{C_l}|\mathbf{y}_t) - V_l(\mathbf{y}_{C_l}) \tag{7}$$

where

$$V_l(\mathbf{y}_{C_l}) = \frac{1}{2} E_{C_l C_l} [d_l^2(\mathbf{y}_{C_l}, \mathbf{y}_{C_l})] \tag{8}$$

and

$$V_l(\mathbf{y}_{C_l}|\mathbf{y}_t) = E_{C_l} [d_l^2(\mathbf{y}_t, \mathbf{y}_{C_l})] \tag{9}$$

are the geometric variability and the relative geometric variability to pattern \mathbf{y}_t . Note that \mathbf{y}_{C_l} refers to those patterns belonging to class C_l . Thus, the DBDA assigns $\widetilde{\mathbf{PSD}}_t$ to C_b , if

$$\phi_l(\mathbf{y}_t) = \min_{s=1, \dots, c} [\phi_s(\mathbf{y}_t)] \tag{10}$$

In practice, suitable estimates of geometric variability and relative geometric variability to pattern \mathbf{y}_t are

$$\hat{V}_l(\mathbf{y}) = \frac{1}{2n_l^2} \sum_{j,j'=1}^{n_l} d^2(\mathbf{y}_{lj}, \mathbf{y}_{lj'}) \tag{11}$$

$$\hat{V}_l(\mathbf{y}|\mathbf{y}_t) = \frac{1}{n_l} \sum_{j=1}^{n_l} d^2(\mathbf{y}_t, \mathbf{y}_{lj}), \tag{12}$$

where \mathbf{y}_{lj} is the sample j of class l . Therefore, the estimate of the proximity function is

$$\hat{\phi}_l(\mathbf{y}_t) = \frac{1}{n_l} \sum_{j=1}^{n_l} d^2(\mathbf{y}_t, \mathbf{y}_{lj}) - \frac{1}{2n_l^2} \sum_{j,j'=1}^{n_l} d^2(\mathbf{y}_{lj}, \mathbf{y}_{lj'}). \tag{13}$$

Following the competition requirements, we have taken into account eight consecutive samples. Thus, the final decision obtained every 62.5 ms is based on the last 0.5 s. The projected sample incoming from a testing set is assigned to class C_l in time t if

$$\bar{\phi}_l(\mathbf{y}_t) = \min_{s=1, \dots, c} [\bar{\phi}_s(\mathbf{y}_t)] \tag{14}$$

where

$$\bar{\phi}_l(\mathbf{y}_t) = \frac{1}{N_{av}} \sum_{i=1}^{N_{av}} \hat{\phi}_l(\mathbf{y}_{t-i+1}) \tag{15}$$

is an average proximity over $N_{av} = 8$ consecutive samples.

2.2.3 Mental tasks transitions detector (MTTD)

With the aim to improve classification accuracy, we have designed a parallel discriminant process guided by a MTTD. For each new incoming sample, after normaliza-

tion and canonical variates projection, the algorithm works as follows:

1. Compute an index to detect transitions. It is easy to detect a mental task transition at time t with the index

$$I(\widetilde{\mathbf{PSD}}_t) = |\Psi(\widetilde{\mathbf{PSD}}_{t-1}, \widetilde{\mathbf{PSD}}_t) - \Psi(\widetilde{\mathbf{PSD}}_{t-2}, \widetilde{\mathbf{PSD}}_{t-1})| \tag{16}$$

if $\min[I(\widetilde{\mathbf{PSD}}_{t-1}), I(\widetilde{\mathbf{PSD}}_t)] > \theta$, where θ is a fixed threshold and $\Psi(\cdot)$ is a dissimilarity function. In this work we use the Euclidean distance. It is worth noting that the detection of a mental task transition needs only four $\widetilde{\mathbf{PSD}}$ patterns, and does not introduce any delay given that detects a sudden change at time t .

2. Classify the sample with DBDA.
3. If $\min[I(\widetilde{\mathbf{PSD}}_{t-1}), I(\widetilde{\mathbf{PSD}}_t)] > \theta$, compute class proportions $p(C_l)$ assigned by DBDA in the gap limited by two last transitions or by first sample and first transition. Otherwise, do nothing.
4. If $\max_h[p(C_h)] > \zeta$, where ζ is a fixed threshold, until next transition remove from training data those samples labeled as C_h and reclassify the new sample once again with DBDA into resting classes. Otherwise, do nothing (maintain classification from step 2).

Note that mental tasks transitions detection yields to use transitions to discard the class that can be assumed as predominant (with a proportion bigger than ζ) in the gap limited by the two last transitions, improving chance classification in next incoming samples from 0.33 to 0.50.

3 Results and discussion

The algorithm was first tested with *sessions 2 and 3*. In order to do this, when the algorithm was tested with the second session, it had been trained with the first session; and when it was tested with the third session, it had been trained with the first two sessions, both individually and jointly. The transition detector threshold was fixed at $\theta = 0.2$, and the probability threshold, at $\zeta = 0.55$.

Table 1 shows the algorithm performance over the three subjects, according to the test conditions mentioned above. For each subject, the first row refers to the performance of the algorithm without including MTTD while the second one refers to the complete algorithm. These results showed two aspects worth highlighting that were considered in the competition testing with *session 4*. On the one hand, the inclusion of MTTD systematically improved the performance of the classification. On the other hand, when the algorithm was tested with the third session, the results indicated it was advisable to train it with the two first sessions jointly. This action produced the best performance

Table 1 Classification accuracy over the three subjects according to different test conditions

Subject	MTTD	Test condition				Competition test 1 + 2 + 3 → 4
		1 → 2	1 → 3	2 → 3	1 + 2 → 3	
1	No	67.4%	69.73%	72.87%	74.86%	75.14%
	Yes	72.84%	72.09%	75.64%	76.46%	79.60%
2	No	51.94%	59.99%	58.64%	62.41%	62.18%
	Yes	59.58%	68.03%	64.86%	68.72%	70.31%
3	No	52.31%	42.97%	38.69%	42.73%	50.83%
	Yes	61.68%	46.45%	39.10%	43.49%	56.02%
Average	No	57.33%	57.56%	56.73%	60.00%	62.72%
	Yes	64.70%	62.19%	59.87%	62.89%	68.65%

over the two first subjects. Similar results to the best performance were obtained over the third subject, which was achieved when only the first session was used to train the algorithm. Thus, all patterns from the first three sessions jointly were taken as a training set for the competition, and the thresholds were fixed at $\theta = 0.2$ and $\xi = 0.55$. Likewise, Table 1 shows the competition results too: the algorithm without MTTD inclusion provides a mean classification accuracy of 62.72% (75.14, 62.18 and 50.83% for each subject), whereas the complete algorithm improves this mean classification accuracy up to 68.65% (79.60, 70.31 and 56.02%).

For each subject, the plots in the first row of Figs. 1, 2, 3 show temporal plots with labeling during the fourth session (1 + 2 + 3 → 4 condition) produced by the algorithm without MTTD, with MTTD, and produced by the subjects (correct labels) respectively, $I(\mathbf{PSD}_t)$ values, and threshold $\theta = 0.2$. In the second row, the same data is displayed, but projected into canonical variates space. These figures help to understand the results obtained and the way the MTTD works. Note that labels 2, 3 and 7 refer to mental tasks: imagination of repetitive self-paced left hand movements, imagination of repetitive self-paced right hand movements, and generation of words beginning with the same random letter respectively.

Temporal plots provide intrasessions information while projections into canonical variates space provide intersessions information (note that we are projecting samples of the fourth session into a space constructed from the first three sessions). In this sense, it is possible to say that the relatively good results of the algorithm over *subject 1* are due to the consistent dissimilarity of different mental task patterns produced in a session, and the ability to maintain this in the same way along different sessions. In this sense, it is observable in the temporal *without MTTD* plot, that in most of the gaps where the subject says to be doing a mental task, there are few samples classified in another class, fitting the subject's labeling. On the other hand, the

similarity between the projections into canonical variates of samples labeled by the algorithm with respect to those labeled by the subject show that feature extraction from the first three sessions constructs a valid space to represent and discriminate samples from different mental activities from *session 4*. For their part, the plots from *subjects 2 and 3* show a very different behavior. These subjects produce poorer discriminable patterns. This is clearly shown in temporal *without MTTD* plots, where the subjects say to be doing a mental task, but there is an important number of samples classified into different classes. Simultaneously, for this reason, mental tasks cannot be represented as consistent patterns along different sessions. This is represented in canonical variates plots where there is a mismatch between the labeling carried out by the subjects and the algorithm classification, showing that canonical variates space obtained from *sessions 1, 2 and 3* is not able to fully represent samples from *session 4*.

Related to the algorithm differential performance over the three subjects, there is a particular explanation for each case. In case of *subject 1*, the algorithm gets the smallest improvement (4.46%) with the MTTD inclusion. This is due to an initial good performance, which is nearest to the maximum possible classification accuracy, achieved by using a good representation space. In this case, the fact of getting $\max_h[p(C_h)] > \xi$ in all temporal gaps does not have many consequences. On the other hand, although *subject 3* does not show much improvement either (5.19%), the reason is totally different. In this case, the inclusion of MTTD does not improve performance substantially because there is one out of eight temporal gaps (specifically the eighth one) achieving $\max_h[p(C_h)] > \xi$, which is not representative of the mental task being executed, thus producing the misclassification process of the next temporal gap. This problem, could be averted by fixing a more conservative threshold ξ . In fact, if it is fixed at $\xi = 0.50$, $\max_h[p(C_h)] > \xi$ is not achieved in the eighth temporal gap and the misclassification process of the ninth one does not

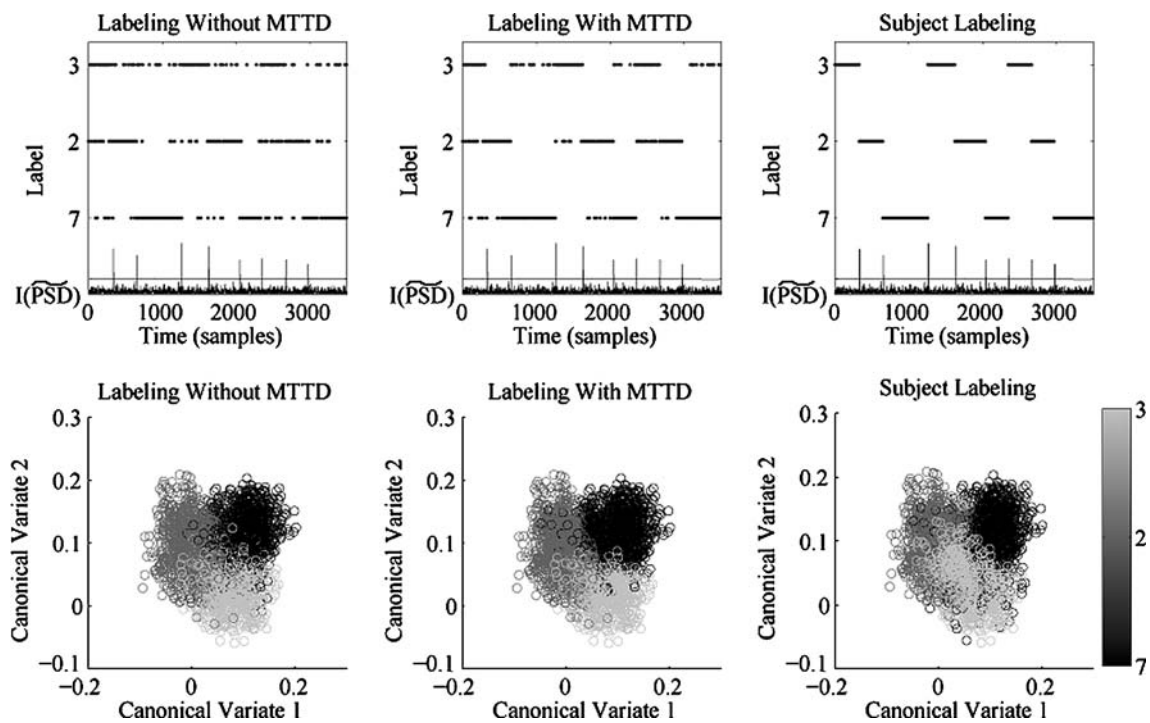


Fig. 1 Above, temporal plots of 1 + 2 + 3 → 4 condition with labeling obtained from the algorithm without MTTD, with MTTD, and *subject 1*. Each one shows labeling, $I(\widehat{PSD}_t)$ values and threshold $\theta = 0.2$. Below, corresponding projections into canonical variates space

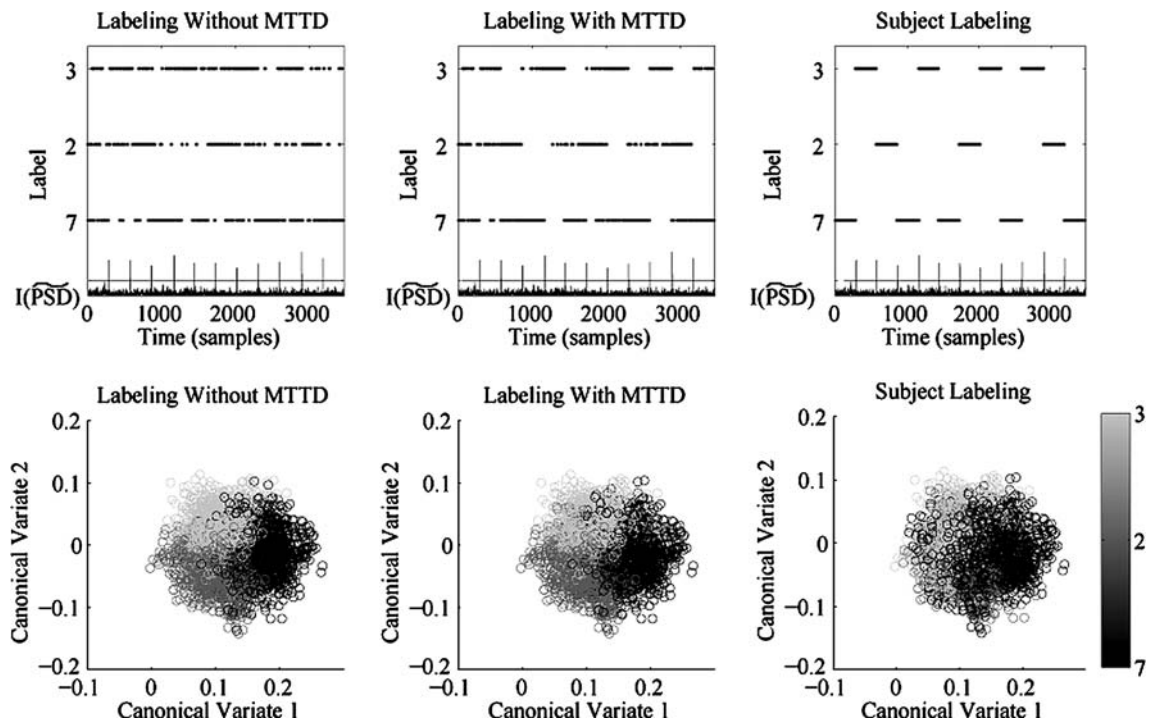


Fig. 2 Above, temporal plots of 1 + 2 + 3 → 4 condition with labeling obtained from the algorithm without MTTD, with MTTD, and *subject 2*. Each one shows labeling, $I(\widehat{PSD}_t)$ values and threshold $\theta = 0.2$. Below, corresponding projections into canonical variates space

occur. In this case, the algorithm gets a classification accuracy of 59.95%. On the other hand, the algorithm performance over *subject 2* shows the greatest improve-

ment with the MTTD inclusion. This is caused by the existence of several gaps (specifically nine) where the expression $\max_h[p(C_h)] > \xi$ is true, jointly with the exist-

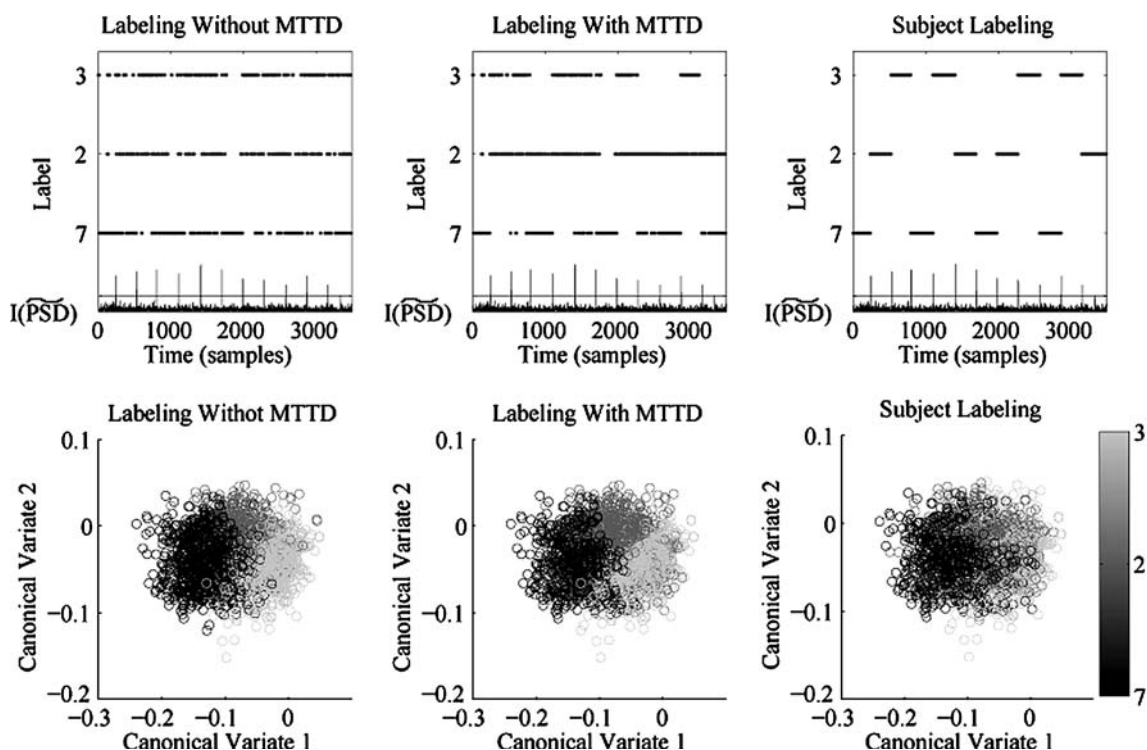


Fig. 3 Above, temporal plots of 1 + 2 + 3 → 4 condition with labeling obtained from the algorithm without MTTD, with MTTD, and *subject 3*. Each one shows labeling, $I(\text{PSD}_t)$ values and threshold $\theta = 0.2$. Below, corresponding projections into canonical variates space

tence of a representation space that, though far from the appropriate one, maintains a basic structure in common with the samples from the fourth session, thus giving a broad margin to modify it. In this case, we can say that this subject is a scarcely consistent one, the kind of subject where the MTTD inclusion produces maximum improvements (8.13% in this case).

In terms of processing time of the algorithm, the MTTD increases it 77 ms per sample (utilizing an Intel CPU T2500 at 2.00 GHz, 2 GB of RAM and MATLAB <http://www.mathworks.com/products/matlab/>), what permits to implement it online.

4 Conclusion

This paper reported the benefits to use mental tasks transitions detection to improve spontaneous mental activity classification for BCI applications. The proposed algorithm showed promising results in a BCI working without online feedback. Some drawbacks as the sampling rate MTTD dependency as well as the simplicity of the heuristic rule implemented on it will guide future extensions of this approach to avoid undesired effects of artifacts detection. These results clearly call for further

studies assessing the algorithm performance on BCI's working in different conditions where the subjects receive online feedback.

Acknowledgments We thank the anonymous reviewers their contribution to improve the quality of the manuscript with their comments and Dr José del R. Millán for valuable discussions.

References

- Blankertz B, Dornhege G, Lemm S, Krauledat M, Curio G, Müller K-R (2006) The Berlin brain-computer interface: machine learning based detection of user specific brain states. *J Univers Comput Sci* 12:581–607
- Blankertz B, Müller K-R, Krusienski D, Schalk G, Wolpaw JR, Schlögl A, Pfurtscheller G, Millán J del R, Schröder M, Birbaumer N (2006) The BCI competition III: validating alternative approaches to actual BCI problems. *IEEE Trans Neural Syst Rehab Eng* 14:153–159
- Boostani R, Graimann B, Moradi MH, Pfurtscheller G (2007) A comparison approach toward finding the best feature and classifier in cue-based BCI. *Med Biol Eng Comput* 45:403–412
- Cuadras CM, Fortiana J, Oliva J (1997) The proximity of an individual to a population with applications in discriminant analysis. *J Classif* 14:117–136
- Krzanowski WJ (1988) *Principles of multivariate analysis*. Oxford University Press, Oxford
- Mahmoudi B, Erfanian A (2006) Electro-encephalogram based brain-computer interface: improved performance by mental

- practice and concentration skills. *Med Biol Eng Comput* 44:959–969
7. Millán J del R (2004) On the need for on-line learning in brain-computer interfaces. In: *Proceedings of international joint conference on neural networks*
 8. Millán J del R, Renkens F, Mouriño J, Gerstner W (2004) Noninvasive brain-actuated control of a mobile robot by human EEG. *IEEE Trans Biomed Eng* 51:1026–1033
 9. Vaughan TM, Wolpaw JR (2006) The third international meeting on brain-computer interface technology: making a difference. *IEEE Trans Rehab Eng* 14:126–127

Appendix C

Detecting Intentional Mental Transitions in an Asynchronous BCI

F. Galán, F. Oliva, J. Guàrdia, P.W. Ferrez, and J. del R. Millán. **Detecting Intentional Mental Transitions in an Asynchronous Brain-Computer Interface.** *Medical and Biological Engineering and Computing*, 2008b. Submitted.

Resum

La introducció de la detecció de transicions entre tasques cognitives ha mostrat la seva utilitat (veure Apèndix A; Galán et al., 2007b) en el procés de transducció d'una interfície cerebral operant en modalitat asíncrona. La detecció de transicions permet extreure informació contextual amb l'objectiu d'inferir la intencionalitat de l'usuari en un moment concret i d'aquesta manera corregir possibles errors de classificació. Malgrat els resultats prometedors de l'algorisme, algunes limitacions com la seva dependència respecte la freqüència de mostreig així com la simplicitat de la regla heurística implementada limiten el seu rendiment.

L'algorisme proposat en aquest article inclou un nou detector de transicions basat en filtres de Kalman, i un supervisor del mòdul classificador basat en heurístics. L'esmentat supervisor treu profit tant de la informació extreta pel detector de transicions com de la detecció d'inconsistències entre la intencionalitat del subjecte i l'electroencefalograma (EEG) associat. D'aquesta manera els heurístics permeten augmentar el rendiment tant en termes de classificació correcta com de capacitat de comunicació.

Aquest nou algorisme ha estat avaluat tant amb el BCI Competition III -Data Set V: Multiclass Problem, Continuous EEG-, com amb dades enregistrades durant quatre sessions experimentals on dos subjectes rebien retroalimentació visual de manera continuada d'un robot real i d'un robot virtual. Els resultats obtinguts mostren que la introducció dels nous components proporcionen una estimació més robusta de les tasques cognitives executades pels subjectes. L'increment obtingut en termes de capacitat de comunicació s'explica principalment per la reducció de la taxa d'error.

La principal limitació d'aquesta versió és la utilització d'heurístics en el mòdul supervisor. El següent pas estarà orientat a formalitzar aquests heurístics en un marc Baiesià i construir models probabilístics per a inferir la intencionalitat dels subjectes com a (Verma i Rao, 2006).

Medical and Biological Engineering and Computing manuscript No. (will be inserted by the editor)
--

Detecting Intentional Mental Transitions in an Asynchronous Brain-Computer Interface

Received: / Accepted:

Abstract The inclusion of mental tasks transitions detection (MTTD) has been proven as a useful tool in guiding the transduction process of a brain-computer interface (BCI) working under an asynchronous protocol [8]. The algorithm proposed in this paper includes a new transitions detector based on Kalman filtering and a classifier supervisor based on heuristics rules. The classifier supervisor exploits transition detection as well as inconsistencies between subject's mental intention and the associated Electroencephalogram (EEG). These heuristic rules

This work was supported in part by Agència de Gestió d'Ajuts Universitaris i de Recerca, Departament d'Universitats Recerca i Societat de la Informació, Generalitat de Catalunya, under Grants 2002FI00437, 2001SGR00139 and 2001SGR00067, by Ministerio de Educación y Ciencia, under Grant MTM2004-00440, by the Swiss National Science Foundation through the National Centre of Research on "Interactive Multimodal Information Management (IM2)", and by the European IST Programme FET Project FP6-003758. This paper only reflects the author's views and founding agencies are not liable for any use that may be made of the information contained herein.

Ferran Galán
IDIAP Research Institute, Martigny, Switzerland
Tel.: +41-27-7217747
Fax: +41-27-7217712
E-mail: Ferran.Galan@idiap.ch

Francesc Oliva
Departament d'Estadística, Facultat de Biologia, Universitat de Barcelona, Barcelona, Spain

Joan Guàrdia
Departament de Metodologia de les Ciències del Comportament, Facultat de Psicologia, Universitat de Barcelona, Barcelona, Spain

Pierre W. Ferrez
IDIAP Research Institute, Martigny, Switzerland

José del R. Millán
IDIAP Research Institute, Martigny, Switzerland

lead to improvements of the BCI in terms of both classification accuracy and channel capacity.

1 Introduction

The possibility of acting upon the environment that surrounds us without using our nervous system's efferent pathway opens the door to new ways of interaction that can compensate for total or partial loss of mobility. Research in brain-computer interface (BCI) has made it possible to transform brain activity into mental commands for navigating in virtual environments [1], controlling prosthetic devices [5], steering mobile robots [14] and wheelchairs [9], or writing on virtual keyboards [3]-[12]-[15]. BCI systems can be characterized along two orthogonal dimensions. The first one is the nature of the recorded brain signals, either invasive (obtained from implanted microelectrodes) or non-invasive (based on electroencephalogram, EEG, measured from scalp electrodes). The second dimension is the interaction protocol, either synchronous (time-locked to externally-paced cues) or asynchronous (guided by the user's self-paced decisions). Our work is focused on asynchronous non-invasive BCIs so that humans can interact with brain-actuated devices as flexibly and naturally as possible.

The algorithm proposed in this paper is an extension of our previous work [8], the winner of the last international BCI Competition III for 'Data set V' [4]. The new algorithm, like its antecessor, is based on canonical variates transformation (CVT) [11] and on distance-based discriminant analysis (DBDA) [6], but it has a new transitions detector based on Kalman filtering. In addition, it includes a classifier supervisor based on heuristics rules that exploit transition detection as well as inconsistencies between subject's mental intent and the associated EEG. These heuristic rules lead to improvements of the BCI in terms of both classification accuracy and channel capacity.

2 Method

2.1 Data Acquisition and Mental Tasks

For the offline assessment of the proposed algorithm we have used two datasets. The first one is the 'Data set V' of the BCI Competition III [4], where subjects did not receive any feedback indicating their performance. The second one comes from feedback experiments. In both datasets, EEG signals were recorded with a portable Biosemi acquisition system from 32 (first dataset) or 64 (second dataset) electrodes. The sampling frequency was 512 Hz. The signal was spatially filtered using a surface Laplacian (first dataset) or common average reference (CAR) (second dataset) previous to the estimation every 62.5 ms. (16 times per second) of the PSD in the band 8-30-Hz, with a resolution of 2Hz over the last 1-second windows. In the first dataset the PSD was estimated on the electrodes C3, Cz, C4, CP1, CP2, P3, Pz, P4; thus obtaining a 96-dimensional vector (8 electrodes \times 12 frequency components) as a pattern. In the second dataset the PSD was estimated on F3, F4, FC1, FC2, C3, C1, C2, C4, CP1 and CP2 obtaining a 120-dimensional vector (10

electrodes \times 12 frequency components). The computation of the EEG patterns, the vector **PSD**, is described in [4]-[13].

Data come from 5 healthy voluntary subjects. Subjects 1, 2 and 3 from the first dataset carried out three mental tasks, two motor imagination tasks (right-left hand movement imagination) and one cognitive task (search of words with the same initial letter) for 15 seconds switching randomly between them at the operator’s request. EEG signals were recorded during 4 non-feedback sessions (see [6] for details). Subjects 4 and 5 executed the same mental tasks also during 4 sessions while receiving continuous visual feedback from the movement of a virtual robot in the case of subject 4, or from a real mobile robot in the case of subject 5. The robots were controlled by the association between the subject’s mental states and high-level commands (right-left hand imagination with right-left turns, and word search with forward movements). In addition, the brain-actuated robots relied on a behavior-based controller that guarantee obstacle avoidance and smoothed turns [14]. These two subjects were at the very beginning of their training with the robots.

For every subject, the first three sessions were used as training and validation sets while the fourth session was the test set.

2.2 Algorithm Description

The proposed algorithm incorporates three components: an *inconsistencies detector* (Section 2.3) between the user’s intent and the measured EEG patterns that assigns a provisional label to each incoming pattern, a *transitions detector* based on Kalman filtering (Section 2.4) that detects patterns not similar to their predecessors, and a *classifier supervisor* based on three heuristic rules (Section 2.5) that determine which of these patterns identified as transitions by the transitions detector are intentional transitions between different mental tasks. Figure 1 depicts a schematic representation of the overall algorithm. The inconsistencies detector, based on a bi-feature extractor and a bi-classifier, works in parallel with the transition detector. Thus, each incoming pattern is first checked for inconsistency and transition. Next, based on three heuristic rules and only using the labels of the three last patterns identified as transitions, the classifier supervisor eventually changes the label of the pattern provided by the inconsistencies detector.

2.3 Inconsistencies Detector

One of the main difficulties of classifying spontaneous brain activity is its variability over time. Physiological reasons, like endogenous brain processes and fatigue, cause slow changes of EEG over time. An approach to deal with this type of non-stationarity is to build adaptive classifiers that track this variability [13]. In addition, rapid shifts in the user’s motivational and attentional states¹ may lead to a mismatch between the user’s intent and the user’s EEG patterns. The aim of

¹ For instance, erroneous responses of the BCI, especially if they are frequent as it is the case at the beginning of the user’s training, may disconcert and frustrate the user.

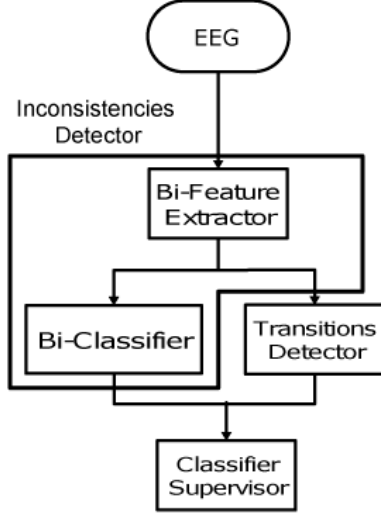


Fig. 1 Schematic representation of the whole algorithm. Note that the inconsistencies detector (based on a bi-feature extractor and a bi-classifier) and the transitions detector work in parallel. The output of the two previous components is used by the classifier supervisor.

the inconsistencies detector is to identify those patterns that likely are inconsistent with the user’s intent.

In order to identify inconsistent patterns we propose to build two canonical spaces by means of a canonical variates transformation (CVT), as in [8]. The first one is based on the original labelling that corresponds to the user’s intent (*intentional* labelling)—i.e., it is obtained by a direct CVT on the training set. In the second case, after building the canonical space as in the first case, we carry out k-means cluster analysis (using Euclidean distance) and generate as many clusters as mental tasks (3, in our case). Then we relabel the patterns in the training set with the labels obtained from the clustering process (*measured* labelling) and build a new canonical space. This Bi-CVT process yields two different canonical spaces, the intentional and the measured canonical spaces (see Figure 2). Afterwards, we project the patterns of the test set onto both canonical spaces and the resulting projections are sent to each DBDA classifier. The outputs of these two classifiers are combined to obtain a final decision, called Bi-DBDA, which labels a pattern as *unknown* if the outputs of the two previous DBDA classifiers are inconsistent—i.e., they are different.

The different steps of the inconsistencies detector are the following²:

1. *Normalization*: Each spectral component h of channel i from the pattern recorded at time t , $PSD_{h_t}(i)$, is normalized by the energy of the channel

$$\widetilde{PSD}_{h_t}(i) = \frac{PSD_{h_t}(i)}{\sum_{h=1}^n PSD_{h_t}(i)} \quad (1)$$

² Note that the first step is the normalization of the frequency components of each electrode.

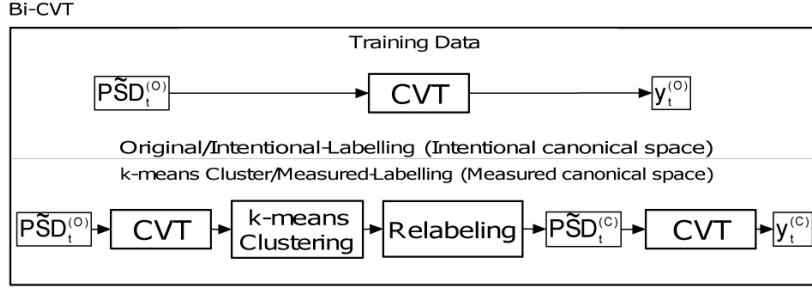


Fig. 2 Bi-feature extractor based on CVT (Bi-CVT). From the training data we build two canonical spaces, the intentional canonical space using the original labelling (top), and the measured canonical space using the k-means cluster labelling (bottom). Patterns whose projections onto the canonical spaces do not match are potentially inconsistent and the Bi-DBDA labels them as *unknown*.

2. *Bi-CVT*: We find the eigenvectors $\mathbf{A}^{(O)}$ and $\mathbf{A}^{(C)}$ of $\mathbf{W}^{-1(O)}\mathbf{B}^{(O)}$ and $\mathbf{W}^{-1(C)}\mathbf{B}^{(C)}$ with eigenvalues greater than zero, where $\mathbf{B}^{(\cdot)}$ and $\mathbf{W}^{(\cdot)}$ are the between- and within-classes dispersion matrices, obtained from the matrices $\widetilde{\mathbf{PSD}}^{(O)}$ and $\widetilde{\mathbf{PSD}}^{(C)}$ of patterns with the original labels (*intentional* labelling) or with the cluster-analysis labels (*measured* labelling), respectively. Then, we compute the projections

$$\mathbf{y}_t^{(O)} = \widetilde{\mathbf{PSD}}_t^{(O)} \mathbf{A}^{(O)} \quad (2)$$

$$\mathbf{y}_t^{(C)} = \widetilde{\mathbf{PSD}}_t^{(C)} \mathbf{A}^{(C)} \quad (3)$$

3. *Bi-DBDA*: The label ν_t of the incoming pattern at time t with projections $\mathbf{y}_t^{(O)}$ and $\mathbf{y}_t^{(C)}$ is

$$\nu_t = \begin{cases} g & \text{if } (\bar{\phi}_g(\mathbf{y}_t^{(O)}) = \min_k [\bar{\phi}_k(\mathbf{y}_t^{(O)})]) \cap (\bar{\phi}_g(\mathbf{y}_t^{(C)}) = \min_k [\bar{\phi}_k(\mathbf{y}_t^{(C)})]) \\ \text{unknown} & \text{otherwise} \end{cases} \quad (4)$$

where k is the number of classes and $\bar{\phi}_g(\mathbf{y}^{(\cdot)})$ is the average of DBDA proximity estimates, $\hat{\phi}_g(\mathbf{y}^{(\cdot)})$ (see appendix), in the corresponding canonical space over $N_{av} = 4$ consecutive patterns

$$\bar{\phi}_g(\mathbf{y}^{(\cdot)}) = \frac{1}{N_{av}} \sum_{i=1}^{N_{av}} \hat{\phi}_g(\mathbf{y}_{t-i+1}^{(\cdot)}) \quad (5)$$

Thus, the final decision is obtained every 0.250 s. In this way, the new pattern is assigned to class C_g only if the two DBDA classifiers agree. See Figure 3 for an example.

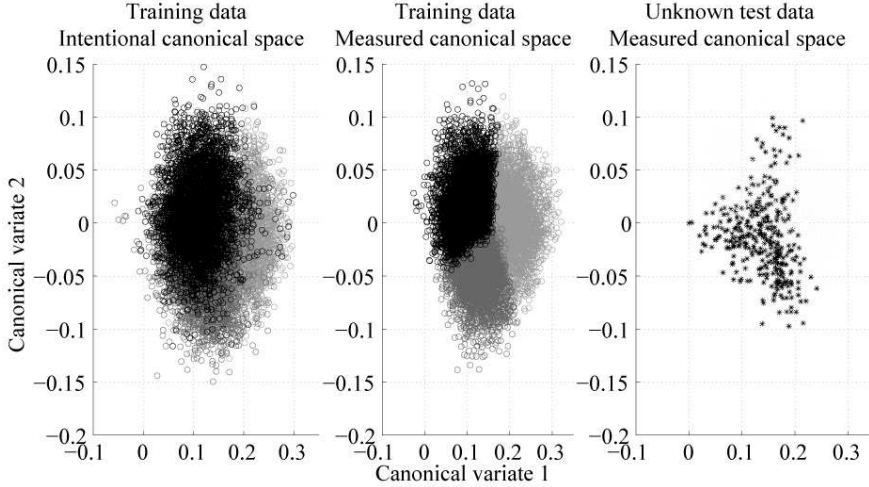


Fig. 3 Bi-DBDA example, subject 1. *Left*: Training data projection with original labels on the intentional canonical space (black: imagination of left hand movement; dark grey: imagination of left hand movement, light grey: word search). *Middle*: Training data projection with cluster labels on the measured canonical space. *Right*: Test data labelled by Bi-DBDA as unknown projected on the measured canonical space. These inconsistent patterns are those projected onto the mismatch areas of the two canonical spaces.

2.4 Transitions Detector Based on Kalman Filtering

Kalman filtering is a principled approach to detect abrupt changes in temporal series [2]. We have used it to build a more robust transitions detector than in the previous algorithm [8]. While the inconsistencies detector filters patterns given the relative positions of its projections on both training canonical spaces, the transitions detector checks for patterns whose distances to their predecessors on the measured canonical space are larger than expected. Thus, the transitions detector filters those patterns that are likely intentional transitions between different mental tasks.

Using the projected patterns ($\mathbf{y}_t^{(C)}$) in the canonical space obtained with labels computed by k-means cluster analysis (*measured* labelling), we have built the linear state dynamical system

$$\begin{aligned} \mathbf{x}_t &= \mathbf{A}\mathbf{x}_{t-1} + \mathbf{w}_{t-1} \\ \mathbf{y}_{t-1}^{(C)} &= \mathbf{H}\mathbf{x}_{t-1} + \mathbf{v}_{t-1} \end{aligned} \quad (6)$$

where \mathbf{x}_t , \mathbf{A} and \mathbf{H} are the state vector, the state matrix and the measurement matrix, respectively. The state noise \mathbf{w}_{t-1} and the measurement noise \mathbf{v}_{t-1} are assumed to be uncorrelated zero-mean Gaussian white-noise processes with covariance matrices \mathbf{Q} and \mathbf{R} . The Kalman filter finds the optimal state estimate $\hat{\mathbf{x}}_t$ (minimizing the variance error estimator, defined as $E[\|\mathbf{x}_t - \hat{\mathbf{x}}_t\|^2]$) given a set of past observations $\{\mathbf{y}_1^{(C)}, \dots, \mathbf{y}_t^{(C)}\}$ in a prediction-correction approach:

1. **Prediction equations.** In this step, the prediction of the state of the system at time t $\hat{\mathbf{x}}_{t|t-1}$ and his variance $\mathbf{P}_{t|t-1}$ are computed from the estimates and $\mathbf{P}_{t-1|t-1}$ at time $t-1$ and the noise covariance \mathbf{Q} :

$$\hat{\mathbf{x}}_{t|t-1} = \mathbf{A}\hat{\mathbf{x}}_{t-1|t-1} \quad (7)$$

$$\mathbf{P}_{t|t-1} = \mathbf{A}\mathbf{P}_{t-1|t-1}\mathbf{A}^T + \mathbf{Q} \quad (8)$$

Initial matrices \mathbf{A} , \mathbf{H} , \mathbf{Q} and \mathbf{R} were estimated with EM algorithm [7] using the third session. As initial values estimates we have fixed $\hat{\mathbf{x}}_{t-1|t-1} = \mathbf{y}_{t-1}^{(C)}$ and $\mathbf{P}_{t-1|t-1} = \mathbf{R}$.

2. **Correction equations.** The obtained estimates in the prediction step are corrected by the innovation process

$$\epsilon_t = \mathbf{y}_t^{(C)} - \mathbf{H}\hat{\mathbf{x}}_{t|t-1} \quad (9)$$

defined as the difference between the new measured value $\mathbf{y}_t^{(C)}$ and the hypothetical measured value given the estimate $\hat{\mathbf{x}}_{t|t-1}$ at time t . Then, the corrected estimates are

$$\hat{\mathbf{x}}_{t|t} = \hat{\mathbf{x}}_{t|t-1} + \mathbf{K}_t[\mathbf{y}_t^{(C)} - \mathbf{H}\hat{\mathbf{x}}_{t|t-1}] \quad (10)$$

$$\mathbf{P}_{t|t} = [\mathbf{I} - \mathbf{K}_t\mathbf{H}]\mathbf{P}_{t|t-1} \quad (11)$$

where the Kalman gain matrix is

$$\mathbf{K}_t = \mathbf{P}_{t|t-1}\mathbf{H}^T\mathbf{S}_t^{-1} \quad (12)$$

and the innovation covariance matrix is

$$\mathbf{S}_t = \mathbf{H}\mathbf{P}_{t|t-1}\mathbf{H}^T + \mathbf{R} \quad (13)$$

If the system works properly, the normalized innovation process $\tilde{\epsilon}_t = \mathbf{S}_t^{-1/2}\epsilon_t$ is a zero-mean Gaussian white-noise process with identity covariance matrix $E[\tilde{\epsilon}_t] = 0$, $E[\tilde{\epsilon}_t\tilde{\epsilon}_t^T] = \mathbf{I}$. Thus, any transition or variation in the model is reflected by a change in the aforementioned statistics.

In order to detect transitions we use the sequence of innovation process sample covariance matrices [10]

$$\mathbf{U}_t = \frac{1}{N_{av} - 1} \sum_{i=t-N_{av}+1}^t [\tilde{\epsilon}_i - \bar{\tilde{\epsilon}}_t][\tilde{\epsilon}_i - \bar{\tilde{\epsilon}}_t]^T \quad (14)$$

where

$$\bar{\tilde{\epsilon}}_t = \frac{1}{N_{av}} \sum_{i=t-N_{av}+1}^t \tilde{\epsilon}_i \quad (15)$$

and $N_{av} = 2$ consecutive patterns. Given a threshold θ , we consider that there is a transition if the following inequality is satisfied

$$I(\mathbf{U}_t) > \theta > I(\mathbf{U}_{t-1}) \quad (16)$$

where

$$I(\mathbf{U}_t) = \Psi[d(\mathbf{U}_t), d(\mathbf{U}_{t-1})] \quad (17)$$

is the Euclidean distance $\Psi[\cdot]$ between the diagonal vectors $d(\mathbf{U}_t)$ and $d(\mathbf{U}_{t-1})$ (variance vectors) of two consecutive sample covariance matrices. In this way, using (16) we only pay attention to abrupt changes in time. Consecutive changes are not considered to be intentional—rather they may indicate periods where the subject cannot sustain attention.

2.5 Classifier Supervisor

As described in Section 2.4, incoming patterns identified as transitions exhibit leaps in the training measured canonical space with respect to their predecessors. Thus these transitions patterns are probably located in different canonical subspaces from their predecessors and Bi-DBDA will have labelled such a transition pattern either as the majority of its predecessors (*within-class transition*) or differently (*intentional* or *unintentional between-class transition*) (see Figure 4). This last scenario reflects a mismatch between the user’s intent and the user’s EEG patterns. The goal of the classifier supervisor is to infer the different kinds of transitions and correct the labelling produced by Bi-DBDA.

To do so we have designed three heuristic rules (HR1, HR2, and HR3). HR1 is the simplest and most conservative rule as it rejects a large number of patterns (labels them as *unknown*) rule from which HR2 and HR3 are derived (see Figures 5 and 6 for a detailed description). The three HR label a new pattern, always every 0.250 s, using information from the last three transitions. The three HR seek to infer the intentional label of the patterns identified as transitions and then reclassify the subsequent patterns, until the next transition, with the same label. In this way the classifier supervisor only changes the labels when a intentional transition between different mental tasks is inferred.

3 Results and Discussion

The advantages of a inconsistencies detector and a classifier supervisor in an asynchronous BCI have been assessed offline by using the first three sessions of each subject as training and validation³ data and the fourth as test data. Performance has been measured in terms of classification accuracy and channel capacity. Given that the different components of the algorithm may reject responses (*unknown* responses), the estimator proposed by [14] has been used as a measure of the channel capacity. Table 1 shows the results for subjects 1, 2 and 3, whose data were used in BCI Competition III. Table 2 shows the results obtained on the subjects who received online feedback.

Regarding the first dataset, all the components of the new algorithm give the best performance for subject 1 and the worst for subject 3, paralleling the results obtained by the different algorithms that participated in the BCI Competition III.

³ k-fold cross-validation was done to select the values of the different hyperparameters of the algorithm—e.g., thresholds of the heuristics rules.

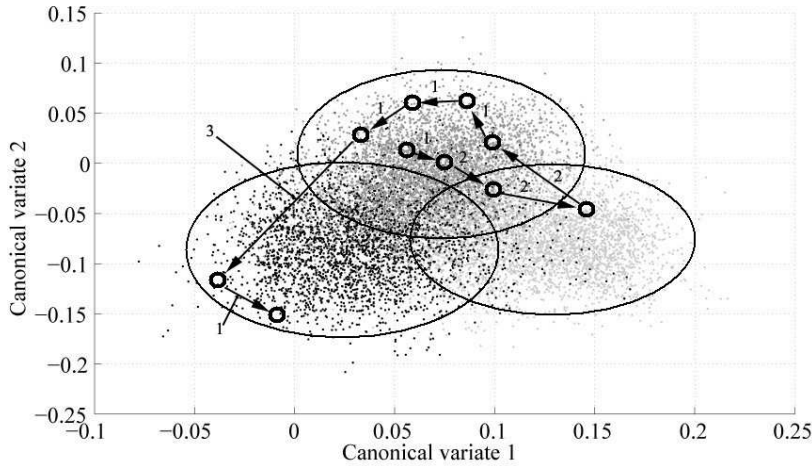


Fig. 4 Examples of projected test patterns identified as transitions on the training measured canonical space (black: imagination of left hand movement; dark grey: imagination of right hand movement; light grey: word search). Dots show the projected training patterns. Big circles represent the location of the three mental tasks in the canonical space. Small circles indicate transitions; i.e., patterns exhibiting leaps in the measured canonical space with respect to their predecessors. In this example the user executes first imagination of right hand movement and then imagination of left hand movement. This example illustrates the three kinds of transitions: **1**, within-class; **2**, unintentional between-class; **3**, intentional between-class transition.

$DBDA^{(O)}$ and $DBDA^{(C)}$ classifiers ($DBDA$ trained with the intentional canonical space, and $DBDA$ trained with measured canonical space respectively) exhibit a very similar performance over the three subjects in terms of both channel capacity and classification accuracy. Note that although the classification accuracy of these simple classifiers are slightly worse than that of the original classifier BCI-III, the channel capacity is similar (or even better) due to the fact that the new algorithm yields faster responses. But the real advantage of the new algorithm appears when the two new components process sequentially the outputs of the two $DBDA$ classifiers. Indeed, the detection of inconsistent patterns (7.82%, 12.18% and 30.75% unknown responses for subjects 1, 2 and 3, respectively) leads to a significant increase of the Bi- $DBDA$ channel capacity since the percentage of patterns incorrectly classified is greatly reduced. In particular, the effects of the inconsistencies detection in subject 3 stands out: the percentages of correctly and incorrectly classified patterns are inverted.

These results are further improved with the use of the different heuristic rules (HR) of the classifier supervisor. HR1 allows to increase the channel capacity for the three subjects, even though it rejects an extremely high percentage of patterns. HR2 rejects much less patterns and improves significantly the channel capacity. Finally, HR3 achieves a still further significant increase of the channel capacity (due to a remarkable increase in classification accuracy) for the first two subjects, but it shows a dramatic decline in performance in terms of channel capacity for subject 3.

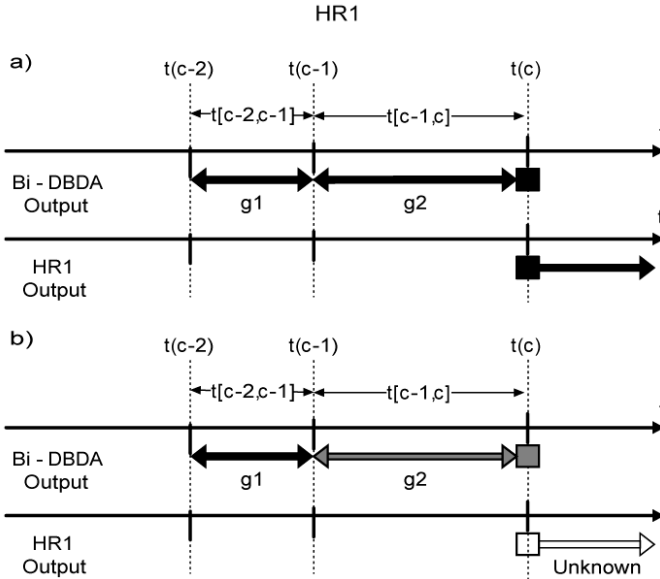


Fig. 5 HR1 changes the label of all *unknown* patterns after a transition if the C_{g1} and C_{g2} classes with maximum labelling proportion assigned by Bi-DBDA, $\max_{k+1}[p(\nu_{t[c-1,c]} = g1)]$ and $\max_{k+1}[p(\nu_{t[c-2,c-1]} = g2)]$, in the two gaps $t[c-2, c-1]$, $t[c-1, c]$ limited by the last three transitions are the same and equal to the label of the last transition $t(c)$ (**HR1.a**). Otherwise, HR1 labels as *unknown* the last transition $t(c)$ and all following patterns (**HR1.b**). Note that the number of classes $k+1$ corresponds to the k mental tasks plus the *unknown* class. Although this labelling rule may delay the detection of an intentional transition, it allows for the filtering of a great number of unintentional transitions. This rule yields a large number of unknown patterns, which limits its suitability to situations where it is useful to be conservative (e.g., at the very early stages of training where there is a higher degree of mismatch between the user's intent and the EEG patterns). Empty squares referred to unknown labels.

Concerning the second dataset where subjects received continuous feedback, we observed the same trend; i.e., the first two DBDA classifiers already achieved similar classification accuracy than the original classifier (and, hence, better channel capacity due to their faster responses), and the channel capacity is further improved through the sequential processing of the outputs of those classifiers by the inconsistencies detector (Bi-DBDA) and classifier supervisor. However, the effects of the different HR on the subjects' performance is not the same as before. For subject 4 we also see a significant improvement after the application of HR1 on the output of the Bi-DBDA and even a higher one with HR2. HR3 also increases the channel capacity with respect to Bi-DBDA, but in a lesser extent than HR1 and HR2. Significantly, all three heuristic rules invert the percentages of correctly and incorrectly classified patterns. For subject 5, only HR1 and HR2 increase the channel capacity with respect to Bi-DBDA, with HR1 outperforming HR2. The disadvantage of HR3 for these two subjects is that it rejects a very short number of patterns and, given that these two subjects are at the very beginning of their training, the BCI makes risky decisions, thus generating a high percentage

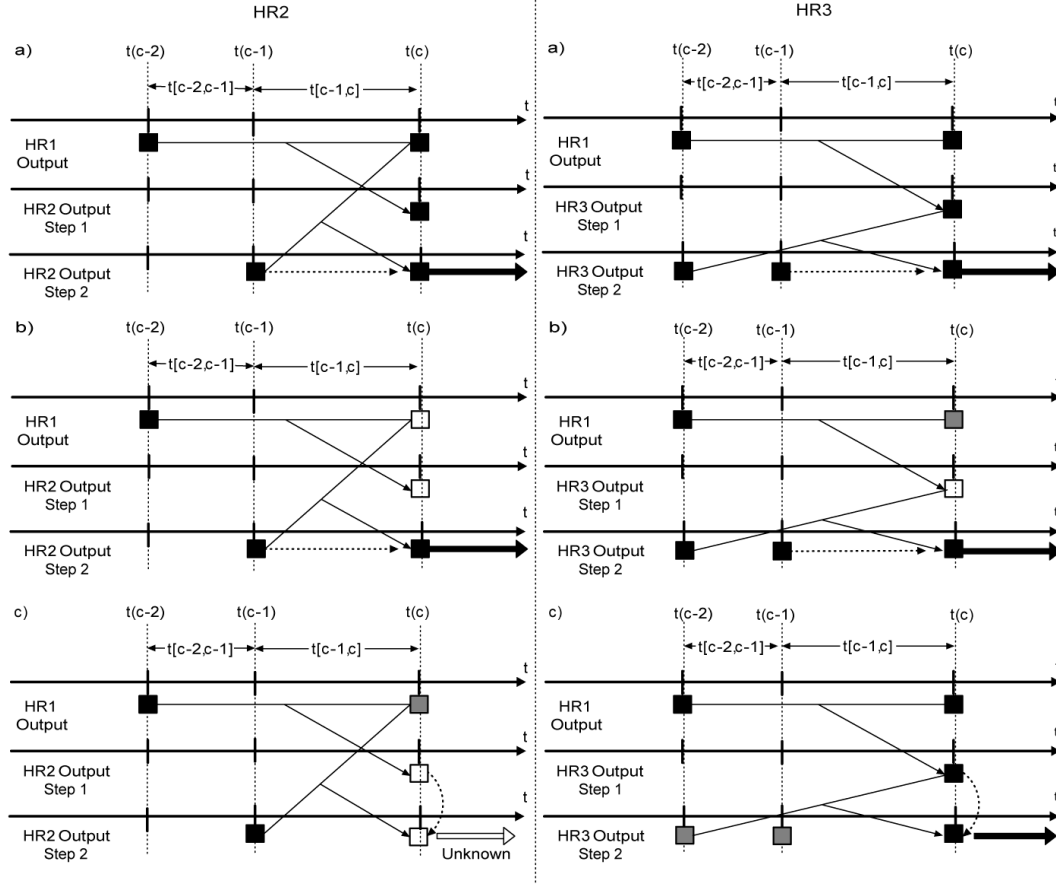


Fig. 6 Rules HR2 and HR3 incorporate two different ways to extend the filtering of unintentional transitions generated by HR1, allowing a more extensive supervision with different degrees of caution. Both of them share the first step where the clear transition $t(c)$ keeps the label it received from HR1 if it is the same as the label HR1 assigned to transition $t(c-2)$, otherwise $t(c)$ is classified as *unknown*. HR2 and HR3 differ in the second step. HR2 re-labels the clear transition $t(c)$ as the previous one $t(c-1)$ if HR1 labelled $t(c)$ either as HR2 labelled $t(c-1)$ (**HR2.a**) or as *unknown* (**HR2.b**), otherwise the output of the first step of HR2 is kept (**HR2.c**). HR3 re-labels the clear transition $t(c)$ as the previous one $t(c-1)$ if HR3 in the first step labelled $t(c)$ either as HR3 labelled $t(c-2)$ in the second step (**HR3.a**) or as *unknown* (**HR3.b**), otherwise the output of the first step of HR3 is kept (**HR3.a**). The difference between both rules is the amount of *unknown* labels generated: HR3 rejects a shorter number of patterns. Empty squares referred to unknown labels.

of misclassifications. Under this condition, more conservative heuristic rules are better suited.

In conclusion, the incorporation of the inconsistencies detector and the classifier supervisor outperforms the original classifier, winner of the BCI Competition III, on all five subjects for both working conditions of a BCI—namely with or without online feedback. Of the three heuristic rules, HR3 only seems suitable

Table 1 Classifiers performance on the BCI Competition III dataset.

Subject1				
Classifier	Channel Capacity	Accuracy	Error	Rejection
<i>DBDA</i> ^(O)	1.69 b/s	70.80 %	29.20 %	-
<i>DBDA</i> ^(C)	1.68 b/s	70.72 %	29.28 %	-
Bi-DBDA	1.96 b/s	67.47 %	24.71 %	7.82 %
HR1	2.90 b/s	54.02 %	5.61 %	40.37 %
HR2	3.91 b/s	72.37 %	4.60 %	23.03 %
HR3	4.34 b/s	90.77 %	8.14 %	1.09 %
BCI-III	1.30 b/s	79.60 %	20.40 %	-
Subject2				
Classifier	Channel Capacity	Accuracy	Error	Rejection
<i>DBDA</i> ^(O)	.85 b/s	59.92 %	40.08 %	-
<i>DBDA</i> ^(C)	.82 b/s	59.44 %	40.56 %	-
Bi-DBDA	1.17 b/s	54.51 %	33.31 %	12.18 %
HR1	1.89 b/s	38.24 %	11.84 %	49.92 %
HR2	2.68 b/s	58.31 %	11.31 %	30.38 %
HR3	2.75 b/s	80.12 %	19.04 %	.84 %
BCI-III	.82 b/s	70.31 %	29.69 %	-
Subject3				
Classifier	Channel Capacity	Accuracy	Error	Rejection
<i>DBDA</i> ^(O)	.30 b/s	48.74 %	51.16 %	-
<i>DBDA</i> ^(C)	.30 b/s	48.77 %	51.13 %	-
Bi-DBDA	.98 b/s	37.00 %	32.25 %	30.75 %
HR1	1.46 b/s	28.78 %	14.52 %	56.70 %
HR2	1.71 b/s	41.81 %	18.49 %	39.70 %
HR3	.49 b/s	52.52 %	46.46 %	1.02 %
BCI-III	.31 b/s	56.02 %	43.98 %	-

DBDA^(O): DBDA trained with training data, original labelling.

DBDA^(C): DBDA trained with training data, cluster labelling.

BCI-III: Winner classifier of the BCI Competition III, which yields a decision every 0.5 s.

Note that the clear algorithm yields a response every 0.250 s, hence achieving a higher channel capacity than the original algorithm for similar classification accuracies.

when the user's performance is already satisfactory (i.e., subjects 1 and 2). Otherwise, it is recommendable to use HR1 or, preferably, HR2. This is the case of subject 3, who has still a poor performance, and of subjects 4 and 5, who are at the beginning of their training or do not yet master the complexity of the online feedback coming from moving robots. Although HR1 and HR2 present a lower performance in terms of classification accuracy than HR3, they succeed notably in limiting the number of incorrect responses, an important aspect in order to avoid processes of discouragement, confusion and frustration that can easily interfere with attentional processes, and thus achieving acceptable levels of channel capacity.

Table 2 Classifiers performance of subjects receiving online feedback.

Subject4				
Classifier	Channel Capacity	Accuracy	Error	Rejection
$DBDA^{(O)}$.11 b/s	42.73 %	57.27 %	-
$DBDA^{(C)}$.10 b/s	42.30 %	57.70 %	-
Bi-DBDA	.22 b/s	40.00 %	52.89 %	7.11 %
HR1	1.10 b/s	17.95 %	13.75 %	68.30 %
HR2	1.48 b/s	26.57 %	10.41 %	63.02 %
HR3	.55 b/s	54.40 %	45.29 %	.31 %
BCI-III	.06 b/s	43.75 %	56.25 %	-

Subject5				
Classifier	Channel Capacity	Accuracy	Error	Rejection
$DBDA^{(O)}$.04 b/s	39.04 %	60.96 %	-
$DBDA^{(C)}$.04 b/s	39.06 %	60.94 %	-
Bi-DBDA	.12 b/s	36.47 %	56.46 %	7.07 %
HR1	.92 b/s	14.25 %	19.11 %	66.64 %
HR2	.85 b/s	18.14 %	27.02 %	54.84 %
HR3	.07 b/s	40.51 %	59.26 %	.23 %
BCI-III	.02 b/s	39.75 %	60.25 %	-

$DBDA^{(O)}$: DBDA trained with training data, original labelling.

$DBDA^{(C)}$: DBDA trained with training data, cluster labelling.

BCI-III: Winner classifier of the BCI Competition III, which yields a decision every 0.5 s.

Note that the clear algorithm yields a response every 0.250 s, hence achieving a higher channel capacity than the original algorithm for similar classification accuracies.

4 Conclusion

In this article we have shown that the inclusion of a inconsistencies detector and a classifier supervisor based on intentional mental transitions detection leads to an effective inference of the user's intended mental task. This approach yields a increase of the channel capacity mainly because it allows to decrease the error rates. Experimental results show the benefits of our algorithm in both working conditions of a BCI, namely with or without online feedback. The main limitation of our approach is the use of ad-hoc heuristic rules. The next step is to formalize those heuristic rules in a Bayesian framework and build probabilistic models for the inference of the user'intent as in [16].

5 Acknowledgements

The authors would like to thank Ricardo Chavarriaga for his useful suggestions and Anna Buttfield for her collaboration in the experimental recordings.

6 Appendix

As described in [6] and [8], given k classes C_1, \dots, C_k and a defined distance function d_g for class C_g , the proximity measurement for pattern w_t with vector

$\mathbf{y}_t = \mathbf{y}(w_t)$, is defined as

$$\phi_g(\mathbf{y}_t) = V_g(\mathbf{y}_{C_g}|\mathbf{y}_t) - V_g(\mathbf{y}_{C_g}) \quad (18)$$

where

$$V_g(\mathbf{y}_{C_g}) = \frac{1}{2}E_{C_g C_g}[d_g^2(\mathbf{y}_{C_g}, \mathbf{y}_{C_g})] \quad (19)$$

and

$$V_g(\mathbf{y}_{C_g}|\mathbf{y}_t) = E_{C_g}[d_g^2(\mathbf{y}_t, \mathbf{y}_{C_g})] \quad (20)$$

are the geometric variability and the relative geometric variability to pattern \mathbf{y}_t . Thus, the DBDA assigns w_t to C_g , if

$$\phi_g(\mathbf{y}_t) = \min_k[\phi_k(\mathbf{y}_t)] \quad (21)$$

In practice, suitable estimates of the geometric variability and the relative geometric variability to pattern \mathbf{y}_t are

$$\hat{V}_g(\mathbf{y}) = \frac{1}{2n_g^2} \sum_{j,j'=1}^{n_g} d^2(\mathbf{y}_{gj}, \mathbf{y}_{gj'}) \quad (22)$$

$$\hat{V}_g(\mathbf{y}|\mathbf{y}_t) = \frac{1}{n_g} \sum_{j=1}^{n_g} d^2(\mathbf{y}_t, \mathbf{y}_{gj}), \quad (23)$$

where n_g is the number of patterns of class C_g and \mathbf{y}_{gj} is the pattern j of class g . Therefore, the estimate of the proximity function is

$$\hat{\phi}_g(\mathbf{y}_t) = \frac{1}{n_g} \sum_{j=1}^{n_g} d^2(\mathbf{y}_t, \mathbf{y}_{gj}) - \frac{1}{2n_g^2} \sum_{j,j'=1}^{n_g} d^2(\mathbf{y}_{gj}, \mathbf{y}_{gj'}) \quad (24)$$

References

1. Bayliss, J. D. (2003) Use of the evoked potential P3 component for control in a virtual apartment. *IEEE Trans. Neural Sys. Rehab. Eng.* 11:113-116.
2. Basseville, M., and Nikiforov, I. V. (1993) *Detection of Abrupt Changes: Theory and Application*. Upper Saddle River, NJ: Prentice-Hall.
3. Birbaumer, N., Ghanayim, N., Hinterberger, T., Iversen, I., Kotchoubey, B., Kübler, A., Perelmouter, J., Taub, E., and Flor, H. (1999) A spelling device for the paralysed. *Nature* 398:297-298.
4. Blankertz, B., Müller, K. R., Krusienski, D., Schalk, G., Wolpaw, J. R., Schlögl, A., Pfurtscheller, G., Millán, J. del R., Schröder, M., and Birbaumer, N. (2006) The BCI competition III: Validating alternative approaches to actual BCI problems. *IEEE Trans. Neural Sys. Rehab. Eng.* 14:153-159.
5. Carmena, J. M., Lebedev, M. A., Crist, R.E., O'Doherty, J. E., Santucci, D. M., Dimitrov, D. F., Patil, P. G., Henriquez, C. S., and Nicolelis, M. A. L. (2003) Learning to control a brain-machine interface for reaching and grasping by primates. *PLoS Biol.* 1:193-208.
6. Cuadras, C. M., Fortiana, J., and Oliva, F. (1997) The proximity of an individual to a population with applications in discriminant analysis. *Journal of Classification* 14:117-136.

-
7. Digalakis, D., Rohlicek, J. R., and Ostendorf, M. (1993) ML Estimation of a Stochastic Linear System with the EM Algorithm and its Application to Speech Recognition. *IEEE Trans. Speech and Audio Proc.* 1:431-442.
 8. Galán, F., Oliva, F., Guàrdia, J. (2007) Using Mental Tasks Transitions Detection to Improve Spontaneous Mental Activity Classification. *Medical and Biological Engineering and Computing.* 45:603-609.
 9. Galán, F., Nuttin, M., Lew, E., Ferrez, P. W., Vanacker, G., Philips, J., Van Brussel, H., and Millán, J. del R. (2007) An Asynchronous and Non-Invasive Brain-Actuated Wheelchair. 13th International Symposium on Robotics Research, Hiroshima. In press.
 10. Hajiyev, C. M., and Caliskan, F. (1999) Fault detection in flight control systems based on the generalized variance of the Kalman filter innovation sequence. *Proc. Amer. Cont. Conf.* 1:109-113.
 11. Krzanowski, W. J. (1988) *Principles of multivariate analysis.* Oxford: Oxford University Press.
 12. Millán, J. del R. (2003) Adaptive brain interfaces. *Comm. of the ACM* 46:75-80.
 13. Millán, J. del R. (2004) On the need for on-line learning in brain-computer interfaces. *Proc. Int. Joint. Conf. on Neural Networks* 4:2877-2882.
 14. Millán, J. del R., Renkens, F., Mouriño, J., and Gerstner, W. (2004) Noninvasive brain-actuated control of a mobile robot by human EEG, *IEEE Trans. Biomed. Eng.* 51:1026-1033.
 15. Obermaier, B., Müller, G. R., and Pfurtscheller, G. (2003) Virtual keyboard controlled by spontaneous EEG activity. *IEEE Trans. Neural Sys. Rehab. Eng.* 11:422-426.
 16. Verma D., and Rao, R. P. N., Goal-based imitation as probabilistic inference over graphical models. *Advances in Neural Information Processing Systems* 18:1393-1400.

Appendix D

Feature Extraction for Multi-class BCI using Canonical Variates Analysis

F. Galán, P. W. Ferrez, F. Oliva, J. Guàrdia, and J. del R. Millán. Feature Extraction for Multi-class BCI using Canonical Variates Analysis. In *Proceedings of the 2007 IEEE International Symposium on Intelligent Signal Processing, WISP 2007, Alcalá de Henares, Spain, 2007a.*

Resum

L'objectiu d'aquest article és proposar un nou extractor de característiques amb solució canònica per a interfícies cerebrals asíncrones multi-classe. El mètode proposat facilita un nombre reduït de patrons espacials canònics discriminants i ordena els canals en funció de la seva capacitat discriminant entre classes.

L'EEG analitzat ha estat enregistrat utilitzant 64 canals mentre 4 subjectes participaven en 20 sessions experimentals. Durant aquestes sessions es va requerir als subjectes executar tres tasques cognitives (imaginació moviment mà dreta, associació de paraules i relaxació), dos assajos per sessió, durant 7 segons cada assaig. Després de separar les dades en conjunt d'entrenament i conjunt de test s'ha ordenat els canals en funció de la seva capacitat discriminant entre classes i s'han obtingut els patrons espacials canònics discriminants per a cada conjunt, tant en el domini temporal com freqüencial. Alhora s'ha comparat la classificació correcta aconseguida per un discriminant lineal en ambdós dominis utilitzant els espais canònics respectius.

La classificació correcta mitjana entre els quatre subjectes utilitzant els espais canònics en ambdós dominis, freqüencial i temporal, és equivalent (57.89% i 59.43% respectivament). Aquests resultats es veuen alhora reflectits en la similitud entre les ordenacions de canals obtinguda en els conjunts d'entrenament i test, tant en el domini temporal com freqüencial.

Aquest estudi mostra que l'anàlisi de variables canòniques és un simple extractor de característiques amb solució canònica útil per a interfícies cerebrals multi-classe. Alho-

ra, pot ser utilitzat tant en el domini temporal com freqüencial. Ambdós trets són noves aportacions respecte als extractors de característiques generalment utilitzats (Ramoser et al., 2000; Lemm et al., 2005).

Feature Extraction for Multi-class BCI using Canonical Variates Analysis

Ferran Galán[†], Pierre. W. Ferrez[†], Francesc Oliva[‡], Joan Guàrdia[§], and José del R. Millán[†]

[†]IDIA Research Institute, 1920 Martigny, Switzerland. E-mail: Ferran.Galan@idiap.ch

[‡]Dept. of Statistics, University of Barcelona, Barcelona, Spain

[§]Dept. of Methodology of the Behavioural Sciences, University of Barcelona, Barcelona, Spain

Abstract – Objective: To propose a new feature extraction method with canonical solution for multi-class Brain-Computer Interfaces (BCI). The proposed method should provide a reduced number of canonical discriminant spatial patterns (CDSP) and rank the channels sorted by power discriminability (DP) between classes. **Methods:** The feature extractor relays in Canonical Variates Analysis (CVA) which provides the CDSP between the classes. The number of CDSP is equal to the number of classes minus one. We analyze EEG data recorded with 64 electrodes from 4 subjects recorded in 20 sessions. They were asked to execute twice in each session three different mental tasks (left hand imagination movement, rest, and words association) during 7 seconds. A ranking of electrodes sorted by power discriminability between classes and the CDSP were computed. After splitting data in training and test sets, we compared the classification accuracy achieved by Linear Discriminant Analysis (LDA) in frequency and temporal domains. **Results:** The average LDA classification accuracies over the four subjects using CVA on both domains are equivalent (57.89% in frequency domain and 59.43% in temporal domain). These results, in terms of classification accuracies, are also reflected in the similarity between the ranking of relevant channels in both domains. **Conclusions:** CVA is a simple feature extractor with canonical solution useful for multi-class BCI applications that can work on temporal or frequency domain.

Keywords – Electroencephalogram, Brain-computer interfaces, Canonical Variates Analysis, Linear Discriminant Analysis.

I. INTRODUCTION

Brain-computer interfacing (BCI) research enables a new interaction modality with the environment. Many applications

This work was supported in part by Agència de Gestió d'Ajuts Universitaris i de Recerca, Departament d'Universitats Recerca i Societat de la Informació, Generalitat de Catalunya, under Grants 2001SGR00139 and 2001SGR00067, by the Spanish Ministerio de Educación y Ciencia, under Grant MTM2004-00440, by the Swiss National Science Foundation through the National Centre of Research on "Interactive Multimodal Information Management (IM2)", and by the European IST Programme FET Project FP6-003758. This paper only reflects the author's views and founding agencies are not liable for any use that may be made of the information contained herein.

have been explored in recent years [1], [2], [3], [4], [5], [6]. Our work is focused on asynchronous and non-invasive electroencephalogram (EEG) based BCI to control robots and wheelchairs [7], [8]. It means that the users drive such devices by learning to voluntarily control specific EEG features. To facilitate this learning process it is necessary to select those subject-specific features that allow to generate the maximum number of discriminant patterns. This process becomes crucial to facilitate the generation of those patterns that will permit an easier execution of those commands needed to drive the different devices. To this end, Common Spatial Patterns (CSP) [9] and his extension Common Spatio Spectral Patterns (CSSP) [10] have been proven very useful. However, *there is no canonical way to choose the relevant CSP patterns for multi-class CSP and only approximative solutions can be obtained* [11]. In the present paper we propose a new feature extraction method with canonical solution for multi-class BCI. The feature extractor utilized relays on Canonical Variates Analysis (CVA) [12], also known as Multiple Discriminant Analysis [13], that provides the canonical discriminant spatial patterns (CDSP) between the classes. The number of CDSP is equal to the number of classes minus one.

The paper is structured as follows: Section II describes CVA and the experimental setup, preprocessing and analysis carried out to assess its usability for multi-class BCI feature extraction; Section III reports the results; and finally in Section IV gives some conclusions and discusses future work.

II. METHODS

A. Canonical Variates Analysis

In our BCI research the user employs the voluntary modulation of different oscillatory rhythms [7] by executing of different mental tasks (motor and cognitive) to drive robots and wheelchairs in virtual [8] and real environments. In these

applications the users utilize more than two commands. To facilitate this voluntary modulation it is necessary to find those subject-specific spatial patterns that maximize the separability between the patterns generated by executing the different mental tasks. In this way, from band-pass filtered EEG signals, the CSP algorithm extracts canonical discriminant spatial patterns which directions maximizes the differences in variance between two classes. *Since the variance of a band-pass filtered signal is a measure for the energy in the corresponding frequency band, the patterns reflect the spatial distributions of event-related (de)synchronization effects* [14]. However, *there is no canonical way to choose the relevant CSP patterns for multi-class CSP and only approximative solutions can be obtained* [11]. This limitation can be avoided in two ways, namely working in frequency domain or working with the squared band-pass filtered EEG signal. In the former case, the energy in the corresponding frequency band is measured by its spectral power. In this domain the spatial distributions of event-related (de)synchronization effects are identified by changes on the spectral power. In the later case, the spatial distributions of event-event-related (de)synchronization effects are identified by changes on the mean, given that the variance of a band-pass filtered EEG signal becomes the mean when the signal is squared (see proof in the appendix). Thus, using CVA it is easy to extract CDSP which directions maximizes the differences in mean, either spectral power in the first case or energy of the original band-pass filtered EEG signal in the second case, between a given number of classes.

Given the $n_i \times c$ matrix, either with the estimated spectral power of a frequency band or the squared band-pass filtered EEG signal, $\mathbf{S}_i = (\mathbf{s}_{i1}, \dots, \mathbf{s}_{in_i})'$ of class $i = 1, \dots, k$, where n_i is the number of samples and c is the number of channels, and $\mathbf{S} = (\mathbf{S}'_1, \dots, \mathbf{S}'_k)'$, the $k-1$ CDSP of \mathbf{S} are the eigenvectors \mathbf{A} of $\mathbf{W}^{-1}\mathbf{B}$ which eigenvalues λ_u , ($u = 1, \dots, k-1$) are larger than 0. Note that the direction of eigenvectors \mathbf{A} maximize the quotient between the between-classes dispersion matrix

$$\mathbf{B} = \sum_{i=1}^k n_i (\mathbf{m}_i - \mathbf{m})(\mathbf{m}_i - \mathbf{m})' \quad (1)$$

and the pooled within-classes dispersion matrix

$$\mathbf{W} = \sum_{i=1}^k \sum_{j=1}^{n_i} (\mathbf{s}_{ij} - \mathbf{m}_i)(\mathbf{s}_{ij} - \mathbf{m}_i)' \quad (2)$$

where

$$\mathbf{m}_i = \frac{1}{n_i} \sum_{j=1}^{n_i} \mathbf{s}_{ij} \quad (3)$$

and

$$\mathbf{m} = \frac{1}{n} \sum_{i=1}^k n_i \mathbf{m}_i \quad (4)$$

are the class and total centroids respectively. Thus, the new features are obtained by the projection

$$\mathbf{Y} = \mathbf{S}\mathbf{A} \quad (5)$$

Once the CDSP are computed, it is useful to know how the original features (electrodes) are contributing in the separability between the classes. It also permits to interpret the space generated by the CDSP, specially when the number of classes is high. In this way, it is possible to rank the channels given their contribution on the new space. We define a new *Discriminant Power* (DP) [15] measure for each channel from the *structure matrix*, pooled correlation matrix between original channels in \mathbf{S} and the new features in \mathbf{Y} . Given the $c \times k-1$ structure matrix \mathbf{T} , where $\mathbf{T} = \sum_{i=1}^k \mathbf{T}_i$, $e = 1, \dots, c$, and the normalized eigenvalues $\gamma_u = \lambda_u / \sum_{u=1}^{k-1} \lambda_u$, the proposed DP can be computed as follows

$$DP_e = \left(\sum_{u=1}^{k-1} \gamma_u t_{eu}^2 / \sum_{e=1}^c \sum_{u=1}^{k-1} \gamma_u t_{eu}^2 \right) \times 100 \quad (6)$$

B. Data Acquisition and Task

Data were recorded from 4 subjects with a portable Biosemi acquisition system using 64 channels sampled at 512Hz and high-pass filtered at 1Hz. The subjects were sitting in a chair looking at a fixation cross placed at the center of a monitor. The subjects were instructed to execute three different mental tasks (left hand imagination movement, rest, and words association) in a self-paced way. The mental task to be executed was previously specified by the operator in order to counterbalance the order, the subjects specify when they started to execute the mental task. Each subject participated in 20 sessions integrated by 6 trials each, 2 trials of each class. The duration of each trial was 7 seconds but only the last 6 seconds were utilized in the analysis to avoid preparation periods. Subjects 1 and 2 had previous experience with the selected mental tasks, while it was the first time for subjects 3 and 4.

C. Preprocessing

To work in frequency domain the signal was spatially filtered using common average reference (CAR) previous to the estimation every 62.5 ms. (16 times per second) of the power spectral density (PSD) in the band 10-14Hz with 2Hz resolution over the last 1-second windows. PSD was estimated by Welch method with 5 overlapped (25%) Hanning windows of 500 ms. length. To work in temporal domain the signal was also spatially filtered by CAR, band-pass filtered in the frequency range 8-16Hz (to get a band-pass filtered signal in the same frequency ranges analyzed in the frequency domain, taking in account the FIR filter transition band) and finally squared. Single trials were obtained by averaging samples within last 1-second window. In both cases only 45 electrodes were utilized, namely: F1, F3, F5, FC1, FC3, FC5, C1, C3, C5, CP1, CP3, CP5, P1, P3, P5, P7, PO3, PO7, O1, Fz, FCz, Cz, CPz, Pz, POz, Oz, F2, F4, F6, FC2,

TABLE I.

LDA CLASSIFICATION ACCURACY OVER THE FOUR SUBJECTS ACCORDING TO THE DIFFERENT TEST SESSIONS USING CVA IN FREQUENCY AND TEMPORAL DOMAINS

Subject	Domain	Test Session					Average
		1	2	3	4	5	
1	F ^a	66.25%	76.04%	71.04%	70.41%	62.92%	69.33%
	T ^b	60.34%	87.05%	74.13%	73.54%	72.42%	73.50%
2	F	72.71%	59.79%	73.54%	69.37%	64.38%	67.95%
	T	62.36%	56.70%	69.81%	61.76%	71.14%	64.35%
3	F	43.54%	49.38%	55.00%	60.21%	50.63%	51.75%
	T	60.32%	60.04%	61.41%	50.28%	55.83%	57.57%
4	F	35.83%	61.45%	48.33%	33.54%	34.16%	42.66%
	T	31.24%	62.17%	35.71%	46.57%	35.95%	42.33%
Average	F						57.89%
	T						59.43%

^afrequency domain, ^btemporal domain

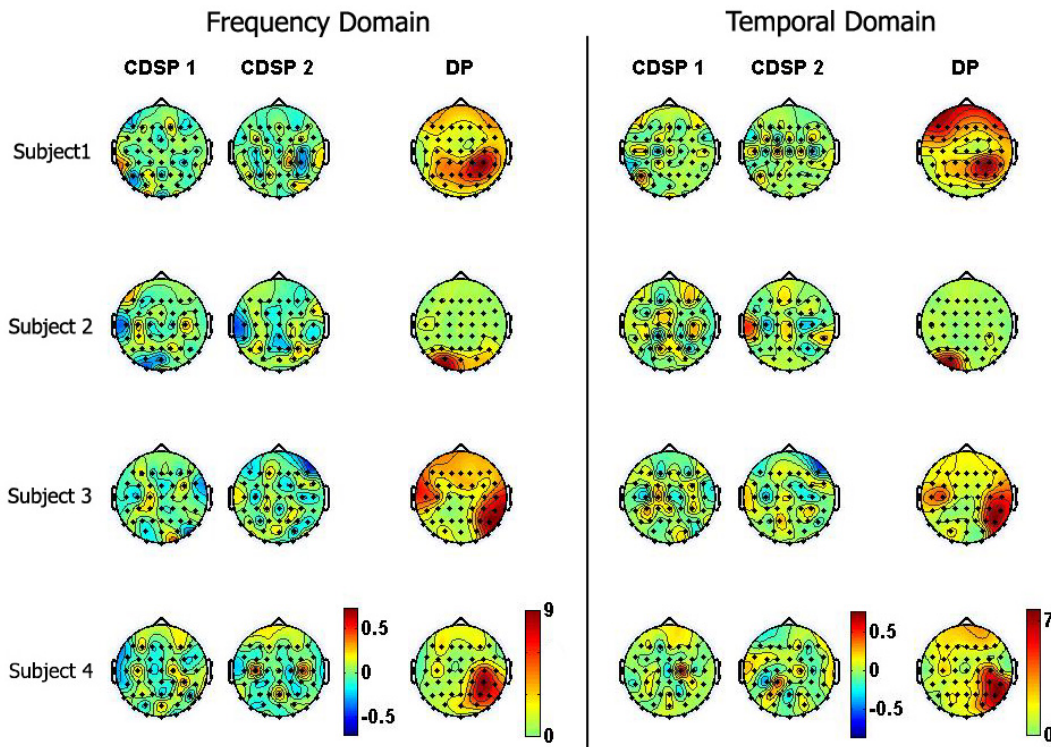


Figure 1. CDSP AND DP FOR EACH SUBJECT IN FREQUENCY AND TEMPORAL DOMAINS COMPUTED FROM TRAINING SET. NOTE THAT DP SCALE IS IN %.

FC4, FC6, C2, C4, C6, CP2, CP4, CP6, P2, P4, P6, P8, PO4, PO8, O2.

D. Analysis

To assess the canonical discriminant spatial patterns stability over time, data were split in two sets, the training set integrated by the trials from the first 15 sessions, and the test set integrated by the trials from the last 5 sessions. In frequency domain a trial was defined by each PSD estimation whereas in temporal domain each trial was defined as the averaged squared band-

pass signal over the last second. After obtain the CDSP from the training set of each domain, training and test trials were projected in the new space using eq. 5. Then, we built one Linear Discriminant Analysis (LDA) classifier per subject and per domain whose parameters are estimated on the corresponding training sets. Finally, we used these LDA classifiers to assess the generalization performances of each subject. Given that the main problem in BCI research is to deal with EEG unstability over time, the use of k-fold crossvalidation was avoided. This non-parametric classification error estimator uses as training and test sets data from all sessions, what never occurs in on-line

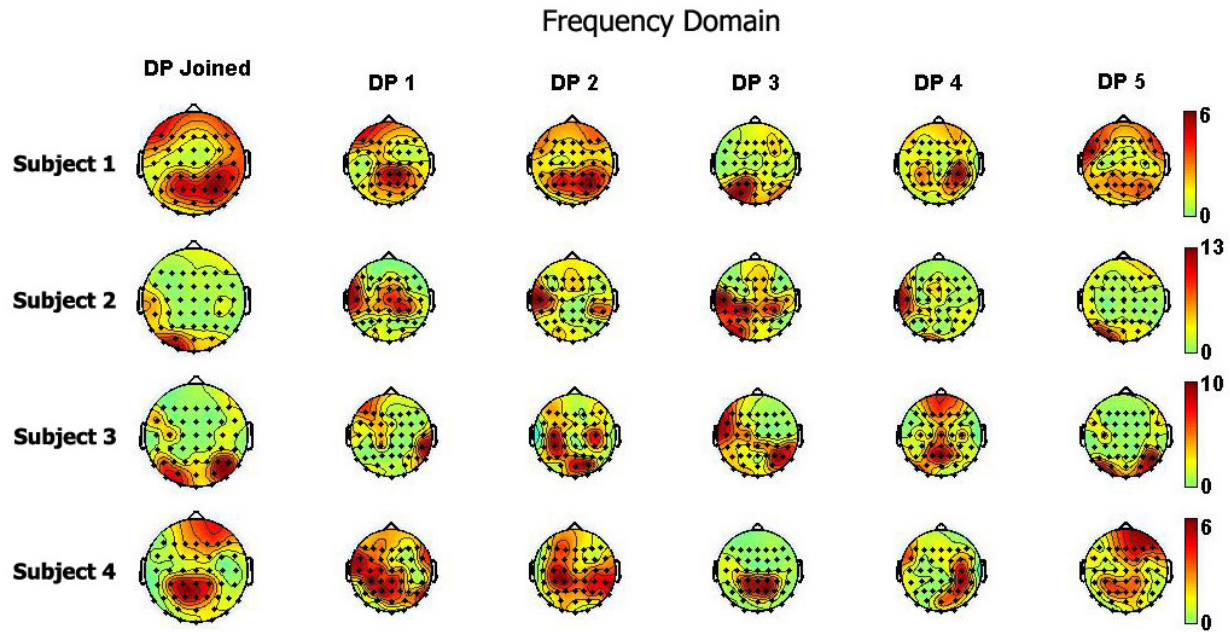


Figure 2. DP FOR EACH SUBJECT IN FREQUENCY DOMAIN COMPUTED JOINING ALL TEST SESSIONS AND FROM EVERY SINGLE TEST SESSION. NOTE THAT DP SCALE IS IN %.

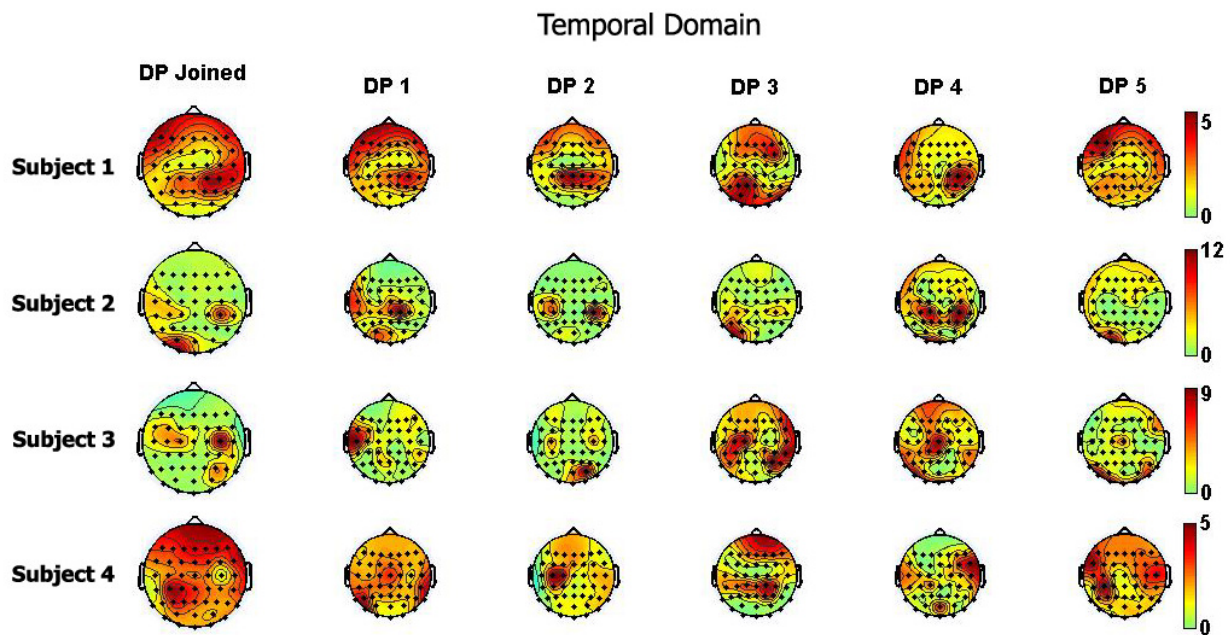


Figure 3. DP FOR EACH SUBJECT IN TEMPORAL DOMAIN COMPUTED JOINING ALL TEST SESSIONS AND FROM EVERY SINGLE TEST SESSION. NOTE THAT DP SCALE IS IN %.

applications and yields optimistic error estimations.

III. RESULTS

Table I reports the LDA classification accuracy over the 5 test sessions using CVA in frequency and temporal domain. In average, the classification accuracies for both domains are equivalent (57.89% in frequency domain vs. 59.43% in temporal domain, random level is 33.3% for a 3-class problem). In the temporal domain, we obtained higher classification accuracies for two subjects, namely subjects 1 and 3 (73.50% and 57.57% vs. 69.33% and 51.75%). In the frequency domain, we obtained higher classification accuracies only for one subject, namely subject 2 (67.95% vs. 64.35%). The performance is equivalent on subject 4 (42.66% vs. 42.33%). Fig. 1 depicts the two CDSP and the DP obtained for each subject in frequency and temporal domains computed on the training set. The CDSP interpretation as a whole it is facilitated by DP maps. DP maps show the electrodes contribution, in percentage, on the space defined by the CDSP. As expected according to the results obtained in terms of classification accuracy, DP maps obtained from both domains show a similar distribution of electrodes contribution in all subjects. Fig. 2 and Fig. 3 depict the DP for each subject in the frequency and temporal domains, respectively, computed joining all test sessions (first column) and also from every single test session (next five columns). These figures show the origin of the intersession variability and allow also to understand the results in terms of classification accuracy (see Table I). In both domains, the classification accuracy is related to the level of similarity between DP maps obtained from the training set (see DP maps in Fig. 1) and DP maps obtained from test sessions (see Fig. 2, frequency domain, and Fig. 3, temporal domain), either joining all test sessions or for each single test session. Higher classification accuracies correspond to higher similarity between the maps, what means that the canonical spaces defined by the CDSP estimated on the training sets are more stable over time. It is also worth noting that the similarity between DP maps obtained from both domains (DP joined in Fig. 2 and Fig. 3, first column) decreases on those subjects with lower classification accuracies.

IV. CONCLUSION AND FURTHER RESEARCH

The objective of this paper is to propose a new feature extraction method with a canonical solution for multi-class BCI. The estimated CDSP yield the space of maximum separability between event-related (de)synchronization effects involved in the execution of different mental tasks. The proposed DP measure rank the electrodes sorted by their contribution in the new space. The average LDA classification accuracies obtained working on frequency and temporal domains are equivalent. Performances are not very high for a 3-class problem because, for comparative purposes, we have classified every single trial obtained from the last second window. The equivalent results, in terms of classification accuracies, are also reflected in the similarity between the DP maps obtained from the training sets

of both domains. On the other hand, the level of similarity between DP maps obtained from the testing sets of both domains decreases for those subjects with lower classification accuracies (subjects 3 and 4). A possible explanation that needs to be explored is that energy (temporal domain) and PSD estimation (frequency domain) do not reflect the same phenomena when the signal is less stationary, what occurs when the subject have difficulties to generate stable EEG patterns during the execution of the mental tasks. Future work will focus on testing different extensions of CVA, assessing the sources of performance variability between both domains on different subjects, and exploring the relation between energy and spectral estimation.

APPENDIX

Theorem 1: Given a band-pass filtered signal $x(t)$, ($t = 1, \dots, T$), its variance is equal to the squared signal's mean:

$$\sigma_{x(t)} = \mu_{x^2(t)} \quad (7)$$

Proof: Given that

$$\mu_{x(t)} = 0 \quad (8)$$

$$\sigma_{x(t)} = \frac{\sum_{t=1}^T (x(t) - \mu_{x(t)})^2}{T} \quad (9)$$

substituting (8) in (9) yields

$$\sigma_{x(t)} = \frac{\sum_{t=1}^T x^2(t)}{T} \quad (10)$$

that, by definition, it is $\mu_{x^2(t)}$ ■

REFERENCES

- [1] J. D. Bayliss, 'Use of the evoked potential P3 component for control in a virtual apartment,' *IEEE Trans. Neural Sys. Rehab. Eng.*, vol. 11, pp. 113–116, 2003.
- [2] M. A. Nicolelis and J. K. Chapin, 'Controlling robots with the mind,' *Sci. Am.*, vol. 287, pp. 46–53, 2002.
- [3] J. M. Carmena, M. A. Lebedev, R. E. Crist, J. E. O'Doherty, D. M. Santucci, D. F. Dimitrov, P. G. Patil, C. S. Henriquez, and M. A. L. Nicolelis, 'Learning to control a brain-machine interface for reaching and grasping by primates,' *PLoS Biol.*, vol. 1, pp. 193–208, 2003.
- [4] N. Birbaumer, N. Ghanayim, T. Hinterberger, I. Iversen, B. Kotchoubey, A. Kübler, J. Perelmouter, E. Taub, and H. Flor, 'A spelling device for the paralysed,' *Nature*, vol. 398, pp. 297–298, 1999.
- [5] B. Obermaier, G. R. Müller, and G. Pfurtscheller, 'Virtual keyboard controlled by spontaneous EEG activity,' *IEEE Trans. Neural Sys. Rehab. Eng.*, vol. 11, pp. 422–426, 2003.
- [6] J. del R. Millán, 'Adaptive brain interfaces,' *Comm. of the ACM*, vol. 46, pp. 75–80, 2003.
- [7] J. del R. Millán, F. Renkens, J. Mouriño, and W. Gerstner, 'Noninvasive brain-actuated control of a mobile robot by human EEG,' *IEEE Trans. Biomed. Eng.*, vol. 51, pp. 1026–1033, 2004.
- [8] E. Lew, M. Nuttin, P. W. Ferrez, A. Degeest, A. Buttfeld, and G. Vanacker, 'Noninvasive brain-computer interface for mental control of a simulated wheelchair,' *Proceedings of the 3rd International Brain-Computer Interface Workshop & Training Course*, 2006.
- [9] H. Ramoser, J. Müller-Gerking, and G. Pfurtscheller, 'Optimal spatial filtering of single trial EEG during imagined hand movement,' *IEEE Trans. Neural Sys. Rehab. Eng.*, vol. 8, pp. 441–446, 2000.
- [10] S. Lemm, B. Blankertz, G. Curio, and K-R. Müller, 'Spatio-spectral filters for improving the classification of single trial EEG,' *IEEE Trans. Biomed. Eng.*, vol. 52, pp. 1541–1548, 2005.

- [11] G. Dornhege, B. Blankertz, G. Curio, and K-R. Müller, 'Increase information transfer rates in BCI by CSP extension to multi-class,' in: S. Thrun, L. Saul, and B. Schölkopf, eds., *Advances in Neural Inf. Proc. Systems*, vol. 16, pp. 733–740, 2004.
- [12] W. J. Krzanowski, *Principles of multivariate analysis*, Oxford University Press, Oxford, 1998.
- [13] R. O. Duda, P. E. Hart, and D. G. Stork, *Pattern Classification*, John Wiley & Sons, 2nd ed., 2001.
- [14] G. Dornhege, B. Blankertz, and G. Curio, 'Speeding up classification of multi-channel brain-computer interfaces: common spatial patterns for slow cortical potentials,' *In Proceedings of the 1st International IEEE EMBS Conference on Neural Engineering*, pp. 591–594, 2003.
- [15] S. L. Gonzalez Andino, R. Grave de Peralta Menendez, G. Thut, J. del R. Millán, P. Morier, and T. Landis, 'Very high frequency oscillations (VHFO) as a predictor of movement intentions,' *Neuroimage*, vol. 32, pp. 170–179, 2006.

Appendix E

Visuo-Spatial Attention Frame Recognition for Brain-Computer Interfaces

F. Galán, J. Palix, R. Chavarriaga, P.W. Ferrez, C.A. Hauert, and J. del. R. Millán. **Visuo-spatial Attention Frame Recognition for Brain-computer Interfaces.** In *Proceedings of the 1st International Conference on Cognitive Neurodynamics, ICCN 2007. Symposium on Advanced Signal Processing Techniques for Brain Data Analysis, Shanghai, China, 2007c.* To appear.

Resum

La introducció d'un enfocament basat en la detecció de *frames* neurals implica un canvi conceptual del sistema de presa de decisions d'una interfície cerebral. Aquest enfocament transforma l'escenari tradicional, un problema de reconeixement de patrons EEG, en un problema de detecció d'esdeveniments. Aquest nou enfocament ha estat avaluat preliminarment en una tasca de reconeixement de *frames* d'atenció visuoespacial.

Els resultats obtinguts han mostrat, primer, la viabilitat de modular ritmes EEG per mitjà de l'orientació visuoespacial de l'atenció. Segon, la intensitat d'aquesta modulació no és sostinguda. Aquest fet pot estar relacionat amb els patrons intermitents d'amplitud modulada induïts de manera activa (*frames*) descrits per Freeman (2005). A diferència dels anteriors, en aquest cas són generats voluntàriament per l'usuari. Tercer, és possible classificar els *frames* generats durant l'orientació de l'atenció a diferents localitzacions espacials amb una alta classificació correcta (superior al 80% en orientar l'atenció a 2 possibles localitzacions, 2 classes). Quart, la classificació correcta d'aquests *frames* s'incrementa utilitzant components freqüencials inclosos a banda gamma ($> 30\text{Hz}$). Cinquè, la classificació correcta utilitzant l'enfocament tradicional, assumint que la modulació dels ritmes EEG és sostinguda en el temps, es situa en nivells al voltant del 50%. Aquest fet suggereix que un enfocament tradicional és subòptim en la tasca de reconeixement de fenòmens EEG induïts,

fet alhora confirmat al comparar la capacitat de comunicació teòrica d'una interfície cerebral utilitzant ambdós enfocaments. Utilitzant l'enfocament basat en la detecció de *frames* neurals la capacitat de comunicació teòrica de la interfície cerebral es multiplica per 10.

El futur treball en aquesta línia de recerca estarà orientat a completar l'estudi amb una major mostra i en el desenvolupament d'algorismes per al reconeixement d'assajos basats en l'acumulació temporal d'evidència. D'aquesta manera, aquests algorismes respondran en intervals variables una vegada l'evidència acumulada superi un nivell estimat de confiança.

Visuo-Spatial Attention Frame Recognition for Brain-Computer Interfaces ^{*}

Ferran Galán^{1,2}, Julie Palix³, Ricardo Chavarriaga¹, Pierre W. Ferrez^{1,4}, Eileen Lew^{1,4}, Claude-Alain Hauert³, and José del R. Millán^{1,4}

¹ IDIAP Research Institute, Martigny, Switzerland,

² University of Barcelona, Barcelona, Spain,

³ Lab. du Développement et des Apprentissages Moteurs, UniGe, Geneva, Switzerland,

⁴ Ecole Polytechnique Fédérale de Lausanne (EPFL), Switzerland.

Ferran.Galan@idiap.ch

Abstract. *Objective:* To assess the feasibility of recognizing visual spatial attention frames for Brain-computer interfaces (BCI) applications. *Methods:* EEG data was recorded with 64 electrodes from 2 subjects executing a visuo-spatial attention task indicating 2 target locations. Continuous Morlet wavelet coefficients were estimated on 18 frequency components and 16 preselected electrodes in trials of 600 ms. The spatial patterns of the 16 frequency components frames were simultaneously detected and classified (between the two targets). The classification accuracy was assessed using 20-fold cross-validation. *Results:* The maximum frames average classification accuracies are 80.64% and 87.31% for subject 1 and 2 respectively, both utilizing frequency components located in gamma band.

1 Introduction

Asynchronous EEG-based brain-computer interfaces (BCI) [1] allow subjects to control devices spontaneously and at their own pace, contrarily to synchronous BCI systems [2], and without requiring external cues such as in the case of relying on evoked potentials [3]. To this end, people learn how to voluntarily modulate different oscillatory EEG rhythms by the execution of different mental tasks. A limitation of using mental tasks as control commands (e.g., imagining movements or doing arithmetics) is that subjects need to keep performing those mental tasks during the whole interaction, what can be exhausting, especially for novel users. An alternative is to exploit conscious behaviors that do not require sustained attention. Recent studies have demonstrated the possibility to modulate EEG alpha band by orienting visuo-spatial attention [4]. In an ideal case, BCI users could make a wheelchair *turn left* just by orienting their attention (without any eye movement) to some location in the left visual field, what is more natural than, for instance, imagining a left hand movement. Moreover, once the wheelchair just turn

^{*} We thank Drs. S. Gonzalez and R. Grave, Geneva Univ. Hospital, for suggesting the use of visuo-spatial attention in BCI. This work was supported in part by the Swiss National Science Foundation through the NCCR ‘IM2’ and by the European IST Programme, Projects FP6-003758 and FP6-IST-027140. This paper only reflects the author’s views and funding agencies are not liable for any use that may be made of the information contained herein.

left, users will simply stop attending to any particular spot of their visual field and the wheelchair, endowed with an intelligent controller [1], will move forward.

In this paper we assess the feasibility of recognizing user’s voluntary modulation of EEG rhythms associated to visuo-spatial attention in an experimental setup close to the ecological conditions of asynchronous EEG-based BCIs. To this end, we compare both, a *traditional BCI approach* and a *frames approach*. These frames, as described by Freeman [5], correspond to active intermittent induced spatial patterns of amplitude modulation of beta-gama oscillations in response to conditioned stimuli. Based on those findings we address the following questions: (i) Does this discontinuous mode of function (i.e., frames) also appear in response to voluntary modulation of EEG rhythms? (ii) In this case, is it possible to classify these frames with respect to the attended location? (iii) Which frequency ranges yields better classification accuracy? (iv) Can this approach improve BCI performance? We hypothesize that *traditional approaches* (assuming sustained modulation of EEG rhythms over time) would face methodological problems: they will label (for training purposes) and classify samples extracted from periods of time where the underlying brain phenomena is either not present or is not salient enough. Then, a *frames approach* (which only classifies those samples where the induced episodic frames are detected) would be more appropriate. This paper addresses these questions and presents some hints for future work.

2 Methods

Data were recorded from 2 subjects with a portable Biosemi acquisition system using 64 channels sampled at 512Hz and high-pass filtered at 1Hz. The sampling rate was fixed at 512Hz to ensure a good estimation of the highest frequency component under analysis. The subjects were sitting in a chair looking at a fixation cross placed at the center of a monitor. The subjects were instructed to covertly attend to one of two possible target locations (lower-left and lower-right monitor’s corners). The target location was specified by the operator in a pseudo-random balanced order. The subjects specified when they started to shift their attention. Each subject participated in 10 sessions composed by 4 trials each, 2 trials for each target. The duration of each trial was 7 seconds but only the first 600ms were utilized in this study.

The signal was spatially filtered using common average reference (CAR) previous to estimate the continuous Morlet wavelet coefficients on 18 frequency components (7, 8, 9, 10, 11, 12, 28, 32, 36, 40, 44, 48, 56, 64, 72, 80, 88, and 96 Hz) and 16 electrodes (F5, FC5, C5, CP5, P5, AFz, Fz, FCz, Cz, PCz, Pz, F6, FC6, C6, CP6, P6). The selection of electrodes was based on preliminary analysis of continuous Morlet wavelet coefficients scalp topography. Thus, each trial is composed by 512×0.6 samples and 18×16 features. The analysis carried on aims to compare the recognition rates over the different frequency components using two different approaches, namely the *traditional BCI approach* and the *frames approach*. The process was structured in two steps:

1. One canonical space was built per each frequency component (18 canonical spaces) [6] using 16-dimensional vectors (estimated wavelet coefficients at 16 electrodes). Since it is a 2-class problem, canonical spaces are defined by 1 canonical function.
2. A linear discriminant classifier (LDA) was built following two different approaches:

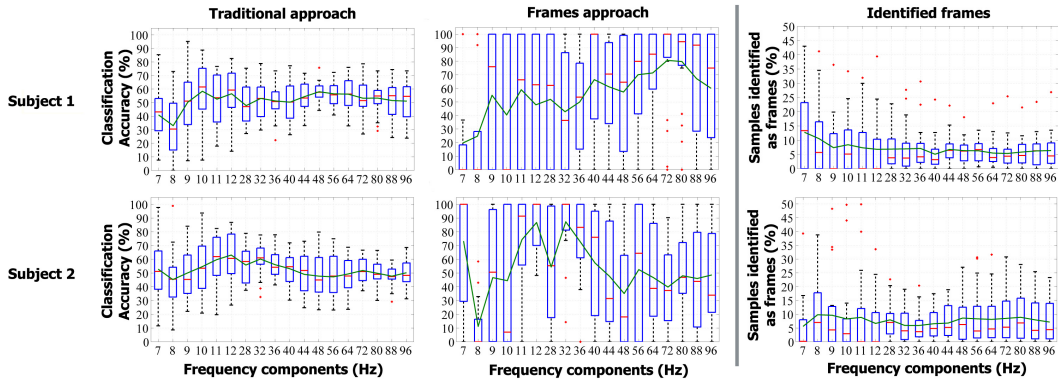


Fig. 1. Classification results using 20-fold crossvalidation over the 18 frequency components. Solid line represents the mean. LDA classification accuracy distributions utilizing traditional approach (*left*) and frames approach (*center*). *Right*, percentage of the total trial samples identified as frames.

- (a) *Traditional BCI approach*: using all the training projected samples on the canonical space and classifying all the test projected samples.
- (b) *Frames approach*: only a subset of the projected samples (i.e. frames) are used for training and classification. A sample was considered as a frame if its projection on the training canonical space was located on the opposite tails of each class distribution. Eight percentiles were utilized as thresholds: P_{40} , P_{35} , P_{30} , P_{25} , P_{20} , P_{15} , P_{10} and P_5 . Thus, a sample was identified as a frame either its projection was below a given percentile (i.e: P_5) of class 1 or above the opposite percentile (i.e: P_{95}) of class 2. From now, the reference to one percentile also includes its opposite.

Both approaches were assessed using k -fold crossvalidation, $k = 20$. Each fold was integrated per one trial of each condition respecting the timing when they were recorded.

3 Results and Conclusions

The average LDA classification accuracy is higher utilizing the frames approach. For both subjects, the maximum classification accuracy is reached utilizing P_5 . We report on detail the results obtained on this percentile. The maximum average classification accuracy classifying all the samples (i.e. traditional approach) is 58.41% at 10Hz and 63.08% at 12Hz for subject 1 and 2 respectively (see Figure 1 *left*), both in the alpha range. Utilizing frames approach, the maximum average classification accuracies are 80.64% at 72Hz, and 87.31% at 32Hz for subject 1 and 2 respectively (see Figure 1 *center*), both in the gamma range. It represents an absolute increase of 22.23% and 27.13% for subject 1 and 2 respectively. Notice that these classification accuracies are computed only on those samples identified as frames. The average percentage of samples identified as frames out of the total of samples of a trial is 5.85% for subject 1 and

5.92% for subject 2 (see Figure 1 *right*) at 72Hz and 32Hz respectively. In case of subject 1, only in 1 fold out of 20 it was not possible to identify any frame. In case of subject 2, it was not possible in 4 out of 20 folds. To understand the implication of these results in a real BCI application, each trial has been labelled according to the class maximum recognized by the classifier, using all the samples in case of traditional approach, and using only frames in case of frames approach. In the first case, the trial classification accuracies are 60.00% and 57.50% for subjects 1 and 2 respectively, what implies that channels capacities are .05 bits/second and .03 b/s (using estimator proposed in [1]). Using frames approach, the trial classification accuracies are 60.00% and 47.50%, but with only 12.50% of error recognition in both cases, what implies that channels capacities are .55 b/s and .46 b/s. Using frames approach the BCI theoretical channel capacity is boosted by 10.

This preliminary study on visuo-spatial attention frame recognition for BCI provides relevant hints for further research. First, it is possible to voluntarily modulate EEG rhythms by orienting visuo-spatial attention in order to use asynchronous noninvasive EEG-based BCI's. Second, the intensity of this modulation is not sustained over time. This fact can be related to the active intermittent induced spatial patterns of amplitude modulation (frames) in response to conditioned stimuli described by Freeman [5]. In this case these patterns are voluntarily driven by the subject. Third, it is possible to classify the frames generated by orienting the attention to different visual locations with high classification accuracies (above 80%). Fourth, these classification accuracies are maximum in gamma band ($> 30\text{Hz}$), corresponding to endogenous shifts of attention effects [7]. Fifth, classification accuracies utilizing a traditional approach, i.e. assuming modulations sustained over time, are around the chance level. It suggests that this approach is not optimal to recognize induced EEG phenomena, what is confirmed comparing the BCI theoretical channel capacity achieved using both approaches. Using frames approach the BCI theoretical channel capacity is drastically increased.

References

- [1] Millán, J. del R., Renkens, F., Mouriño, J., Gerstner, W.: Noninvasive brain-actuated control of a mobile robot by human EEG. *IEEE Trans. Biomed. Eng.* **51** (2004) 1026–1033.
- [2] Birbaumer, N., Ghanayim, N., Hinterberger, T., Iversen, I., Kotchoubey, B., Kübler, A., Perelmouter, J., Taub, E., Flor, H.: A spelling device for the paralysed. *Nature* **398** (1999) 297–298.
- [3] Kelly, S. P., Lalor, E. C., Reilly, R. B., Foxe, J. J.: Visual spatial attention tracking using high-density SSVEP data for independent brain-computer communication. *IEEE Trans. Neural Sys. Rehab. Eng.* **13** (2005) 172–178.
- [4] Thut, G., Nietzel, A., Brandt, S., Pascual-Leone, A.: Alpha-band electroencephalographic activity over occipital cortex indexes visuospatial attention bias and predicts visual target detection. *J. Neurosci.* **26** (2006) 9494–9502.
- [5] Freeman, W. J.: Origin, structure, and role of background EEG activity. Part 3. Neural frame classification. *Clin. Neurophysiol.* **116** (2005) 1118–1129.
- [6] Galán, F., Ferrez, P. W., Oliva, F., Guàrdia, J., Millán, J. del R.: Feature extraction for multi-class BCI using canonical variates analysis. *IEEE Int. Symp. Intell. Signal Process.* (2007).
- [7] Palix, J., Hauert, C. A., Leonards, U.: Brain oscillations: Indicators for serial processing in inefficient visual search? *Perception* **35** (2006) 234.

Appendix F

A Brain-Actuated Wheelchair: Asynchronous and Non-Invasive Brain-Computer Interfaces for Continuous Control of Robots

F. Galán, M. Nuttin, E. Lew, P. W. Ferrez, G. Vanacker, J. Philips, H. Van Brussel, and J. del R. Millán. A Brain-Actuated Wheelchair: Asynchronous and Non-Invasive Brain-Computer Interfaces for Continuous Control of Robots, *Clin. Neurophysiol.*, 2008a. To appear.

Resum

L'objectiu d'aquest article ha estat avaluar la robustesa d'una interfície cerebral asíncrona i no invasiva per a la conducció d'una cadira de rodes mitjançant l'execució de tasques cognitives.

En el primer experiment es va demanar a 2 subjectes que conduïssin mentalment una cadira de rodes, real i virtual, d'un punt de partida a un punt final seguint un trajecte prèviament especificat. En aquest article únicament s'inclouen els resultats obtinguts amb la cadira de rodes virtual. Cada subjecte va participar en 5 sessions experimentals integrades per 10 assajos cadascuna. Les sessions experimentals es van portar a terme amb períodes temporals variables entre elles (de 1 hora a 2 mesos) per avaluar la robustesa temporal del sistema. Alhora, el trajecte especificat es va dividir en 7 trams per avaluar la robustesa contextual del sistema. Per a una avaluació més completa, el subjecte 1 va participar en un segon experiment integrat per 10 assajos en el qual es va demanar de conduir la cadira de rodes seguint 10 trajectes complexos mai executats amb anterioritat.

En el primer experiment ambdós subjectes van poder conduir la cadira de rodes fins al punt final en un 100% (subjecte 1) i un 80% (subjecte 2) dels assajos a les millors sessions experimentals. Els resultats varien temporalment i contextual, fet que demostra

que el rendiment és temporalment i contextualment dependent. En el segon experiment, el subjecte 1 va ser capaç de conduir satisfactòriament la cadira de rodes fins al punt final seguint un 80% dels trajectes.

Aquests resultats mostren que el sistema pot ser controlat sense necessitat de llargues sessions d'entrenament. A més a més, pot ser controlat de manera autònoma per l'usuari sense la necessitat d'algorismes adaptatius calibrats externament per un operador expert en ordre a minimitzar l'impacte de la no-estacionarietat del senyal EEG. Això és gràcies a dos components. Primer, la selecció de característiques EEG estables que maximitzen la separabilitat entre els patrons EEG generats durant l'execució de diferents tasques cognitives. Segon, la inclusió d'un sistema de control compartit entre la interfície cerebral i la cadira de rodes intel·ligent.

A Brain-Actuated Wheelchair: Asynchronous and Non-Invasive Brain-Computer Interfaces for Continuous Control of Robots

F. Galán ^{a,*} M. Nuttin ^b E. Lew ^c P. W. Ferrez ^c G. Vanacker ^b
J. Philips ^b J. del R. Millán ^{c,*}

^a*IDIAP Research Institute, Martigny, Switzerland*
University of Barcelona, Barcelona, Spain

^b*Dept. of Mechanical Engineering, Katholieke Universiteit Leuven, Leuven, Belgium*

^c*IDIAP Research Institute, Martigny, Switzerland*
Ecole Polytechnique Fédérale de Lausanne, Lausanne, Switzerland

Abstract

Objective: To assess the feasibility and robustness of an asynchronous and non-invasive EEG-based Brain-Computer Interface (BCI) for continuous mental control of a wheelchair.

Methods: In experiment 1 two subjects were asked to mentally drive both a real and a simulated wheelchair from a starting point to a goal along a pre-specified path. Here we only report experiments with the simulated wheelchair for which we have extensive data in a complex environment that allows a sound analysis. Each subject participated in 5 experimental sessions, each consisting of 10 trials. The time elapsed between two consecutive experimental sessions was variable (from one hour to two months) to assess the system robustness over time. The pre-specified path was divided in 7 stretches to assess the system robustness in different contexts. To further assess the performance of the brain-actuated wheelchair, subject 1 participated in a second experiment consisting of 10 trials where he was asked to drive the simulated wheelchair following 10 different complex and random paths never tried before.

Results: In experiment 1 the two subjects were able to reach 100% (subject 1) and 80% (subject 2) of the final goals along the pre-specified trajectory in their best sessions. Different performances were obtained over time and path stretches, what indicates that performance is time and context dependent. In experiment 2, subject 1 was able to reach the final goal in 80% of the trials. **Conclusions:** The results show that subjects can rapidly master our asynchronous EEG-based BCI to control a wheelchair. Also, they can autonomously operate the BCI over long periods of time without the need for adaptive algorithms externally tuned by a human operator to minimize the impact of EEG non-stationarities. This is possible because of two key components: first, the inclusion of a shared control system between the BCI system and the intelligent simulated wheelchair; second, the selection of stable user-specific EEG features that maximize the separability between the mental tasks. **Significance:** These results show the feasibility of continuously controlling complex robotics devices using an asynchronous and non-invasive BCI.

Key words: Brain-computer interfaces, electroencephalogram (EEG), asynchronous protocol, feature selection, intelligent wheelchair, shared control.

* Corresponding author.

IDIAP Research Institute

Centre du Parc. Av. des Prés-Beudin 20

CH-1920 Martigny, Switzerland

Tel: (+41) 277217747

Fax: (+41) 277217712

Email addresses: ferran.galan@idiap.ch (F. Galán),
jose.millan@idiap.ch (J. del R. Millán).

1 Introduction

The possibility to act upon the surrounding environment without using our human nervous system's efferent pathways enables a new interaction modality that can boost and speed up the human sensor-effector loop. In recent years, brain-computer interface (BCI) research is exploring many applications in different fields: communication, environmental control, robotics and mobility, and neuroprosthetics (Birbaumer et al., 1999; Obermaier et al., 2003; Bayliss, 2003; Millán, 2003; Nicoletis and Chapin, 2002; Millán et al., 2004; Carmena et al., 2003). Our work in the MAIA project¹ aims at developing asynchronous and non-invasive BCI to control robots and wheelchairs (Millán et al., 2004; Lew et al., 2006). It means that users control such devices spontaneously and at their own paced, by learning to voluntary control specific electroencephalogram (EEG) features measured from the scalp. To this end, users learn how to voluntary modulate different oscillatory rhythms by execution of different mental tasks (motor and cognitive). To facilitate this learning process, we rely upon machine learning techniques, both to find those subject-specific EEG features that maximize the separability between the patterns generated by executing the mental tasks (Galán et al., 2007), and to train classifiers that minimize the classification error rates of these subject-specific patterns (Millán et al., 2004). Finally, to assist the control task, different levels of intelligence are implemented in the device jointly with shared control techniques between the two interacting agents, the BCI system and the intelligent device (Philips et al., 2007; Vanacker et al., 2007).

One of the main challenges of a non-invasive BCI based on spontaneous brain activity is the non-stationary nature of the EEG signals. Shenoy and co-workers (Shenoy et al., 2006) describe two sources of non-stationarity, namely differences between samples extracted from calibration measurements (training data set) and samples extracted during the online operation of the BCI system (test data set), and changes in the user's brain processes during the online operation (e.g., due to fatigue, change of task involvement, etc). Such kind of phenomena have motivated that BCI research groups develop adaptive algorithms to deal with these shifts in the distributions of samples (Shenoy et al., 2006; Buttfeld et al., 2006; Vidaurre et al., 2006; Millán et al., 2007). Unfortunately, current adaptive solutions have two main limitations. Firstly, they are based on supervised approaches requiring the correct output for every sample and so the user cannot operate the BCI autonomously. Secondly, adaptation in the wrong moment (e.g., when the user is not executing properly the mental tasks because of fatigue, distraction, etc) will incorrectly change the feedback (the device's behavior) and will disrupt user's learning process. Given this scenario, two questions arise. Is it possible to find (rather) stable subject-specific

¹ MAIA—*Mental Augmentation through Determination of Intended Action*,

<http://www.maia-project.org>

EEG features to reduce the differences between samples extracted from calibration and online operation sessions? How shared control techniques can minimize the impact of changes in the user's EEG signals during the online operation?

In this paper we describe an asynchronous brain-actuated wheelchair that can be operated autonomously and report results obtained by two subjects while continuously driving a simulated version of the wheelchair. Our brain-actuated wheelchair exhibits two key components, namely the selection of stable user-specific EEG features that maximize the separability between the different mental tasks, and the implementation of a shared control system (Philips et al., 2007; Vanacker et al., 2007) between the BCI and the intelligent simulated wheelchair.

2 Methods

2.1 EEG Data Acquisition and Preprocessing

EEG Data were recorded from 2 healthy subjects with a portable Biosemi acquisition system using 64 channels sampled at 512Hz and high-pass filtered at 1Hz. Then, the signal was spatially filtered using a common average reference (CAR) before estimating the power spectral density (PSD) in the band 8-48 Hz with 2 Hz resolution over the last 1 second. The PSD was estimated every 62.5 ms (i.e., 16 times per second) using the Welch method with 5 overlapped (25%) Hanning windows of 500 ms. Thus, an EEG sample is a 1344-dimensional vector (64 channels times 21 frequency components). Obviously, not all these 1344 features are used as control signals. Sections 2.2 and 2.3 describe the algorithms to estimate the relevance of the features for discriminating the mental commands and the procedure to select the most stable discriminant features that will be fed to the classifier embedded in the BCI. This classifier processes each of the EEG samples and the BCI combines 8 consecutive responses to deliver a mental command every 0.5 seconds.

2.2 Calibration Sessions and Feature Extraction

To extract stable discriminant EEG features (see Sect. 2.3.2) and build the statistical Gaussian classifier embedded in the BCI (see Sect. 2.3.3), both subjects participated in 20 calibration sessions recorded in the same day than the test driving session 1. The calibration sessions were recorded during the morning and the test driving session 1 during the afternoon. As in the driving sessions, the subjects sat in a chair

looking at a fixation point in the center of a monitor. The display was also the same, the simulated wheelchair in a first person view (see Fig. 1 *Left*). The subjects were instructed to execute the three mental tasks (left hand imagination movement, rest, and words association²), tasks utilized as mental commands to operate the wheelchair, in a self-paced way. The mental task to be executed was selected by the operator in order to counterbalance the order, while the subjects decided when they started to execute the mental task. Each calibration session was integrated by 6 trials each, 2 trials of each class. The duration of each trial was 7 seconds but only the last 6 seconds were utilized in the analysis to avoid preparation periods where the subjects were not yet engaged in the execution of the mental task. A trial started when subjects informed the operator they were executing the requested mental task. In these sessions the subjects did not receive any feedback, so the monitor display was static—i.e., the simulated wheelchair did not move.

The data from the 20 calibration sessions were grouped in 4 blocks (B1, B2, B3 and B4) of 5 consecutive sessions. Taking into account the recordings timing, there were different configurations of training and testing sets (train-test): B1–B2, B1–B3, B1–B4, B2–B3, B2–B4, B3–B4, (B1+B2)–B3, (B1+B2)–B4, (B1+B2+B3)–B4. Feature selection was done in a sequential way, where we first picked stable frequency components and then chose the best electrodes. To assess the stability of the frequency components we applied 21 canonical variates analysis (CVA), one per frequency component, on the training set of each configuration. For each canonical space we ranked the electrodes according to their contribution to this space (see Sect. 2.3.2). Then, we built up to 15 linear discriminant (LDA) classifiers³, each using those electrodes that contributed more than $c\%$, with $c \in \{1.0, 2.0, \dots, 15.0\}$. We used the stability of the classifier accuracy over the different configurations to select the frequency components. In particular, we selected those frequencies that performed systematically among the top 5. Afterwards, for each selected frequency, we took the configuration of electrodes (out of the 15 possible ones) that yielded the highest classification accuracy on the configuration (B1+B2+B3)–B4. Finally, we tested the different combinations of selected frequencies (with their associated electrodes) on the configuration (B1+B2+B3)–B4 and chose the best one. At the end of this sequential process the selected frequencies were 12 Hz for subject 1 and $\{10, 12, 14\}$ Hz for subject 2. We then built the statistical Gaussian classifier

² The mental tasks consisted in imagining repetitive self-paced movements of the left hand, getting relaxed centering attention on the fixation point placed on the center of the monitor, and searching words starting with the same letter.

³ The reasons for using a LDA classifier for feature extraction rather than the final Gaussian classifier are the simplicity and speed of training of the former. Furthermore, LDA is a special case of our Gaussian classifier.

(see Sect. 2.3.3) for each subject using their individual selected features from all the data of the calibration sessions. Table 1 reports the LDA classifier accuracies on the configuration (B1+B2+B3)-B4 using the selected features for each subject. Accuracies are not very high, what is normal for a first session without feedback, but still well above random level (33.3% for a 3-class classification problem).

Fig. 2 depicts the electrodes contribution, for each selected frequency component for each subject, and the associated scalp distribution of the averaged logarithmic transform of the PSD ($\text{Log}(PSD_e)$) for each mental task. The $\text{Log}(PSD_e)$ scalp distributions show that the differences between the mental tasks, localized in those electrodes with higher D_e values (see Sect. 2.3.2), are bigger for subject 2. This is in agreement with the train classification accuracies, 59% and 85% for subjects 1 and 2, respectively.

2.3 System Description

The system is integrated by two entities, the intelligent wheelchair and the BCI system. Environmental information from the wheelchair’s sensors feeds a contextual filter that builds a probability distribution $P_{Env}(C)$ over the possible user’s mental steering commands, $C = \{Left, Right, Forward\}$. The BCI system estimates the probabilities $P_{EEG}(C)$ of the different mental commands from the EEG signals. Both streams of information are combined to produce a filtered estimate of the user’s intent $P(C) = P_{EEG}(C) \cdot P_{Env}(C)$. The shared control system also uses the environmental information from the wheelchair’s sensors to map these high-level commands into appropriate motor commands, translational and rotational velocities, that generates a smooth and safe driving behavior. This is achieved by constantly adapting the level of assistance provided to the user to negotiate obstacles. Thus, the intelligent wheelchair, via shared control, will significantly help when the subject’s performance (BCI accuracy) is low whereas it will decrease its role when the BCI accuracy is higher. In other words, the intelligent wheelchair will take over control to avoid obstacles if subjects cannot deliver the proper mental commands to stay at a safe distance from obstacles and will not activate any assisting behavior in case subjects can safely drive the wheelchair. Obstacle avoidance is the only assisting behavior used in the experiments. Fig. 3 depicts a schematic representation of the shared control architecture of the brain-actuated wheelchair. See (Philips et al., 2007; Vanacker et al., 2007) for a detailed description. As for the BCI, it has two components: a feature extractor and a Gaussian classifier. The former selects the most relevant features of the EEG signals based on canonical variates analysis (Galán et al., 2007). Based on these features, the Gaussian classifier estimates the probability distributions of the three mental commands (Millán et al., 2004).

2.3.1 Context-Based Filter

Context estimation is done by defining a general, a priori-known user intention (smooth and efficient forward navigation through the environment) on the one hand and a constant automatic estimation of the environmental situation on the other hand. The situations are modelled as the number and location of openings: wide, open spaces to which the user might safely navigate. The principle is as follows: suppose the wheelchair is approaching a crossroad, as depicted in Fig. 4. The laser scanner in front of the wheelchair scans 180 degrees and senses the distance to the environment for every degree. The algorithm then searches for regions with consecutive scans for which the distance is larger than a certain threshold T . This results in a number of regions that qualify as candidates for an opening. Next, for each of the resulting regions, the width of the opening O is calculated: $O = \sqrt{s_1^2 + s_2^2 - 2s_1s_2\cos(t_2 - t_1)}$. This length is then compared to the physical dimensions of the wheelchair. If the length O exceeds the wheelchair width augmented with a safety margin, the corresponding region is accepted as an opening. Its orientation with respect to the current wheelchair position is then $\frac{\pi}{2} - \frac{t_2 - t_1}{2}$.

Each opening then represents a general direction in which the user might opt to continue his navigation. With this knowledge about the current situation, a probability distribution concerning the possible local user actions is built. Note that inferring these probabilities requires the knowledge of the global intention of the human. In this case, it is supposed that the user wishes to navigate safely and efficiently through the environment without halting or going backwards. In other cases, a user might also wish to stop at certain locations, or dock at particular places. When the directions in which the robot can travel are orthogonal, as in Fig. 4, it is possible to summarize the environmental belief in four quadrants, as depicted in Fig. 5. The figure shows how the regions West and North are deemed probable navigation directions, as extracted from the environment (see Fig. 4). The regions East and South are improbable (as the scanner sees a wall on the right hand, and going backwards is also not probable given the intention of smooth forward navigation). If the wheelchair is oriented North, the controller attaches a probability of 0.5 to *Forward* and *Left*. $P_{Env}(Right)$ is set to zero, because rotating to the right would make the robot turn towards an obstacle (the wall). The possibility of turning into the corridor to the left is reflected in $P_{Env}(Left) = 0.5$. If the wheelchair is oriented 45 degrees North-West, $P_{Env}(Forward)$ has become zero, while the possible commands now are *Left* and *Right*, with equal probability, reflecting the belief that one of the orthogonal directions North or West should be chosen. When the wheelchair is turning further towards West, *Forward* becomes possible again, and $P_{Env}(Right)$ stays constant while $P_{Env}(Left)$ diminishes completely. At the boundary between the probable directions and those that are improbable, the controller attaches a maximum belief to those commands that would keep the wheelchair in the half plane of high probability. Between the above-described orientations, the probabilities are interpolated linearly. This is depicted in Fig. 5 as the linearly changing transparency of the respective circle. See (Vanacker et al., 2007) for a detailed description.

2.3.2 Feature Extractor

Our approach is based on a mutual learning process where the user and the BCI are coupled together and adapt to each other. To facilitate and accelerate this process, it is necessary to select the relevant EEG features that best discriminate among the mental tasks executed by the user. The feature selection process is based on Canonical Variates Analysis (CVA) (Krzanowski, 1998), also known as Multiple Discriminant Analysis (Duda et al., 2001), which provides a canonical solution for multi-class problems. In our case, CVA extract Canonical Discriminant Spatial Patterns (CDSP) whose directions maximize the differences in mean spectral power between a given number of classes.

Let's $\mathbf{S}_k = (\mathbf{s}_{k1}, \dots, \mathbf{s}_{kn_k})'$ be the $n_k \times c$ matrix with the estimated spectral power of a frequency band for class $k = 1, \dots, l$, where n_k is the number of samples and c is the number of channels. Now, given $\mathbf{S} = (\mathbf{S}'_1, \dots, \mathbf{S}'_l)'$, the $l - 1$ CDSP of \mathbf{S} are the eigenvectors \mathbf{A} of $\mathbf{W}^{-1}\mathbf{B}$ whose eigenvalues λ_u , ($u = 1, \dots, l - 1$) are larger than 0. Note that the direction of the eigenvectors \mathbf{A} maximizes the quotient between the between-classes dispersion matrix \mathbf{B} and the pooled within-classes dispersion matrix \mathbf{W} . Thus, the CDSP are obtained by projecting $\mathbf{X} = \mathbf{S}\mathbf{A}$.

Once the CDSP are computed, it is useful to know how the original channels are contributing to the separability among the classes. To measure this contribution we compute a *Discrimination* index for each channel from the *structure matrix*—the pooled correlation matrix between the original channels in \mathbf{S} and the CDSP \mathbf{X} . Given the $c \times (l - 1)$ structure matrix \mathbf{T} , where $\mathbf{T} = \sum_{k=1}^l \mathbf{T}_k$, $e = 1, \dots, c$, and the normalized eigenvalues $\gamma_u = \lambda_u / \sum_{u=1}^{l-1} \lambda_u$, the proposed discrimination index is computed as $D_e = (\sum_{u=1}^{l-1} \gamma_u t_{eu}^2 / \sum_{e=1}^c \sum_{u=1}^{l-1} \gamma_u t_{eu}^2) \times 100$. See (Galán et al., 2007) for more details.

2.3.3 Classifier

The classifier utilized is a statistical Gaussian classifier, (Millán et al., 2004) for more details. The output of this statistical classifier is an estimation of the posterior class probability distribution for a sample; i.e., the probability that a given single trial belongs to each mental task (or class). Each class is represented by a number of Gaussian prototypes, typically less than four. That is, it is assumed that the class-conditional probability function of class k is a superposition of N_k Gaussian prototypes. It is also assume that all classes have equal prior probability. All classes have the same number of prototypes N_p , and for each class each prototype has equal weight $1/N_k$. Then, dropping constant terms, the activity of the i^{th} prototype of class k for a given sample \mathbf{x} is the value of the Gaussian with center μ_k^i and covariance matrix Σ_k^i . From this we calculate the posterior probability y_k of the class k , which is the sum of the activities of all the prototypes of class k divided by

the sum of the activities of all the prototypes of all the classes. The classifier output for input vector \mathbf{x} is then the class with the highest probability. In order to smooth this output, we average the class-conditioned probabilities of the last 8 consecutive input vectors \mathbf{x} . Thus, the BCI responds every 0.5 s. Usually each prototype of each class would have an individual covariance matrix Σ_k^i , but to reduce the number of parameters the model has a single diagonal covariance matrix common to all the prototypes of the same class. During offline training of the classifier, the prototype centers are initialized by any clustering algorithm or generative approach. This initial estimate is then improved by stochastic gradient descent to minimize the mean square error $E = \frac{1}{2} \sum_k (y_k - t_k)^2$, where \mathbf{t} is the target vector in the form 1-of-C; that is, if the second of three classes was the desired output, the target vector is (0,1,0). The covariance matrices are computed individually and are then averaged over the prototypes of each class to give Σ_k .

2.4 Experimental Tasks

2.4.1 Task 1

Both subjects sat in a chair looking at a fixation point placed in the center of a monitor. The monitor displayed a simulated wheelchair in a first person view moving in a simulated world. The subjects were asked to mentally drive the simulated wheelchair from a starting point to a goal following a pre-specified path by executing three different mental tasks (*left* hand imagination movement to turn *Left*, rest to go *Forward*, and words association to turn *Right*). Fig. 1 depicts the monitor display and the pre-specified path. Every subject participated in 5 experimental sessions, each consisting of 10 trials. The time elapsed between two consecutive experimental sessions was variable to assess the system robustness over time: 1 day between sessions 1 and 2, 2 months between sessions 2 and 3, 1 hour between sessions 3 and 4, and finally 1 day between sessions 4 and 5.

2.4.2 Task 2

To further assess the performance of the brain-actuated wheelchair, Subject 1 participated in a second experiment four months later. He performed 10 trials in the same simulated environment where he was asked to drive the simulated wheelchair following 10 different complex and random paths never tried before. Fig. 6 depicts the 10 complex and random paths. Subject 2 did not participate in this task because she was not available.

2.5 Analysis

The system's robustness was assessed in task 1 on three criteria, namely the percentage of goals reached, the BCI classification accuracy, and the shared control accuracy (the actual mental commands sent to the wheelchair after combining the probability distributions from the BCI and contextual filter). The three criteria were analyzed over time (5 sessions) and context. For the contextual analysis, the path was split in 7 stretches. Thus, the system's performance was measured over the final goal (complete path) and subgoals (path stretches). Additionally, we compared the performance of the 2 subjects to that of a random BCI to further assess their level of mental control. In this case, we use the percentage goals reached by a random BCI as a reference.

The analysis of the accuracies of the BCI and shared control has a main limitation since it requires to know the subject's intent. It is true, however, that in the experiments subjects had to inform verbally the operator whenever they switched mental task so that the latter could label the data. Unfortunately, this approach is far from optimal. Indeed, providing this information interferes with, and so hampers, the driving task. As a consequence, the subject may deliver wrong or delayed mental commands leading to poor trajectories that the subject needs to correct by rapidly switching between mental commands—and the subject does not have time to inform the operator of all those switches and their exact timing. It follows that using the subject's stated intent for labelling data yields a pessimistic and/or wrong estimate of the accuracies of the BCI and the shared control. For this reason the accuracies were estimated in a different way. Each path stretch was labelled with the command that makes the wheelchair reach the next subgoal. Only those samples where the subject's stated intent corresponds to the stretch label were utilized to compute the accuracies. Fig. 7 shows the 7 labelled stretches.

To avoid the limitations described before, in task 2 the subject drove the wheelchair without informing the operator about the mental command he was executing. In this way, the subject could drive the simulated wheelchair in real conditions that allow a better assessment of the brain-actuated wheelchair. In this case only the behavioral performance (percentage of goals reached) was assessed.

An issue to be ruled out in any BCI system is the use of eye movements or muscular activity components embedded in the EEG as control signals. In the experiments described in this paper this issue was not assessed directly, but it was in posterior experiments with the real wheelchair where the two subjects utilized the same statistical Gaussian classifier as here. In these experiments we monitored eye movements and muscular activity by means of bipolar electrooculogram (EOG) using surface electrodes placed below and laterally to the left eye, and by bipolar electromyogram (EMG) using 2 surface electrodes placed on the forearm muscle Extensor Digitorum. The analysis of EOG and EMG activity showed that eye move-

ments were equally distributed among the classes and that there was no significant muscular activity. Thus, we can conclude that subjects did not use any EOG and/or EMG feature as control signals. Also, the fact that the selected band frequency is 10-14 Hz makes it very improbable to have EOG/EMG artifacts. Furthermore, in the experiments reported in this article, we did not observe any overt movement of the subjects' left hand.

3 Results

3.1 Task 1

3.1.1 Global Performance

Fig. 8 depicts the percentage of final goals reached over the 5 sessions for the 2 experimental subjects. Subject 1 reached more final goals in all the sessions. For both subjects, session 1 and session 3 are the sessions with less reached final goals (40% and 10% in session 1, 50% and 40% in session 3). Note that between session 2 and session 3 passed 2 months, so sessions 1 and 3 can be considered as sessions where the subjects learn (session 1) and re-learn (session 3) how to interact with the system and its dynamics. If these sessions were not considered, the average percentage of reached final goals are 86.7% and 66.7% for subjects 1 and 2, respectively. Regarding the maximum performances, subject 1 reached the final goal 100% of the trials in session 4, and subject 2 reached the final goal 80% of the trials in session 2. It is worth noting that even in the first session where the subjects had the lowest performance (40% and 10% of reached goals), they significantly outperformed the random BCI that only reached the goal along the pre-specified path in 1% of the cases. This figure was obtained by running 100 trials.

Table 2 displays the percentage of reached local goals, the average BCI classification accuracy and the shared control accuracy on each session over the 7 path stretches (local goals) for the two subjects, and the percentage of reached goals for the random BCI. This table makes it clear the reasons why subjects couldn't reach the final goal—they failed sometimes to turn *Left* at the stretch L and/or to turn *Right* at the stretches R1 and R2. Interestingly, in these three stretches shared control performed generally worse than the BCI, what could indicate that subjects tried to deliver mental commands that the shared control system considers impossible to execute. On the contrary, shared control significantly improved the performance of BCI at stretches F1, SD1, SD2 and F2, where the wheelchair was supposed to go straight. The average difference over these stretches is 35% for subject 1 (24% BCI

vs. 59% shared control) and 20% for subject 2 (34% BCI vs. 55% shared control). These ‘poor’ accuracies of the BCI and shared control indicate that to drive the wheelchair straight subjects cannot simply deliver the mental command *Forward*, but needed to steer *Left* and *Right*. Furthermore, shared control helped to generate smoother trajectories, especially in the vicinity of walls.

Subject 1 failed to reach the final goal in session 1 because he could not turn *Left* at stretch L in 30% of the cases and, afterwards, he failed to turn *Right* in 40% of the cases that he successfully arrived to stretch R2. In this session, subject 1 always performed correctly the optimal action for all other stretches he went through. As mentioned before, at these ‘hard’ stretches, L and R2, shared control degraded the BCI performance (50% vs. 62% in L and 47% vs. 53% in R2). Regarding session 3, subject 1 failed to reach the final goal because he could not turn *Left* at stretch L 50% of the cases. This was due to a low BCI accuracy (42%) and a lower shared control accuracy (37%). Finally, in sessions 2, 4 and 5 subject 1 reached the final goal 70% (or more) of the trials and each local goal over 88%.

Subject 2 failed to reach the final goal in session 1 because he could not turn *Right* at stretch R1 in 90% of the cases. This was due to a very low BCI and shared control accuracy (29%). In sessions 3 and 5, the poor final performance was due to failures in turning *Left* at stretch L—accuracies of 50% and 40%, respectively. Similarly to subject 1, also in these two sessions shared control degraded the BCI performance although less severely (38% vs. 37% in session 3, 48% vs. 39% in session 5). Finally, in sessions 2 and 4 subject 2 reached the final goal 70% (or more) of the trials and each local goal over 80%.

Regarding the random BCI, it reached the final goal a mere 1% of the trials because it was able to turn *Right* at stretch R1 and to turn *Left* at stretch L only 16% and 6% of the trials, respectively, percentages significant lower than those achieved by subjects 1 and 2.

3.1.2 System Performance in Single Trials

Here we analyze the performance of the brain-actuated wheelchair in a few single trials to show emergent behaviors originated by the interaction of the BCI system and the shared control system in particular contexts. The experimental results show that subjects cannot execute a given mental task with the same level of proficiency all across the trajectories and over time. But, is this the only reason of the inter-trial differences in BCI classification accuracy for the same path stretch? We have observed that the interaction of the BCI system and the shared control system in a particular context plays also a significant role. We have already mentioned in the previous section that, for some stretches, shared control degraded the performance of the BCI, what could indicate that subjects tried to deliver mental commands that

the shared control system considers impossible to execute. Here we take a closer look at this situation.

Table 3 shows the performance for subject 1 in session 4 for trials 2 and 8 at two stretches, R1 and R2, requiring the same command. Subject 1 always succeeded in making the wheelchair turn *Right*. However, the BCI and shared control performances were rather different. Thus, we can see that whenever the BCI accuracy is sufficiently high (92% in trial 2 stretch R1, 74% in trial 8 stretch R2) the shared control accuracy is much lower (67% and 53%, respectively). The opposite happens when the BCI accuracy is not that good (trial 2 stretch R2 and trial 8 stretch R1). The implication for the subjects is that they need to learn a model of the shared control system (and its interaction with the BCI) to develop successful driving strategies, otherwise their BCI proficiency cannot be fully exploited and, eventually, can hamper the behavior of the wheelchair. But for the subjects to learn that model they need to have a stable performance of the brain-actuated wheelchair. Table 2 shows that, in many cases, the shared control accuracy is rather stable independently of the performance of the BCI (see, in particular, trial 2).

3.2 Task 2

Subject 1 reached the final goal 80% of the trials. He failed in the last 2 trials, where he was not able to turn *Right* at the starting point. Making this first *Right* turn requires a very high BCI performance because the subject has to rotate the wheelchair by 90 degrees almost in place (i.e., without entering the corridor it is facing). Indeed, the execution of even a short number of wrong commands in this context makes the shared control system to move the wheelchair *Forward*. Once the wheelchair is in the corridor, the shared control system makes it very hard to turn back (180 degrees) rapidly and the trial is considered a failure. To illustrate the behavior of the brain-actuated wheelchair in this task, we have included a supplementary video clip (WMV file, supplementary material) which contains the trajectories generated on trials 7 (successful) and 10 (unsuccessful).

4 Conclusions

In this paper we have presented an asynchronous and non-invasive EEG-based BCI prototype for brain-actuated wheelchair driving. The system can be autonomously operated by the user without the need for adaptive algorithms externally tuned by a human operator to minimize the impact of EEG non-stationarities. Our brain-actuated wheelchair has two key components. First, the selection of stable user-

specific EEG features that maximize the separability between the patterns generated by executing different mental tasks. Second, the inclusion of a shared control system between the BCI system and the intelligent simulated wheelchair. The reported experiments with two subjects have shown that both were able to reach 90% (subject 1) and 80% (subject 2) of the goals one day after the calibration of the BCI system, and 100% (subject 1) and 70% (subject 2) two months later. It is worth noting that both subjects reached less goals in the first session (one hour after the calibration of the BCI system) and in the third session (two months after the calibration of the BCI system), sessions where the subjects learn or re-learn how to interact with the system and its dynamics. As a consequence, subjects need to cope with the need to generate stable EEG patterns even in the presence of distracting events such as unexpected trajectories of the wheelchair due to the interaction between its intelligence and the context. However, even in these sessions, the subjects showed significant brain-actuated control of the simulated wheelchair: indeed, a random BCI can only reach a mere 1% of the goals.

In agreement with the results obtained in (Vanacker et al., 2007), the analysis over different path stretches shows that the shared control system boosts the BCI performance when it is low, while it may even degrade it when the BCI performance is higher because the user driving strategy it is not compatible with the context-based filter. This could explain why subject 1 achieves better performance in task 1 than subject 2 despite the lower LDA classification accuracies on the calibration session (see Table 1). As a consequence, the subject has to learn when these situations occur in order to develop successful driving strategies compatible with the rules of the shared control system. On the other hand, a low BCI accuracy during the driving tasks does *not* necessarily imply that the BCI is not working correctly. This accuracy is *estimated* according to the user's stated intent and/or the optimal command for each stretch, while for a proper control of the wheelchair subjects need to make steering corrections and so switch rapidly between mental commands. For this reason we believe that the assessment of an intelligent brain-actuated device cannot simply be based on the BCI performance. As illustrated by the results achieved in task 2, our approach makes it possible for subject 1 to drive along complex paths once he was "free" to concentrate on the task, as he did not need to inform the operator of the mental commands he intended to deliver to the wheelchair.

In this article we have demonstrated our approach with healthy subjects. However, it is worth noting that our approach should also work for disabled people since it is based on an individual calibration. This calibration procedure, which is common to all users, selects user-specific features that are relevant and stable. In addition, the approach is not based on a fixed set of mental tasks, but subjects can choose those tasks they feel more comfortable with and yield EEG patterns that are more discriminant among themselves.

This discussion brings up a critical issue of a BCI, namely training. Several groups have demonstrated that subjects can learn to control their brain activity through

appropriate, but lengthy, training in order to generate fixed EEG patterns that the BCI transforms into external actions (Birbaumer et al., 1999; Wolpaw and McFarland, 2004). In this case the subject is trained over several months to modify the amplitude of their EEG signals following bio-feedback approaches. Contrarily, we follow a mutual learning process to facilitate and accelerate the user's training period. Subjects still need to learn to modulate their EEG but not all the training burden is on their shoulders-the use of statistical machine learning facilitates the selection of relevant, stable EEG features and the design of optimal classifiers. As shown for the experiments in task 1, subjects can control the wheelchair since the first day with a performance significantly better than a random BCI.

5 Acknowledgements

This work was supported in part by the European IST Programme FET Project FP6-003758 (MAIA), by the Swiss National Science Foundation through the National Centre of Research on "Interactive Multimodal Information Management (IM2)", and by FWO Flanders project G.0317.05. This paper only reflects the author's views and funding agencies are not liable for any use that may be made of the information contained herein.

References

- Bayliss JD. Use of the evoked potential P3 component for control in a virtual apartment. *IEEE Trans. Neural Sys. Rehab. Eng.* 2003; 11:113–116.
- Birbaumer N, Ghanayim N, Hinterberger T, Iversen I, Kotchoubey B, Kübler A, Perelmouter J, Taub E, Flor H. A spelling device for the paralysed. *Nature* 1999; 398:297–298.
- Buttfield A, Ferrez PW, Millán J del R. Towards a robust BCI: Error potentials and online learning. *IEEE Trans Neural Sys Rehab Eng.* 2006; 14:164–168.
- Carmena JM, Lebedev MA, Crist RE, O'Doherty JE, Santucci DM, Dimitrov DF, Patil PG, Henriquez CS, Nicolelis MAL. Learning to control a brain-machine interface for reaching and grasping by primates. *PLoS Biol* 2003; 1:193–208.
- Duda RO, Hart PE, Stork DG. *Pattern Classification*, 2nd ed. John Wiley & Sons, 2001.
- Galán F, Ferrez PW, Oliva F, Guàrdia J, Millán J del R. Feature Extraction for Multi-class BCI using Canonical Variates Analysis. In Proc. 2007 IEEE Int. Symposium on Intelligent Signal Processing (WISP) 2007. (Available at <http://ieeexplore.ieee.org>)

- Krzanowski WJ. Principles of Multivariate Analysis. Oxford: Oxford University Press, 1988.
- Lew E, Nuttin M, Ferrez PW, Degeest A, Buttfeld A, Vanacker G, Millán J del R. Noninvasive brain-computer interface for mental control of a simulated wheelchair. In Proc. 3rd Int. Brain-Computer Interface Workshop & Training Course 2006.
- Millán J del R. Adaptive brain interfaces. *Comm. of the ACM* 2003; 46:75–80.
- Millán J del R, Renkens F, Mouriño J, Gerstner W. Noninvasive brain-actuated control of a mobile robot by human EEG. *IEEE Trans. Biomed. Eng.* 2004; 51:1026–1033.
- Millán J del R, Buttfeld A, Vidaurre C, Krauledat M, Schögl A, Shenoy P, Blankertz B, Rao RPN, Cabeza R, Pfurtscheller G, Müller K-R. Adaptation in brain-computer interfaces. In: Dornhege G, Millán J del R, Hinterberger T, McFarland D, Müller K-R, editors. *Towards Brain-Computer Interfacing*, Cambridge: MIT Press, 2007:303–325.
- Nicolelis MAL, Chapin JK. Controlling robots with the mind. *Sci. Am.* 2002; 287:46–53.
- Obermaier B, Müller GR, Pfurtscheller G. Virtual keyboard controlled by spontaneous EEG activity. *IEEE Trans. Neural Sys. Rehab. Eng.* 2003; 11:422–426.
- Philips J, Millán J del R, Vanacker G, Lew E, Galán F, Ferrez PW, Van Brussel H, Nuttin M. Adaptive shared control of a brain-actuated simulated wheelchair. In Proc. 10th Int. Conf. Rehabilitation Robotics 2007. (Available at <http://ieeexplore.ieee.org>)
- Shenoy P, Krauledat M, Blankertz B, Rao RPN, Müller K-R. Towards adaptive classification for BCI. *J. Neural. Eng.* 2006; 3:13–23.
- Vanacker G, Millán J del R, Lew E, Ferrez PW, Galán F, Philips J, Van Brussel H, Nuttin M. Context-based filtering for assisted brain-actuated wheelchair driving. *Computational Intelligence and Neuroscience* 2007; Article ID 25130.
- Vidaurre C, Schlogl A, Cabeza R, Scherer R, Pfurtscheller G. A fully on-line adaptive BCI. *IEEE Trans. Biomed. Eng.* 2006; 53:1214–1219.
- Wolpaw JR, McFarland DJ. Control of a two-dimensional movement signal by a noninvasive brain-computer interface in humans. *PNAS* 2004; 101:17849–17854.

Table 1

LDA train-test classification accuracies on the configuration (B1+B2+B3)-B4 using the selected features for each subject.

Subject	Train	Test
1	59.0%	54.7%
2	85.0%	61.2%

Table 2

Percentage of local goals reached (subgoals), average BCI classification accuracy and average shared control accuracy over the 7 path stretches.

Subject	Criterion	Session	Path Stretch							
			F1	R1	SD1	L	SD2	R2	F2	
1	Subgoals (%)	1	100	100	100	70	100	57	100	
		2	100	100	100	90	100	100	100	
		3	100	100	100	50	100	100	100	
		4	100	100	100	100	100	100	100	
		5	100	90	100	89	100	88	100	
	BCI / Shared Control Accuracy (%)	1	18/45	73/62	20/40	62/50	18/33	53/47	23/67	
		2	22/52	73/70	26/53	57/55	20/58	68/67	19/58	
		3	34/62	70/59	22/46	42/37	15/78	69/63	29/85	
		4	28/55	70/63	22/66	54/51	16/57	69/64	25/68	
		5	33/62	56/51	29/62	53/52	29/63	56/47	30/75	
	2	Subgoals (%)	1	100	10	100	100	100	100	100
			2	100	100	100	90	100	89	100
			3	100	100	100	40	100	100	100
			4	100	80	100	88	100	100	100
			5	100	100	100	50	100	100	100
BCI / Shared Control Accuracy (%)		1	40/61	29/29	17/42	89/89	25/83	61/68	36/50	
		2	33/41	71/68	40/62	57/59	26/48	66/65	35/61	
		3	40/55	77/75	40/57	38/37	26/56	73/67	48/70	
		4	38/46	62/63	46/62	49/53	38/48	77/77	35/61	
		5	31/42	65/63	27/43	48/39	27/43	77/74	24/54	
Random	Subgoals (%)	-	100	16	100	6	100	100	100	

Table 3

Inter-trial differences in performance: subject 1, session 4.

Trial	Stretch	BCI Acc.	Shared control Acc.	Wheelchair Behavior
2	R1	92%	67%	<i>Right</i>
	R2	48%	68%	<i>Right</i>
8	R1	65%	76%	<i>Right</i>
	R2	74%	53%	<i>Right</i>

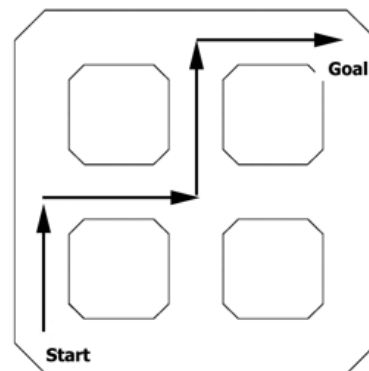
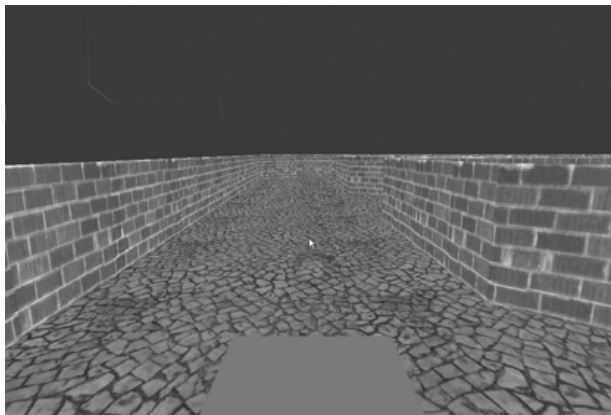


Figure 1. *Left*: monitor display in a first person view from the Start. The white cursor at the center is the fixation point. The rectangle at the bottom is the simulated wheelchair. *Right*: top view of the simulated world and the pre-specified path.

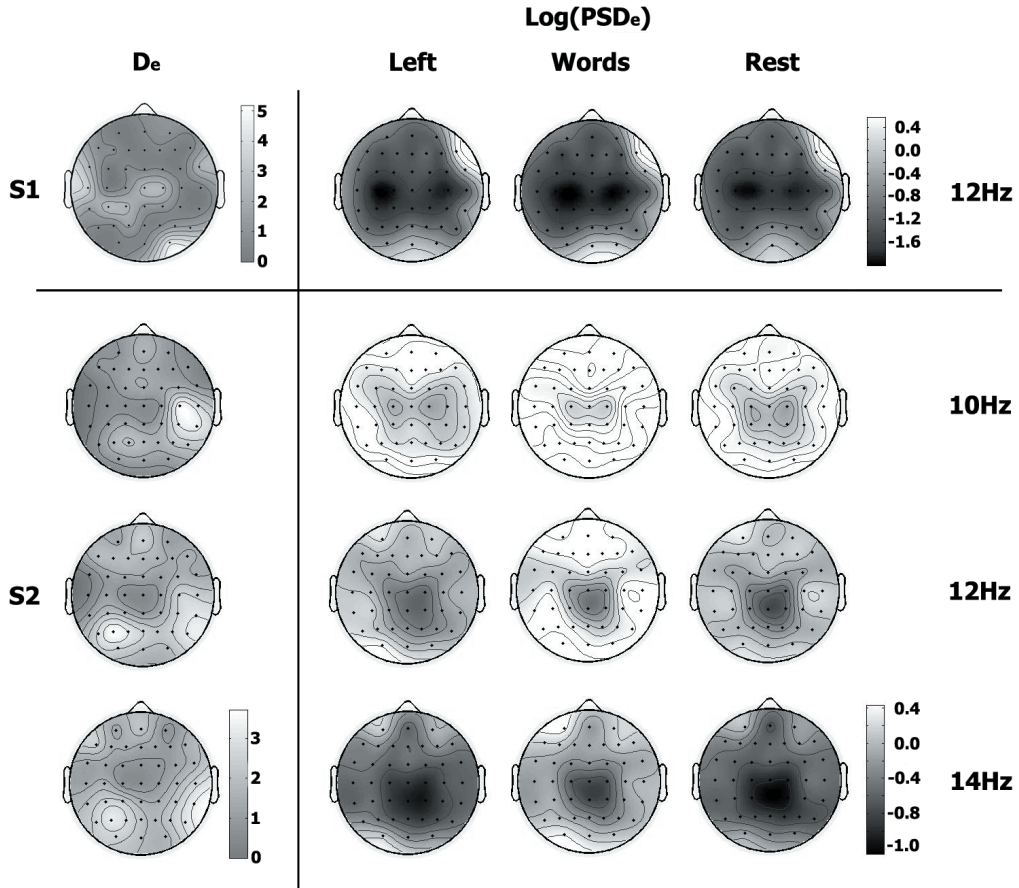


Figure 2. Electrode discrimination index values D_e (see Sect. 2.3.2) for the selected frequencies for each subject, and the associated scalp distribution of the averaged logarithmic transform of the power spectral density, $\text{Log}(PSD_e)$, for each class. For subject 1, D_e is higher at left temporal, central and right occipital areas. For subject 2, at 10 Hz it is higher at right centro-parietal areas, and at 12 and 14 Hz it is higher at bilateral parietal areas. These areas correspond with those where the differences between the averaged $\text{Log}(PSD_e)$ patterns associated to each mental task is the biggest.

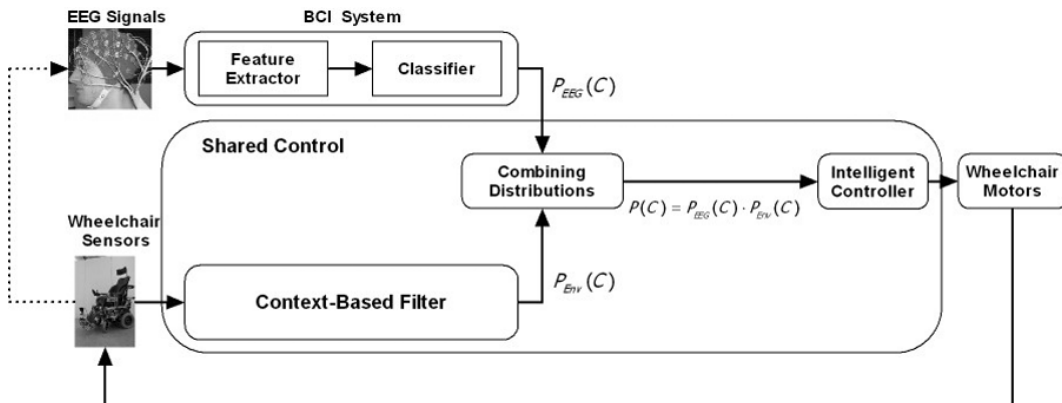


Figure 3. Architecture of the brain-actuated wheelchair.

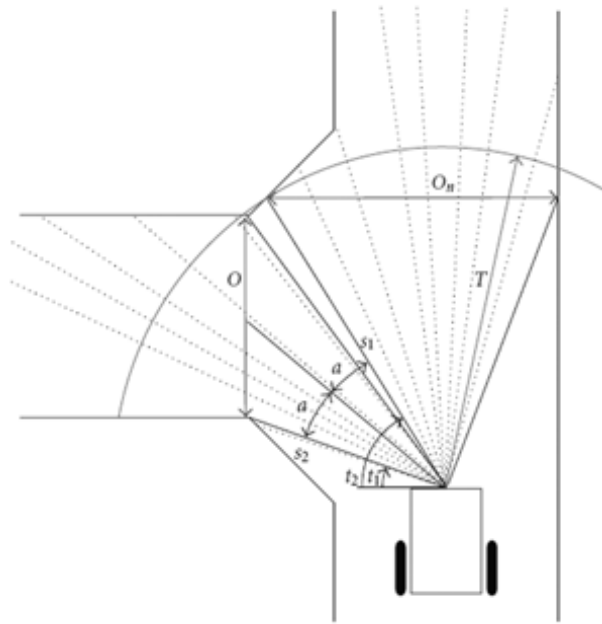


Figure 4. Principle of context estimator. With a laser range scanner, a set of regions that provide safe manoeuvrable openings in the environment is detected. The figure shows how the region to the left and the one in front of the wheelchair are detected as openings.

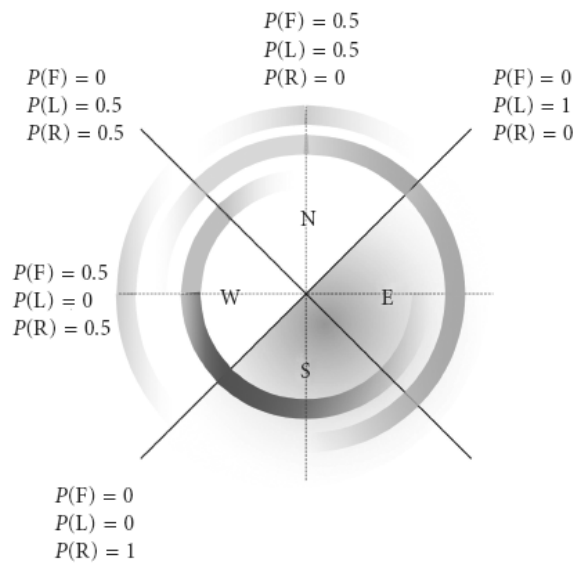


Figure 5. Extracting user intent from the context in function of the wheelchair orientation. Four quadrants are shown, representing a situation in which possible directions are arranged orthogonal. The inner circle shows the probability of a *Right* command, the middle circle the probability of a *Left* command and the outer circle the probability of a *Forward* command.

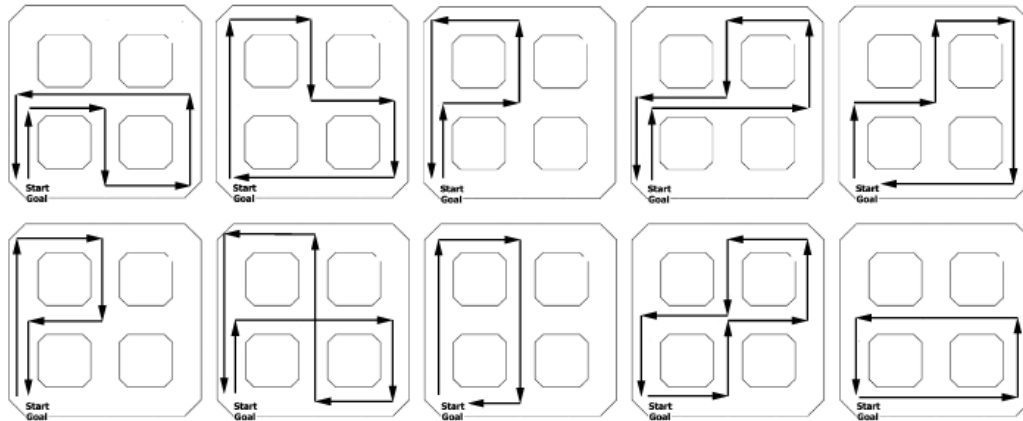


Figure 6. Top view of the random paths in Task 2. Trial 1 placed in upper row, first column. Trial 10 placed in second row, last column.

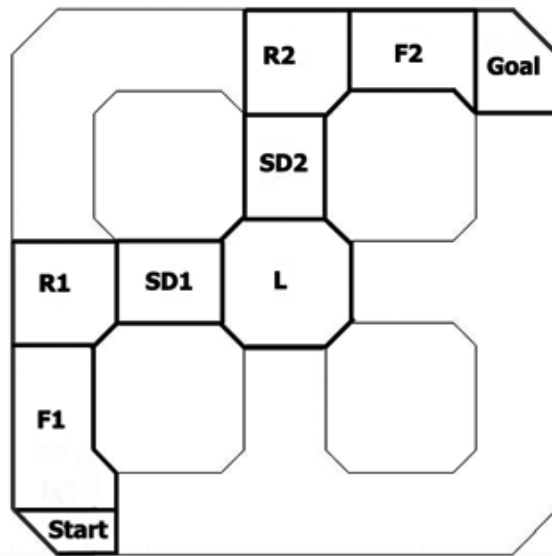


Figure 7. Top view of the world and the path stretches. Stretches F1 and F2 were labelled as *Forward*, R1 and R2 labelled as *Right*, L labelled as *Left*, and SD1 and SD2 labelled as strategy dependent. The subjects can go through SD1 by means of two strategies, either executing *Forward* or executing *Right* followed by *Left*. Through SD2, subjects can execute either *Forward* or *Left* followed by *Right*.

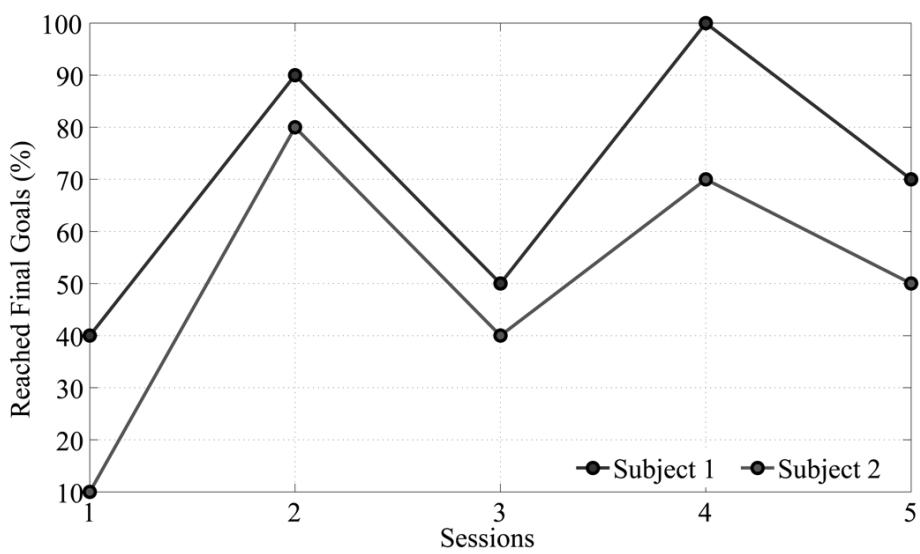


Figure 8. Percentage of reached final goals over sessions. The time elapsed between sessions was: 1 day between sessions 1 and 2, 2 months between sessions 2 and 3, 1 hour between sessions 3 and 4, and 1 day between sessions 4 and 5.

Appendix G

Adaptive Shared Control of a Brain-Actuated Simulated Wheelchair

J. Philips, J. del R. Millán, G. Vanacker, E. Lew, F. Galán, P.W. Ferrez, H. Van Brussel, and M. Nuttin. Adaptive shared control of a brain-actuated simulated wheelchair. In *Proceedings of the 10th International Conference on Rehabilitation Robotics, ICORR 2007*, Noordwijk, The Netherlands, 2007.

Resum

La utilització de tècniques de control compartit han tingut un gran impacte en el rendiment d'un assistent robòtic controlat mitjançant senyals cerebrals humanes. Tanmateix, aquest control compartit assisteix d'una manera constant i idèntica en cada moment. L'actuació d'un nivell adaptatiu d'assistència complementant les capacitats de l'usuari seria més apropiat. En aquest escenari, a millor rendiment de l'usuari menor assistència seria proporcionada pel control compartit i viceversa. Per tal de desenvolupar aquest concepte és necessari inferir quan i de quina manera l'usuari necessita assistència. Un cop detectada la necessitat d'assistència, un comportament assistent apropiat d'acord a una situació específica seria activat.

Aquest article presenta un sistema de control compartit adaptatiu per assistir a un usuari d'una interfície cerebral en la conducció d'una cadira de rodes virtual. Com més dificultats tingui l'usuari per conduir la cadira, més assistència serà proporcionada. Resultats experimentals amb 2 subjectes mostren l'increment del rendiment en la conducció de la cadira utilitzant el sistema de control compartit proposat.

Adaptive Shared Control of a Brain-Actuated Simulated Wheelchair

Johan Philips, José del R. Millán, Gerolf Vanacker, Eileen Lew, Ferran Galán,
Pierre W. Ferrez, Hendrik Van Brussel and Marnix Nuttin

Abstract—The use of shared control techniques has a profound impact on the performance of a robotic assistant controlled by human brain signals. However, this shared control usually provides assistance to the user in a constant and identical manner each time. Creating an adaptive level of assistance, thereby complementing the user’s capabilities at any moment, would be more appropriate. The better the user can do by himself, the less assistance he receives from the shared control system; and vice versa. In order to do this, we need to be able to detect when and in what way the user needs assistance. An appropriate assisting behaviour would then be activated for the time the user requires help, thereby adapting the level of assistance to the specific situation. This paper presents such a system, helping a brain-computer interface (BCI) subject perform goal-directed navigation of a simulated wheelchair in an adaptive manner. Whenever the subject has more difficulties in driving the wheelchair, more assistance will be given. Experimental results of two subjects show that this adaptive shared control increases the task performance. Also, it shows that a subject with a lower BCI performance has more need for extra assistance in difficult situations, such as manoeuvring in a narrow corridor.

I. INTRODUCTION

Nowadays, most people who are paraplegic or have another physical impairment at the lower limbs can be provided with a fair amount of mobility and independence through the use of an ordinary wheelchair, either manual or electrical. However, the use of such a mechanical device cannot provide aid to all people. Imagine someone with an uncontrollable tremor in his hand or arm trying his best to make a safe passage through a narrow corridor using an electrical wheelchair. For those people an intelligent controller inside the wheelchair together with range sensors, detecting nearby obstacles, could solve many of problems [1]. Theoretically, the person could then switch on this controller and it would autonomously drive the wheelchair through the corridor, while avoiding all obstacles. Though this might be appropriate for other applications, the wheelchair user loses the feeling of continuous control. This loss of independence is undesirable and therefore, shared control between the user and the controller is more suitable in these cases. There have been promising results in this field recently, where the shared control system estimates the user’s intention and provides aid accordingly [2], [3].

Nevertheless, there are still people who cannot directly benefit from this technology due to their severe physical impairment. Tetraplegics, whose paralysis prevents them

This work is supported by the European IST Programme FET Project FP6-003758. This paper only reflects the authors’ views and funding agencies are not liable for any use that may be made of the information contained herein.



Fig. 1. The subject wearing an electroencephalogram (EEG) sensor cap is manoeuvring the robot wheelchair *Sharioto* through a natural indoor environment. The electrodes on the sensor cap are connected to the BCI system through an analogue to digital converter and amplifier.

from using an ordinary joystick of an electrical wheelchair by hand or patients with locked-in syndrome, require other technologies. Examples are the chin joysticks, which can be mounted on the wheelchair, or the eye and gaze tracking techniques [4]. Another promising technology is brain-computer interface (BCI) control of a mechanical device.

Although the idea of mentally controlling a common apparatus is certainly appealing, the complexity of an everyday environment increases the difficulty to design a robust system, capable of coping with such a complexity. Nevertheless, more recently, there seems to be an increase in the research done on non-invasive brain-computer interfaces. The key motivation of this research is to provide aid for people whose impairment is so severe that current solutions are not suitable. BCI control could offer them a way to improve their communication, increase their mobility and independence again. Typical applications would be spelling devices, prostheses and mobility aids, such as a wheelchair.

More recently, in the MAIA project ¹ the asynchronous IDIAP BCI [5] has been integrated with the intelligent wheelchair *Sharioto* of the KU Leuven [6] to allow a person to continuously drive it in natural environments, as shown in Figure 1. This brain-actuated wheelchair incorporates the advances in adaptive shared autonomy, on-line adaptation, as well as the on-line use of both high frequency bands and estimated local field potentials [7], four of the achievements of the MAIA project.

This paper presents this adaptive shared control system for the BCI controlled wheelchair where several behaviours are enabled simultaneously and will be activated only when the user is in need of them. In this paper, we will focus on these aspects that have been tested in simulation in order to evaluate the proposed approach. The use of shared control techniques has a profound impact on the performance during BCI control of a robotic assistant [8]. Yet, most of the time, shared control techniques assist the user in a constant and identical manner every time. In other words, the level of assistance is constant.

A next step in the development of shared control techniques would be to make the robot’s assistance level adaptive so as to complement the user’s capabilities at any moment. The better the user can do by himself, the less assistance he receives from the shared control system; and vice versa. In this way, the user remains in maximal control of the brain-actuated robot, which is considered to be desirable for people in need of such systems [1]. To implement this principle, it is necessary for the shared control module to detect when and in what way the user needs assistance. An appropriate assisting behaviour would then be activated for the time that the user needs help. In other words, the system should be able to constantly adapt the level of assistance to the specific situation. More assistance when the user needs it, less when the user is sufficiently capable of controlling the robot himself.

In the experiment presented in this paper, we tested this concept of adaptive shared control by introducing three levels of assistance which are activated only when the user needs them. The first two, collision avoidance and obstacle avoidance, prevent the user from colliding with obstacles. The third level of assistance is called orientation recovery and will be triggered whenever the user has difficulties in driving the wheelchair towards the goal.

In this case, however, rather than choosing one of them, all behaviours are enabled, but they will only be active if their respective assisting behaviour is required. Therefore, the user has complete control over the wheelchair until he or she requires assistance. The goal of this experiment is to indicate the need for such an adaptive shared control as well as the benefits the user will gain from it. This paper

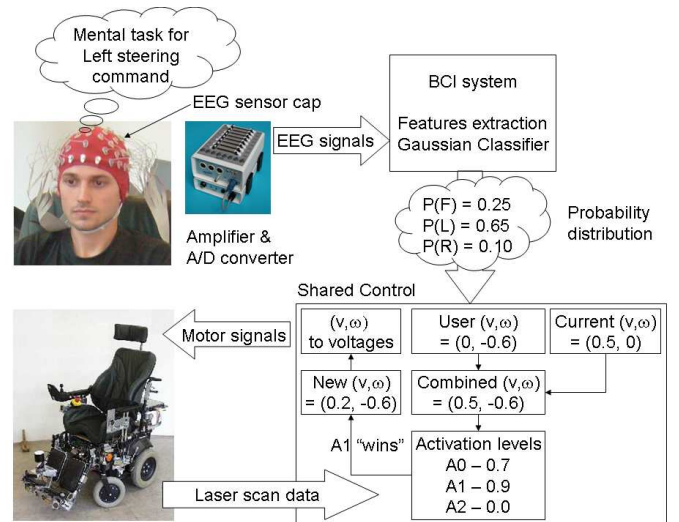


Fig. 2. Diagram of how a mental steering command is integrated in the shared control system and eventually converted into motor signals. Shown here, the user’s mental task corresponds to moving the wheelchair left. In this case, obstacle avoidance is the winning behaviour and adjusts the (v, ω) velocities to prevent collision.

focuses on the shared control framework, rather than on the BCI itself.

II. APPROACH

A. Brain-Computer Interface

The mental commands are obtained from a BCI based on non-invasive electroencephalogram (EEG) signals. These signals are measured by placing electrodes on the scalp, after preparing the scalp area by applying a conductive gel to reduce impedance. The electrodes are part of the EEG cap, worn by the subjects. The measured EEG signals represent an electrical signal (post-synaptic potentials) from a large number of neurons. An amplifier is connected to the electrodes on the EEG cap to amplify the voltage signal. The resulting signal is filtered by a high-pass filter and a low-pass filter. Finally, the signal is sent through an analogue to digital converter. EEG potentials were recorded at 512Hz with 64 electrodes covering the whole scalp. An example of such a configuration is depicted in Figure 1.

There are three possible discrete mental steering commands: Forward, Left and Right. An asynchronous BCI, which responds every 0.5 seconds, sends a probability distribution over the three mental commands to the shared control system. This probability distribution is estimated by a statistical Gaussian classifier that takes as inputs samples made of the power spectrum density, computed over the last second, at several frequency bands for a number of channels. Frequency bands and channels were individually selected using feature selection techniques, yielding 4 bands (from 8 – 14Hz to 192 – 208Hz) and 4 to 8 electrodes per experimental subject. Details of the BCI and the statistical classifier can be found in [5], [7], [9].

¹MAIA or Mental Augmentation through Determination of Intended Action, is a EU STREP IST project (6th FWP). The coordination is done by IDIAP, Martigny, Switzerland and other partners are Katholieke Universiteit Leuven (B), University Hospital of Geneva (CH), Fondazione Santa Lucia-Rome (I) and Helsinki University of Technology (F). More information can be found on <http://www.maia-project.org>

B. Shared control

The estimated probability distribution is sent from the BCI system to the shared control system, which translates these probabilities to proper joystick-like input values, represented by a translational (v) and rotational (ω) velocity. The steering command with the highest probability is considered the user's current steering intent and used further on as input. This steering command will result in the proper motion of the wheelchair. Issuing a Forward command, i.e. the probability of Forward was higher than the probability of Left and the probability of Right, results in an increase of the translational velocity v . Left and right steering commands represent the user's intent to rotate the wheelchair and decrease or increase the rotational velocity ω , depending on the direction. After sending a Forward command, it is maintained for some time, to provide a smoother motion of the wheelchair and avoiding the need to reissue the same command every 0.5 seconds. If the user sends a Left or Right command during this time, the resulting joystick input will be a combination of an positive translational velocity and, depending on the direction, a positive or negative rotational velocity.

Instead of directly executing the user's steering commands, the shared control system evaluates the situation. The current environment, registered through a laser scanner, is taken into account. All assisting behaviours have an appropriateness level. Given the environmental information, each behaviour calculates its appropriateness. The shared control system then applies *winner-takes-all* to determine which behaviour it activates. For example, if the user steers too close to an obstacle, an avoidance behaviour of the shared control system will be activated to prevent collision.

A diagram of the translation from mental steering command to actual motor signals is shown in Figure 2. In this case, the actual steering command is adjusted by obstacle avoidance to prevent collision with nearby obstacles.

C. Adaptive levels of assistance

The shared control framework we propose here introduces three levels of assistance, named respectively $A0$, $A1$ and $A2$, which are only activated when the user requires them. The first two, collision avoidance and obstacle avoidance, will be activated near obstacles to prevent collisions. A third level of assistance, called orientation recovery, will trigger whenever the user's direction is misaligned too much with respect to the goal direction.

1) $A0$ - collision avoidance: The collision avoidance acts as an emergency stop. If the user steers the wheelchair too close to an obstacle, this behaviour decreases the translational velocity until the wheelchair comes to a full stop. The laser scanner, in front of the wheelchair, is used to determine the activation of this behaviour. The activation threshold in this experiment was set at $0.4m$. If the system detects obstacles within this threshold, the appropriateness level of this behaviour is high, otherwise it is low.

2) $A1$ - obstacle avoidance: Unlike the previous behaviour, obstacle avoidance calculates a proper (v, ω) pair to steer the wheelchair away from the obstacle. During

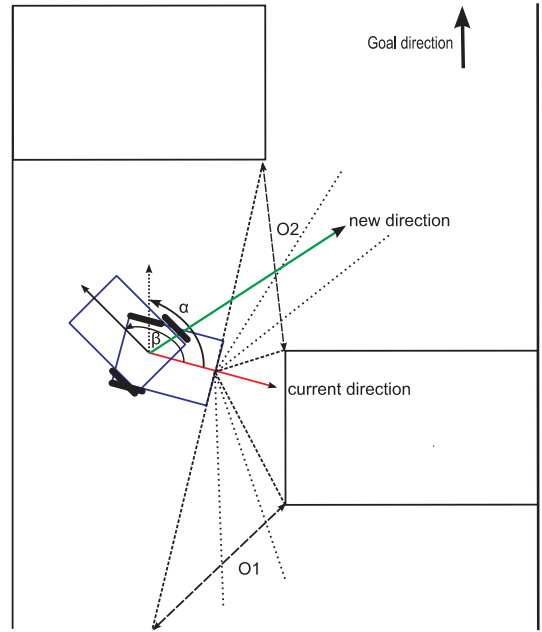


Fig. 3. The orientation recovery behaviour. If the angle between the current orientation of the wheelchair and the goal direction, given by α , reaches a certain threshold, the behaviour will correct the orientation as follows: first, the wheelchair will be rotated over a certain angle, given by β , in order to scan for valid openings; secondly the opening with a direction closest to the goal direction is chosen; finally the wheelchair will center its direction towards the chosen opening direction. In this case the direction of opening $O2$ is closest to the goal direction and is chosen, even though the larger opening more south, $O1$, is a valid opening.

calculation the input of the user and the environment itself are taken into account, to assist appropriately. The activation threshold of this behaviour is set at $0.5m$. Details of the both avoidance algorithms, $A0$ and $A1$, can be found in [10].

3) $A2$ - orientation recovery: The orientation recovery algorithm corrects the orientation of the wheelchair if it is too misaligned with respect to the goal orientation. Figure 3 illustrates this behaviour. The rectangle represents the wheelchair with its current orientation towards the south east. If in this case the user keeps turning right, the angle α , which measures the angle between the current orientation of the wheelchair and the goal direction, will increase. Whenever α reaches a certain threshold, in this experiment set at 105 degrees, orientation recovery will be activated.

First, the direction, in which the wheelchair needs to turn to realign with the goal direction, is calculated. Depending on the current orientation of the robot and the goal orientation, the shortest path is chosen. In Figure 3, the desired direction is left. In the next step the algorithm calculates the best nearby opening. Best in this case is defined as having an orientation closest to the goal direction. A candidate opening is a set of consecutive distance measurements of a scan, which are larger than some threshold. If the width of the opening is larger than the width of the robot increased with a safety margin, the opening is considered as valid for the robot to pass through safely. Because no global map is used, it is necessary to scan through the environment for openings in order to determine the best one. If a global map would

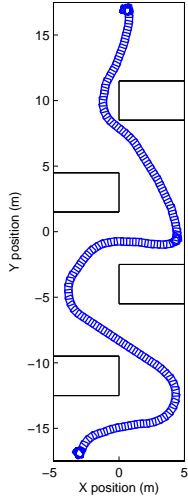


Fig. 4. The environment in which the experiment was performed. The trajectory of the wheelchair during the session is depicted as a sequence of squares.

be used, the best opening will be known at all times without needing to rotate the robot.

The algorithm rotates the wheelchair around its axis for a certain amount of degrees, given by the angle β . In this experiment β was set at 150 degrees. At each step, the laser scanner will scan for 180 degrees in front of the robot and for each of the 180 measurements the distance to the closest obstacle is given. Using these scan data, openings are calculated. In Figure 3, O_1 and O_2 are considered valid openings for the first step. During the rotation all the other valid openings are also stored. Each valid opening has an orientation, relative to the wheelchair. Out of all the candidate openings, the one with an orientation closest to the goal direction is chosen. If no openings were found, the search radius is widened, by increasing the angle β .

Finally, the robot will be rotated towards the selected opening. The direction to turn towards is recalculated to ensure the shortest angle is chosen.

III. EXPERIMENTS AND RESULTS

A. Setup

Experiments were carried out in a simulated environment by two healthy voluntary subjects. In two half days, the two subjects were asked to control the simulated wheelchair and drive it through the environment from the starting position at the bottom to a goal region at the top as depicted in Figure 4. The sequence of squares represents the trajectory of the simulated wheelchair during one of such sessions. The position is given in meters on each axis. Each subject had one half of the day to perform several sessions. Subject 1 did 9 sessions in the morning, while subject 2 did 10 in the afternoon. Both subjects had already experience with controlling the simulated wheelchair by BCI commands. Before each session, the level of assistance of the shared control system was set to either enable or disable the orientation recovery behaviour to establish the need for such a behaviour.

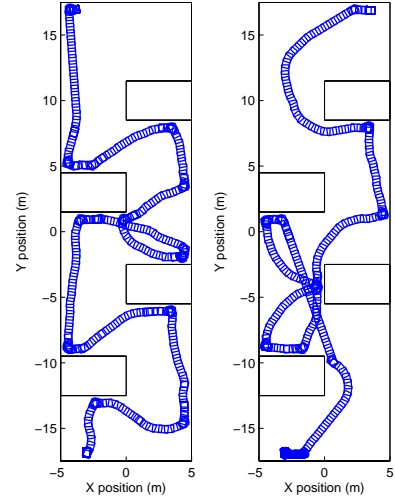


Fig. 5. The left trajectory is from a session of subject 1 and the right one is from a session of subject 2. In both cases orientation recovery is disabled.

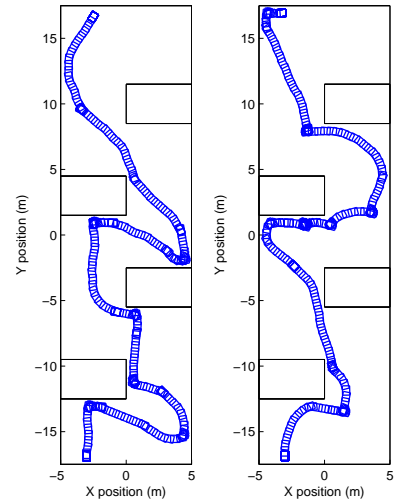
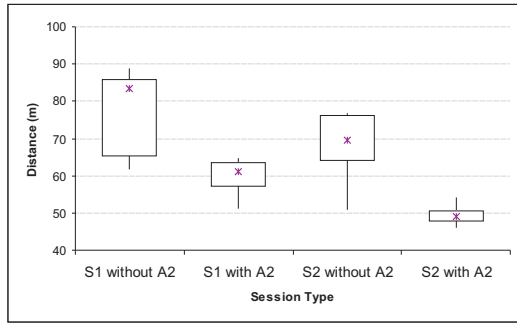


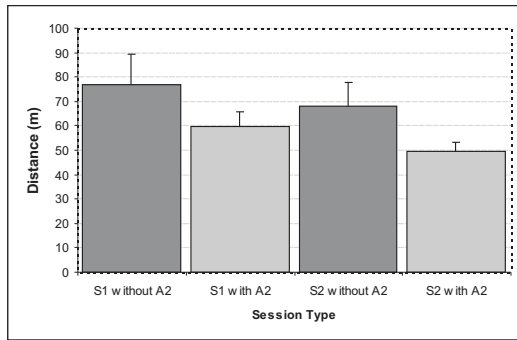
Fig. 6. At the left, orientation recovery is disabled and at the right it is enabled. Both trajectories are executed by subject 1.

B. Experiment

The idea of the experiment was to test the need for the orientation recovery behaviour (A_2), providing more assistance when the user needs it. During the whole session the two avoidance behaviours were enabled, to prevent collisions with any obstacles. Although they were enabled, the behaviours only actively intervened when the user moved too close to an obstacle. The need for the additional orientation recovery behaviour can be expressed in the difference in performance between sessions where A_2 was enabled and sessions where it was not. Performance criteria were distance of the trajectory and elapsed time to reach the goal region. Besides these two criteria, the BCI performance and the number of times A_2 is needed were compared to see if there might be any correlation.



(a) Box plots



(b) Averages

Fig. 7. Box plots and averages of travelled distance with respect to different session types.

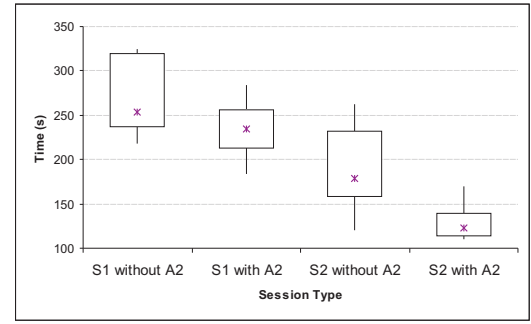
C. Results

During the experiment, data were logged on different levels. First of all, the incoming mental commands, sent by the BCI classifier, together with the user's intent were saved. Also, the total time spent and total amount of distance travelled in each session was logged. The activation of the different levels of assistance was also stored, to be able to calculate the percentage of activation of orientation recovery in the sessions where it was enabled. Finally, the wheelchair's position and orientation were logged to make a plot of the trajectory, such as the one shown in Figure 4, and to calculate the need of A2 in the sessions where it was disabled.

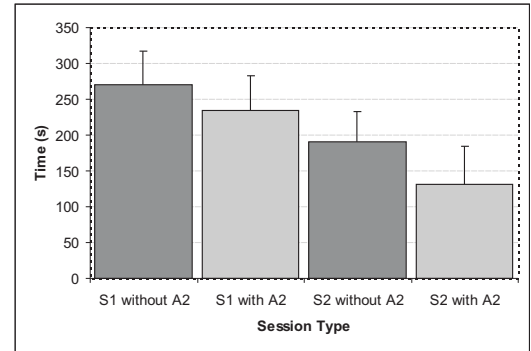
1) *Distance*: For both subject 1 and subject 2, the sessions where orientation recovery was enabled are executed with a lower total amount of travelled distance. Figure 5 shows that both subjects do make some loops when A2 is disabled (7 on 4 sessions and 6 on 6 sessions, respectively). Thus, orientation recovery could definitely help here. Figure 6 shows the difference in turns between sessions where orientation recovery is turned off and a session where it is turned on. Both trajectories were executed by subject 1.

In Figure 7(a) the data on the distance is plotted in several box plots and below, in Figure 7(b), the averages are plotted with their respective standard deviations. For each subject, Figure 7 shows an overall statistic over all his or her sessions, a plot of the sessions without A2 and a plot for the ones with A2 enabled.

First of all, it seems that subject 2 performed much better



(a) Box plots



(b) Averages

Fig. 8. Box plots and averages of elapsed time with respect to different session types.

than subject 1 (with an average of 60.57m versus 69.23m for subject 1). This is explained by a better BCI performance, measured by the percentage of correctly classified steering commands, (58.10% versus 53.69% for subject 1) as well as a better driving strategy: subject 1 took wider turns and switched slowly between BCI commands, while subject 2 took sharp turns and was able to switch faster.

Secondly, the standard deviation of the average distances between the different sessions where A2 is turned on, and the interquartile distances in the box plots are also smaller than the ones between the sessions where it is turned off. When the user is doing really bad and no orientation recovery is turned on, many loops will occur and the distance will be much larger. However, if the agent is turned on, the performance of the user is more constant, because the agent reorients the wheelchair, whenever it is off course.

It is also noticeable that, even though subject 2 seems to have a better overall performance than subject 1, he still performs better with the orientation recovery behaviour turned on, than without it.

To conclude we could state that regarding distance travelled, A2 is a benefit. Inexperienced users will travel much less distance and the behaviour will be frequently active. Experienced users, although they might not need it all the time, can still rely on orientation recovery to help them in the few cases they do make a wrong turn (due to concentration problems or fatigue, for instance).

TABLE I
AVERAGE BCI PERFORMANCE OF BOTH SUBJECTS COMPARED WITH
THE AVERAGE NUMBER OF TIMES THEY NEEDED *A2*

Subject	BCI Performance	# <i>A2</i> needed
1	53.69%	5
2	58.10%	1.7

2) *Time*: The elapsed time is also reduced, on average, although the difference is smaller than the difference with respect to distance travelled (see Figure 8). This is due to the fact that the orientation recovery agent needs to scan the environment, looking for the most suitable opening to reorient the wheelchair towards. While *A2* scans through the local environment, by rotating the wheelchair, time is lost.

Overall, there is still a noticeable difference between the sessions where orientation recovery was enabled, and where it was not. By activating *A2*, loops cannot occur. Not only the travelled distance but also the elapsed time decreases significantly by preventing loops.

3) *The need for A2*: Finally, if we compare, on average, the need for *A2* (i.e. the number of times *A2* could have helped by reorienting but was disabled or did help by reorienting when it was enabled) with the BCI performance for both subject 1 and subject 2, we can see that with a higher BCI performance the number of times *A2* was active or could have been active is lower than with a lower BCI performance. This can be seen in Table I. An experienced user has less need for *A2* than an inexperienced one.

IV. CONCLUSIONS AND FUTURE WORK

We have shown that the use of an adaptive level of assistance increases the task performance. The assisting behaviours will only be activated when the user requires assistance and depending on the situation, the proper behaviour is activated. By introducing this adaptivity, the users remain in maximal control. An inexperienced user will receive more assistance than an experienced one. If, after some time, the performance of the user has improved, the assisting behaviours will be activated less.

In the experiment we showed the travelled distance and elapsed time of a session decreased while orientation recovery was active, resulting in an increase of the task performance. Also the need for this behaviour was given. It can be beneficial for both inexperienced and experienced users. The former will have a much shorter trajectory due to a frequently active *A2* behaviour and the latter, although

it might not always be required, can still rely on orientation recovery. In the few cases they do make a wrong turn, the *A2* behaviour can also assist them.

A weak point of the proposed approach are the fixed activation levels, which do not integrate the user's experience or performance. The behaviour will always be activated when the activation threshold is reached, even though an experienced user might still be able to recover from this disorientation on his own.

We could increase the performance if we could build a model of the user at runtime and estimate the level of experience to determine the thresholds when the behaviour should be activated or not.

REFERENCES

- [1] M. Nuttin, E. Demeester, D. Vanhooydonck, and H. Van Brussel, "Obstacle avoidance and shared autonomy for electric wheel chairs: An evaluation of preliminary experiments," in *Robotik 2002, Ludwigsburg, Germany*, June 2002.
- [2] D. Vanhooydonck, E. Demeester, M. Nuttin, and H. Van Brussel, "Shared control for intelligent wheelchairs: an implicit estimation of the user intention," in *ASER*, Bardolino, Italy, March 2003, pp. 176–182.
- [3] E. Demeester, M. Nuttin, D. Vanhooydonck, and V. B. H., "A model-based, probabilistic framework for plan recognition in shared wheelchair control: Experiments and evaluation," in *IEEE/RSJ International Conference on Intelligent Robots and Systems (IROS)*, Las Vegas, Nevada, October 2003, pp. 1456–1461.
- [4] M. Betke, J. Gips, and P. Fleming, "The camera mouse: Visual tracking of body features to provide computer access for people with severe disabilities," *IEEE Transactions on Neural Systems and Rehabilitation Engineering*, vol. 10, no. 1, pp. 1–10, 2002.
- [5] J. del R. Millán, P. W. Ferrez, and A. Buttfield, *Towards Brain-Computer Interfacing*. Martigny, Switzerland: MIT Press, 2006, no. 86, maia-in book *The IDIAP Brain-Computer Interface: An Asynchronous Multi-Class Approach*.
- [6] K. U. Leuven, "Mobile learning robots research group (mlr)," URL, Februari 2007. [Online]. Available: <http://www.mech.kuleuven.be/mlr/>
- [7] P. W. Ferrez, F. Galán, A. Buttfield, S. L. Gonzalez, R. Grave de Peralta, and J. del R. Millán, "High frequency bands and estimated local field potentials to improve single-trial classification of electroencephalographic signals," in *Proceedings of the 3rd International Brain-Computer Interface Workshop & Training Course 2006, Graz*, 2006.
- [8] E. Lew, M. Nuttin, P. Ferrez, A. Degeest, A. Buttfield, G. Vanacker, and J. del R. Millán, "Non-invasive brain computer interface for mental control of a simulated wheelchair," in *Proceedings of the 3rd International Brain-Computer Interface Workshop & Training Course 2006, Graz*, 2006.
- [9] J. del R. Millán, F. Renkens, J. Mouriño, and W. Gerstner, "Non-invasive brain-actuated control of a mobile robot by human eeg," *IEEE Trans Biomed Eng*, vol. 51, pp. 1026–1033, 2004.
- [10] M. Nuttin, D. Vanhooydonck, E. Demeester, and H. Van Brussel, "Selection of suitable human-robot interaction techniques for intelligent wheelchairs," in *Proceedings of 11th IEEE International Workshop on Robot and Human Interactive Communication ROMAN, Berlin*, September 2002, pp. 146–151.

Appendix H

Context-based Filtering for Assisted Brain-Actuated Wheelchair Driving

G. Vanacker, J. del R. Millán, E. Lew, P.W. Ferrez, F. Galán, J. Philips, H. Van Brussel, and M. Nuttin. Context-based filtering for assisted brain-actuated wheelchair driving. *Computational Intelligence and Neuroscience*, 2007.

Resum

Controlar un dispositiu robòtic utilitzant senyals cerebrals humanes és una tasca interessant i desafiant. El dispositiu pot ser complicat de controlar i la natura no estacionària dels senyals cerebrals proporciona entrades inestables. Utilitzant algorismes intel·ligents de processament adaptats a la tasca es pot incrementar el rendiment del control del dispositiu en qüestió.

Aquest article introdueix un sistema de control compartit que assisteix a un usuari d'una interfície cerebral en la conducció d'una cadira de rodes. La intenció direccional de l'usuari és estimada mitjançant l'electroencefalograma (EEG) i introduïda al sistema de control compartit abans de ser enviada als agents motrius de la cadira. Resultats experimentals mostren la possibilitat d'augmentar notòriament el rendiment en la conducció quan el sistema de control compartit és utilitzat. Aquests resultats s'han obtingut amb 2 subjectes sans novells durant el seu primer dia d'entrenament amb la cadira de rodes.

Research Article

Context-Based Filtering for Assisted Brain-Actuated Wheelchair Driving

Gerolf Vanacker,¹ José del R. Millán,² Eileen Lew,² Pierre W. Ferrez,² Ferran Galán Moles,² Johan Philips,¹ Hendrik Van Brussel,¹ and Marnix Nuttin¹

¹The Department of Mechanical Engineering, Katholieke Universiteit, 3001 Leuven, Belgium

²The IDIAP Research Institute, 1920 Martigny, Switzerland

Correspondence should be addressed to Gerolf Vanacker, gerolf.vanacker@mech.kuleuven.be

Received 18 February 2007; Accepted 23 May 2007

Recommended by Fabio Babiloni

Controlling a robotic device by using human brain signals is an interesting and challenging task. The device may be complicated to control and the nonstationary nature of the brain signals provides for a rather unstable input. With the use of intelligent processing algorithms adapted to the task at hand, however, the performance can be increased. This paper introduces a shared control system that helps the subject in driving an intelligent wheelchair with a noninvasive brain interface. The subject's steering intentions are estimated from electroencephalogram (EEG) signals and passed through to the shared control system before being sent to the wheelchair motors. Experimental results show a possibility for significant improvement in the overall driving performance when using the shared control system compared to driving without it. These results have been obtained with 2 healthy subjects during their first day of training with the brain-actuated wheelchair.

Copyright © 2007 Gerolf Vanacker et al. This is an open access article distributed under the Creative Commons Attribution License, which permits unrestricted use, distribution, and reproduction in any medium, provided the original work is properly cited.

1. INTRODUCTION

The continuing progress in the research for noninvasive BCI classification systems gives rise to a wealth of potential practical applications. The prospect of humans interfacing the mechanical world through brain-coupled devices and thereby controlling everyday machines through the process of mere thought is certainly an appealing one as discussed in [1–3]. A promising class of applications are those concerning assistive devices for people with serious impairments. The classical interfaces that disabled people commonly used to control or manipulate an assistive device typically require the patient to have adequate control over one or more physical components of his or her body. Typically, that would be one of the limbs: an arm, hand, or finger. Bioprosthetic systems that are controlled directly through brain signals on the other hand could provide for a more natural extension of human capabilities. Especially in the case where the patient is completely paralysed, this technology may provide for the only possible way for him/her to gain control over basic aspects of his/her daily life.

Amongst these, the ability to control the personal mobility is generally considered an important one. The reduction in mobility that many people experience, due to various impairments or simply due to the effects of ageing, often has a profound impact on the person's independence, social activity, and self-esteem. For many people suffering from a diverse range of impairments, the primary device that could provide for that mobility is the electrical wheelchair. It is worth noting, however, that in case of locked-in patients their highest priority is not mobility. Still, learning how to make it possible to drive complex devices such a wheelchair will also lead to better communication and domestic tools. Many patients, however, do not have the ability to exercise the demanding fine control that wheelchair steering requires, even with an input device capable of communicating a high level of detail, such as the classical joystick. Problems regarding not only the physical inability to accurately manipulate the joystick, but also a reduced kinematical and dynamical insight in the wheelchair motion regularly occur, as was seen in earlier work [4]. Therefore, the prospect of wheelchair control through a brain-coupled control interface, which is in general less reliable than a classical interface, may seem a



FIGURE 1: A subject controlling our robotic platform Sharioto in a natural indoor environment through noninvasive EEG. Visible are the sensors of the platform: a laser range scanner in front and sonar sensors all around.

remote one. Nevertheless, recent results have shown the feasibility of such brain-actuated wheelchairs; see Figure 1 and [1].

Over the past years, important advances in research concerning *shared control* techniques have been made, as may be seen in [4–7]. Shared control systems typically feature one or more intelligent algorithms that aim at assisting the human to execute some task at hand. Both human(s) and intelligent controller(s) then *share* the control over a device whereby each of the actors may exercise influence through the manipulation of some control variables. Together, through cooperative behavior, they aim at completing the task in a way which is hoped to be superior to the situation where only a single actor is in control. In the specific case of assisted wheelchair driving, the actors are the patient and an intelligent controller. The variables to be shared are the translational and rotational velocity of the robot (v, ω). Also, in this class of applications, the human typically has *supervisory* control, meaning that it is him or her that defines the *global plan* that has to be executed. The other actors then need to adopt this plan and cooperate accordingly. Furthermore, an intelligent actor cooperating in a shared control system that is designed to operate with a brain computer interface (BCI) as the human input needs to accommodate for the specific properties that this particular input has.

This paper presents a shared control system for use with a brain computer interface (BCI). The intelligent controller is designed to *filter* out the possible erroneous mental commands inferred by the BCI from noninvasive electroencephalogram (EEG) signals. It estimates the environmental *context* and uses that to detect illogical steering signals, according to the intention—the global plan—the human has. In the proposed framework, the patient has *continuous* control over the wheelchair, parallel to classical joystick control. This allows for a more natural interaction with the robotic assistant, as well as *fine motion* control. The organization of

this paper is as follows. In Section 2, we will briefly discuss related work in shared control techniques for wheelchair navigation. Section 3 introduces our new shared control system based on context estimation and signal filtering. In Section 4, we then present experimental results that validate this approach. Finally, Sections 5 and 6 present, respectively, a discussion of the results and the general conclusions of this work.

The brain-actuated wheelchair described in this paper is an extension of the brain-actuated mobile robot developed by Millán et al. [1]. In this paper, we focus on the main innovation of such first prototype, namely, novel features of the shared control framework specifically designed to work with a BCI. Details of the BCI can be found in [1].

2. RELATED WORK

In the past years, a fair number of research groups have ventured into the search for shared control techniques in order to provide assistance to patients as they experience problems when driving an electrical wheelchair. Because of the many different types of manoeuvres that may induce driving problems, for example, driving through a door, obstacle avoidance, driving in a small corridor, docking at a table and others, different algorithms have been developed to cope with these specific situations. This led to the fact that most of the existing approaches focus on the development and selection of such discrete *modes*. Roughly speaking, one may divide the approaches in those that require the user to *explicitly* choose the mode [8–12] on the one hand and those that provide automatic—*implicit*—mode changes based on an interpretation of the surroundings and the user input [6, 7, 13, 14].

Not only the latter group of approaches provide for a more natural interaction between patient and robot, but automatic mode changes are also necessary for a group of patients that are physically unable to communicate their choice on the provided interface. Consider, for example, an array of buttons, each of which activates another assistance mode. A patient suffering from, for instance, multiple sclerosis might experience large difficulties to accurately reach and press the wanted button. The central problem in these implicit approaches therefore is the question: “What is the user’s intention?” [6, 7]. Research addressing that question is performed at the *Mobile Learning Robot* (MLR) research group of the Department of Mechanical Engineering at the K. U. Leuven.¹ Another approach centres on establishing a relation between the steering commands that a capable able-bodied user would give—the so-called *reference* signals—and the signals of the specific patient, given the same situation and the same global intention, introduced in [5]. Knowledge over both allows for a conversion of the less than optimal patient steering signals to the optimal reference signals, thereby *filtering* out the steering handicap.

A similar technique filtering may be used to improve the driving performance of a BCI-controlled wheelchair, keeping in mind the specifics of this particular interface. In

¹ <http://www.mech.kuleuven.be/mlr>.

comparison with the classical analog joystick, as used in [5], the BCI input generally has a limited resolution and higher uncertainty.

3. APPROACH

This paper presents an assistive algorithm specifically designed to help a BCI subject navigate an electrical wheelchair in an everyday environment. It uses an estimate of the environmental *context* to build a probability distribution over the possible steering commands and uses that information to “filter” out possible erroneous user signals. The hypothesis is that with this assistance, the overall driving performance will improve, especially for “novel” subjects, that is, subjects with little or no former experience in BCI control. Figure 2 illustrates the general architecture of the brain-actuated wheelchair.

3.1. BCI-generated commands and interpretation

The nature of BCI-classified mental commands, generated by the subject to indicate some desired movement is quite different from those generated by a continuous joystick. First and foremost, there is an important reduction in resolution due to the limited amount of different mental commands that a BCI classifier can reliably discern. As a consequence, a command-to-movement scheme must be adopted which ensures that smooth motion will result from these discrete input signals. The EEG classifier system used in this work (see [1]) is able to distinguish three discrete commands that may express the need for movement into a certain direction. The steering signals that the classifier outputs consist of a probability distribution over these three discrete steering commands: *Forward*, *Left*, and *Right*. In order to provide intuitive control, we would like to enable the patient to exercise *velocity control* over the platform, so the probability distribution expresses the BCI’s belief about the intent of the user to alter the current *velocity* of the wheelchair. *Forward* means that the translational speed v should be increased or maintained—when the maximum speed is already reached. A *Left* or *Right* signal means that the user intends to rotate the wheelchair in the respective direction, thus increasing or decreasing the rotational velocity ω . Both velocities are superimposed, so that a command to turn when the wheelchair is already moving forward will result in a smoothly curved path.

To accommodate for smooth motion, the system maintains the translational speed for a number of seconds, so that the human does not have to constantly generate *Forward* commands when driving straight on. This also prevents the robot from coming to a halt when taking turns. When for a certain period no *Forward* command is issued, however, the robot does effectively stop. For similar reasons, a signal that triggers a rotational command is only executed for a small amount of time. This prevents that the platform keeps turning for too long and overshoots the direction in which the subject intended to continue his travel.

3.2. Context

In typical everyday life, a wheelchair user may come to face a large number of different situations. The nature of a situation is primarily dependent on the environmental settings. Together with the *intention* (the plan) of the user, this environmental situation is part of the *context* in which the controller needs to operate. The assistive system should be able to provide help in as many of these contexts as possible. Because of the different nature of each situation, the controller should be able to detect the specific type of context at hand automatically if it is to help the human in an appropriate manner.

3.2.1. Estimating the context

For this work, context estimation was done by defining a general, a priori-known user intention (smooth and efficient forward navigation through the environment) on the one hand and a constant automatic estimation of the environmental situation on the other hand. The situations were modelled as the number and location of *openings*: wide, open spaces to which the user might safely navigate. The principle is as follows: suppose the wheelchair is approaching a crossroad, as depicted in Figure 3. The laser scanner in front of the wheelchair scans 180 degrees and senses the distance to the environment for every degree. The algorithm then searches for regions with consecutive scans for which the distance is larger than a certain threshold T . This results in a number of regions that qualify as candidates for an opening. Next, for each of the resulting regions, the width of the opening O is calculated:

$$O = \sqrt{s_1^2 + s_2^2 - 2s_1s_2 \cos(t_2 - t_1)}. \quad (1)$$

This length is then compared to the physical dimensions of the wheelchair (its width). If the length O exceeds the wheelchair width augmented with a safety margin, the corresponding region is accepted as an opening. Its orientation with respect to the current wheelchair position is then $\pi/2 - (t_2 - t_1)/2$.

3.2.2. Extracting a belief in user actions

Each opening then represents a general direction in which the user might opt to continue his travel. With this knowledge about the current situation, a probability distribution concerning the possible *local* user actions may be built. Note that inferring these probabilities requires the knowledge of the global intention of the human. In this case, it is supposed that the user wishes to navigate safely and efficiently through the environment without halting or going backwards. In other cases, a user might also wish to stop at certain locations, or dock at particular places.

When the directions in which the robot can travel are orthogonal, as in Figure 3, we can summarize the environmental belief in four quadrants, as depicted in Figure 4. The figure shows how the regions West and North are deemed probable navigation directions, as extracted from the environment (see Figure 3). The regions East and South, on the other

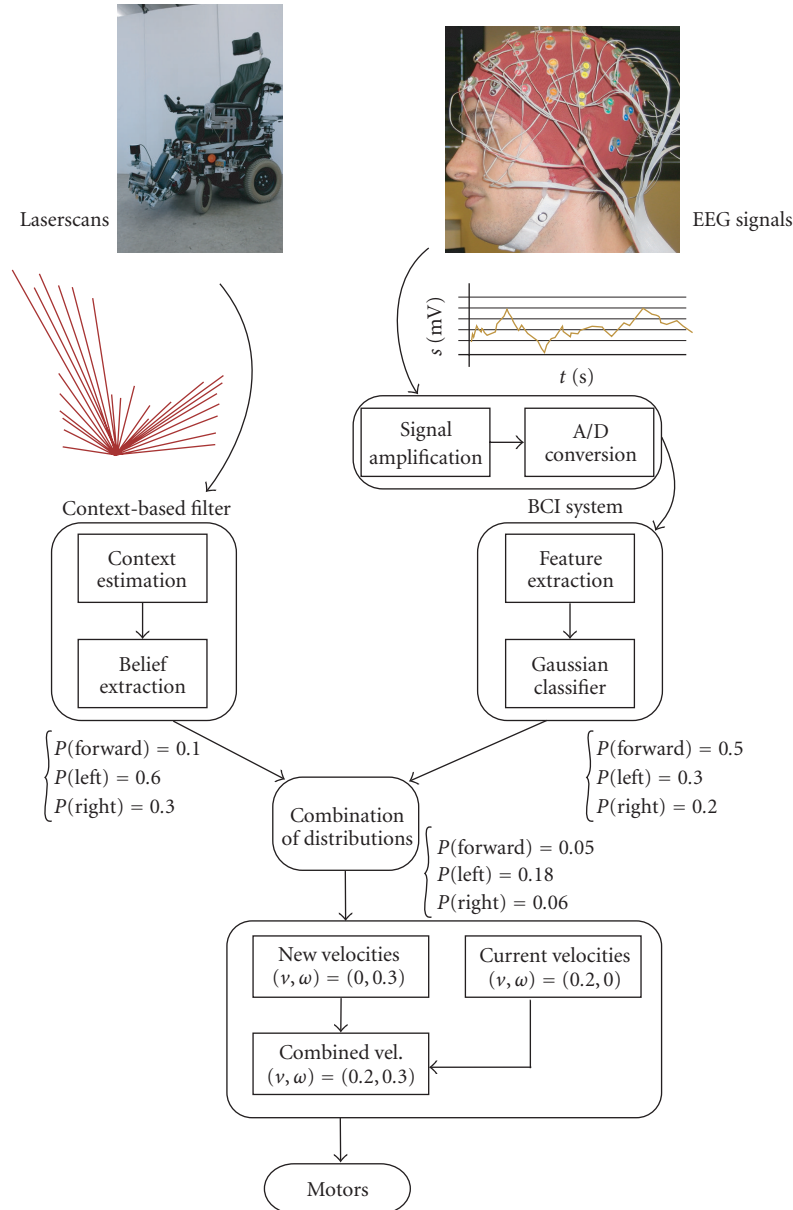


FIGURE 2: A schematic diagram showing the flow of information in the system. On the left-hand side, environmental information from the wheelchair’s sensors (the laser range scanner) feeds the contextual filter that builds a probability distribution over the possible (local) user steering actions. On the right-hand side, the EEG data is fed into the BCI system that estimates the probability of the different mental commands. Both streams of information are combined to form a filtered estimate of the user’s steering intent which is eventually sent to the wheelchair’s motors as explained in Section 3.1.

hand, are improbable (as the scanner sees a wall on the right hand, and going backwards is also not probable given the intention of smooth forward navigation). If the wheelchair is oriented North, the controller attaches a probability of 0.5 to *Forward* and *Left*. $P_{\text{env}}(\text{Right})$ is set to zero, because rotating to the right would make the robot turn towards an obstacle (the wall). The possibility of turning into the corridor to the left is reflected in $P_{\text{env}}(\text{Left}) = 0.5$. If the wheelchair is oriented 45 degrees North-West, $P_{\text{env}}(\text{Forward})$ has become

zero, while the possible commands now are *Left* and *Right*, with equal probability, reflecting the belief that one of the orthogonal directions North or West should be chosen. When the wheelchair is turning further towards West, *Forward* becomes possible again, and $P_{\text{env}}(\text{Right})$ stays constant while $P_{\text{env}}(\text{Left})$ diminishes completely. At the boundary between the probable directions and those that are improbable, the controller attaches a maximum belief to those commands that would keep the wheelchair in the half plane of high

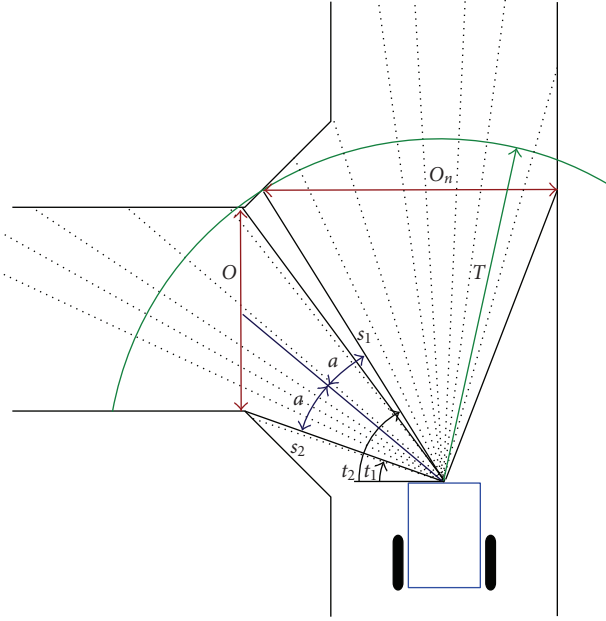


FIGURE 3: The principle of the context estimator. With a laser range scanner, a set of regions is detected that provide safe manoeuvrable openings in the environment. The number and location of these openings, together with the intention of the human, then provides the context. The figure shows how the region to the left and the one in front of the robot are detected as openings.

probability. Between the above-described orientations, the probabilities are interpolated linearly. This is depicted in Figure 4 as the linearly changing transparency of the respective circle.

3.2.3. Combining the beliefs

The intelligent controller now needs to combine the signals coming from the EEG classifier with the probability distribution generated from the environmental knowledge, so as to get a better estimation of the user's local steering intent. Different ways of combining the probabilities from EEG classifier and environment may be chosen [15]. In this work, the *product* operator was used, mainly because the classifier can occasionally attribute a high probability to the wrong class, and averaging the contributions of EEG classifier and environment may still lead to a fairly high probability for a command that is in fact very unlikely. Using the product in this case yields more likely combinations. The resulting probability for a certain class C thus becomes

$$P(C) = P_{\text{EEG}}(C) \cdot P_{\text{env}}(C). \quad (2)$$

From the resulting distribution, the command with the *highest* probability is selected and applied to the wheelchair motors.

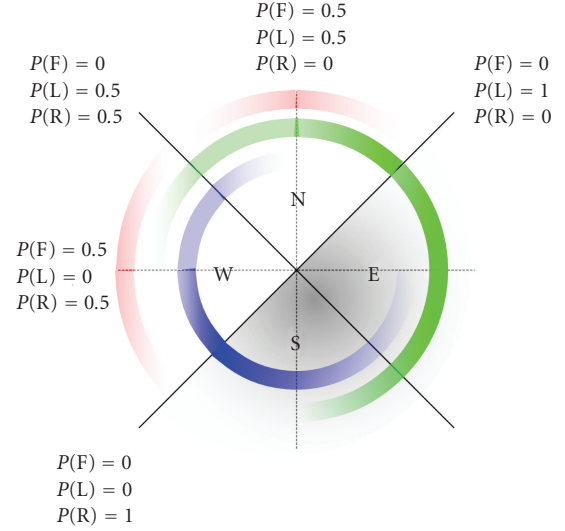


FIGURE 4: Extracting beliefs from the context in function of the wheelchair orientation. Four quadrants are shown, representing a situation in which possible directions are arranged orthogonal. The inner circle shows the probability of a *Right* command, the middle circle the probability of a *Left* command, and the outer circle the probability of a *Forward* command.



FIGURE 5: A subject controlling an intelligent wheelchair in a simulated environment. Visible is the EEG sensor cap with the cables that are connected to the BCI system and the computer that runs the shared control system.

4. EXPERIMENTS AND RESULTS

4.1. Setup

Experiments were conducted with a commercially available EEG system feeding the data to the BCI that estimates the user's mental commands. The classifier uses power spectrum information computed from the EEG as its input and outputs the estimated probability distribution over the classes *Left*, *Forward*, and *Right* at a rate of 2 Hz. A second computer running the shared control system is attached to the classifier system and uses its output to control the wheelchair. In this work, a simulated environment was used (mainly for safety reasons) in which a wheelchair was modelled featuring

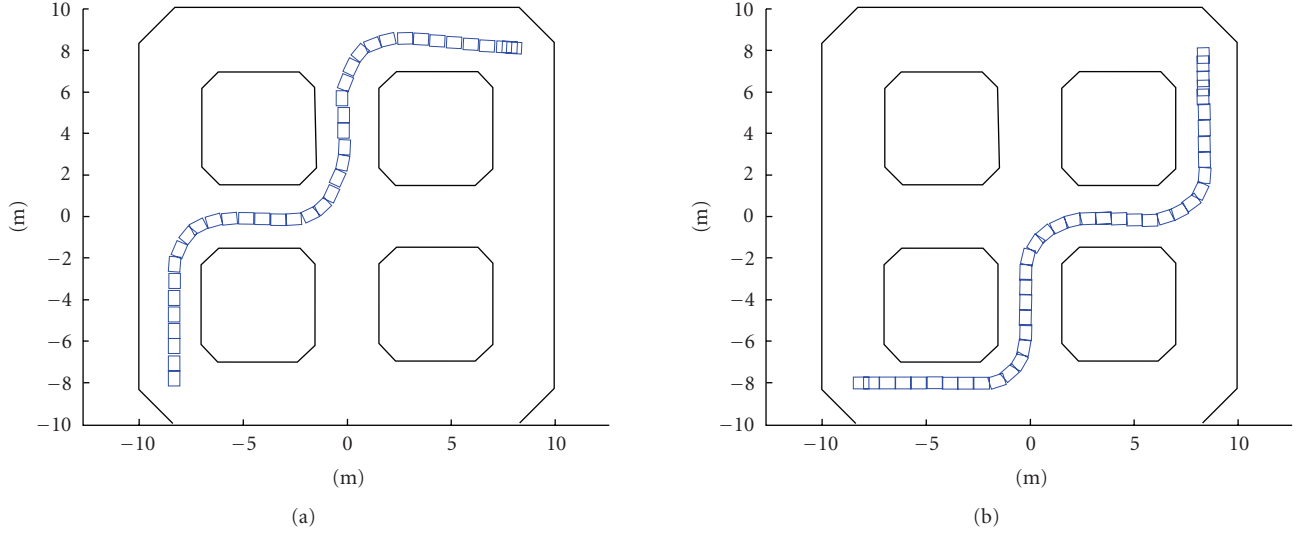


FIGURE 6: The environment in which the experiments were performed. The wheelchair’s position is depicted as a small rectangle at consecutive time steps. Both the paths that the subjects were instructed to follow are shown. It is also worth noting that the initial orientation for each of the paths is different.

a laser range scanner in front capable of scanning 180 degrees (1 scan for each degree) at 5 Hz. The maximum range of this scanner was fixed to 4.5 m, in accordance with the real physical scanner on our platform Sharioto. The wheelchair was placed in the environment shown in Figure 6. The figure also shows the two paths the subjects were asked to follow. Figure 5 shows a subject during one of the sessions.

Furthermore, because of the inherent nonstationary nature of EEG data, a mild form of online learning was used in the EEG classifier system to continually track the subject’s brain signals [16].

4.2. Experimental design

For the experiments, two able-bodied voluntary subjects were asked to control the wheelchair for a large number of sessions spanning over several days. This not only allowed to test the performance of the proposed shared control system, but also the *evolution* of the subject’s control with and without filter. In between the sessions, the filter was occasionally (de-)activated without the subject’s knowledge to investigate the effects of mental model switches and phenomena such as mode confusion [14]. Both subjects were novel with respect to BCI control as well as control of an electrical wheelchair. On the first day we asked the subjects to simply control the wheelchair regardless of any goals in the map, allowing them to get accustomed to using the system. On days 2 through 5, the subjects were instructed to follow a path to reach a certain goal position (see Figure 6). While driving, the subject continuously expressed his/her intended direction orally, allowing logging and comparison. When the wheelchair came too close to an obstacle (a wall), obstacle avoidance (OA, see [4] for details) was activated, to prevent the robot from getting stuck. Finally, the subject was allowed to take resting points while driving (simply because BCI con-

trol requires deep concentration which cannot be endured for long periods). When the user calls out “stop,” the classifier is paused and no new steering commands are generated. The robot will continue the path it is currently following while the shared control system (obstacle avoidance in this case) would lead it safely away from obstacles, if necessary. For the interpretation of the BCI commands, the following scheme was used:

$$\begin{aligned}
 v_{\text{inc}} &= 0.5 \text{ m/s}, \\
 \omega_{\text{inc}} &= 0.2 \text{ rad/s}, \\
 v_{\text{max}} &= 1 \text{ m/s}, \\
 \omega_{\text{max}} &= 0.6 \text{ rad/s}, \\
 v_{\text{new}} &= \begin{cases} \max \{v_{\text{curr}} + v_{\text{inc}}, v_{\text{max}}\} & \text{if } \delta t_v < 10 \text{ s}, \\ 0 & \text{if otherwise,} \end{cases} \\
 \omega_{\text{new}} &= \begin{cases} \max \{\omega_{\text{curr}} \pm \omega_{\text{inc}}, \omega_{\text{max}}\} & \text{if } \delta t_\omega < 1 \text{ s}, \\ 0 & \text{if otherwise,} \end{cases}
 \end{aligned} \tag{3}$$

where δt_v and δt_ω are the number of seconds since the last received command for, respectively, translational and rotational motion.

4.3. Results

Data was gathered on two distinct levels. First, every command sent by the classifier was logged, as well as the intent of the subject at that time. This allows to compare the output of the classifier with the actual intention of the human on the *individual command* level. Second, when driving towards the goal position, global measures such as the total time needed, the total distance travelled, and the percentage of the time that obstacle avoidance was active were logged to quantify *task performance*.

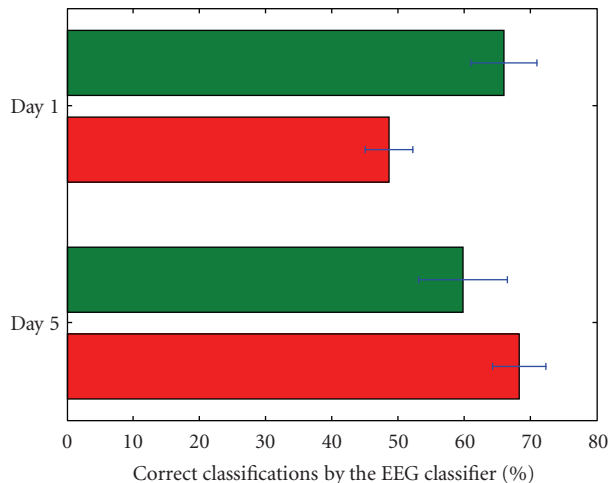


FIGURE 7: The EEG classifier performance for days 1 and 5 for subject 1. The lower bar in each day depicts the performance when driving without filter, the upper one shows the performance for sessions when filtering was active.

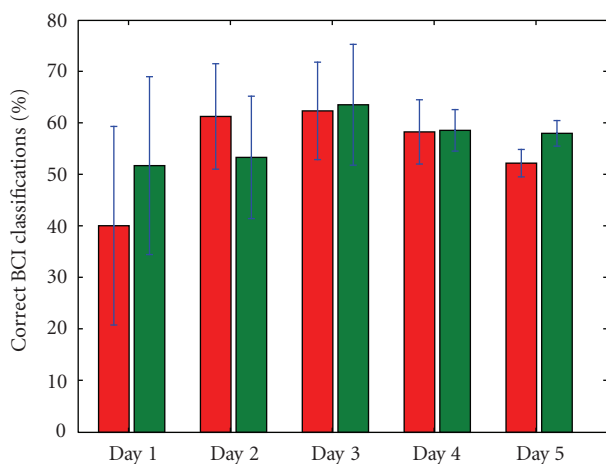


FIGURE 8: The EEG classifier performance for all days for subject 2. The left bar in each day depicts the performance when driving without filter, the right one shows the performance for sessions when filtering was active.

4.3.1. Individual command level

When comparing the number of times that the intended direction (*Forward, Left, Right*) was deemed the most likely one by the EEG classifier (attaching it the highest probability), subject 1 showed an overall increase in performance over the course of the five days (from 57.24% on day 1 to 63.98% on day 5). It has to be noted in this respect that this subject was completely new to BCI control as well as wheelchair control. The witnessed evolution may thus be attributed to the human gradually learning to control the system. Subject 2 shows a similar improvement over the first days, from 46.61% on day 1 to 63.14% on day 3 (although performance declines afterwards).

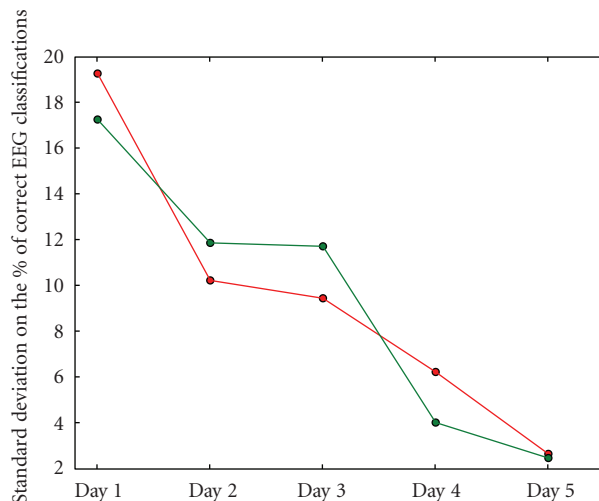


FIGURE 9: The standard deviations on the EEG classifier performance during the five days for subject 2; sessions with and without filter are shown in green and red, respectively. We can see that the subject shows a more constant performance over the sessions during one day as his experience with controlling the system develops.

For both subjects the classifier performance is different when controlling with or without the environmental filter as is visible in Figures 7 and 8. When the overall BCI performance is rather bad, it is much better to drive with the filter (e.g., subject 1, day 1). On the other hand, when the BCI performance is exceptionally good, driving with the shared control system may make it worse (e.g., subject 1, day 5). It is also worth mentioning that although subject 2 did not show the same increase in average classifier performance over all days (see Figure 8), he showed a steady improvement regarding the standard deviation on the performance (depicted in Figure 9). This reflects the gradually more constant driving behavior of the subject, as his mental driving models become more mature.

A similar picture is visible when we look at the actual resulting number of correct *decisions* that were sent to the wheelchair motors (the number of times that the speeds sent to the motors were in accordance with the subject's intent). Without filtering, this number equals that of the "raw" classifier performance. When environmental filtering is used, we get significantly more correct classifications if the EEG signal in itself is rather bad, but we can see that if the BCI performance gets very good (subject 1, day 5 and subject 2, day 2), the filter may actually deteriorate the percentage of correctly executed decisions (see Figures 10 and 11). We may conclude that if there is ample room for improvement (because of a bad EEG signal), the filter improves the situation. Whenever the human (and classifier) perform very well, however, the filter may actually hold back. However, the fact that the filter may impair the performance depends on the driving behavior of the subject, as can be seen in Figure 11, when we compare day 2 with day 3. Both days show almost the same performance without filter, but the performance *with* filtering is different. The difference may be attributed to a change

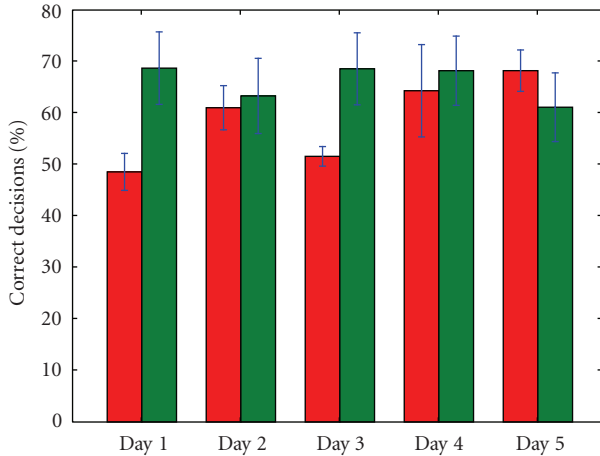


FIGURE 10: The percentage of control variables (v, ω) that is in accordance with the human’s intention, for subject 1. On the left for each day, we see the performance without environmental filtering. On the right, the results when filtering is active. Also shown are the standard deviations.

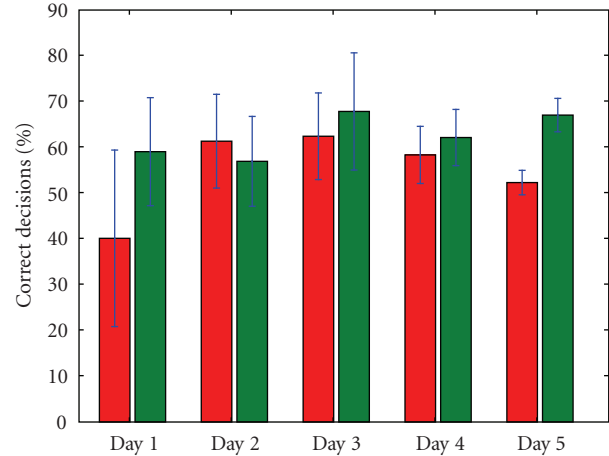


FIGURE 11: The percentage of control variables (v, ω) that is in accordance with the human’s intention, for subject 2. On the left for each day, we see the performance without environmental filtering. On the right, the results when filtering is active. Also shown are the standard deviations.

in driving behavior. In the detail of Figure 12, for instance, we can see that the subject tries to turn 180 degrees in a corridor, behavior which is not deemed likely by the filter (remember that the filter assumes the intention of smooth and efficient *forward* motion). Because it is not deemed likely, many of the subject’s steering commands during this manoeuvre are filtered out, which explains the decrease in classifier performance. During day 2 (from which Figure 12 was taken), subject 2 supposedly was still exploring the details of the driving model of the system *with* environmental filter and hence he tried some steering that is incompatible with the filtering assumptions. On day 3, manoeuvres as the one shown in Figure 12 were less in number, supposedly because the mental model that the subject had of the system was more mature by then. All in all, Figure 10 shows that the filter keeps the performance (on the individual command level) more or less constant over all days, roughly between 61% and 69%, in contrast with the more variable decision performance when no filtering is used. Over all sessions and days, the environmental filter improved the individual decision performance with 7.25% for subject 1 and 7.70% for subject 2.

4.3.2. The task level

Interesting in itself, the results obtained on the individual command level do not reflect the *driving behavior*. Even if the speeds that are sent to the motors are *on average* very much what the subject wants them to be, that does not necessarily result in good driving behavior. Much more is involved when controlling mobile robots such as the wheelchair. For one, *timing* is critical. When the corner arrives, the steering needs to be correct *at that very moment*, not just on average over the whole session. Also, the human needs to have good understanding of the kinematic and dynamical constraints of the robot, to predict its movement and hence correctly time the steering. To get a qualitative feeling of the typical driving

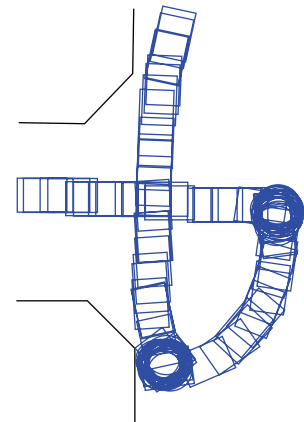


FIGURE 12: A detail of one trajectory followed by subject 2 on day 2. We can see that the subject tries to turn 180 degrees in a corridor, behavior which is deemed unlikely by the environmental filter.

problems that may occur, see Figure 13. It is clearly visible at Figure 13(a) that steering commands may arrive rather late, when the opportunity of turning into the corridor has already passed. Two main causes underlie this behavior. On the one hand, the subject’s kinematic insight is impaired by the large mental workload that the fine steering requires. Therefore, the commands for turning may be generated too late or too soon. On the other hand, switching directions (i.e., from *Forward to Right*) always takes some time, because the user has to shift his/her thoughts to another mental task to generate another steering signal. While this switching is occurring, the wheelchair simply drives on and critical moments are passing by. Figure 16 schematically shows this process. Also visible is that a fair amount of “wall following” is occurring, that is, the subject gets too close to a wall and obstacle avoidance is activated, leading the wheelchair alongside the wall. When the subject does not take action to get away from

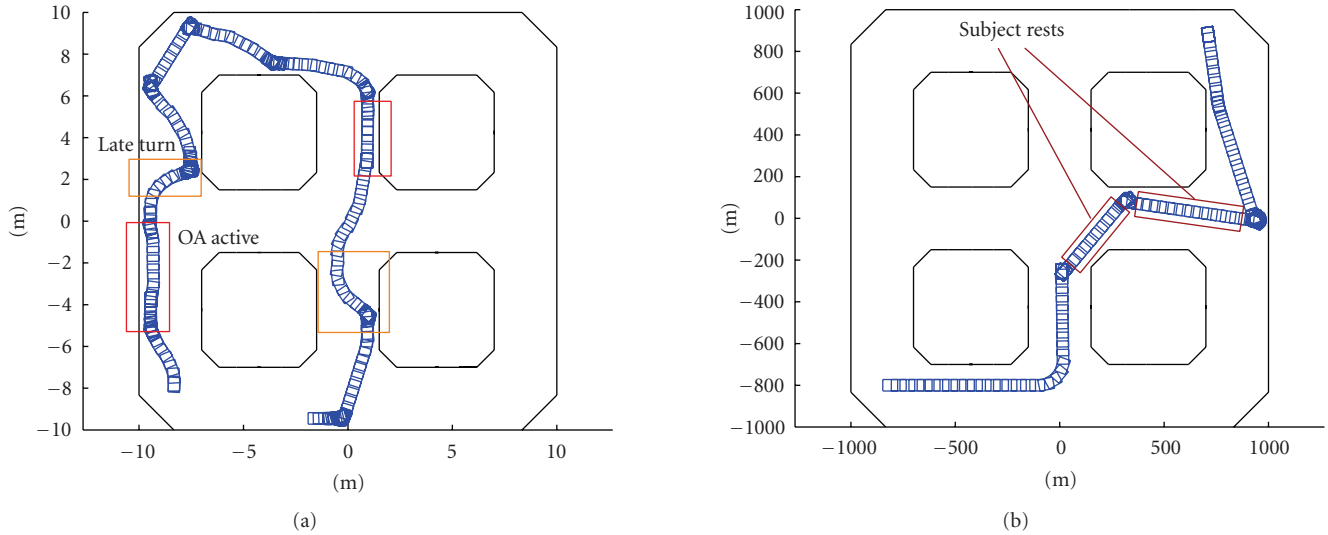


FIGURE 13: Typical problems that occur while driving. On the left, a path is shown that is driven without the environmental filter. We can see that there are many near collisions (obstacle avoidance gets active), resulting in a rather jagged path. On the right a session with filtering is shown. It is clear that the overall path is more smooth, although near collisions still occur (mainly due to inappropriate resting periods).

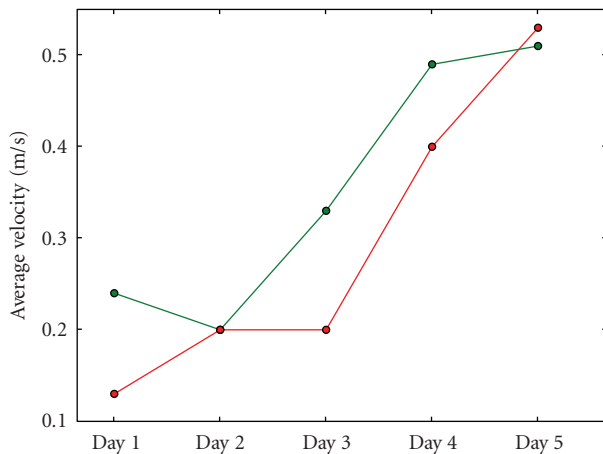


FIGURE 14: The evolution of the average velocity during sessions over all five days for subject 1. The lower line represents the performance when driving without filter, the upper one the average velocity when the filter is active. It is clear that the overall performance (with and without filter) improves significantly over the course of days.

the wall, a large percentage of the session time may be spent in OA mode. This is undesirable, as it results in a reduction of the average velocity and thus in a degraded overall task performance.

When driving with environmental filtering, the path is typically much smoother (see Figure 13(b)). Problems that may occur are that the subject chooses his/her resting periods at inappropriate moments. When driving the wheelchair, resting periods are most appropriate when driving straight on in a corridor. The robot will stay on course. Whenever a choice in the path (e.g., the possibility to turn left or right)

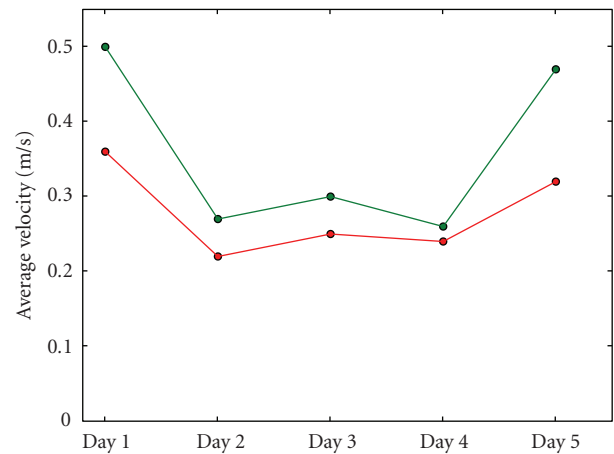


FIGURE 15: The evolution of the average velocity during sessions over all five days for subject 2. The lower line represents the performance when driving without filter, the upper one the average velocity when the filter is active. We can see that the average velocities are much higher when driving with filtering, especially during the first and last days.

arises, however, the subject needs to take control and convey his/her intention to the system. In other words, resting periods cannot be chosen arbitrarily but must be appropriately timed as well. For instance, as shown in Figure 13, the subject takes two long rests, right at the moment when he/she needs to decide over the general direction to take. This behavior has a negative impact on the smoothness of the path and the resulting average velocity.

It is also noteworthy to mention that the overall average velocity for subject 1 rises over the days as Figure 14 shows, indicating that the subject's driving skills improve gradually.

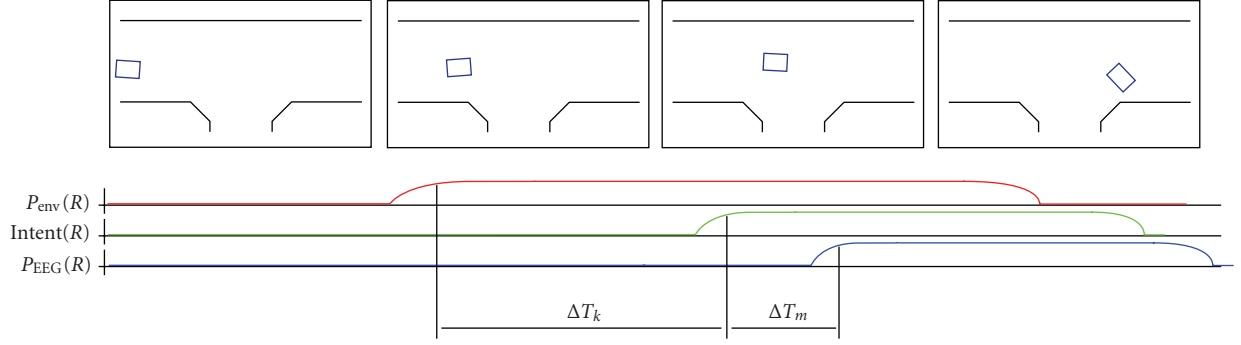


FIGURE 16: The timing problem. The upper row of figures shows a few frames in the path a subject may follow when the task is to turn south into the T -shaped corridor. We can see the evolution of the probabilities for *Right* commands as seen from the environmental filter and the BCI. Also visible is the moment at which the user decides to start turning, shown as *intention*(R). The timing issue has 2 components. First, there is a delay δT_k that denotes the suboptimal kinematic prediction by the subject; the turn should have started earlier for the current speed of the platform. Secondly, a mental task switching delay T_m occurs which increases the total time delay even more. Eventually, the opportunity has passed by and the wheelchair crashes into the wall.

TABLE 1: The percentage of sessions in which subject 1 reached the goal position within 4 minutes.

Day	Overall (all sessions)	Sessions without filtering	Sessions with filtering
Day 2	60%	40%	80%
Day 3	80%	66.67%	85.71%
Day 4	70%	60%	80%
Day 5	80%	100%	60%

TABLE 2: The time subject 2 needed to reach the goal position (in s).

Day	Overall (all sessions)	Sessions without filtering	Sessions with filtering
Day 2	151.32	164.25	138.4
Day 3	120.37	144.6	115.52
Day 4	138.7	145.6	127.2
Day 5	110.26	126.01	84.01

Subject 2 does not show a similar evolution (see Figure 15), but *in both cases* we can see that the average velocities are much higher when filtering is active. For subject 1, the average improvement the filter offers regarding the average velocity is 17.58%. For subject 2 the gain is even higher: 22.72%.

Another interesting factor is the time the user spent in obstacle avoidance mode, as this reflects an undesirable aspect: namely that the subject is controlling the robot to a lesser extent when in this mode. Furthermore, OA is designed as a safety measure, not to provide continuous navigational assistance. All in all, spending much time in OA does not constitute what we regard as “good driving behavior” and it slows the navigation down significantly. When we compare the average amount of time spent in OA mode when driving without filter to the amount when driving with environmental filtering, we see an overall 13.3% (subject 1) and 17.44%

(subject 2) decrease for the latter case. This is reflected in the more efficient (centre of corridor) driving behavior.

Now, if we consider the task that the subjects had to perform (driving to a certain goal pose, if possible via a predetermined path, as shown in Figure 6) we get the results for subject 1 listed in Table 1. This table shows the figures for day 2 through 5 (there was no goal-directed task in day 1). It is clear that for the majority of days, the environmental filter significantly increases the probability of reaching the goal position within 4 minutes. Only during the last day, the subject had better control without the filter and could reach the goal 100% of the time. All sessions together, the filter proves to increase the task performance by about 10%. Considering only days 2 through 4, we see an increase of more than 26%. Subject 2 on the other hand, did not show a large difference in probability of reaching the goal with or without filtering (+7.5% when filtering is active). However, the *time* needed to reach the goal is significantly lower when using the environmental filter, as Table 2 shows. In total, subject 2 reached the goal 19.87% more rapidly when driving with filter compared to driving without.

5. DISCUSSION

The experiments were conducted with two subjects that had no previous experience in BCI control nor control of differentially driven robots such as the electrical wheelchair. From the data collected over all five days, we can clearly see how the subjects have gradually learned to improve this control. Yet, the problem of predicting the kinematic behavior of the wheelchair accurately remains a mentally demanding task. This may cause erroneous timing when initiating a turn into a corridor, leading to a worse overall driving behavior; refer to Figure 16 for a graphical overview of this problem.

During the course of the first days, when the subjects were still performing rather bad, the filter acts as a correctional tool that rectifies much of the misclassifications coming from the EEG classifier. This is visible in Figures 10,11, 14,15 and Table 1. As a result, filtering enables a novel subject

to achieve good levels of performance even on the *first* day of usage. It is clear from Figures 10 and 11 that the filter keeps the performance on the level of the individual commands more or less stable over all days. The environmental filter may thus be seen as a *learning tool* that keeps the subjects performance on a workable level even if that subject is just taking the first steps in learning to use BCI control for driving a wheelchair. Later on, when the subject shows an improved control, the filter corrects less, up to the point that the control is so good that the filter actually holds back. It is remarkable that on the first day, when the subjects still were completely new to the task, for some (filtered) sessions very good performance could be noted.

However, the collected data and the performance figures extracted from the experiments are to a large extent dependent on the *driving strategy* the subject employs. As the subjects gradually learned to control the system, different strategies were explored. One example is visible in Figure 13(a), where the subject exploited the behavior provided by the obstacle avoidance algorithm to lead the robot without much control effort alongside a wall. Similarly, the subject occasionally exploited the OA safety behavior to let the robot ride until it approaches a wall. At that point, OA slows the robot down and the subject has more time to choose the direction he/she wants to go into. This is, for instance, visible in Figure 13(b). Now, while exploring alternative strategies, the performance measures naturally change as well.

A further source of “noise” on the collected data is caused by inappropriate usage of the resting possibility, as already discussed before. Figure 13-right shows an example. Of course, this strategy also has a negative influence on the resulting performance.

Furthermore, the filter was regularly switched on and off in between sessions, without the subject’s knowledge. Because of the fact that the driving system is different when the filtering is applied, the subject needs to use another mental model (or at least adapt his/her existing one) when the filter is switched on or off. Also, the subjects were not told how the environmental filter internally works, so that they needed to learn an appropriate mental model from scratch while driving. The result is that when the subject’s acquired strategies built up using the one driving system (i.e., without filtering) were applied to the other situation, performance was seriously weakened. This effect is sometimes referred to as *mode confusion* [14] and it is a common problem in shared control systems. An illustrative example is that when driving without filtering, the subjects learned at a certain moment to turn 180 degrees in a corridor, whenever they got orientated in the wrong direction (see Figure 12). When the filter was switched on, he/she tried to use that same strategy. Because the filter assumes smooth and efficient forward motion, such behavior was deemed unlikely and the filter made it a difficult manoeuvre. This leads to a situation in which the environmental filter is actually working *against* the user’s intention.

6. CONCLUSIONS AND FURTHER WORK

We have shown that the usage of an environmental filtering technique, which uses knowledge about the current con-

text to filter out erroneous steering commands, can improve the overall driving behavior. Especially when the subject is not already trained for the task, the filter provides significant benefits. However, when the subject is performing really well and employs driving behavior that is not compatible with the logic of the filter, performance may be weakened. All in all, the subjects declared that driving with filtering was *more easy* to do, especially during the first days. As such, the system proves most useful as a learning tool, when the subject is in the learning phase of BCI control.

Probably the most notable weakness of the filter in its current form is the fixed user model. The system assumes a certain driving behavior that would lead to smooth and efficient forward motion. Whenever strategies are employed that contradict with this assumption, the performance gets worse (i.e., 180-degree turning in a corridor). Therefore, we need an *adaptive* model that constantly adapts to whatever strategies the user might employ. Besides that, we could also benefit from a detection mechanism that simply switches off the filter if user performance gets high, or more generally some mechanism to regulate the amount of influence the filter has. Also, a user model incorporating the specific BCI profile the particular subject has (how likely it is that he/she generates the correct steering commands) might lead to a better filtering of the individual commands.

ACKNOWLEDGMENTS

This research was funded by a Ph.D. grant of the Institute for the Promotion of Innovation through Science and Technology in Flanders (IWT-Vlaanderen). This work is supported by the Swiss National Science Foundation NCCR “IM2” and by the European IST Programme FET Project FP6-003758. This paper only reflects the authors’ views and funding agencies are not liable for any use that may be made of the information contained herein.

REFERENCES

- [1] J. d. R. Millán, F. Renkens, J. Mouriño, and W. Gerstner, “Non-invasive brain-actuated control of a mobile robot by human EEG,” *IEEE Transactions on Biomedical Engineering*, vol. 51, no. 6, pp. 1026–1033, 2004.
- [2] J. d. R. Millán, “Brain-computer interfaces,” in *Handbook of Brain Theory and Neural Networks*, M. A. Arbib, Ed., pp. 178–181, MIT Press, Cambridge, Mass, USA, 2002.
- [3] J. d. R. Millán, F. Renkens, J. Mouriño, and W. Gerstner, “Brain-actuated interaction,” *Artificial Intelligence*, vol. 159, no. 1-2, pp. 241–259, 2004.
- [4] M. Nuttin, D. Vanhooydonck, E. Demeester, and H. Van Brussel, “Selection of suitable human-robot interaction techniques for intelligent wheelchairs,” in *Proceedings of the 11th IEEE International Workshop on Robot and Human Interactive Communication (ROMAN ’02)*, pp. 146–151, Berlin, Germany, September 2002.
- [5] G. Vanacker, D. Vanhooydonck, E. Demeester, et al., “Adaptive filtering approach to improve wheelchair driving performance,” in *Proceedings of the 15th IEEE International Symposium on Robot and Human Interactive Communication (ROMAN ’06)*, pp. 527–532, Hatfield, UK, September 2006.

- [6] D. Vanhooydonck, E. Demeester, M. Nuttin, and H. Van Brussel, "Shared control for intelligent wheelchairs: an implicit estimation of the user intention," in *Proceedings of the 1st International Workshop on Advances in Service Robotics (ASER '03)*, pp. 176–182, Bardolino, Italy, March 2003.
- [7] E. Demeester, M. Nuttin, D. Vanhooydonck, and H. Van Brussel, "A model-based, probabilistic framework for plan recognition in shared wheelchair control: experiments and evaluation," in *Proceedings of IEEE/RSJ International Conference on Intelligent Robots and Systems (IROS '03)*, vol. 2, pp. 1456–1461, Las Vegas, Nev, USA, October 2003.
- [8] N. I. Katevas, N. M. Sgours, S. G. Tzafestas, et al., "The autonomous mobile robot SENARIO: a sensor-aided intelligent navigation system for powered wheelchairs," *IEEE Robotics & Automation Magazine*, vol. 4, no. 4, pp. 60–70, 1997.
- [9] E. Prassler, J. Scholz, and M. Strobel, "MAid: mobility assistance for elderly and disabled people," in *Proceedings of the 24th Annual Conference of the IEEE Industrial Electronics Society (IECON '98)*, vol. 4, pp. 2493–2498, Aachen, Germany, August–September 1998.
- [10] H. Yanco, *Shared user-computer control of a robotic wheelchair system*, Ph.D. thesis, Massachusetts Institute of Technology, Cambridge, Mass, USA, September 2000.
- [11] G. Bourhis, O. Horn, O. Habert, and A. Pruski, "An autonomous vehicle for people with motor disabilities," *IEEE Robotics & Automation Magazine*, vol. 8, no. 1, pp. 20–28, 2001.
- [12] R. S. Rao, K. Conn, S. H. Jung, et al., "Human robot interaction: application to smart wheelchairs," in *Proceedings of IEEE International Conference on Robotics and Automation (ICRA '02)*, vol. 4, pp. 3583–3588, Washington, DC, USA, May 2002.
- [13] R. C. Simpson, S. P. Levine, D. A. Bell, L. A. Jaros, Y. Koren, and J. Borenstein, "NavChair: an assistive wheelchair navigation system with automatic adaptation," in *Proceedings of the Assistive Technology and Artificial Intelligence, Applications in Robotics, User Interfaces and Natural Language Processing*, vol. 1458 of *Lecture Notes in Computer Science*, pp. 235–255, 1998.
- [14] T. Röfer and A. Lankenau, "Architecture and applications of the Bremen autonomous wheelchair," in *Proceedings of the 4th Joint Conference on Information Systems*, vol. 1, pp. 365–368, Association for Intelligent Machinery, October 1998.
- [15] L. I. Kuncheva, *Combining Pattern Classifiers: Methods and Algorithms*, John Wiley & Sons, New York, NY, USA, 2004.
- [16] A. Buttfield, P. W. Ferrez, and J. d. R. Millán, "Towards a robust BCI: error potentials and online learning," *IEEE Transactions on Neural Systems and Rehabilitation Engineering*, vol. 14, no. 2, pp. 164–168, 2006.

Appendix I

Demonstrations

This Appendix includes a CD-ROM with demonstrations carried out with the real wheelchair at 2006 and 2007 in the laboratories of the Katholieke Universiteit Leuven (Slalom.wmv and Docking.wmv), and the supplementary material of the publication included in Appendix F (Galán et al., 2008) (Simulation.wmv). CD-ROM at the back cover.

Aquest apèndix inclou un CD-ROM amb les demostracions portades a terme amb la cadira de rodes al 2006 i al 2007 als laboratoris de Katholieke Universiteit Leuven (Slalom.wmv i Docking.wmv), i el material suplementari de la publicació inclosa a l'apèndix F (Galán et al., 2008) (Simulation.wmv). CD-ROM a la contraportada.

Apèndix J

Resum

La idea de controlar diferents tipus de dispositius amb el pensament (mitjançant l'activitat cerebral) ha fascinat a la humanitat des de sempre. Investigadors treballant en àrees multidisciplinars entre l'estadística, la ciència computacional, la neurociència i l'enginyeria biomèdica han començat a desenvolupar les primeres proves de concepte d'interfícies cerebrals que permeten navegar en entorns virtuals (Bayliss, 2003), controlar pròtesis (Nicoletti and Chapin, 2002), conduir dispositius mòbils com robots (Millán et al., 2004) o cadires de rodes (Galán et al., 2008a), i escriure utilitzant teclats virtuals (Birbaumer et al., 1999; Millán, 2003; Oberbayer et al., 2003).

Una interfície cerebral és un sistema de cicle tancat que monitoritza l'activitat cerebral de l'usuari i transforma la seva intencionalitat en accions sense necessitat d'utilitzar l'activitat muscular o el sistema nerviós perifèric (Wolpaw et al., 2002). L'aspecte central d'aquest tipus d'interfície és la capacitat de reconèixer patrons d'activitat cerebral, patrons cadascun dels quals està associat a una intenció o tasca cognitiva. D'aquesta manera, una interfície cerebral és un desenvolupament tecnològic assistencial que estableix una nova modalitat interactiva entre l'usuari i l'entorn (veure Fig. J.1).

Com funciona una interfície cerebral? L'activitat cerebral, enregistrada amb un sistema d'adquisició, és posteriorment processada i transformada per un mòdul de processament de senyals on es selecciona les característiques rellevants que permeten a un mòdul de reconeixement de patrons, normalment un classificador estadístic, identificar el tipus d'activitat generada per l'usuari i associar-la a comandes que permetin controlar un dispositiu. Finalment, el feedback juga un paper essencial en el procés d'aprenentatge de l'usuari facilitant informació sobre la manera en que el sistema ha executat la comanda desitjada. La Fig. J.2 mostra l'arquitectura general d'una interfície cerebral.

J.1 Interfícies Cerebrals a l'IDIAP Research Institute

Les interfícies cerebrals desenvolupades a l'IDIAP Research Institute (IDIAP BCI) segueixen quatre principis (veure apèndix A; Millán et al., 2008). El primer, un protocol asíncron amb el qual els usuaris decideixen voluntàriament quan executar una tasca cognitiva, se-

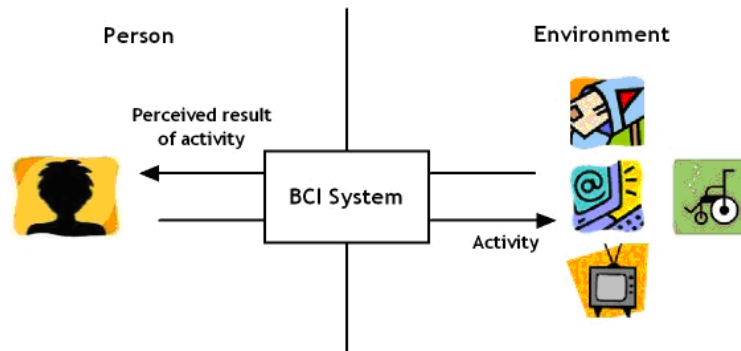


Figura J.1: Model d'una interfície cerebral com a desenvolupament tecnològic que estableix una nova modalitat interactiva entre l'usuari i l'entorn.

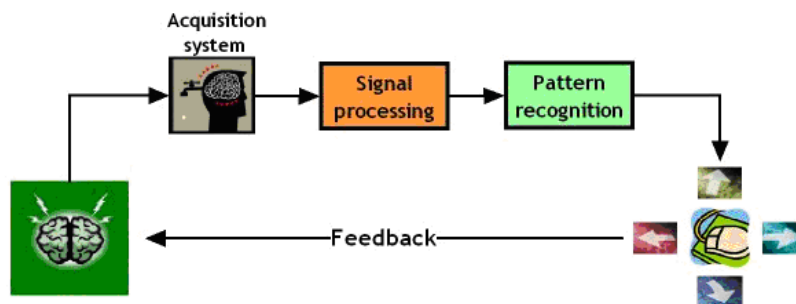


Figura J.2: Representació esquemàtica de l'arquitectura d'una interfície cerebral.

guint el seu propi ritme, sense la necessitat d'un senyal extern que marqui la pauta d'execució. El segon, aprenentatge mutu entre la interfície i l'usuari. IDIAP BCI utilitza tècniques d'aprenentatge estadístic per descobrir els patrons EEG característics de cada usuari associats a l'execució de les diferents tasques cognitives que permeten la modulació voluntària dels diferents ritmes EEG. El tercer principi és la combinació de la intel·ligència de l'usuari i la intel·ligència artificial implementada en els diferents dispositius amb l'objectiu de facilitar la interacció i reduir la càrrega cognitiva de l'usuari. Aquest principi és particularment útil per al control de dispositius mòbils com robots i cadires de rodes. Finalment, el quart principi consisteix en el reconeixement d'estats cognitius de l'usuari associats a la percepció d'errors. D'aquesta manera, el sistema únicament executa aquelles comandes no percebudes per l'usuari com comandes erròniament reconegudes per la interfície. Les següents seccions introdueixen breument cada principi.

J.1.1 Protocol Asíncron i Espontani

Les interfícies cerebrals no invasives basades en EEG es poden classificar en síncrones o asíncrones. La necessitat d'un senyal extern que indiqui a l'usuari quan pot començar a executar una tasca cognitiva restringeix l'aplicabilitat dels sistemes síncrons. Una modalitat interactiva alternativa i més apropiada es fonamenta en l'anàlisi dels components associats amb activitat cognitiva espontània i intencional. Particularment, aquest és el cas en el control de dispositius robòtics. Les interfícies cerebrals síncrones estan limitades per una reduïda capacitat de comunicació, per sota de 0.5 bits/segon (Wolpaw et al., 2002). El principal motiu és la repetició del senyal extern cada 4-10 segons, fet que limita la freqüència de resposta de la interfície (Birbaumer et al., 1999; Pfurtscheller et al., 2001; Wolpaw et al., 2004). Els protocols síncrons faciliten l'anàlisi de l'EEG donat que es coneix en tot moment l'instant quan l'usuari comença l'execució d'una determinada tasca cognitiva. Aquest fet permet amplificar les diferències respecte l'EEG basal, malauradament alenteix dramàticament la interacció. Contràriament, l'IDIAP BCI utilitza protocols asíncrons més flexibles amb els quals els usuaris executen comandes quan ells així ho desitgen, sense la necessitat d'esperar un senyal extern. Aquest tipus de protocol permet a l'usuari començar o canviar voluntàriament de tasca cognitiva i executar comandes en qualsevol moment (Birch et al., 2002; Millán et al., 2004). D'aquesta manera el temps de resposta de la interfície pot ser inferior a un segon. Concretament, IDIAP BCI respon cada 1/2 segon. Aquest fet, juntament amb el rendiment de la interfície, facilita una capacitat de comunicació entre 1 i 1.5 bits/segon.

J.1.2 La Via de l'Aprenentatge Estadístic en Interfícies Cerebrals

Un aspecte crític per al desenvolupament d'una interfície cerebral no invasiva basada en EEG és l'entrenament dels usuaris, com els usuaris aprenen a operar la interfície. Alguns grups han demostrat que alguns individus poden aprendre a controlar la seva activitat cerebral satisfactòriament, després de llarg temps entrenant, amb l'objectiu de generar patrons EEG estables que són transformats per la interfície en accions externes (Birbaumer et al., 1999; Wolpaw et al., 2004). En aquests casos els usuaris són entrenats durant mesos per modificar l'amplitud dels senyals EEG. L'IDIAP BCI utilitza un procés d'aprenentatge mutu (entre l'usuari i la interfície) per facilitar i accelerar aquest procés d'entrenament. Aquest aprenentatge mutu ha permès aconseguir rendiments satisfactoris necessitant poques hores d'entrenament (Millán et al., 2004; Galán et al., 2008a). La majoria d'interfícies cerebrals basades en EEG reconeixen dos tasques cognitives (Babiloni et al., 2000; Pfurtscheller et al., 2001; Blankertz et al., 2006a; Birch et al., 2002). L'IDIAP BCI mostra una taxa d'error inferior al 30% reconeixent tres tasques cognitives. Això és possible principalment gràcies a la utilització de tècniques d'aprenentatge estadístic implementades en dos nivells, en la selecció de característiques EEG i en l'entrenament d'un classificador integrat a la interfície. Aquest plantejament pretén descobrir patrons espai-freqüencials específics de

cada usuari immersos en el senyal EEG. En el primer nivell es seleccionen aquelles característiques (espacials i freqüencials) que són més rellevants per discriminar entre diferents tasques cognitives. Les característiques seleccionades satisfan dos criteris: maximització de la separabilitat entre les tasques cognitives, i estabilitat d'aquesta separabilitat en el temps. La selecció d'aquestes característiques es basa en l'anàlisi de variables canòniques (veure apèndix D; Galán et al., 2007a). En el segon nivell, IDIAP BCI implementa un classificador estadístic Gaussià (Millán et al., 2004). La sortida d'aquest classificador és una estimació de les distribucions de probabilitats posteriors per a cada classe, és a dir la probabilitat que un patró EEG a temps t pertanyi a cada tasca cognitiva (o classe). Veure apèndix F (Galán et al., 2008a) per a més detalls.

J.1.3 Combinació d'Intel·ligències

Els sistemes d'interfícies cerebrals són utilitzats per augmentar les capacitats comunicatives dels seus usuaris, possibilitar noves formes d'entreteniment, i establir noves formes de control de dispositius físics. Fins fa poc, les interfícies cerebrals basades en EEG havien estat considerades massa lentes per controlar seqüències ràpides i complexes de moviments. IDIAP BCI ha mostrat com una anàlisi asíncrona de l'EEG permet controlar de manera continuada un robot seguint trajectòries complexes requerint canvis ràpids entre tasques cognitives (Millán et al., 2004). Un aspecte clau d'aquest robot és la introducció de control compartit entre els dos agents intel·ligents, l'usuari i el robot, de manera que l'usuari únicament proporciona comandes cognitives d'alt nivell que el robot executa de manera autònoma. Específicament, els estats cognitius de l'usuari són associats a comandes d'alt nivell que són executats de manera autònoma pel robot utilitzant la informació enregistrada pels seus sensors. El robot executa les comandes d'alt nivell gràcies a un controlador comportamental que garanteix l'evitació d'obstacles i el seguiment de trajectòries suaus.

J.1.4 Reconeixement d'Estats Cognitius

Les interfícies cerebrals poden posar a l'abast noves eines comunicatives i de control a persones amb diferents tipus de discapacitat. Tanmateix, com qualsevol altre sistema basat en senyals fisiològiques, les interfícies cerebrals són susceptibles de cometre errors en la tasca de reconèixer la intencionalitat de l'usuari. A diferència d'altres modalitats interactives, una especificitat del *canal cerebral* és la possibilitat d'extreure tant informació utilitzada per a la execució de comandes mentals com informació sobre els estats cognitius de l'usuari que pot ser utilitzada per optimitzar el procés interactiu. Un d'aquests estats cognitius és l'associat a la percepció de comissió d'errors. El treball portat a terme per Ferrez i Millán (Ferrez and Millán, 2005; Ferrez and Millán, 2007a; Ferrez and Millán, 2007b) ha descrit la presència d'un tipus de potencials d'error (ErrP) immersos en l'EEG dels usuaris elícit pel reconeixement erroni, per part de la interfície, de la seva intencionalitat. En els últims estudis publicats, Ferrez (Ferrez, 2007) ha mostrat la viabilitat de reconèixer potencials d'error en

temps real. D'aquesta manera, el procés interactiu pot ser optimitzat únicament executant aquelles comandes no percebudes per l'usuari com comandes erròniament reconegudes per la interfície.

J.2 Projecte MAIA

L'objectiu del projecte europeu MAIA (Mental Augmentation through determination of Intended Action) ha estat desenvolupar interfícies cerebrals que reconeguin les tasques cognitives executades pels usuaris i executin els necessaris passos de baix nivell que permetin completar tasques complexes. El projecte ha estat finançat pel Sisè Programa Marc (FP6), va començar al setembre 2004 i ha finalitzat al desembre 2007. Els socis integrants han estat l'IDIAP Research Institute (coordinador, Suïssa), Katholieke Universiteit Leuven (Bèlgica), University Hospital of Geneva (Suïssa), Fondazione Santa Lucia (Itàlia) i Helsinki University of Technology (Finlàndia). Els principis innovadors del projecte han estat la utilització d'estimacions d'activitat intracranial des de l'EEG per al reconeixement de la intencionalitat de l'usuari, el control compartit adaptatiu entre l'usuari i el robot, la utilització de feedback vibro-tàctil per accelerar l'entrenament de l'usuari, la integració de la detecció d'estats cognitius d'alt nivell (detecció de comissió d'errors) per augmentar la robustesa de la interfície, i finalment la adaptació en línia de la interfície al subjecte per monitoritzar contínuament els canvis de l'activitat cerebral. Els principals èxits del projecte han estat ambdues demostracions al 2006 i 2007 de la primera cadira de rodes controlada mentalment (veure Apèndix I) portades a terme als laboratoris de Katholieke Universiteit Leuven.

J.3 Objectius de la Tesi

El propòsit d'aquesta tesi ha estat desenvolupar mètodes per interfícies cerebrals asíncrones i no invasives basades en EEG que permetin augmentar la robustesa de dispositius controlats mentalment. Dintre del marc establert pel projecte MAIA, aquests mètodes han estat orientats a augmentar la robustesa de la interfície integrada a la cadira de rodes.

La cadira de rodes controlada mentalment desenvolupada al projecte MAIA s'integra per dos entitats diferenciades, la cadira de rodes intel·ligent i la interfície cerebral. La informació de l'entorn enregistrada pels sensors de la cadira és introduïda a un filtre contextual que construeix una distribució de probabilitat $P_{Env}(C)$ sobre les possibles comandes direccionals de l'usuari, $C = \{Esquerra, Dreta, Endavant\}$. La interfície cerebral estima les probabilitats $P_{EEG}(C)$ de les diferents comandes cognitives des de l'EEG. Ambdós fluxos d'informació es combinen produint una estimació filtrada de la intencionalitat de l'usuari $P(C) = P_{EEG}(C) \cdot P_{Env}(C)$. El sistema de control compartit també inclou la informació de l'entorn enregistrada pels sensors de la cadira per transformar les esmentades probabilitats

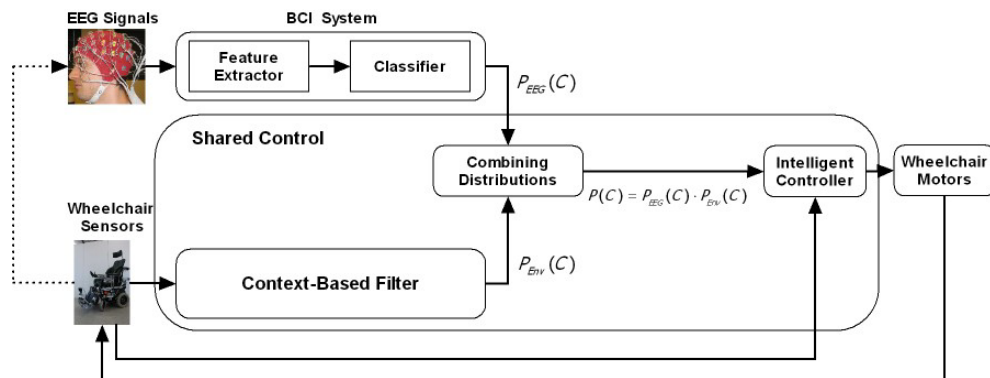


Figura J.3: Arquitectura de la cadira de rodes.

corresponents a comandes d'alt nivell $P(C)$ en comandes motrius apropiades, velocitats translacionals i rotacionals, que permetin generar una conducció suau. Això és realitzat per un controlador intel·ligent que activa un comportament apropiat d'assistència en la conducció quan l'usuari necessita ajuda. D'aquesta manera, el sistema adapta constantment el grau d'assistència a una situació específica. Aquesta assistència ajuda significativament quan el rendiment de l'usuari (rendiment de la interfície cerebral) és baix, mentre que el seu rol decreix quan el rendiment de l'usuari és alt. La Fig. J.3 mostra una representació esquemàtica de l'arquitectura de control compartit implementada a la cadira de rodes. Veure Apèndixs G i H (Philips et al., 2007; Vanacker et al., 2007) per a una descripció detallada.

Les principals contribucions d'aquesta tesi són tres. Primer, la utilització de la detecció de transicions entre tasques cognitives (MTTD) per guiar algorismes de postprocessament encarregats de suavitzar el procés de presa de decisions de la interfície cerebral. Segon, la utilització d'un nou mètode d'extracció de característiques de solució canònica per interfícies cerebrals que facilita un reduït nombre de patrons espacials discriminants canònics i ordena els diferents canals EEG per capacitat discriminant entre les classes (tasques cognitives). Tercer, la introducció d'un enfocament basat en el reconeixement de *frames* neurals (Freeman, 2005), patrons intermitents espacials induïts d'amplitud modulada, per a guiar nous processos de presa de decisions. Mentre que les primeres dues aportacions consisteixen en afegir o modificar mòduls a l'actual arquitectura de la cadira de rodes d'acord a enfocaments convencionals d'interfícies asíncrones (Blankertz et al., 2006a; Birch et al., 2002; Millán et al., 2004), la tercera s'allunya radicalment dels enfocaments convencionals i implica canviar el procés de presa de decisions de la interfície. La Fig. J.4 mostra on encaixen les esmentades aportacions a la present arquitectura de la cadira de rodes.

Tant la recerca desenvolupada pel grup de recerca IDIAP BCI com les aportacions de la tesi han estat àmpliament descrites en les següents publicacions:

1. J.del R. Millán, P. W. Ferrez, F. Galán, E. Lew, and R. Chavarriaga. Non-Invasive Brain-Machine Interaction. *International Journal of Pattern Recognition and Artifi-*

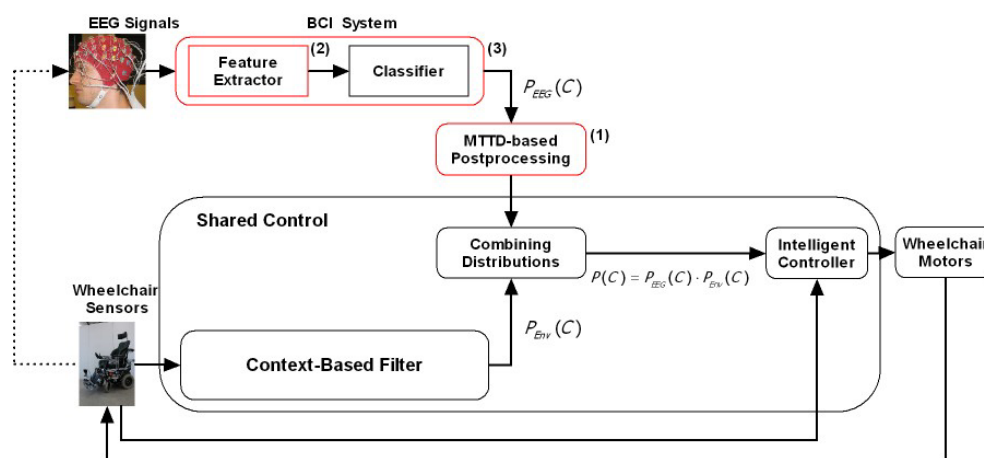


Figura J.4: Arquitectura de la cadira de rodes després d'incloure les tres contribucions d'aquesta tesi. (1) El mòdul de postprocessament basat en la detecció de transicions entre tasques cognitives (MTTD) representa un nou mòdul entre la interfície cerebral i la posterior combinació de distribucions. (2) L'extractor de característiques proposat és situa en el mòdul d'extracció de característiques. (3) L'enfocament basat en el reconeixement de *frames* neurals implica el canvi complet del sistema de presa de decisions de la interfície cerebral.

cial Intelligence, 2008. To appear.

2. F. Galán, F. Oliva, and J. Guàrdia. Using Mental Tasks Transitions Detection to Improve Spontaneous Mental Activity Classification. *Medical and Biological Engineering and Computing*, 45: 603-609, 2007b.
3. F. Galán, F. Oliva, J. Guàrdia, P.W. Ferrez, and J. del R. Millán. Detecting Intentional Mental Transitions in an Asynchronous Brain-Computer Interface. *Medical and Biological Engineering and Computing*, 2008b. Submitted.
4. F. Galán, P. W. Ferrez, F. Oliva, J. Guàrdia, and J. del R. Millán. Feature Extraction for Multi-class BCI using Canonical Variates Analysis. In *Proceedings of the 2007 IEEE International Symposium on Intelligent Signal Processing, WISP 2007*, Alcalá de Henares, Spain, 2007a.
5. F. Galán, J. Palix, R. Chavarriaga, P.W. Ferrez, C.A. Hauert, and J. del. R. Millán. Visuo-spatial Attention Frame Recognition for Brain-computer Interfaces. In: Wang, R., Gu, F., and Shen, F. (Eds.) *Advances in Cognitive Neurodynamics ICCN 2007. Proceedings of the International Conference on Cognitive Neurodynamics. ICCN 2007 Proceedings*. Springer, Shangai, China, 2007c. To appear.

6. F. Galán, M. Nuttin, E. Lew, P. W. Ferrez, G. Vanacker, J. Philips, H. Van Brussel, and J. del R. Millán. A Brain-Actuated Wheelchair: Asynchronous and Non-Invasive Brain-Computer Interfaces for Continuous Control of Robots, *Clin. Neurophysiol.*, 2008a. To appear.

La publicació 1 descriu la recerca portada a terme pel grup de recerca IDIAP BCI. Les publicacions 2 i 3 inclouen dues versions diferenciades del detector de transicions entre tasques cognitives (MTTD), la publicació 4 descriu la utilització de l'anàlisi de variables canòniques per a l'extracció de característiques en interfícies cerebrals multi classe. La publicació 5 proposa l'enfocament basat en la detecció de *frames* neurals, i finalment la publicació 6 descriu la darrera versió de la cadira de rodes virtual. Aquesta versió de la cadira de rodes virtual i la cadira de rodes real ja implementen l'extractor de característiques descrit a la publicació 4.

J.4 Resultats i Conclusions

El primer algorisme de postprocessament basat en MTTD (veure Apèndix B; Galán et al. (2007b)) ha mostrat el seu potencial en guanyar el concurs internacional BCI Competition III -Datata Set V: Multiclass Problem, Continous EEG- (Blankertz et al., 2006b) assolint una classificació correcta mitjana sobre tres subjectes de 68.65% (79.60%, 70.31% i 56.02% respectivament) en un problema de tres classes. La introducció de MTTD representa un increment absolut del 6% en classificació correcta mitjana respecte la versió de l'algorisme que no incorpora MTTD. Malgrat aquests bons resultats, l'algorisme presenta alguns inconvenients com la dependència a la freqüència de mostreig i la simplicitat de la regla heurística implementada. Aquests inconvenients poden explicar el comportament irregular de l'algorisme quan ha estat avaluat en condicions on els subjectes reben feedback. Per corregir aquestes deficiències s'ha proposat un segon algorisme (veure Apèndix C; Galán et al. (2008b)). Aquest últim implementa un MTTD basat en un filtre de Kalman i tres regles heurístiques que exploten tant la informació extreta de la detecció de transicions com la extreta de la detecció d'inconsistències entre la intencionalitat de l'usuari i l'EEG associat. Aquest enfocament facilita un important increment del rendiment de la interfície tant en termes de classificació correcta com en termes de capacitat de comunicació del sistema. L'increment en la capacitat de comunicació s'explica principalment per dos motius, tant per la reduïda taxa d'error facilitada com per oferir una resposta cada 250 mil·lisegons. Els resultats experimentals han mostrat la superioritat d'aquest algorisme respecte el seu predecessor en ambdues condicions, tant en condicions on els subjectes reben retroalimentació on-line com en condicions on els subjectes no reben retroalimentació. El principal inconvenient d'aquest algorisme és la utilització de regles heurístiques. El següent pas a seguir és la formalització d'aquestes regles heurístiques en un marc Baiesià i construir models probabilístics per a la inferència de la intencionalitat de l'usuari seguint la idea de

Verma i Rao (2005). D'aquesta manera serà factible implementar l'algorisme a la cadira de rodes controlada mentalment per combinar les distribucions de probabilitats posteriors amb les facilitades pel filtre contextual (veure Fig. J.3).

L'extractor de característiques amb solució canònica per interfícies cerebrals multi classe (veure Apèndix D; Galán et al. (2007a)) facilita l'espai de màxima separabilitat entre efectes ERD/ERS ((de)sincronització relacionada a esdeveniments) (Pfurtscheller i Lopes da Silva, 1999) involucrats en la execució de diferents tasques cognitives. Addicionalment, la mesura DP proposada ordena els elèctrodes EEG en funció de la seva contribució en l'esmentat espai. Resultats experimentals han mostrat l'obtenció de solucions equivalents treballant en els dominis temporal i freqüencial. Addicionalment, aquests també han mostrat que els resultats en termes de classificació correcta són reflectits en la similitud entre els mapes DP obtinguts dels conjunts d'entrenament i test d'ambdós dominis. Per altra banda, la similitud entre els mapes DP obtinguts en cada domini, utilitzant els conjunts test, disminueix en aquells subjectes amb menor classificació correcta. Una possible explicació que requereix una major exploració és el fet que l'energia d'un senyal (domini temporal) i l'estimació dels seus components freqüencials utilitzant la PSD (domini freqüencial) no capturen el mateix fenomen quan el senyal és menys estacionari. Aquest fet esdevé especialment quan l'usuari de la interfície té dificultats de generar patrons EEG estables durant la execució de les diferents tasques cognitives. L'extractor de característiques proposat ha estat satisfactòriament implementat en ambdós algorismes de postprocessament basats en la detecció de transicions entre tasques cognitives (Galán et al., 2007b; Galán et al., 2008b). Tanmateix, juga un paper essencial en el procés de detecció de *frames* neurals (Galán et al., 2007c), i és utilitzat en la darrera versió de la cadira de rodes (Galán et al., 2008a).

La introducció d'un enfocament basat en la detecció de *frames* neurals (veure Apèndix E; Galán et al. (2007c)) implica un canvi conceptual del sistema de presa de decisions de la interfície cerebral. Aquest enfocament transforma l'escenari tradicional, un problema de reconeixement de patrons EEG, en un problema de detecció d'esdeveniments. Aquest nou enfocament ha estat avaluat preliminarment en una tasca de reconeixement de *frames* d'atenció visuoespacial. Els resultats obtinguts han mostrat, primer, la viabilitat de modular ritmes EEG per mitjà de l'orientació visuoespacial de l'atenció. Segon, la intensitat d'aquesta modulació no és sostinguda. Aquest fet pot estar relacionat amb els patrons intermitents d'amplitud modulada induïts de manera activa (*frames*) descrits per Freeman (2005). A diferència dels anteriors, en aquest cas són generats voluntàriament per l'usuari. Tercer, és possible classificar els *frames* generats durant l'orientació de l'atenció a diferents localitzacions espacials amb una alta classificació correcta (superior al 80% en orientar l'atenció a 2 possibles localitzacions, 2 classes). Quart, la classificació correcta d'aquests *frames* s'incrementa utilitzant components freqüencials inclosos a banda gamma (> 30Hz). Cinquè, la classificació correcta utilitzant l'enfocament tradicional, assumint que la modulació dels ritmes EEG és sostinguda en el temps, es situa en nivells al voltant del 50%. Aquest fet suggereix que un enfocament tradicional és subòptim en la tasca de reconeixement de fenòmens EEG induïts, fet ahora confirmat al comparar la capacitat

de comunicació teòrica d'una interfície cerebral utilitzant ambdós enfocaments. Utilitzant l'enfocament basat en la detecció de *frames* neurals la capacitat de comunicació teòrica de la interfície cerebral es multiplica per 10. El futur treball en aquesta línia de recerca estarà orientat a completar l'estudi amb una major mostra i en el desenvolupament d'algorismes per al reconeixement d'assajos basats en l'acumulació temporal d'evidència. D'aquesta manera, aquests algorismes respondran en intervals variables una vegada l'evidència acumulada superi un nivell estimat de confiança.

Les tres contribucions d'aquesta tesi, així com la cadira de rodes desenvolupada pel projecte MAIA, representen diferents línies actives de recerca en diferent estats de desenvolupament. A dia d'avui, únicament l'extractor de característiques ha estat implementat en la interfície cerebral integrada en la cadira de rodes. L'arquitectura de la última versió ha estat descrita a la secció I.3 (veure també Apèndix F, G i H; Galán et al., 2008a; Philips et al., 2007; Vanacker et al., 2007). El sistema pot ser controlat de manera autònoma per l'usuari sense la necessitat d'algorismes adaptatius calibrats externament per un operador expert en ordre a minimitzar l'impacte de la no-estacionarietat del senyal EEG. Això és gràcies a dos components. Primer, la selecció de característiques EEG estables que maximitzen la separabilitat entre els patrons EEG generats durant l'execució de diferents tasques cognitives. Segon, la inclusió d'un sistema de control compartit entre la interfície cerebral i la cadira de rodes intel·ligent. Els experiments portats a terme on es requeria a dos subjectes conduir mentalment la cadira de rodes d'un punt de sortida a un punt d'arribada seguint una trajectòria preespecificada han mostrat que ambdós subjectes han estat capaços d'assolir 90% (subjecte 1) i 80% (subjecte 2) dels objectius un dia després del calibratge de la interfície, i 100% (subjecte 1) i 70% (subjecte 2) dos mesos més tard. És important destacar que ambdós subjectes van assolir menys objectius en les sessions primera, una hora després del calibratge de la interfície, i tercera, primera sessió després de dos mesos, sessions en les quals els subjectes van haver d'aprendre o recordar com interactuar amb la cadira de rodes i la seva dinàmica. De totes maneres, tot i en aquestes sessions, els subjectes van mostrar un control de la cadira significativament més elevat que l'aconseguit per una interfície aleatòria, la qual sols va aconseguir un 1% dels objectius.

En els darrers anys, la recerca en interfícies cerebrals asíncrones i no invasives ha mostrat la possibilitat de controlar mentalment diferents tipus de dispositius. El següent pas és desenvolupar dispositius intel·ligents i optimitzar la interacció. El desafiament és establir interaccions cerebrals intel·ligents.

Bibliography

F. Babiloni, F. Cincotti, L. Lazzarini, J. del R. Millan, J. Mouriño, M. Varsta, J. Heikkonen, L. Bianchi, and M.G. Marciani. Linear classification of low-resolution EEG patterns produced by imagined hand movements. *IEEE Trans Rehabil Eng.*, 8(2):186–188, 2000.

C. Barber and T. Blum (Eds.). *Evoked Potentials III*, Butterworth, 1988.

J.D. Bayliss. Use of the evoked potential P300 component for control in a virtual apartment. *IEEE Trans. Neural Sys. Rehab. Eng.*, 11:113-116, 2003.

M. Basseville and I. V. Nikiforov, *Detection of Abrupt Changes: Theory and Application*, Prentice-Hall, Upper Saddle River, NJ, 1993.

N. Birbaumer, N. Ghanayim, T. Hinterberger, I. Iversen, B. Kotchoubey, A. Kubler, J. Perelmouter, E. Taub, and H. Flor. A spelling device for the paralysed. *Nature*, 398:297–298, 1999.

G.E. Birch, Z. Bozorgzadeh, and S.G. Mason. Initial on-line evaluation of the LF-ASD braincomputer interface with able-bodied and spinal-cord subjects using imagined voluntary motor potentials. *IEEE Trans. Neural Sys. Rehab. Eng.*, 10: 219-224, 2002.

B. Blankertz, G. Dornhege, S. Lemm, M. Krauledat, G. Curio, and K-R. Müller. The Berlin brain-computer interface: Machine learning based detection of user specific brain states. *J. Universal Computer Sci.*, 12:581-607, 2006a.

B. Blankertz, G. Dornhege, C. Schäfer, R. Krepki, J. Kohlmorgen, K-R. Müller, V. Kunzmann, F. Losch, G. Curio. Boosting Bit Rates and Error Detection for the Classification of Fast- Paced Motor Commands based on Single-Trial EEG Analysis. *IEEE Trans. Neural Sys. Rehab. Eng.* 11: 127–131, 2003.

B. Blankertz, K-R. Müller, D. Krusienski, G. Schalk, J.R. Wolpaw, A. Schlögl, G. Pfurtscheller, J. del R. Millán, M. Schröder, and N. Birbaumer. The BCI competition III: validat-

ing alternative approaches to actual BCI problems. *IEEE Trans. Neural Sys. Rehab. Eng.*, 14:153-159, 2006b.

A. Buttfield, P. W. Ferrez, and J. del R. Millán. Towards a robust BCI: Error potentials and online learning. *IEEE Trans Neural Sys Rehab Eng.*, 14:164-168, 2006.

E. Callaway, P. Tueting, and S. Koslow (Eds.). *Event-Related Brain Potentials in Man*. New York, Academic Press, 1978.

J.M. Carmena, M.A. Lebedev, R.E. Crist, J.E. O'Doherty, D.M. Santucci, D.F. Dimitrov, P.G. Patil, C.S. Henriquez, and M.A.L. Nicolelis. Learning to control a brain-machine interface for reaching and grasping by primates. *PLoS Biology*, 1:193–208, 2003.

Y.L. Chen, F.T. Tang, W.H. Chang, M.K. Wong, Y.Y. Shih, and T.S. Kuo. The new design of an infrared-controlled human–computer interface for the disabled. *IEEE Trans. Neural Syst. Rehabil. Eng.*, 7(4):474–481, 1999.

S. Coyle, T. Ward, and C. Markham. An optical brain computer interface. *Biomedizinische Technik*, 49(1):45–46, 2004a.

S. Coyle, T. Ward, C. Markham, and G. McDarby. On the suitability of near-infrared (NIR) systems for next-generation brain-computer interfaces. *Physiol. Meas.*, 25:815–822, 2004b.

C.M. Cuadras, J. Fortiana, and J. Oliva. The proximity of an individual to a population with applications in discriminant analysis. *Journal of Classification*, 14:117-136, 1997.

E. Curran, P. Sykacek, S. Roberts, W. Penny, M. Stokes, I. Jonsrude, and A. Owen. Cognitive tasks for driving a Brain Computer Interfacing System: a pilot study. *IEEE Transactions on Rehabilitation Engineering*, 12(1): 48-55, 2004.

V. Digalakis, J. R. Rohlicek and M. Ostendorf. ML Estimation of a Stochastic Linear System with the EM Algorithm and its Application to Speech Recognition, *IEEE Trans. Speech and Audio Proc.*, 1:431-442, 1993.

E. Donchin, K.M. Spencer, and R. Wijesinghe. The mental prosthesis: assessing the speed of a P300-based brain-computer interface. *IEEE Transactions on Rehabilitation Engineering*, 8:174-179, 2000.

G. Dornhege, B. Blankertz, and G. Curio. Speeding up classification of multi-channel brain-computer interfaces: common spatial patterns for slow cortical potentials. In *Pro-*

ceedings of the 1st International IEEE EMBS Conference on Neural Engineering, 591-594, 2003.

G. Dornhege, B. Blankertz, G. Curio, and K-R. Müller. Increase information transfer rates in BCI by CSP extension to multi-class. In: S. Thrun, L. Saul, and B. Schölkopf (Eds.), *Advances in Neural Inf. Proc. Systems*, 16: 733-740, 2004.

T. Elbert, B. Rockstroh, W. Lutzenberger, and N. Birbaumer. Biofeedback of slow cortical potentials. *Electroencephalography and Clinical Neurophysiology*, 48:293–301, 1980.

L.A. Farwell and E. Donchin. Talking off the top your head: toward a mental prosthesis utilizing event-related brain potentials. *Electroencephalography and Clinical Neurophysiology*, 70:510–523, 1988.

P.W. Ferrez. *Error-Related EEG Potentials in Brain-Computer Interfaces*. Ph.D. Thesis, Ecole Polytechnique Fédéral de Lausanne, Switzerland, 2007.

P.W. Ferrez, and J. del R. Millán. You Are Wrong!—Automatic Detection of Interaction Errors from Brain Waves. In *Proc. 19th International Joint Conference on Artificial Intelligence*, Edinburgh, UK, 2005.

P.W. Ferrez, and J. del R. Millán. Error-Related EEG Potentials in Brain-Computer Interfaces. In: Dornhege, G., Millán, J.d.R., Hinterberger, T., McFarland, D., Müller, K.-R. (Eds.) *Towards Brain-Computer Interfacing*. MIT Press, Cambridge, Massachusetts, 2007a.

P.W. Ferrez, and J. del R. Millán. Error-Related EEG Potentials Generated during Simulated Brain- Computer Interaction. *IEEE Trans. Biomed. Eng.*, 2007b. To appear.

W.J. Freeman. Origin, structure, and role of background EEG activity. Part 3. Neural frame classification. *Clin. Neurophysiol.* 116, 1118-1129, 2005.

F. Galán, P. W. Ferrez, F. Oliva, J. Guàrdia, and J. del R. Millán. Feature Extraction for Multi-class BCI using Canonical Variates Analysis. In *Proceedings of the 2007 IEEE International Symposium on Intelligent Signal Processing, WISP2007*, Alcalá de Henares, Spain, 2007a.

F. Galán, M. Nuttin, E. Lew, P. W. Ferrez, G. Vanacker, J. Philips, H. Van Brussel, and J. del R. Millán. A Brain-Actuated Wheelchair: Asynchronous and Non-Invasive Brain-Computer Interfaces for Continuous Control of Robots. *Clin. Neurophysiol.*, 2008a. To appear.

F. Galán, F. Oliva, and J. Guàrdia. Using Mental Tasks Transitions Detection to Improve Spontaneous Mental Activity Classification. *Medical and Biological Engineering and Computing*, 45: 603-609, 2007b.

F. Galán, F. Oliva, K. Guàrdia, P.W. Ferrez, and J. del R. Millán. Detecting Intentional Mental Transitions in an Asynchronous Brain-Computer Interface. *Medical and Biological Engineering and Computing*, 2008b. Submitted.

F. Galán, J. Palix, R. Chavarriaga, P.W. Ferrez, C.A. Hauert, and J. del R. Millán. Visuo-spatial Attention Frame Recognition for Brain-computer Interfaces. In: Wang, R., Gu, F., and Shen, F. (Eds.) *Advances in Cognitive Neurodynamics ICCN 2007. Proceedings of the International Conference on Cognitive Neurodynamics. ICCN 2007 Proceedings*. Springer, Shanghai, China, 2007c. To appear.

X. Gao, X. Dingfeng, M. Cheng, and S. Gao. A BCI-based environmental controller for the motion-disabled. *IEEE Trans. Neural Syst. Rehabil. Eng.*, 11: 137—140, 2003.

A.P. Georgopoulos, F.J. Langheim, A.C. Leuthold, and A.N. Merkle. Magnetoencephalographic signals predict movement trajectory in space. *Exp. Brain Res.*, 167:132–135, 2005.

A.A. Glover, M.C. Onofrj, M.F. Ghilardi, and I. Bodis-Wollner. P300-like Potentials in the Normal Monkey using Classical Conditioning and the Auditory ‘oddball’ Paradigm. *Electroencephalography and Clinical Neurophysiology*, 65: 231-235, 1986.

W.R. Goff, T. Allison, and H.G. Jr. Vaughan. The functional neuroanatomy of event-related potentials. In: E. Callaway, P. Tueting, and S. Koslow (Eds.) *Event-Related Brain Potentials in Man*. New York, Academic Press, 1-80, 1978.

S.L. Gonzalez Andino, R. Grave de Peralta Menendez, G. Thut, J. del R. Millán, P. Morier, and T. Landis. Very high frequency oscillations (VHFO) as a predictor of movement intentions. *Neuroimage*, 32:170-179, 2006.

W.M. Grill and J.T. Mortimer. Neural and connective tissue response to long-term implantation of multiple contact nerve cuff electrodes. *J. Biomed. Mater. Res.*, 50:213–220, 2000.

C. M. Hajiyev and F. Caliskan. Fault detection in flight control systems based on the generalized variance of the Kalman filter innovation sequence. In *Proc. Amer. Cont. Conf.*, 1999.

S.A. Hillyard and D. Woods. Electrophysiological analysis of human brain function. In:

M. Gazzaniga (Ed.) *Handbook of Behavioral Neurobiology*, Vol. 2. New York, Plenum Press, 345-378, 1979.

L.R. Hochberg, M.D. Serruya, G.M. Friehs, J.A. Mukand, M. Saleh, A.H. Caplan, A. Branner, D. Chen, R.D. Penn, and J.P. Donoghue. Neuronal ensemble control of prosthetic devices by a human with tetraplegia. *Nature*, 442:164-171, 2006.

R. Karrer, J.Cohen, and P. Tuetting (Eds.) *Brain and Information: Event-Related Potentials*, *Annals of the New York Academy of Sciences*, New York, The New York Academy of Sciences, 1984.

P. Kennedy, R. Bakay, M. Moore, K. Adams, and J. Goldwithe. Direct control of a computer from the human central nervous system. *IEEE Transactions on Rehabilitation Engineering*, 8:198-202, 2000.

H.H. Kornhuber and L. Deecke. Hirnpotentialänderungen beim Menschen vor und nach Willkürbewegungen, dargestellt mit Magnetbandspeicherung und Rückwärtsanalyse. *Pflügers Arch. Ges. Physiol.*, 1964.

A. Kostov and M. Polak. Parallel man-machine training in development of EEG-based cursor control. *IEEE Transactions on Rehabilitation Engineering*, 8:203–204, 2000.

W.J. Krzanowski. *Principles of multivariate analysis*. Oxford University Press, Oxford, 1988.

S. Lemm, B. Blankertz, G. Curio, and K-R. Müller. Spatio-spectral filters for improving the classification of single trial EEG. *IEEE Trans. Biomed. Eng.*, 52:541-1548, 2005.

E.C. Leuthardt, G. Schalk, J.R. Wolpaw, J.G. Ojemann, and D.W. Moran, A brain-computer interface using electrocorticographic signals in humans. *J. Neural Eng.*, 1:63-71, 2004.

M. Middendorf, G. McMillan, G. Calhoun, and K.S. Jones. Brain-computer interfaces based on steady-state visual evoked response. *IEEE Transactions on Rehabilitation Engineering*, 8:211–213, 2000.

J. del R. Millán, J. Mourino, M. Franze, F. Cincotti, M. Varsta, J. Heikkonen, and F. Babiloni. A local neural classifier for the recognition of EEG patterns associated to mental tasks. *IEEE Transactions on Neural Networks*, 13:678-686, 2002.

J. del R. Millán. Adaptive brain interfaces. *Communications of the ACM*, 46:75-80, 2003.

J. del R. Millán. On the need for on-line learning in brain-computer interfaces. In *Proc. Int. Joint Conf. Neural Networks*, 2004.

J. del R. Millán, A. Buttfeld, C. Vidaurre, M. Krauledat, A. Schögl, P. Shenoy, B. Blankertz, R. P. N Rao, R. Cabeza, G. Pfurtscheller, and K-R. Müller. Adaptation in brain-computer interfaces. In: G. Dornhege, J. del R. Millán, T. Hinterberger, D. McFarland, K-R. Müller (Eds.) *Towards Brain-Computer Interfacing*, Cambridge: MIT Press, 2007.

J. del R. Millán, P. W. Ferrez, F. Galán, E. Lew, and R. Chavarriaga. Non-Invasive Brain-Machine Interaction. *International Journal of Pattern Recognition and Artificial Intelligence*, 2008. To appear.

J. del R. Millán, F. Renkens, J. Mouriño, and W. Gerstner. Noninvasive brain-actuated control of a mobile robot by human EEG. *IEEE Trans. Biomed. Eng.*, 51:1026-1033, 2004.

M.A. Nicolelis, and J.K Chapin. Controlling robots with the mind. *Sci Am.*, 287:46-53, 2002.

B. Obermaier, G.R. Muller, and G. Pfurtscheller. Virtual keyboard controlled by spontaneous EEG activity. *IEEE Trans. Neural Syst. Rehabil. Eng.*, 11: 422–426, 2003.

J. Palix, C.A. Hauert, U. Leonards. Brain oscillations: Indicators for serial processing in inefficient visual search?. *Perception*, 35:234, 2006.

W.D. Penny, S.J. Roberts, E.A. Curran, and M.J. Stokes. EEG-based communication: a pattern recognition approach. *IEEE Transactions on Rehabilitation Engineering*, 8:214–215, 2000.

W.D. Penny, S.J. Roberts, and M.J. Stokes, Imagined hand movements identified from the EEG mu-rhythm, *J. Neurosci. Methods*, 1998. Submitted.
<http://citeseer.ist.psu.edu/penny98imagined.html>.

G. Pfurtscheller, C. Guger, G.Müller, G Krausz, and C. Neuper. Brain oscillations control hand orthosis in a tetraplegic. *Neuroscience Letters*, 292:211-214, 2000.

G. Pfurtscheller and F.H. Lopes da Silva. Event-related EEG/EMG synchronization and desynchronization: basic principles. *Clin. Neurophysiol.*, 110:1842-1857, 1999.

G. Pfurtscheller and C. Neuper. Motor imagery and direct brain-computer communication. *Proceedings of the IEEE*, 89:1123-1134, 2001.

T.W. Picton, S.A. Hillyard. Endogenous Event-Related Potentials. In: T. W. Picton (Ed.) *Human Event-Related Potentials – Handbook of Electroencephalography and Clinical Neurophysiology, Vol. 3*. Amsterdam, Elsevier, 1988.

J. Philips, J. del R. Millán, G. Vanacker, E. Lew, F. Galán, P.W. Ferrez, H. Van Brussel, and M. Nuttin. Adaptive shared control of a brain-actuated simulated wheelchair. In *Proceedings of the 10th International Conference on Rehabilitation Robotics, ICORR 2007*, Noordwijk, The Netherlands, 2007.

V. S. Polikov, P. A. Tresco, and W. M. Reichert. Response of brain tissue to chronically implanted neural electrodes. *J. Neurosci. Meth.*, 148: 1–18, 2005.

H. Ramoser, J. Müller-Gerking, and G. Pfurtscheller. Optimal spatial filtering of single trial EEG during imagined hand movement. *IEEE Trans. Neural Sys. Rehab. Eng.*, 8:441–446, 2000.

G. Schalk, J.R. Wolpaw, D.J. McFarland, and G. Pfurtscheller. EEG-based Communication: Presence of an Error Potential. *Clin. Neurophysiol.* 111:2138–2144, 2000.

R. Scherer, G.R. Müller, C. Neuper, B. Graimann, and G. Pfurtscheller. An asynchronously controlled EEG-based virtual keyboard: Improvement of the spelling rate. *IEEE Trans. Biomed. Eng.*, 51:979–984, 2004.

M.D. Serruya, N.G. Hatsopoulos, L. Paninski, M.R. Fellows, and J.P. Donoghue. Instant neural control of a movement signal. *Nature*, 416:141–142, 2002.

P. Shenoy, M. Krauledat, B. Blankertz, R. P. N. Rao, and K-R. Müller. Towards adaptive classification for BCI. *J. Neural. Eng.*, 3:13–23, 2006.

E.E. Sutter. The brain response interface: communication through visually induced electrical brain responses. *Journal of Microcomputer Applications*, 15:31–45, 1992.

S. Sutton, M. Braren, J. Zubin, and E. John. Evoked potential correlates of stimulus uncertainty. *Science*, 150:1187–1188, 1965.

D.H. Szarowski, M.D. Andersen, S. Retterer, A.J.W. Spence, M. Isaacson, H.G. Craighead, J.N. Turner, and W. Shain. Brain responses to micro-machined silicon devices. *Brain Res.*, 983: 23–35, 2003.

D.M. Taylor, S.I. Helms Tillery, and A.B. Schwartz. Direct cortical control of 3D neuroprosthetic devices. *Science*, 296:1829–1832, 2002.

G. Thut, A. Nietzel, S. Brandt, and A. Pascual-Leone. Alpha-band electroencephalographic activity over occipital cortex indexes visuospatial attention bias and predicts visual target detection. *J. Neurosci.*, 26: 9494-9502, 2006.

G. Vanacker, J. del R. Millán, E. Lew, P.W. Ferrez, F. Galán, J. Philips, H. Van Brussel, and M. Nuttin. Context-based filtering for assisted brain-actuated wheelchair driving. *Computational Intelligence and Neuroscience*, 2007.

D. Verma and R. P. N. Rao, 'Goal-based imitation as probabilistic inference over graphical models,' *Advances in Neural Information Processing Systems (NIPS 2005)*, 18:1393-1400, 2006.

R.J. Vetter, J.C. Williams, J. Hetke, E.A. Nunamaker, and D.R. Kipke. *Chronic neural recording using silicon-substrate microelectrode arrays implanted in cerebral cortex. IEEE Trans. Biomed. Eng.*, 51(2): 896–904, 2004.

J.J. Vidal. Toward direct brain-computer communication. *Annual Review of Biophysics and Bioengineering*, 2:157–180, 1973.

J.J. Vidal. Real-time detection of brain events in EEG. *Proceedings IEEE*, 65:633—641, 1977.

W.G. Walter, R. Cooper, V. Aldridge, W.C. McCallum, and A.L. Winter. Contingent negative variation: An electrical sign of sensorimotor association and expectancy in the human brain. *Nature*, 203:380-384, 1964.

N. Weiskopf, K. Mathiak, S.W. Bock, F. Scharnowski, R. Veit, W. Grodd, R. Goebel, and N. Birbaumer. Principles of a brain-computer interface (BCI) based on real-time functional magnetic resonance imaging (fMRI). *IEEE Trans. Biomed. Eng.*, 51(6):966–970, 2004.

J.R. Wolpaw, N. Birbaumer, D.J. McFarland, G. Pfurtscheller, and T.M. Vaughan. Brain-computer interfaces for communication and control. *Clinical Neurophysiology*, 113:767–791, 2002.

J.R. Wolpaw and D.J. McFarland. Control of a two-dimensional movement signal by a noninvasive brain-computer interface in humans. *PNAS*, 101:17849–17854, 2004.

J.R. Wolpaw, D.J. McFarland, T.M. Vaughan, and G. Schalk. The Wadsworth Center brain-computer interface (BCI) research and development program. *IEEE Trans. Neural Syst. Rehabil. Eng.*, 11:204-207, 2003.